A LOW DILUTION FUSION TECHNIQUE FOR THE DETERMINATION OF MAJOR, MINOR AND TRACE ELEMENTS IN LAMPROITE AND KIMBERLITE SAMPLES BY X-RAY FLUORESCENCE SPECTROMETRY

by

JULIE EASTELL

Department of Geochemistry
University of Cape Town
July 1986

Thesis submitted in fulfilment of the requirements for the degree of Master of Science at the University of Cape Town.

This thesis is dedicated to the

loving memory of my late husband

Stephen John Eastell

A Low Dilution Fusion technique for the determination of Major, Minor and Trace elements in Lamproite and Kimberlite samples by X-ray Fluorescence Spectrometry.

ABSTRACT

A low dilution fusion technique using a 2:1 flux:sample ratio has been developed for the accurate determination of major, minor and trace elements by X-ray fluorescence spectrometry (XRFS). This method has been used to analyze geological samples of widely varying and unusual composition such as lamproites and kimberlites. The results are shown to be of comparable if not better accuracy than other methods of sample preparation for XRFS. Analytical conditions, including corrections for spectral line interferences are reported for all the elements determined.

For major element analysis three methods of calculating appropriate alpha coefficients were investigated, namely (1) multiple regression analysis, (2) Norrish and Hutton method and (3) a computer program, NBSGSC, involving fundamental parameters and the COLA equation. Methods (1) and (2) gave poor results for rock types of widely varying composition. The third method requires that the variation of alpha coefficients with varying weight fraction of the analyte element be taken into account when calculating alpha coefficients if accurate values for major and minor elements are to be obtained on low dilution fusion discs.

For trace element analysis the average relative error was less than 5% and there was a decrease in sensitivity by about a factor of 2 compared with XRFS determinations on powder pellets. The elimination of particle size effects in the homogeneous glass fusion discs is a major advantage over the use of powder pellets, especially for the determination of elements such as Ba, Cr and the REEs.

A loss on fusion technique has been employed to ensure complete loss of volatiles from the rock samples. Data presented highlight the problems encountered in the determination of the volatile content in geological samples. The oxidation and retention of sulphur in the discs was also investigated.

CONTENTS

Abstract i
List of figures v
List of tables vii

CHAPTER 1

INTRODUCTION

Introduction 1

Background to the development of fusion methods. 6

CHAPTER 2

THE LOW DILUTION FUSION TECHNIQUE AND LOSS ON FUSION

Introduction 9

Flux : Sample ratio 11

Choice of Flux 12

Problems 14

Use of a heavy absorber 16

Choice of oxidant 17

Loss on fusion 22

Retention of sulphur 25

Sulphur determination 27

Determination of H_2O+, CO_2 and FeO content of lamproite and kimberlite samples 31

Loss of volatile elements 37

Fluorine 38

Summary 40

CHAPTER 3

TRACE ELEMENT ANALYSIS

Introduction 41

Mass Absorption coefficients 42

Analytical run - Nb, Zr, Y, Sr, Rb, U, Th, Pb . . . 47

Analytical run - Zn, Cu, Ni 60

Analytical run - Sc 64

Analytical run - Co, Cr, V 66

Analytical run - La, Ce, Nd 71

Analytical run - Sr, U, Th, Pb, Br, Se, Bi, As, W, Ga 81

Barium 87

Summary 94

Further work 105

CHAPTER 4

MAJOR ELEMENT DATA REDUCTION

Introduction 106

Relationship between intensity and concentration in major element oxide analysis 114

Alpha coefficients 116

Previous calculation procedures for low dilution fusions 120

Multiple regression analysis - XRF4 124

Theoretical calculation of alpha coefficients by the Norrish and Hutton method 135

Major element analysis using fundamental parameters 154

Fused disc system 162

Oxide system 173

CHAPTER 5

SUMMARY and CONCLUSIONS

Summary 189

Conclusion 197

ACKNOWLEDGEMENTS 198

REFERENCES 200

APPENDICES

A. Calculation of loss on fusion

B. FeO determinations

H_2O^+ and CO_2 analysis

C. Calculation of oxide content and m.a.c.s. of Johnson and Matthey Spectroflux 100B

MATH/1000

D. Spread sheets from MATH/1000 for calculation of Norrish type alpha coefficients

E. Oxide alpha coefficients calculated using NBSGSC and Thinh and Leroux algorithm

G. Concentration data for Lamproite and kimberlite samples analysed using low dilution fusion technique and Le Roex and Thinh's oxide alpha coefficients for major element data reduction

List of Figures

2:1 Calibration curve for sulphur determined on low dilution fusion discs 28
2:2 Wavelength scans showing the position of Fluorine . 39
3:1 Wavelength scan showing position second and third order La K_a peaks 50
3:2 Wavelength scan showing an asymmetric Nb K_a peak 50
3:3 Wavelength scan showing second order La K_a interference on Nb K_a 51
3:4 Wavelength scan showing the position of Ba $K_{a1,2}$ in relation to Zr K_a and Sr K_b spectral lines . . . 52
3:5 (a) Calibration curve for Sr (<5000ppm) using Rb m.a.c.s 55
(b) Calibration curve for Sr (<15000ppm) using Rb m.a.c.s 55
3:6 (a) Calibration curve for Pb using W X-ray tube with no correction for Lanthanum interference . . . 56
(b) Calibration curve for Pb using W X-ray tube with correction for Lanthanum interference 56
3:7 Wavelength scan showing the interference of Ba and Ti on Vanadium 68
3:8 Wavelength scan showing positions of La, Ce, Nd and Ba in the 100 - 140° 2θ 73
3:9 Position of the Ba L absorption edges in relation to the La, Ce and Nd analyte lines 75
3:10 Position of La, Ce and Nd analyte lines in relation to the Titanium K absorption edge 78
3:11 Calibration curve for Pb using Mo X-ray tube with no correction for Lanthanum interference 84
3:12 (a) Calibration curve for Ba using Cr and K m.a.c.s for powder pellets 88
(b) Calibration curve for Ba using Cr and K m.a.c.s for low dilution fusion discs 88
3:13 Position of the absorption edges in relation to Ba $L\alpha$ analyte line 89
3:14 (a) Calibration curve for Ba using Cr and Sc m.a.c.s for powder pellets 90
(b) Calibration curve for Ba using Cr and Sc m.a.c.s for low dilution fusion discs 90
3:15 Comparison of INAA, international standards and low dilution fusion disc data for lanthanum 96
3:16 Comparison of INAA, international standards and low dilution fusion disc data for cerium 97
3:17 Comparison of INAA, international standards and low dilution fusion disc data for neodymium 98
3:18 Comparison of INAA, international standards and low dilution fusion disc data for scandium 99
3:19 Comparison of INAA, international standards and low dilution fusion disc data for cobalt 100
3:20 Comparison of INAA, international standards and low dilution fusion disc data for rubidium 101
3:21 Comparison of INAA, international standards and low dilution fusion disc data for thorium 102
4:1 Basic shapes of intensity/concentration curves (after Jenkins 1980) 107
4:2 Interference of Zr on P background positions 111
4:3 Mutual interference of Ti K_a and Ba L_a 112
4:4 Interference of third order Ba L_a on Al K_a 112

4:5 Calibration curve for SiO_2 from XRF4 using Lucas-Tooth and Pyne (1963) correction model 126
4:6 Calibration curve for CaO from XRF4 using Lucas-Tooth and Pyne (1963) correction model 127
4:7 Calibration curve for Fe_2O_3 from XRF4 using Lucas-Tooth and Pyne (1963) correction model 127
4:8 Calibration curve for SiO_2 from XRF4 using Lachance-Traill (1966) correction model 129
4:9 (a)-(c) M.A.C. for major element analyte lines using Heinrichs Tables (1966) - correction for oxygen 136
4:10 Silica - standard concentration vs uncorrected concentrations 149
4:11 Calculated Cr X-ray tube spectrum from NBSGSC . . . 157
4:12 (a) Silica - NBSGSC theoretical alpha coefficients for fused disc system 179
(b) Silica - NBSGSC theoretical alpha coefficients for oxide system 180
4:13 (a) Magnesium - standard concentration vs uncorrected concentrations 181
(b) Magnesium - NBSGSC theoretical alpha coefficients for fused disc system 182
(c) Magnesium - NBSGSC theoretical alpha coefficients for oxide system 183
4:14 (a) Aluminium - standard concentrations vs uncorrected concentrations 184
(b) Aluminium - NBSGSC theoretical alpha coefficients for oxide system using Heinrich's (1966) m.a.c. algorithm 185
(c) Aluminium - NBSGSC theoretical alpha coefficients for oxide system using Thinh and Leroux's (1979) m.a.c. algorithm 186

C:1 Mass absorption coefficients for flux components (Jenkins et al 1970) C4

List of Tables

1:1 Comparison of concentrations of selected elements in 'normal' rocks and lamproites 2
1:2 Glossary of frequently used terms 5
2:1a Composition of low dilution fusion discs used in this study 9
2:1b Method of preparation of Low dilution fusion discs . 10
2:2 Compositional limitations for preparation of glass discs (after Haukka and Thomas 1977) 15
2:3 Comparison of calculated LOI values and experimentally determined LOF values using ammonium nitrate as oxidant 20
2:4 Comparison of degree of oxidation of a basalt using different oxidants in differing proportions as shown by amount of FeO remaining after fusion 21
2:5a Comparison of experimentally determined LOI and LOF using ammonium nitrate as oxidant 23
2:5b Duplication of LOF values using ammonium nitrate as oxidant 23
2:6 Comparison of LOF values using lithium nitrate as oxidant with calculated loss/gain values from international standards data 24
2:7 Duplication of LOF values using lithium nitrate as oxidant 25
2:8 Comparison of sulphur net intensities obtained from low dilution fusion discs 27
2:9 Comparison of recommended international standards data with data obtained from LDF discs for Sulphur . 28
2:10 Sulphur concentrations in powders and fusion discs of selected lamproite and kimberlite samples determined by LECO sulphur analyzer (Geological Survey, Pretoria) 29
2:11 Comparison of sulphur data from LDF discs and powder pellets (XRFS), U.C.T. and powders analysed on LECO analyzer, Geol. Survey, Pretoria 30
2:12 Comparison of LOF and H_2O^+ and CO_2 data with total $Fe_2O_3$3 and S values 32
2:13 H_2O- and H_2O+ data for several lamproites analysed at Geological Survey, Pretoria 33
2:14 Loss on ignition data for lamproite samples, data reported at 750°C and 850°C 34
2:15 FeO content of lamproite and kimberlite samples, determined by titration and gain by oxidation to Fe_2O_3 35
2:16 Comparison of calculated "loss" and LOF values corrected for the oxidation of Fe and S 36
2:17 Comparison of potassium data obtained by XRFS and AA (Gurney 1968) and by the low dilution fusion technique 38
3:1 Analytical conditions for the determination of Molybdenum Compton mass absorption coefficients, on a Philips PW1220 XRF spectrometer 42
3:2 Comparison of given and calculated Mo mass absorption coefficients, using the Compton scatter method 44
3:3 Primary and secondary m.a.c.s. used to correct for matrix differences for elements with wavelengths between the Fe and Ca K absorption edges 46
3:4a Analytical conditions for the determination of Mo, Nb, Zr, Y, Sr, U, Rb, Th, and Pb in the low

dilution fusion discs using a Philips PW1400 XRF spectrometer with a W X-ray tube at 50 kV, 55mA, and a LiF (200) analyzing crystal 47
3:4b Possible spectral line interferences on elements Nb, Zr, Y, Sr, U, Rb, Th, and Pb using analytical conditions outlined in table 3:4a 48
3:5 Comparison of Nb - Pb data obtained by low dilution fusion method with international standards data . . 58
3:6 Lower limits of detection and counting errors for low dilution fusion discs analysed by XRFS using the analytical conditions outlined in Table 3:4 59
3:7a Analytical conditions for the determination of Zn, Cu, and Ni on low dilution fusion discs analysed on a Philips PW1400 XRF spectrometer using a Au X-ray tube at 60 kV, 45mA, and a LiF (220) analyzing crystal 60
3:7b Possible spectral line interference in elements Zn, Cu and Ni using analytical conditions outlined in Table 3:7a 60
3:8 Comparison of Zn, Cu and Ni data obtained on low dilution fusion discs with international standards data 62
3:9 Lower limits of detection and counting errors for Zn, Cu and Ni for low dilution fusion discs analysed by XRFS using conditions outlined in Table 3:7 63
3:10 Analytical conditions for the determination of Sc on low dilution fusion discs analysed on a Siemens SRS-1 XRF spectrometer using a Cr X-ray tube at 50kV, 60mA and LiF (200) analyzing crystal 64
3:11 Comparison of Scandium data from the low dilution fusion discs with international standards data . . . 65
3:12 Lower limits of detection and counting errors for Scandium determined on Siemens SRS-1 spectrometer using conditions outlined in Table 3:10 65
3:13a Analytical conditions for the determination of Co, Cr, V in low dilution fusion discs analysed on a Philips PW1400 XRF spectrometer using a W X-ray tube at 50kV, 55mA, and a LiF (220) analyzing crystal 66
3:13b Possible spectral line interferences on elements Co, Cr, and V using analytical conditions outlined in Table 3:13a 66
3:14 Comparison of Co, Cr, V data obtained by the low dilution fusion technique with international standard values 69
3:15 Lower limits of detection and counting errors for Co, Cr and V determined using conditions outlined in Table 3:13 70
3:16a Analytical conditions for the determination of La, Ce, and Nd on low dilution fusion discs analysed on a Philips PW 1400 XRF spectrometer using a W X-ray tube at 50kV, 55mA, and LiF (220) analyzing crystal 71
3:16b Possible spectral line interferences on elements La, Ce and Nd using analytical conditions outlined in Table 3:16a 71
3:17 Comparison of calculated background factors for La, Ce and Nd showing the interference of barium 72
3:18 Comparison of La, Ce and Nd data obtained from the

low dilution fusion discs with international standards data 76
3:19 Lower limits of detection and counting errors for La, Ce and Nd analysed by XRFS using the conditions outlined in Table 3:16 76
3:20 Comparison of La, Ce, and Nd data analysed by INAA (Max Planck), XRFS- powder pellets (UCT) and XRFS- low dilution fusion discs (UCT) 80
3:21a Analytical conditions for the determination of Sr, U, Rb, Th, Pb, Br, Se, Bi, As, Ge, W and Ga on low dilution fusion discs analysed on a Philips PW1400 XRF spectrometer using a Mo X-ray tube at 50kV, 55mA and a LiF (200) analyzing crystal 81
3:21b Possible spectral line interferences on elements Sr, U, Rb, Th, Pb, Br, Se, Bi, As, Ge, W and Ga using analytical conditions outlined in Table 3:21a 82
3:22 Comparison of Sr, U, Rb, Th, Pb and Ga data obtained by low dilution fusion technique with international standards data 85
3:23 Lower limits of detection and counting errors for low dilution fusion discs analysed by XRFS using conditions as detailed in Table 3:21 86
3:24 Comparison of barium data obtained from low dilution fusion discs, international recommended values and artificial standards 92
3:25 Lower limits of detection and counting errors for Ba determined using conditions outlined in Table 4:1 92
3:26 Average relative errors for trace elements determined on low dilution fusion discs for concentrations greater than 20 ppm 93
3:27 Reproducibility of La, Ce and Nd data analysed on low dilution fusion discs 104
4:1a Analytical conditions for the determination of the 12 major element oxides using a Philips PW1400 XRF spectrometer with a Cr X-ray tube operating at 50kV and 55mA 108
4:1b Possible spectral line interferences on major elements determined using analytical conditions outlined in Table 4:1a 109
4:2 Summary of blank fusions discs used for the calculation of background factors 113
4:3 Mathematical correction models relating intensity to concentration 115
4:4 Comparison of alpha coefficients for CaO and BaO calculated using XRF4 and the Lachance-Traill correction model using the same standards set . . . 130
4:5 Absolute and relative errors for the international rock standards used for calibration of the major element oxides by multiple regression analysis . . . 131
4:6 Approximate composition range in the lamproites and kimberlites and the spiked standards 131
4:7 Absolute and relative errors for the "spiked" rock standards used for calibration of the major element oxides by multiple regression analysis . . . 132
4:8 Data for two lamproite samples using multiple regression analysis and "spiked" standards to calculate alpha coefficients 133
4:9 Comparison of alpha coefficients determined by multiple regression analysis and theoretical alphas (after Lachance) 134

4:10 Method of calculating Norrish-type alpha factors . . 137
4:11 General relationship between intensity and concentration using the Norrish and Hutton (1969) method of calculating alpha coefficients 138
4:12 Comparison of reported and calculated Heinrich mass absorption coefficient values for oxygen at K_a wavelengths 139
4:13 Norrish and Hutton (1969) published matrix correction factors for discs containing lanthanum oxide 143
4:14 Calculated Matrix correction factors (this work) using Norrish and Hutton method [Table 4:10] for fusion discs containing lanthanum oxide 144
4:15 Comparison of average absolute and relative errors for the calculated and published coefficients using the Norrish and Hutton (1969) technique 145
4:16 Comparison of concentration data obtained using calculated and published coefficients 145
4:17 Calculated matrix correction factors (this work) using Norrish and Hutton (1969) technique [Table 4:10] for low dilution fusion discs 146
4:18 Average absolute and relative errors for the low dilution fusion discs using theoretical alphas from Table 4:17 151
4:19 Comparison of Kimberlite data obtained using the Norrish and Hutton technique (published alphas) and the low dilution technique (calculated Norrish-type alphas) 151
4:20 Comparison of data obtained using Multiple regression analysis (XRF4) and Norrish method of calculating alpha coefficients for low dilution fusion discs 152
4:21 The COLA equation as used in NBSGSC 155
4:22 Cr X-ray tube spectrum as calculated by NBSGSC . . . 158
4:23 Alpha coefficients for fused disc system for the Norrish and Hutton flux calculated by NBSGSC 163
4:24 Average absolute and relative errors for Norrish and Hutton fusion discs using alpha coefficients calculated by NBSGSC - calibration curve $Y = A1 * X + A2 * X^2$ 164
4:25 Comparison of international standards data with data obtained from NBSGSC for Norrish and Hutton fusion discs 165
4:26a Alpha coefficients calculated using the fused disc system of NBSGSC for low dilution fusion discs (Heinrich,1966) 167
4:26b Alpha coefficients calculated using the fused disc system of NBSGSC for low dilution fusion discs (Thinh & Leroux,1979) 168
4:27 Average absolute and relative errors for "spiked" and international LDF rock standards using $Y = A1 * X + A2 * X^2$ calibration curve and fused disc system alpha coefficients calculated using Heinrich's or Thinh and Leroux's algorithm . . 166
4:28 Comparison of international standards data with data obtained from NBSGSC for low dilution fusion discs using Heinrich's and Thinh and Leroux's algorithms 169
4:29 Major element data obtained from NBSGSC using fused disc system, Heinrich's algorithm and calibration curve, $Y = A1 * X + A2 * X^2$ 171

4:30 Comparison of data for the standards used to calibrate the low dilution fusion discs using the oxide alpha coefficients - Heinrich and Thinh and Leroux's algorithms 175
4:31 Average absolute and relative errors for international and "spiked" standards using oxide alpha coefficients 176
4:32 Average absolute and relative errors for the oxide alpha coefficient system using Thinh and Leroux's algorithm for the four different calibration curves 188
5:1 Trace elements determined on low dilution fusion discs by previous workers and this work 192

CHAPTER 1

INTRODUCTION

Introduction

This thesis investigates analytical problems experienced in X-ray fluorescence spectrometric analysis of geological rock samples.

A low dilution fusion technique, based on those of Haukka and Thomas (1977), Thomas and Haukka (1978) and Lee and McConchie (1982), is used for the determination of major, minor and trace elements in lamproites, kimberlites and other rock types on a single homogeneous glass disc. The "loss" from a sample, which represents the net physical loss in weight due to the evolution of volatiles and the gain in weight by ferrous iron and sulphides during oxidation, is determined by measuring the loss on fusion.

Lamproites and kimberlites present significant analytical problems when analyzed by the present X-ray fluorescence analytical techniques used in the Department of Geochemistry, U.C.T.. These techniques can be summarized as follows: whole rock powder pellets are used for elements with concentrations less than 1000 - 1500 ppm and fusion discs with a heavy absorber, as outlined by Norrish and Hutton (1969), for major and minor elements; total volatiles are determined by roasting at 850 - 1000^{o}C and, if considered necessary, CO_2 and H_2O+ are determined by gas chromatography.

Initial data, obtained by the above methods, indicated that many lamproites contained concentrations of barium in excess of 1 wt. percent. At these concentration levels barium, a heavy absorber of X-ray fluorescence radiation, has to be analyzed as a major element so that the relevant matrix corrections can be

performed. Lamproites and kimberlites also contain many trace and some major elements at concentrations greater than 'normal' rocks such as granites and basalts. Examples are presented in Table 1:1.

Data obtained by Smith (pers.comm) at U.C.T. by XRFS and at the Max Planck Institute for Cosmochemistry, Mainz by INAA indicated that severe mineralogical effects exist for the XRFS determination of Ce, La and Nd in kimberlites. These effects are discussed in Chapter 3.

Table 1:1

Comparison of concentrations of selected elements in 'normal' rocks and lamproites. Data reported in ppm except TiO_2.

	BASALT	GRANITE	LAMPROITE	KIMBERLITE
Ba	330	400-900	>3000	200-5000
La	10	40	110-400	20-400
Ce	60 Ave.		170-750	40-750
Nd	28 Ave.		50-250	20-400
Sr	465	285	500-2500	200-1900
TiO_2%	2.30	0.30	4-7	0.3-5.0

Note: Granite and basalt data taken from Turekian and Wedepohl (1961), lamproite data from Hawkesworth (pers. comm.) except Sr from U.C.T., and kimberlite data from Smith (in press).

It is proposed that the method described in this thesis be used to overcome additional problems associated with sample preparation. Rocks such as kimberlites and mantle nodules which contain abundant sheet silicate minerals (phlogopite, biotite)

and quartz-rich rocks such as granites and sediments can give problems during sample preparation. Sheet silicate minerals tend to slide over one another during grinding, resulting in an inhomogeneous powder, increased particle size and mineralogical effects. Silica-rich rocks, during the pelleting stage of sample preparation, present problems as the compacted sample powder tends to expand and crack once the pressure from the hydraulic press has been released resulting in a very unstable pellet.

The low dilution fusion method described in this thesis eliminates all the above sample preparation problems. XRF spectrometric analysis of major, minor and trace elements is carried out on the same homogeneous glass fusion disc. The use of a fusion method eliminates particle size effects including mineralogical and chemical effects.

Particle size effects (Jenkins 1974, Bertin 1978) is a general term referring to grain size, intermineral and mineralogical effects which are best described using a two phase heterogeneous powder. Grain size effects occur when the analyte is present in only one of the phases, with both phases having similar mass absorption coefficients for the analyte line. The intensity of the analyte line is therefore dependent on the percentage of the analyte phase present in the analytical layer. Intermineral effects occur when the analyte is present in one of the phases and the two phases have substantially different mass absorption coefficients for the analyte wavelength. Mineralogical effects are present when the analyte occurs in both phases, with each phase having different mass absorption coefficients for the analyte wavelength. These effects can be minimized by grinding the sample to a fine powder, the ideal powder should have an

overall particle size which is less than one fifth of the penetration depth of the measured wavelength. This can be very difficult to achieve.

Variations in chemical state can cause wavelength shifts (Zemany 1960, Bertin 1978), these chemical effects occur for elements Na through to Cl where electron transitions from unfilled 3p orbitals give rise to K_b lines, the wavelengths of these lines are affected by oxidation or coordination state of the element. Wavelength shifts are observed for elements such as Al, Si, and Mg when analyzed as a metal and an oxide, and S when analyzed in the sulphide or sulphate form. Fortunately, this is not usually a problem with the K_a lines used for analysis.

Roasting the lamproites at 850 - 1000 ^{o}C to determine volatile content is, in many cases, insufficient to breakdown refractory minerals and remove all the volatiles from the rock. In addition talc-rich rocks present serious analytical problems as talc only decomposes at temperatures in excess of 1100^{o}C, resulting in incorrect loss on ignition, and consequently low analytical totals. A loss on fusion method has been used to overcome the inaccuracy of the loss on ignition method. The results of the loss on fusion method of volatile determination and the retention of sulphur as sulphate (SO_4^{2-}) during the fusion process are discussed.

International standards (Govindaraju 1984, Abbey 1986) were used to calibrate the data, and data obtained are compared with recommended values for international rock standards. Average absolute and relative errors for major elements and lower limits of detection and counting errors for trace elements are reported. Some calibration curves are presented. All relevant

analytical interferences on background and peak angular positions are discussed within the various sections. For major element oxide analysis, various methods of calculating matrix correction coefficients are critically discussed.

Certain trace elements have been determined by INAA (Fraser et al. 1986) and Smith (pers. comm.) and their results are compared with data obtained by the proposed method.

A glossary of frequently used terms in this thesis is given in Table 1:2.

TABLE 1:2

Glossary of frequently used terms

a_{ij} or α_{ij}	alpha coefficient, effect of element j on element i.
abs. edge	absorption edge of an element
kV	Kilovolt
mA	milliamp
m.a.c.s)	
)	mass absorption coefficient
μ/ρ)	
λ	wavelength in Angstroms
i	analyte matrix element
j	interferring matrix element
K)	
)	series x-ray spectral lines
L)	
Ψ_1	angle between specimen surface and centre of X-ray beam
Ψ_2	take-off angle of spectrometer (angle between axis of collimator and specimen surface)
xtal	analyzing crystal
COL	Collimator
DET	Detector / counter
FS	Flow and scintillation counter
FC	Flow counter
SC	Scintillation counter
UPL	Pulse height analyzer - upper window level
LWL	Pulse height analyzer - lower window level
s	counting time in seconds
c.p.s	counts per second (net)
S.D.	standard deviation
ppm	parts per million
wt. %	weight percent

Background to the development of fusion methods.

The past 3 decades have seen many developments in the preparation of samples and methods of data reduction for X-ray fluorescence spectrometry. Experimental work on the analysis of major rock forming elements has been directed towards the preparation of homogeneous glass fusion discs that eliminate some of the problems outlined previously.

Claisse (1956) introduced the use of a flux in a ratio of 100:1 (flux:sample) to dissolve the rock powder and produce a homogeneous glass disc. Rose et al. (1962) introduced the use of lithium tetraborate as a flux in the ratio of 4:1 and lanthanum oxide as an heavy absorber to reduce matrix effects.

Norrish and Hutton (1969) proposed a method of preparation of fusion discs along with experimental, theoretical and 'preferred' values of correction coefficients for the calculation of accurate concentrations from major element intensities. The method of calculation of these coefficients is discussed in Chapter 4. The flux used, in a flux:sample ratio of 5.4:1, consisted of lithium tetraborate, lithium carbonate, and lanthanum oxide in the ratio 2.9:2.3:1 . Lithium carbonate lowers the melting point of the flux and lanthanum oxide reduces matrix effects. Sodium because of its low atomic number and long wavelength, has a low analyte line intensity which is reduced further by dilution with a flux and absorption of the analyte line by the diluent. Sodium is therefore measured on a pressed powder pellet. The addition of $NaNO_3$ as an oxidant also prevents Na determinations on the Norrish and Hutton (1969) glass fusion discs.

Haukka and Thomas (1977) and Thomas and Haukka (1978) investigated the use of a lower dilution ratio in order to analyze trace elements as well as major and minor elements on a single glass disc. Lithium metaborate was used as the flux in a flux:sample ratio of 2:1, with and without lanthanum oxide. The matrix coefficients used by Haukka and Thomas (1977) are discussed in Chapter 4. Data produced by this method indicated a relative precision and accuracy between 0.4 - 6.6% for major, minor and trace elements. The loss of volatiles or gain by oxidation of reduced species by a sample was reported as the difference from 100 % and treated as a variable dilution.

Hutton and Elliott (1980) published results for trace elements determined on a glass disc using a flux:sample ratio of 2:1. Their flux contained lanthanum oxide and they adapted Norrish and Hutton's (1969) matrix correction coefficients to suit their sample:flux ratio.

Lee and McConchie (1982) using lithium tetraborate and lithium carbonate in a flux:sample ratio of 2:1 successfully analyzed major, minor and selected trace elements. Mass absorption differences for trace elements were corrected using the Compton scatter method (Reynolds 1963) and matrix correction coefficients calculated by de Jongh's method (1973) for major and minor elements. The average relative error for this method was 8%.

Bower and Valentine (1986) critically compared sample preparation methods for major and trace element determinations using XRFS. They concluded that any dilution ratio could be adopted depending on the type of analysis and the degree of

accuracy required. They also concluded that pressed powder pellets for trace element analysis have no real advantage over glass fusion discs as the latter are homogeneous and particle size, mineralogical and chemical effects are eliminated.

All the fusion methods outlined above where carried out on 'normal' rock types, for example granites and basalts. There has been no published data on lamproites or kimberlites analyzed by these low dilution fusion techniques. The high concentrations of barium in lamproites present serious problems as barium acts as a heavy absorber of radiation but also enhances its own radiation (Joslin and Salt, 1985).

The documented low dilution fusion methods generally use ignited sample material and problems of incomplete loss of volatile components have generally not been discussed.

CHAPTER 2

LOW DILUTION FUSION TECHNIQUE

AND

LOSS ON FUSION

THE LOW DILUTION FUSION TECHNIQUE AND LOSS ON FUSION.

Introduction

The term "low dilution fusion technique" implies that the dilution of the sample powder by a fluxing reagent is kept to a minimum to ensure sufficient count rates for trace element analysis.

The sample:flux ratio, choice of fluxing reagent and oxidant used in the proposed low dilution fusion technique are discussed in this section. The constituents and preparation technique of the discs are outlined in Table 2:1(a) and (b).

Results for the loss on fusion technique to determine volatile content (CO_2, H_2O, F), gain by the oxidation of reduced species (FeO to Fe_2O_3, S to SO_4^{2-}) and the possible loss of volatile analyte elements (S, Na, K, P, Pb, F) are presented and discussed.

TABLE 2:1(a)

Composition of Low Dilution Fusion Discs used in this study.

Flux:Sample ratio of 2:1

2g ± .001g of sample dried at 110°C

4g ± .001g of Johnson Matthey Spectroflux 100B dried at 450°C

Flux contains 80% lithium metaborate
20% lithium tetraborate

0.6g of lithium nitrate as oxidant

Fusion discs weigh approximately 6.1g and measure ≈ 3.3mm in thickness.

TABLE 2:1(b)

Method of Preparation of Low Dilution Fusion Discs.

---

1 - Weigh dried flux (450°C)
dried lithium nitrate (110°C)
dried sample powder (110°C)

2 - Store 3 constituents in a dry clean sealed glass vial, mix contents thoroughly. Keep prepared mixtures in a desiccator.

3 - Handle Pt-Au crucibles with Pt-tipped or titanium tongs at all times. Weigh a clean, dry Pt-Au crucible, record weight. Leave crucible on balance and add mixture of flux, nitrate and sample. Record weight.

4 - Transfer crucible to Fisher burner (at 1000-1100°C), allow mixture to melt, swirling the sample to ensure the removal of trapped air bubbles.

5 - When melt is homogeneous allow to cool for about 10 minutes in the crucible, preferably with the crucible at an angle.

6 - When a glass has been formed, transfer the crucible to a desiccator and leave to cool to room temperature (approximately 30 minutes).

7 - Reweigh the cold crucible, record weight and reheat crucible and glass to form a melt.

8 - Cast a disc by pouring melt on to a graphite mould, dimensions as illustrated in the diagram below, and quenching with an aluminium plunger. Mould and plunger is kept at a temperature of 260°C.

9 - Transfer the disc to an asbestos pad on a hot plate (220°C) and allow to anneal for ≈ 1 hour.

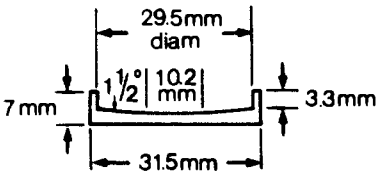

Flux:Sample Ratio

In XRFS analysis the flux:sample ratio in fusion discs has been varied between 2:1 to 100:1. The ratio chosen is normally dependent on the constituents sought and the nature of the samples.

To analyze for major, minor and trace elements on a single glass fusion disc the dilution ratio has to be low enough to produce high count rates for the trace elements but high enough to produce homogeneous glass. Previous workers have used ratios of 2:1 (Haukka and Thomas, 1977 and Lee and McConchie, 1982). This ratio has been adopted but the amount of flux and sample powder has been increased to 4g and 2g respectively in order to ensure infinite thickness for the measurement of short (0.74Å) X-ray wavelengths (ZrK_a and NbK_a). Further increasing the ratio of rock powder to flux results in segregation of the constituents, as the flux is less reactive and consequently the rock powder less soluble. The low flux to sample ratio of this fusion method requires higher fusion temperatures than usual, in the region of 1050-1100^{o}C.

Weighing errors are lower in the low dilution fusion technique, due to the greater sample mass used, than, for example, in the Norrish and Hutton (1969) technique, 2g vs 0.28g. Weighing limits for the flux and the sample are set at 4.000g ± .001g and 2.000g ±.001g respectively. Consequently the maximum weight correction factor for the sample mass is +.05% relative, which is so small that corrections for weight differences from the nominal 2g are unnecessary as they are within the desired precision of the analyses.

Choice of Flux

Lithium metaborate and lithium tetraborate are important fluxing reagents. The low atomic numbers of the elements in the lithium borates mean that none of these elements emit detectable X-rays.

Lithium metaborate is a more reactive flux than lithium tetraborate. It rapidly attacks most silicates and many non-silicates, yielding a glass that is mechanically strong and reasonably non-hygroscopic. Lithium metaborate is essential for chromite dissolution and attacks refractory rock forming minerals more effectively than lithium tetraborate.

Norrish and Hutton (1969) used a flux containing lithium tetraborate, lithium carbonate and lanthanum oxide with a flux:sample ratio of 5.4:1 for major element analysis only. The addition of lithium carbonate to the tetraborate forms a eutectic mixture which has a melting point several hundred degrees lower than that of pure lithium tetraborate. The use of lanthanum oxide will be discussed later.

A suitable flux was required for this study that would dissolve major rock forming silicate and sulphide minerals during the fusion process in a dilution ratio low enough to allow the analysis of trace elements in addition to major and minor elements.

For the quantitative analysis of rocks by XRFS the following types of fusion discs are required: blanks, interference standards and calibration standards. The preparation of blank discs is very important but can be problematic as they usually contain either a pure oxide or a mixture of two oxides which can be difficult to dissolve. Blank discs are used to calculate

background factors for elemental analysis. Generally a fusion disc made with Johnson Matthey Specpure silicon dioxide will be a good blank for all elements except Si. In the Geochemistry Department, U.C.T. for the Norrish and Hutton (1969) technique a mixture of Johnson Matthey Specpure Fe_2O_3 and $CaCO_3$ is used as silica blank. Johnson Matthey Specpure Al_2O_3 is also a good blank for silica and has been used by other workers (Haukka and Thomas, 1977; Lee and McConchie, 1982) in their low dilution fusion techniques.

Previous workers using a low dilution fusion method of 2:1 (flux:sample) have used either pure lithium metaborate (Haukka and Thomas, 1977) or a mixture of 56% lithium tetraborate and 44% lithium carbonate (Lee and McConchie, 1982). The latter flux is not commercially available in South Africa, but Lee (pers.comm) has successfully used a mixture of lithium metaborate and lithium tetraborate. As with the addition of lithium carbonate, the addition of lithium as lithium metaborate results in the flux being more fluid at the fusion temperature. The fusion mixture is easier to handle and homogeneity is more rapidly attained.

Initial work was carried out using Lee and McConchie's (1982) original flux by combining the two chemicals in the proportions of 56% lithium tetraborate and 44% lithium carbonate during the weighing procedure prior to fusion. The presence of carbonate in the mixture caused problems as this generated CO_2 during the initial heating stages resulting in ejection of material from the crucible. In an attempt to prevent this, the flux mixture was first heated in a furnace with the temperature being increased slowly. This still did not solve the problem

completely and was very time consuming. The few fusion discs produced by this method indicated that this flux was unsatisfactory, as pure Al_2O_3 and a mixture of Fe_2O_3 and $CaCO_3$ would not dissolve to form a glass.

The flux recommended by Lee (pers.comm.) was readily available in South Africa from Johnson Matthey as Spectroflux 100B, consisting of 80% lithium metaborate and 20% lithium tetraborate. Initial tests showed that fusion discs containing 4g of flux and 2g of either pure silicon dioxide or aluminium oxide could be produced.

Problems

Various difficulties have been encountered in the production of fusion discs and certain points should be noted.

(1) A glass will only be produced by a fusion method if there is enough silica or aluminium present, as these act as network forming elements. Non-silicate materials usually require the addition of silica or aluminium to form satisfactory discs. Carbonatites and magnesites fall into this category. An important table (Haukka and Thomas, 1977, Table 1) outlining the limiting compositions of the major oxides for which homogeneous glass discs can be prepared using lithium metaborate in a flux to sample ratio of 2:1 is reproduced in Table 2:2.

(2) In the low dilution fusion method, it is of vital importance to mix the sample and flux thoroughly before fusion. For artificial standards where 1-5% of an oxide is added to quartz, the mixture of flux, oxide and quartz requires mixing in a pestal and mortar as local concentrations of quartz and oxide

TABLE 2:2

Compositional limitations for preparation of glass discs (after Haukka and Thomas, 1977).

oxide	Maximum digestible % [a]	Other oxides present [c]	Additions needed for higher percentages [d]
Na_2O	60	Mainly SiO_2 (or Al_2O_3)	SiO_2, Al_2O_3, BeO or B_2O_3
MgO	60	Mainly SiO_2 (or Al_2O_33)	SiO_2, Al_2O_3, BeO or B_2O_3
Al_2O_3	100		Flux or SiO_2
SiO_2	100		Flux or Li_2O
$Ca_3(PO_4)_2$	100	BeO (5-10% in flux)	Flux
K_2O	60	Mainly SiO_2 (or Al_2O_3)	SiO_2, Al_2O_3, BeO or B_2O_3
CaO	60	Mainly SiO_2 (or Al_2O_3)	SiO_2, Al_2O_3, BeO or B_2O_3
TiO_2	20	Mainly SiO_2	Flux
$FeTiO_2$	45	BeO 5%, B_2O_3 30% in flux	Flux, SiO_2
$FeCr_2O_4$ [b]	15	Mainly SiO_2 + alkalis	Flux
MnO	60	Mainly SiO_2	SiO_2, Flux
Fe_2O_3	60	Mainly SiO_2	SiO_2, Flux
BaO	60	Mainly SiO_2	SiO_2 or Al_2O_3

a Expressed as % of 1.0g sample with 2.0g flux weight.

b The digestion in alkaline and oxidising conditions, temperature 1200°C, fine grinding, B_2O_3 addition after dissolving.

c Other oxides present which gave maximum amounts ([b]) digestible

d Additives required for increasing the range of samples which can be dissolved.

disperse very slowly in the viscous melt and are sometimes impossible to dissolve.

(3) The melt must be homogeneous, if not the disc is liable to break or shatter.

(4) For high silica rocks and artificial standards higher fusion temperatures are required due to the high viscosity which results in the entrapment of minute air bubbles causing disc inhomogeneity.

(5) The sample powder used for low dilution fusion discs must be ground to -300 mesh particle size as the high sample content of the mixture means that the flux must be more active in its dissolution effects and the finer the sample powder the more efficient the dissolution.

Use of a Heavy Absorber

Heavy absorbers are used to reduce the interelement effects by strong absorption of primary and secondary X-ray radiation. This leads to the reduction of curvature and degree of scatter about the calibration curves and permits the analysis of a broad range of concentrations independent of the matrix. Norrish and Chappell (1967) discussed the properties of a heavy absorber in reducing matrix effects for alumino-silicates and showed that the effects are selective as elements of high atomic number are influenced more than the low ones.

Oxides of lanthanum, barium, cerium and strontium have all been used as a heavy absorber in fluxes used for major element analysis by XRFS.

The Norrish and Hutton (1969) flux contains about 21% lanthanum oxide which controls the overall mass absorption coefficient of

the mixture and helps to reduce the degree of correction required to a maximum of approximately 4% relative.

A heavy absorber is detrimental to the analysis of minor and trace elements in a glass fusion disc as it considerably reduces the count rate (hence sensitivity) and consequently increases the lower limit of detection (LLD). In addition, the use of one of the above mentioned heavy absorbers would mean that the discs could not be used to analyze for that particular element and certain others due to spectral interferences. Work by Baker (1982) indicated that the presence of lanthanum oxide frequently induces crystallisation in fusion discs resulting in heterogeneous and unstable discs.

Lamproites, for which this method was developed, can contain up to 3% BaO, so the use of a flux containing an additional heavy absorber would reduce the count rate and sensitivity even more drastically.

Joslin and Salt (1985) in their investigation on the analysis of baryte by XRFS showed that the presence of La_2O in fusion discs enhances Si and Fe radiation and absorbs Ba radiation. Consequently the combined absorption and enhancement effects of lanthanum and barium can cause severe matrix problems.

Choice of Oxidant

In the production of fusion discs, a nitrate is used as an oxidising agent to ensure the complete oxidation of reduced species - Fe, Mn and sulphides. The Norrish and Hutton (1969) technique adopted by the Geochemistry Department, U.C.T. uses sodium nitrate as the oxidant. In the low dilution fusion

method, the discs are produced for the determination of all elements normally analyzed by XRFS including Na, and consequently sodium nitrate cannot be used as an oxidising agent.

Lee and McConchie (1982) used lithium nitrate, the nitrate portion of the compound being removed during the fusion process. The additional lithium oxide, resultant from the breakdown of $LiNO_3$, increases the fluidity of the melt at fusion temperature and effectively shifts the composition of the flux towards the eutectic composition located close to lithium metaborate, thus lowering the melting point. It should be noted that lithium does not emit detectable X-rays. Lithium nitrate also increases the alkalinity and oxidising strength of the flux (Baker, 1982).

Specpure lithium nitrate was not commercially available in South Africa, and ammonium nitrate was first used as an oxidant. Ammonium nitrate is desirable as an oxidant as the compound is volatile and consequently completely lost during the fusion process.

The first low dilution fusion discs were produced with 0.2g of ammonium nitrate. It was noted that high iron samples were only partially oxidised during the fusion process. The international rock standard MRG-1, containing 8.26% Fe_2O_3 and 8.63% FeO gave an experimental "loss" of 1.24% instead of the expected 1.019% if all the FeO had been oxidised to Fe_2O_3 and S to SO_3. Other examples are given in Table 2:3.

It should be noted that S is present in the form of sulphide minerals in most fresh igneous rock types and as sulphide, sulphate or sulphite minerals in sedimentary rocks.

Bower and Valentine (1986) used 0.2g ammonium nitrate as an oxidant in 10g fusion discs with flux:sample ratios ranging from 50:1 to 3.5:1, however no iron, loss on ignition or loss on fusion data was reported. If the latter samples were ignited prior to fusion this small amount of ammonium nitrate would be sufficient to complete the oxidation process.

In the Norrish and Hutton (1969) fusion technique, the rock samples are ignited at temperatures between 850°C - 1000°C and then fused using sodium nitrate to ensure complete oxidation. Willis (pers.comm) reports that roasting at these temperatures results in the oxidation of at least 85% of FeO to Fe_2O_3, depending on quantity of sample, length of time ignited and oxidation conditions in the furnace.

In the low dilution fusion technique all the oxidation takes place during the fusion process and consequently there must be sufficient oxidant to ensure that complete oxidation occurs. Investigations into the effectiveness of various oxidants were carried out. A basalt containing 15.11% FeO, determined by titration (Appendix B), was used. Several fusion discs were produced using different nitrates in differing proportions, Table 2:4. The amount of unoxidised FeO remaining in the fusion discs was determined by titration. The data in Table 2:4 illustrates that ammonium nitrate is a less effective oxidant than lithium or sodium nitrate. As already mentioned, sodium nitrate was not considered as an oxidant as the discs were to be analyzed for sodium.

Further tests were carried out on a basalt containing 10.7% FeO using lithium nitrate as the oxidant. The "gain on fusion" values for the rock ranged between 0.52% - 0.61%. The sample,

after roasting for 8 hours at 950°C, had a gain in weight of 0.37%. The roasted sample was then fused and an additional gain of 0.17% was recorded, which increased the total gain in weight of the roasted sample to 0.54%, within the range of the fusion

Table 2:3

Comparison of calculated LOI values and experimentally determined LOF values using ammonium nitrate as oxidant.
(data for LOI calculations, Fe_2O_3, FeO, CO_2, H_2O^+, S, F from Govindaraju 1984)

		calculated LOI *	experimental LOF	Iron content Fe_2O_3	Iron content FeO
MRG-1	Gabbro	0.988	1.24	8.26	8.63
PCC-1	Pyroxenite	4.283	4.82	2.85	5.24
GSP-1	Granite	0.424	0.39	1.70	2.32
NIM-G	Granite	0.439	0.51	0.58	1.30

* calculated using the following equations :-

Total volatile loss = $H_2O+ + CO_2 + F$

$Fe_2O_3^{@}$ = FeO value x 1.1113

$SO_3^{@}$ = S x 2.4969

Gain by Oxidation of FeO = $Fe_2O_3^{@} - FeO = Fe^{ox}$

Gain by Oxidation of S = $SO_3^{@} - S = S^{ox}$

Calculated LOI = Total volatile loss - Fe^{ox} - S^{ox}

values. The data confirmed that igniting samples at 950°C is only about 90% efficient in oxidising FeO.

The addition to the flux-sample mixture of 0.6g $LiNO_3$ as the oxidant was adopted as this ensured complete oxidation. Lithium nitrate is extremely deliquescent so the weighing procedure should be as short as possible to minimize errors and should be carried out in low humidity conditions if possible. Other workers (Lee pers.comm.) have added lithium nitrate in solution form with some success, this method has not been investigated here.

Table 2:4

Comparison of the degree of oxidation of a basalt using different oxidants in differing proportions as shown by percentage of FeO remaining after fusion.
(FeO determined by titration - appendix B)

OXIDANT	%FeO	%OXIDATION
NIL	15.11	0
0.2g NH_4NO_3	1.20-1.04	92-93
0.3g NH_4NO_3	0.44	97
0.4g NH_4NO_3	0.40	97.3
0.2g $NaNO_3$	0.48	96.8
0.2g $LiNO_3$	0.20	98.7
0.4 $LiNO_3$	0.12	99.2
0.6g $LiNO_3$	0.08	99.5

Loss on Fusion

The "loss" from a sample during the fusion process represents the difference between the physical loss in weight from the evolution of volatiles (H_2O, CO_2, F) and the gain in weight by the oxidation of reduced species, namely Fe and S.

Complete oxidation (see earlier), coupled with FeO determinations allows the calculation of the volatile content of the rock. A loss on fusion technique has been adopted to determine the percentage of volatiles in the rocks because the simple roasting technique normally employed in the Geochemistry Department, U.C.T. did not always breakdown the refractory minerals and remove all the volatiles in certain rock types.

The sample powders and lithium nitrate were dried at 110°C and the flux at 450°C prior to fusing and weighing. The fusion method is outlined in Table 2:1(b). The volatile loss and oxygen gain by the mixture of sample, nitrate and flux was determined by weighing cold mixture before and after fusing at temperatures between 1050 - 1100°C. The loss from the flux was determined by fusing dried flux and the loss from the lithium nitrate is determined by calculation, as the lithium remains as lithium oxide. The calculation procedures involved in determining the loss on fusion values are detailed in Appendix A.

The computer program MATH/1000 (Comprog 1981-1984) was used to generate a spread sheet to calculate the loss on fusion values for the individual samples. These data including the dilution ratios are reported in Appendix A.

Comparison of experimentally determined LOI and LOF values are given in Table 2:5 (a) and the duplication of LOF values for two

discs of the same rock are given in Table 2:5 (b) for fusion discs made using ammonium nitrate as oxidant. The agreement between the results of the two methods for international rock standards indicates that LOF is an acceptable method for determining the "loss" from a rock sample. The high relative difference for S-7 in Table 2:5 (a) could be related to the higher iron content of this sample compared to other examples. The incomplete oxidation of FeO to Fe_2O_3 by ammonium nitrate was discussed earlier.

Table 2:5(a)

Comparison of experimentally determined LOI and LOF using ammonium nitrate as oxidant. (wt.%)

	Expt. LOI + H_2O^-	Expt. LOF + H_2O^-	Rel. Diff %
S-7 kimberlite	11.78	11.21	4.84
S-8 carbonatite	39.41	39.38	0.08
S-11 magnesite	48.89	48.82	0.14
S-15 serpentinite	16.09	15.98	0.68

Table 2:5(b)

Duplication of LOF values using ammonium nitrate as oxidant. (wt.%)

Sample	Disc A	Disc B	Rel. Diff. %
NIM P pyroxenite	-0.37	-0.39	5.40
PK2/19 lamproite	1.17	1.17	0.00
K2/6F kimberlite	13.49	13.01	3.56

Comparison of LOF values using lithium nitrate as oxidant and calculated loss/gain values from published international standards data are reported in Table 2:6. The loss/gain values were calculated using equations as given in Table 2:3.

The deliquescent nature of lithium nitrate can lead to poor duplication of LOF values. Experiments indicated that the best duplication was achieved on days of low humidity. The duplication of LOF values using lithium nitrate are reported in Table 2:7.

Table 2:6

Comparison of LOF values using lithium nitrate as oxidant with calculated loss/gain values from international standards data. (Govindaraju 1984)

	Loss (H_2O+,CO_2,F)	Gain Fe+S*	Total Loss-Gain calculated	LOF	Rel. Diff.% (calc-meas)
MRG-1	2.06	1.05	1.01	0.95	-5.94
BCR-1	0.85	1.05	-0.20	-0.16	-20.0
BHVO-1	0.31	0.99	-0.68	-0.74	- 8.8
NIM-N	0.87	0.94	-0.07	-0.02	-71.4

S* corrected for gain in weight by oxidation of S to SO_3
Data reported in weight percent

Table 2:7

Duplication of LOF values using lithium nitrate as oxidant.
(wt.%)

sample		Disc A	Disc B	Rel. Diff.(%)
CKP 9	kimberlite	12.94	13.01	1.16
PK20/1	lamproite	4.90	4.78	2.45
PK20/2	lamproite	1.57	1.62	3.18
NIM-L	lujavrite	2.71	3.02	11.43
NIM-D	dolerite	-0.39	-0.30	23.07

Problems did occur with the quantification of LOF values as the use of lithium nitrate as an oxidant resulted in the retention of sulphur contained in the rock samples probably as sulphate (SO_4^{2-}). It was also noted that several of the lamproite samples tended to gain moisture rapidly when exposed to the atmosphere. This is discussed in detail later.

Retention of Sulphur

The use of fusion discs for X-ray fluorescence analysis has proven very successful for a wide variety of sample types. A major problem is still encountered with sulphide-rich rocks. During the fusion process sulphur is liberated and platinum ware can undergo sulphide attack depending on the oxidising conditions. Baker (1982) tested a variety of fluxes and nitrates to determine their ability to quantitatively retain sulphur during the fusion process and to prevent sulphide attack on the platinum ware. Results showed that temperature and time of fusion are very important factors and that sulphur can only be

retained in its highest oxidation state as a sulphate (SO_4^{2-}). The following flux mixtures were found to be suitable:

1. 80% $Na_2B_4O_7$
   20% Na_2O_3

2. 80% $Li_2B_4O_7$
   20% $LiNO_3$

3. 80% $Li_2B_4O_7$
   20% $CsNO_3$

The flux used in the low dilution fusion disc method (this study), is similar to the second flux of Baker's (1982), except for the $LiNO_3$ content.

Preliminary results on low dilution discs indicate that sulphur was retained, probably semi-quantitatively but reproducibly, using 0.6g (9 %) of lithium nitrate as an oxidant. A kimberlite sample, S-7, shows similar net counts per second for S K_a for four different spiked fusion discs. A lamproite and a kimberlite sample also show similar net counts per second for S K_a for duplicate discs. This data is summarized in Table 2:8.

Joslin and Salt (1985) investigated the retention of sulphate sulphur in barytes. They prepared two discs containing the same amount of SO_4^{2-} using ammonium sulphate and barium sulphate and found that there were no significant differences in measured intensities for sulphur. The retention of sulphur in the low dilution fusion discs is dependent on whether the oxidant is strong enough to completely and rapidly oxidize to sulphate the sulphur present in sulphide minerals prior to sulphur being volatilized as SO_2. Work was carried out on sulphide-rich rocks but the mixture was very viscous and difficult to pour.

Table 2:8

Comparison of sulphur net intensities obtained from low dilution fusion discs.

	Sulphur Net Intensity c.p.s.
S-7	1140
S-7 5%TiO_2	1159*
S-7 10%TiO_2	1174*
S-7 5% BaO	1104*
K4/423 F	123.5
K4/423 F B	123.7
PK16/8	215.4
PK16/8 B	206.9

* corrected for addition of TiO_2 + BaO

Sulphur determination.

The reproducibility of the sulphur counts for duplicate samples suggested that sulphur could be standardized using the intensities from the low dilution fusion discs. Analytical conditions for the determination of sulphur by XRF spectrometry are reported in Table 4:1. The calibration curve is presented in Figure 2:1. Unfortunately only three of the international standards analyzed contained sulphur. The data from the low dilution fusion discs are compared to the international standards data in Table 2:9.

Figure 2:1 Calibration curve for sulphur analysed by XRFS on low dilution fusion discs.

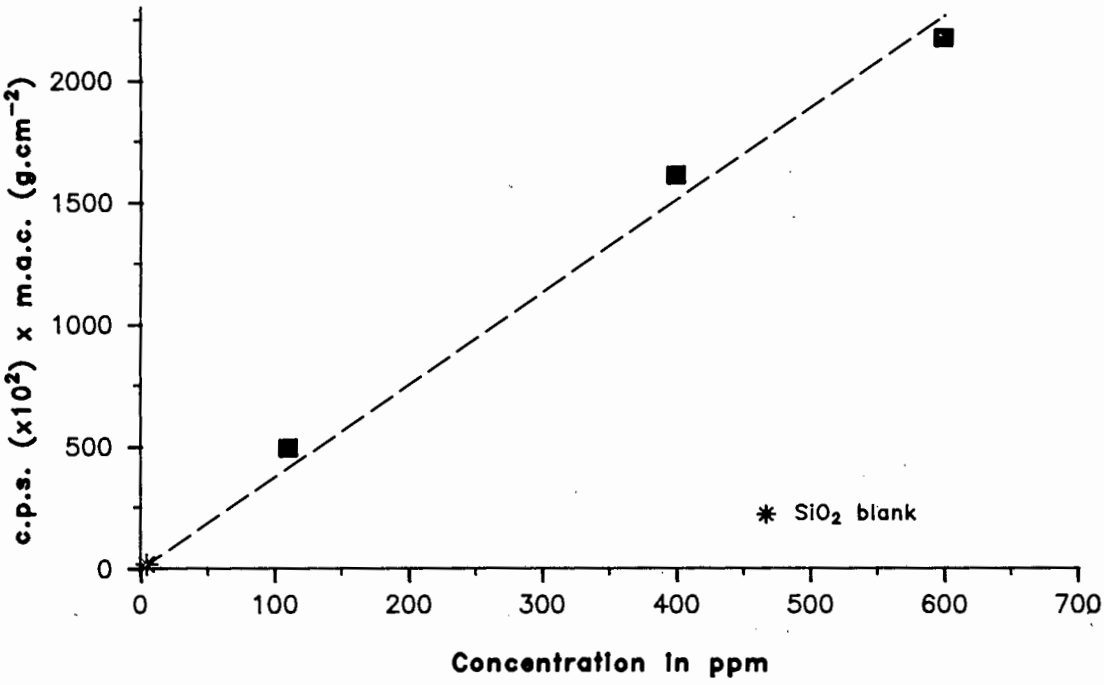

Table 2:9

Comparison of recommended international standards data for S with data obtained from LDF discs. (standards data from Govindaraju 1984)

	Int. Std. Data (ppm S)	LDF Data (ppm S)	Rel. Diff. (%)
BCR-1	400.	435.	+8.8
BHVO-1	110.	133.	+20.9
MRG-1	620.	588.	-5.2

To confirm the sulphur data several lamproite and kimberlite samples were sent to the Geological Survey, Pretoria where sulphur was determined using a LECO sulphur analyzer. In addition several fusion discs were also analyzed for sulphur using the LECO analyzer. The results are detailed in Table 2:10.

Table 2:10

Sulphur concentrations in powders and fusion discs of selected lamproite and kimberlite samples determined by LECO sulphur analyzer.
(Geol. Survey, Pretoria)

	Powder sample % S	Fusion disc % S	Diff. % (powder-fusion)
CKP 9	.602	.512	-14.9
MAIN 15/1	.201	.045	-77.6
PK7/2	.149	.018	-87.9
PK9/4	.006	<.003	-50.0
PK2/19	.076		
PK3/3	.035		
PK9/1	.005		

The agreement of the sulphur concentrations in the fusion discs with that in the powders detailed in Table 2:10 is extremely poor. These poor results of sulphur concentration in the fusion discs from the LECO analyzer at the Geological Survey, Pretoria could be due to either inhomogeneity of the sulphur distribution within the fusion disc or the fact that the LECO analyzer can not accurately determine sulphate sulphur. Using the calibration curve in Figure 2:1 for sulphur analyzed on the low dilution fusion discs by XRFS there seems to be relatively good agreement with the sulphur concentrations obtained from the LECO analyzer on powders. Powder pellets of the lamproite and kimberlite samples were also analyzed for sulphur and calibrated using the data from the LECO analyzer (Geol. Survey). These results are compared in Table 2:11. The analysis of sulphur on powder

pellets by XRF spectrometry is difficult as sulphur can be affected by mineralogical and chemical effects as discussed earlier, depending on whether the sulphur is present as a sulphide or sulphate. The powder pellets are also contaminated with sulphur from backstreaming of oil vapour from the vacuum pump each time they are analyzed in an XRF spectrometer.

The determination of sulphur in the LDF discs requires further investigation. It should be noted that the use of a fusion disc for sulphur analysis eliminates mineralogical and chemical effects.

The data in Table 2:11 show reasonable agreement for sulphur determined by XRFS on the powder pellets and the low dilution fusion discs. These two sets of data were generated using different standards and calibration curves.

Table 2:11

Comparison of Sulphur data from LDF discs and powder pellets (XRFS) and powders analyzed on LECO analyzer (Geol Survey).
(in wt percent)

	S (LECO)	S (XRFS) LDF*	S (XRFS) Pellets**
CKP 9	.602	.598	.612
MAIN 15/1	.201	.239	.145
PK2/19	.076	.102	.098
PK7/2	.149	.189	.165
PK3/3	.035	.053	.056
PK9/4	.006	.022	.019
PK9/1	.005	.014	.014

* standards used as detailed in Table 2:9
** standard used was Allende containing 21000ppm S

Determination of H_2O+, CO_2 and FeO content of lamproite and kimberlite samples.

To confirm that the LOF values represent the loss of H_2O+ and CO_2, and gain by oxidation of reduced species (FeO and S) some of the lamproite and kimberlite samples were analyzed for H_2O+ and CO_2 and FeO content to see if a mass balance was achieved.

A HP 185B Carbon-Hydrogen-Nitrogen analyzer was used to determine the H_2O+ (water chemically bound in minerals) and CO_2 in the rocks (Appendix B). FeO content was determined by titration (see later section). The results for the lamproite and kimberlite samples are reported in Appendix G.

The results for several of the lamproite and kimberlite samples are presented in Table 2:12. On examination of the data it is obvious that there are discrepancies between the LOF, and total H_2O+ and CO_2 data. The LOF values have not been corrected for gain in weight by oxidation of Fe and S and the data presented in Table 2:12 indicates that the oxidation gain can not account for the differences.

Skinner (1980) showed that these samples contain up to 50% devitrified glass consisting of abundant clay minerals and it is possible that these absorb moisture rapidly from the air. In a simple experiment an accurately weighed and sample (dried at 110^{o}C) of PK20/1 gained approximately 3% of its weight in half an hour when left in a watch glass on a bench. Consequently some of the differences in the values in Table 2:12 may be attributed to the uptake of moisture by the sample from the atmosphere.

Table 2:12

Comparison of LOF and H_2O+ and CO_2 data with total Fe_2O_3 and S values.

sample	HP 185B Total CO_2+H_2O+ (%)	XRFS S (ppm)	Gain by S (%)	Total Fe as FeO(%)**	Gain by Fe (%)	Total - gain	LOF
PK13/2	4.49	105.	.016	6.36	0.71	3.76	2.65
PK12/2	5.50	118.	.018	6.58	0.73	4.75	4.11
PK12/1	5.63	35.	.005	7.99	0.89	4.73	4.31
PK11/1	4.20	151.	.023	6.07	0.68	3.49	3.20
PK20/1	7.11	182.	.027	6.91	0.77	6.31	4.90
PK19/2	2.56	176.	.026	7.68	0.86	1.67	2.80
PK9/3	2.76	718.	.107	6.57	0.73	1.92	2.20

** maximum gain in weight if all Fe was FeO

In an attempt to clarify the problems encountered, the samples detailed in Table 2:12, were analyzed for H_2O- and H_2O+ at the Geological Survey in Pretoria (Table 2:13) in order to confirm the U.C.T. data. However this data further confused the issue.

The H_2O+ data from the Geological Survey was only determined at only 755°C and in the technique used the heating is very rapid and of short duration (less than 6 minutes per sample).

Consequently the seven lamproite samples were dried at 110°C, weighed and then ignited at 750°C for eight hours, then cooled, reweighed and ignited at 850°C for a further eight hours. The results of this procedure are presented in Table 2:14.

Comparison of the data in Table 2:14 with that reported in Table 2:13 indicates that not all the H_2O+ was removed from the rock samples at 755°C in the Geological Survey method. The LOF values reported in Table 2:12 are in closer agreement with the LOI values in Table 2:14.

Table 2:13

H_2O^- and H_2O^+ data for several lamproites analyzed at Geol. Survey, Pretoria. (in wt. percent)

	H_2O- (110°C)	H_2O+ (755°C)
PK13/2	2.23	2.03
PK12/2	2.59	3.27
PK12/1	2.96	3.37
PK11/1	2.49	1.84
PK20/1	2.79	3.42
PK19/2	1.84	2.20
PK9/3	0.97	1.44

Table 2:14.

Loss on ignition data for lamproite samples, data reported at 750°C and 850°C.(in wt. percent.)

	Loss at 750°C	Additional loss at 850°C	Total loss at 850°C	LOF
PK13/2	2.40	0.83	2.73	2.65
PK12/2	2.47	0.41	3.88	4.11
PK12/1	3.44	0.30	3.74	4.31
PK11/1	2.15	1.00	3.15	3.20
PK20/1	4.00	0.84	4.84	4.90
PK19/2	2.45	0.30	2.75	2.80
PK9/3	1.62	0.46	2.08	2.20

The brief discussion above highlights the problems encountered in the determination of volatiles in geological samples. The three methods investigated (Table 2:12, 2:13 and 2:14) all yielded significantly different results and further detailed work is required to quantify the losses and gains which occur during the sample preparation and fusion processes.

FeO Determinations.

The amount of FeO in 3 of the lamproites was determined by titration (Appendix B). The results are reported in Table 2:15. The data for FeO content of the two kimberlites MAIN 15/1 and CKP 9 are taken from Smith (in press).

Table 2:15

FeO content of lamproites and kimberlites, determined by titration and gain in weight due to oxidation of FeO to Fe_2O_3. (in wt. percent)

	FeO	Gain by oxidation to Fe_2O_3
PK20/1	1.14	0.127
PK20/2	2.18	0.243
PK12/2	0.74	0.082
CKP 9	5.55	0.617
MAIN 15/1	3.20	0.356

Mass balance calculations involving CO_2, H_2O+, FeO and S content of some of the lamproite and kimberlite samples were performed. Several examples are detailed in Table 2:16.

The data presented in Table 2:16 appear to support the hypothesis that sulphur is retained as sulphate quantitatively during the fusion process. The data in Table 2:16 suggest that mass balance was achieved. The average relative difference between the calculated "loss" and the LOF value corrected for the oxidation of FeO and S was less than 2.1%. Further investigation is required in this direction to confirm that the sulphur is completely retained.

Table 2:16

Comparison of calculated "loss" and LOF values corrected for the oxidation of FeO and S. (data in wt. percent)

	CKP 9 kimberlite	MAIN 15/1 kimberlite	PK20/2 lamproite
FeO content	5.55	3.20	2.18
Gain by Fe*	0.62	0.36	0.24
S content	0.60	0.20	0.10
Gain by S*	0.898	0.299	0.149
$H_2O+ + CO_2$ (Total loss)	14.67	12.98	2.03
Total loss − Gain by Fe + S (calculated "loss")	13.15	12.32	1.64
LOF	12.94-13.01	12.84	1.57-1.62

* assuming complete oxidation to Fe_2O_3 and SO_3

Loss of volatile elements

Volatile elements, K, Rb, Pb, Na, Al, P and Zn, may be lost during the fusion process. According to Maessen and Boumanns (1968) the evaporation behaviour of these elements is dependent on the chemical composition of the sample, added reagents and the mineralogical location of the element. An element mechanically mixed into a matrix as an oxide is less stable than an element located in a lattice position in a mineral. Their experiments showed that a synthetic mixture of volatile elements lost volatile trace elements at lower temperatures than natural samples.

Data obtained by Gurney (1968) for four kimberlite samples (KDB 9, KBEL 2, KDT 24, KDT 28) indicated that potassium was lost either during the roasting or fusion process. This was confirmed by Gurney (1968) as the samples were analyzed by whole rock pellet using XRFS and by Atomic Absorption analysis. The potassium data is detailed in Table 2:17. Gurney (1968) noted that during the roasting stage a brown gas was emitted by the samples that damaged the furnace lining. During the preparation of the low dilution fusion discs no trace of any coloured gas was seen. Data obtained from low dilution fusion discs are also presented in Table 2:17 for comparison. These data indicate that potassium was not lost during the low dilution fusion process. It is thought that the brown gaseous phase observed by Gurney (1968) was responsible for the loss of potassium.

Other data obtained for low dilution fusion discs confirm that none of the other volatile elements have been lost during the fusion process. If volatiles trace elements such as Rb had been lost, one would expect non-linear calibration curves. The only

element that presents problems in this direction is lead and this is discussed later.

Table 2:17

Comparison of potassium data obtained by XRFS and AA (Gurney 1968) and by the Low Dilution fusion technique.
Data reported in wt. % K.

	Whole Rock Pellets XRFS	Norrish Fusion XRFS	Atomic Absorption	LD Fusion XRFS
KDT 24	0.96	0.62	0.92	0.98
KDT 28	1.31	0.95	1.27	1.29
KDB 9	1.20	0.92	1.20	1.27
KBEL 2	1.59	1.36	-	1.71

Fluorine

Fluorine can be detected by XRFS using a PX-1 analyzing crystal. Normally during the fusion process fluorine, a volatile element is lost. Tests were carried out to confirm whether fluorine had been retained in the low dilution fusion discs. The wavelength scan in Figure 2:2 (a) shows the fluorine peak at 42.99° 2θ in a pressed powder pellet of SY-3, a syenite containing 6600 ppm fluorine (Abbey 1986). In Figure 2:2 (b) a wavelength scan from a low dilution fusion disc of SY-3, the F peak is absent and this clearly indicates that fluorine was lost during the fusion process. A wavelength scan of a lamproite sample, Figure 2:2 (c) also indicates that F was not present in the fusion disc.

Figure 2:2. Wavelength scans showing position of Fluorine.

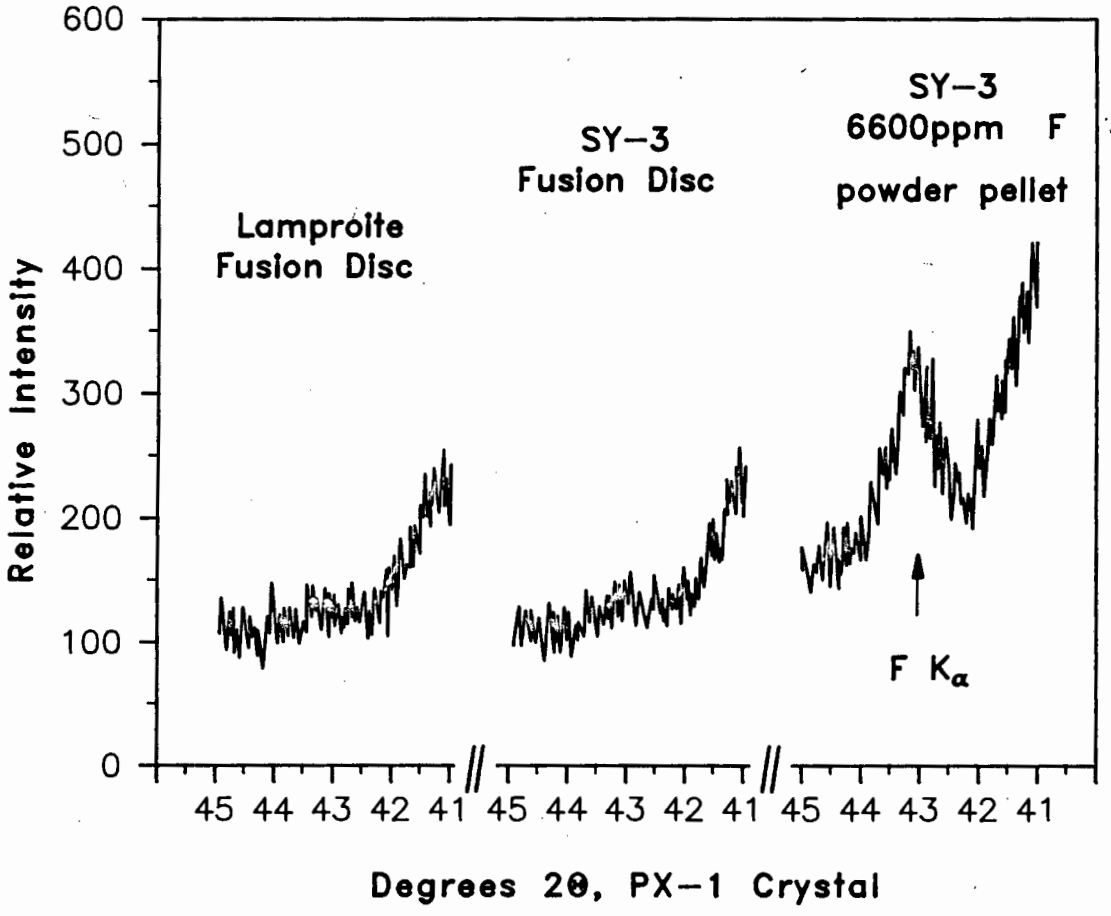

Summary

The 2:1 flux:sample ratio used in this low dilution fusion technique was sufficient to produce homogeneous glass discs for blanks, artificial standards and samples for XRF spectrometric analysis.

The use of a flux that does not contain a heavy absorber means that the composition of the flux from one batch to another will remain relatively stable resulting in the standards being used many times. The analytical surface of the fusion disc discs may be easily cleaned (acetone wash) something that can not be done to powder pellets.

Data presented here indicate that the loss on fusion values using lithium nitrate as an oxidant are difficult to quantify. The retention of minor concentrations of sulphur as sulphate can lead to serious loss/gain and interelement correction errors. Further work on the retention of sulphur in the fusion discs is required if the loss on fusion method is to be employed to determine the volatile content of rocks. The calculations detailed in Table 2:16 tend to support the hypothesis that sulphur is retained as sulphate and that complete oxidation of S to SO_3 occurred.

The uptake of moisture from the atmosphere by some of the lamproites is difficult to control. Despite constant use of a desiccator some of the samples (e.g. PK20/1) gained moisture during the weighing procedure as shown by a continually increasing mass while on the balance pan, making accurate weight mesurements impossible.

CHAPTER 3

TRACE ELEMENT ANALYSIS

TRACE ELEMENT ANALYSIS

Introduction

In trace element analysis it is important to note that correcting the net intensity data for absorption differences between samples and standards, eg. by a method such as Compton scattering, does not compensate for spectral line overlaps and fluorescence enhancement. The raw intensity data obtained for all the analytical runs (major and trace element) were corrected for instrumental drift, dead time, backgrounds, spectral line overlap, and tube peak interference, where necessary, using the program TRACE (written by A.R.Duncan). Background corrections were made by measuring the intensity at peak and interference free spectral positions and calculating background factors from intensity measurements at these spectral positions on fusion discs made from flux + Specpure SiO_2 or Al_2O_3 ("blank" samples) Spectral line interferences were corrected for by calculating interference correction factors from intensity measurements made on specially prepared "interference standards" containing 2000ppm of a single relevant Specpure oxide. An iterative procedure was applied in cases where spectral line interference involved 2 or more elements. Corrections for the concentrations of Ni and Cu in the Au X-ray tube and Cr in the W X-ray tube were made using "blank" samples and correction factors calculated by either ratioing the net tube impurity peak to the measured intensity of a primary tube peak (eg. Au L_a for the Au X-ray tube) or the net tube peak to the mass absorption coefficient of the sample (eg. for W X-ray tube).

Differences in the absorption of the samples where corrected using either the Compton scatter method (Reynolds 1963) or mass

absorption coefficients calculated from the major element compositions. Prior to processing the samples, net intensities were obtained for standards from TRACE and appropriate calibration curves were prepared to check the linearity of the calibration curve. Recommended concentrations for international standards (Govindaraju 1984, Abbey 1986) were plotted against (net intensity x m.a.c) to obtain calibration curves.

Data for some lamproite and kimberlite samples obtained by INAA (Fraser et al. 1986, Smith (pers. comm)) are compared to data obtained by this low dilution fusion method.

Table 3:1

Analytical conditions for the determination of mass absorption coefficients using the Molybdenum K_a Compton peak, on a Philips PW1220 XRF spectrometer.

- Mo X-ray tube, 70 kV, 28 mA
- LiF (220) analyzing crystal
- Compton peak angle 29.95°2θ
- Fine collimator
- Scintillation counter
- Pulse Height window - upper level 700
- lower level 300
- standards with a range of mass absorption coefficients (see Table 3:2)

MASS ABSORPTION COEFFICIENTS

Variations in the mass absorption coefficients of substances are of critical importance in XRFS because :

$C = K \times I \times (\mu/\rho)$ where C = concentration

K = slope of the calibration curve

I = intensity

μ/ρ = total mass absorption coefficient (primary and secondary)

Mass absorption coefficients, at the Mo K_a wavelengths, for the low dilution fusion discs were determined using the Mo K_a Compton peak intensity. Compton peak intensities for standard rock samples were calibrated against m.a.c.s values which had previously been determined by the transmission method. The analytical conditions are summarized in Table 3:1. The use of Compton scattered radiation for m.a.c. determinations has been well documented in the literature, (e.g.Reynolds,1963). The Compton scatter intensity is a measure of the average atomic number of a sample, which is directly related to the mass absorption coefficient. Compton scatter intensity is inversely proportional to mass absorption coefficient (μ/ρ).

The m.a.c.s measured at MoK_a are normally used to correct for matrix differences between samples for the following elements - Mo, Nb, Zr, Y, Sr, U, Rb, Th, Pb, Zn, Cu and Ni. MoK_aCompton m.a.c.s can be used here, as these elements have shorter analyte wavelengths than the $FeK_{abs.edge}$ at 1.743 Å. The MoK_aCompton m.a.c.s for the low dilution fusion discs were determined using

pressed powder pellets as standards. Comparison of the standards data are given in Table 3:2.

If the element of interest is present in minor (0.5-1.0%) to major (>1.0%) concentrations care must be taken to choose the correct mass absorption coefficient. For minor concentrations of Sr for example, the m.a.c. determined by the MoK_a Compton peak method is incorrect and a m.a.c. at a wavelength longer than the $SrK_{abs.\ edge}$ (0.77 Å) and shorter than the $FeK_{abs.\ edge}$ (1.743 Å) should be used. The high Sr concentrations of the lamproite and kimberlite samples necessitated the use of m.a.c.s calculated from major element compositions at the RbK_a wavelength to correct matrix differences of the samples and standards for the elements Zr, Y, Sr, U, Rb, Th and Pb.

Table 3:2

Comparison of standard and calculated Mo mass absorption coefficients for powder pellets using the Compton scatter method at the Mo K_a wavelength.

Standard	std value	calc value	Rel. Error %
MRG-1	9.30	9.31	0.11
NIM-D	7.48	7.43	0.67
NIM-G	4.50	4.50	0.00
NIM-N	6.71	6.70	0.15
NIM-S	5.43	5.40	0.55
G-2	4.85	4.90	1.03
GSP-1	5.38	5.36	0.37
BCR-1	7.59	7.66	0.93

Primary and secondary m.a.c.s are used to correct matrix differences between the samples for the following elements - Cr, V, Co, Ba, Sc, La, Ce, and Nd. The analyte lines used to determine these elements lie between the Fe K and Ca K

absorption edges. The total m.a.c.s of the samples are calculated using the following relationship :

$$\text{Total m.a.c} = \mu_{primary} + 1.347 \times \mu_{secondary}$$

where 1.347 = geometric constant ($\sin\psi_1 / \sin\psi_2$) spectrometer dependent

μ_{pri} = m.a.c. of matrix element for wavelength in primary beam (absorption of incoming radiation).

μ_{sec} = m.a.c. of same matrix element for secondary wavelength (absorption by the sample matrix of the emergent radiation).

The combination of primary and secondary m.a.c.s used for these elements are listed in Table 3:3.

The m.a.c.s at Rb, La, Ce, K, V, Cr, Sc analyte wavelengths (Tables 3:4, 3:10, 3:13, 3:16, 4:1) used for the accurate determination of Zr, Y, Sr, U, Rb, Th, Pb, Cr, V, Co, Ba, Sc, La, Ce and Nd were calculated for the standards and samples using a routine in the computer program, MATH/1000 (COMPROG 1981-1984). This program was used to generate a spreadsheet (FUSMAC, detailed in Appendix C) to calculate the m.a.c.s. Input to the spreadsheet included the m.a.c.s of the flux components and major element oxides at the various wavelengths and the major oxide data of the samples including any "trace" elements existing in minor to major concentrations. Mass absorption coefficients were taken from Jenkins et al. (1970). The m.a.c.s of the flux at the required wavelengths were calculated as detailed in Appendix C.

The m.a.c.s of the pure samples at for example RbK_a, prior to dilution by the flux, are calculated from the product of the weight fraction of the elements in the samples and the appropriate m.a.c. at the exciting wavelength. An example of this is given in Appendix C.

Table 3:3

Primary and secondary m.a.c.s. used to correct for matrix differences for elements with wavelengths between the Fe and Ca K absorption edges.

Element	$\mu_{primary}$ wavelength	$\mu_{secondary}$ wavelength
Co	Rb K_a	Cr K_a
Cr	Rb K_a	Cr K_a
V	Rb K_a	V K_a
Ce	Rb K_a	Ce L_b
Nd	Rb K_a	Ce L_b
La	Rb K_a	La L_a
Ba	Cr K_a	Sc K_a
Sc	Cr K_a	Sc K_a

Table 3:4(a)

Analytical conditions for the determination of Mo, Nb, Zr, Y, Sr, U, Rb, Th and Pb in the Low Dilution Fusion discs using a Philips PW1400 XRF spectrometer with a W X-ray tube at 50 kV, 55 mA, and a LiF (200) analyzing crystal.

Coll = collimator Det = detector UPL = PHA upper window level LWL = PHA lower window level

Element, Line and order	Time (s)	Coll	Det	UPL	LWL	peak ($^{o}2\theta$)	background +off* ($^{o}2\theta$)	background -off* ($^{o}2\theta$)
Mo K_a (1)	80	Fine	SC	68	35	20.335	0.64	1.84
La K_a (2)	80	Fine	SC	68	35	21.240	-	1.24
Nb K_a (1)	120	Fine	SC	68	35	21.400	-	-
Zr K_a (1)	80	Fine	SC	68	35	22.555	-	-
Y K_a (1)	80	Fine	SC	68	35	23.815	0.80	0.64
Sr K_a (1)	80	Fine	SC	68	35	25.175	0.62	-
U L_a (1)	80	Fine	SC	68	35	26.185	-	-
Rb K_a (1)	80	Fine	SC	68	35	26.640	-	-
Th L_a (1)	80	Fine	SC	68	35	27.515	-	-
Pb L_b (1)	80	Fine	SC	68	35	28.290	1.00	-

Note:

A secondary collimator was positioned in front of the scintillation counter on the PW 1400. This collimator reduced the intensity by about 75% but decreases tailing of the peaks.

For La, peak and background measured with PHA set for second order

Counting times on background positions were 40 seconds

Samples analyzed under vacuum.

The following background positions were used :-

Mo	-	Mo-, Mo+
La	-	La-
Nb, Zr	-	Mo+, Y-
Y	-	Y-, Y+
Sr	-	Y+, Sr+
U, Rb, Th, Pb	-	Sr+, Pb+

* $\pm$ background angle offset relative to peak angle

Table 3:4(b)

Possible spectral line interferences on elements, Nb, Zr, Y, Sr U, Rb, Th and Pb using analytical conditions outlined in Table 3:4(a).

Element		Possible Spectral Line Interference
Nb K_a	-	Y K_{b1}, U $L_{b2,4,7}$, Th $L_{b1,3,5}$, La $K_{a1,2}$(2)
Zr K_a	-	Sr $K_{b1,2}$, Th $L_{b2,4,7}$, Pb $L\gamma_4$, U L_{b6} Ba $K_{a1,2}$(2)
Y K_a	-	Pb $L\gamma_{1,2,3,8}$, Rb $K_{b1,2}$, Th L_{b6}
Sr K_a	-	Pb $L\gamma_5$
U L_a	-	Rb K_a
Rb K_a	-	U L_a
Th L_a	-	Pb $L_{b3,5}$
Pb L_b	-	Th L_{a2} La $K_{b1,3}$(3)

Note: interference by adjacent elements on background positions is common.

ANALYTICAL RUN - Nb-Zr-Y-Sr-Rb-U-Th-Pb

The analytical conditions for the determination of these elements are detailed in Table 3:4(a). Possible spectral line interferences are detailed in Table 3:4(b). Pulse height selection is used to reduce interference from higher order spectral lines and reduce backgrounds giving lower limits of detection for trace elements. Mo concentration data are not reported as the lamproite and kimberlite net c.p.s. are all below detection limit.

Wavelength scans from $18^{o}2\theta$ to $33^{o}2\theta$ were carried out to check for any interferences from barium, lanthanum, cerium, and neodymium. A wavelength scan of a fusion disc containing 2% La_2O and 98% SiO_2 is shown in Figure 3:1, the second order K_a peaks of La at approximately 21.25 $^{o}2\theta$ are visible. In addition, several lamproites were scanned to check for any spectral interferences or additional unexpected analyte elements. The wavelength scan in Figure 3:2 indicates an asymmetric peak for niobium K_a. This was investigated further and it was found to be due to second order lanthanum K_{a1} and K_{a2} interfering with niobium K_a. Pulse height selection was obviously not sufficient to completely eliminate the higher order lines. A 2% La_2O + 98% SiO_2 and a 100% SiO_2 fusion disc were scanned with the pulse height analyzer (PHA) set for second order, to show the effect of the La peaks, Figure 3:3. The international rock standard, NIM-L was scanned with PHA set for first order to show the position of Nb $K_{a1,2}$ peaks.

A further interesting feature of the scan is the position of the iodine absorption edge in the second order lying exactly between the LaK_{a1} and K_{a2} peaks. The iodine absorption edge arises from

Figure 3:1. Wavelength scan showing positions of La K lines in in the second and third order.

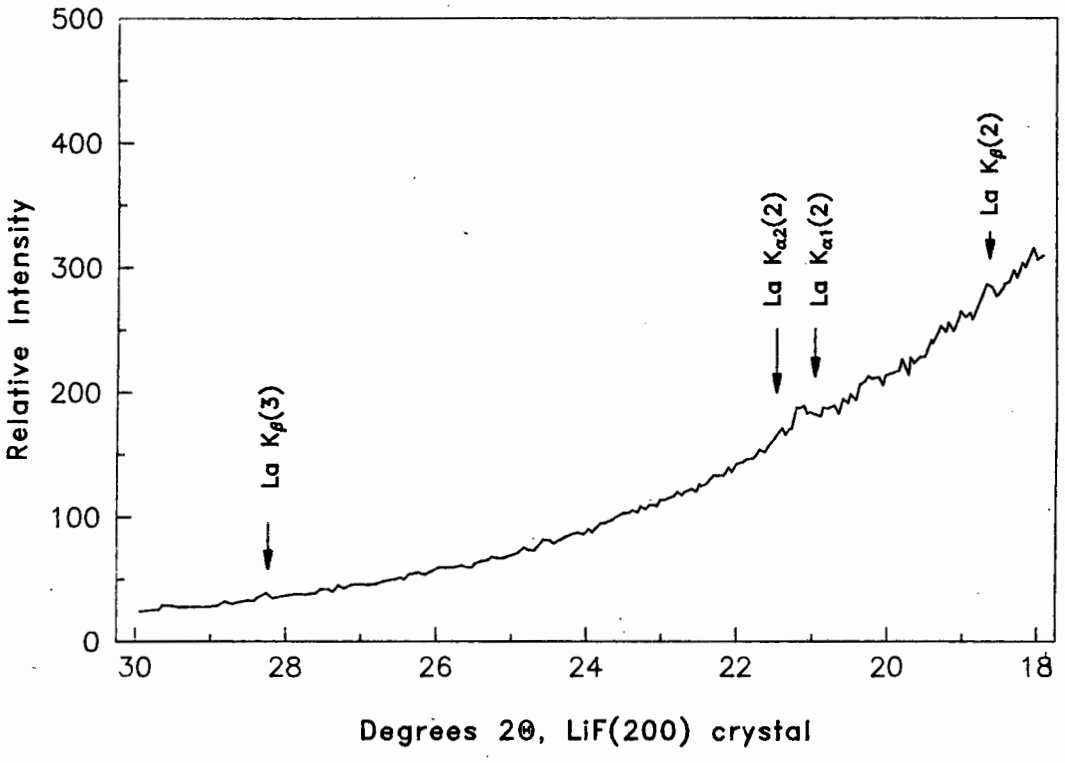

Figure 3:2. Wavelength scan showing position of Nb K_α

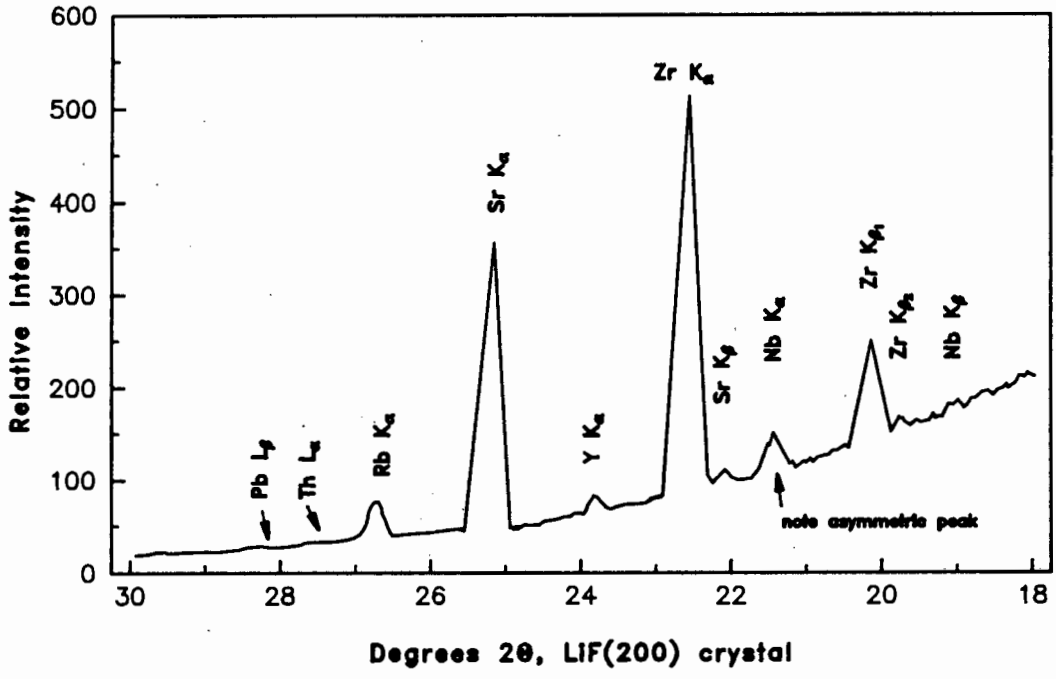

Figure 3:3. Second order La interference on Nb K_α

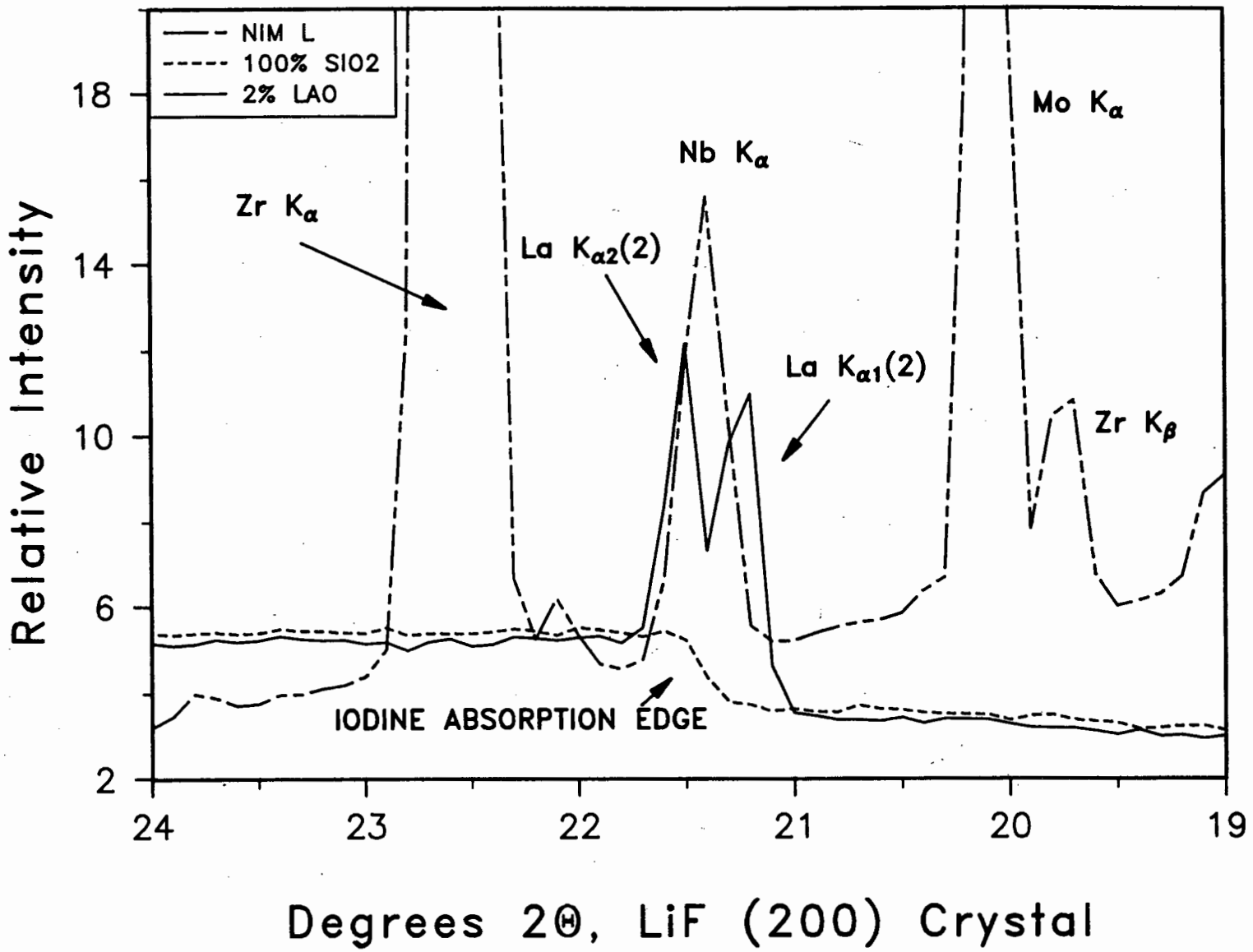

Figure 3:4. Wavelength scan showing position of Ba K lines in the second order.

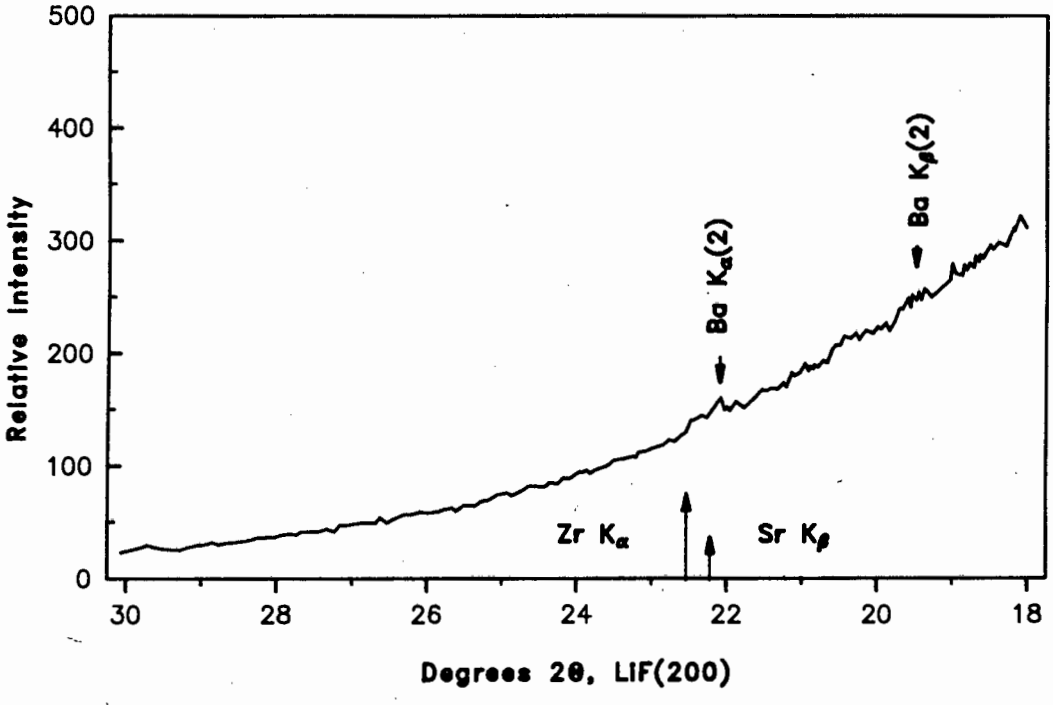

the sodium iodide crystal in the scintillation counter. The effect of this absorption edge is shown by the unusual relative intensity of the two La K_a peaks. Normally the ratio of K_{a1} to K_{a2} is 2:1, but in this instance the ratio is approximately 1:1. Removing the effect of the iodine absorption edge from the K_{a2} peak increases the ratio slightly. This unusual relationship is thought to be due to the absorption of LaK_{a1} by the iodine and the absorbed intensity being partially transferred into an escape peak. To correct for the La interference, LaK_{a1} was measured with the PHA set for second order with one background position on the low angle side to avoid problems of crossing the iodine absorption edge. The fusion discs are not infinitely thick for La K_a radiation but the correction made is only for spectral interference and not to determine La concentrations.

The wavelength scans indicated that $BaK_{a1,2}$ in the second order could be a problem as the peak is very close to ZrK_a. On further investigation it was observed that $BaK_{a1,2}$ in the second order interferes with SrK_b. This is illustrated in Figure 3:4 where the position of ZrK_a is indicated relative to the SrK_b. Net counts per second at the ZrK_a peak position for a low dilution fusion disc containing 2% BaO and 98% SiO_2 are below the detection limit, and consequently for concentrations of BaO of 2% or less in the sample the interference is insignificant and can be ignored.

For this analytical run - Mo, Nb, Zr, Y, Sr, U, Rb, Th, Pb and La interference standards were analyzed. The interference standards contained Specpure SiO_2 and 2000 ppm of the analyte except for the La interference standard, which contained 2% La_2O and 98% SiO_2.

These interference standards are used to correct for analyte line overlap (e.g. RbK_b on YK_a) and "tailing" of analyte peaks on background positions (e.g. SrK_a on background position between SrK_a and RbK_a). Higher concentrations of strontium occurring in the lamproites required the preparation of artificial standards to aid with the calibration of this element. The Geochemistry Department, U.C.T collection of international reference standards does not contain standards with high Sr concentrations. Fusion discs containing 0.5%, 1.0% and 2.0% SrO in Specpure quartz were made. The calibration curve for Sr using Rb m.a.c.s are presented in Figure 3:5 (a) and (b). The 1% and 2% SrO artificial standards do not lie on this curve. These two standards have too low an intensity compared to the concentration. The low intensity is probably due to a combination of three effects. (1) The artificial SrO fusion disc standards may not have infinite thickness for Sr due to the overall low m.a.c. of Specpure SiO_2. (2) The high concentrations of Sr will result in a broader peak and consequently the intensity at the background positions will be elevated due to this "tailing" and a lower net analyte peak intensity will result. (3) The use of interference standards only containing 2000 ppm of the analytes will therefore not have the required effect and could result in incorrect interference corrections and consequently incorrect intensity measurements. These three points require further investigation.

The calibration curve for lead shown in Figure 3:6 (a) indicates that there are severe problems with analyzing Pb by the fusion method. The calibration curve is non linear and does not pass through the origin. In a subsequent analytical run, where La interference on NbK_a was corrected for, the Pb data showed some

Figure 3:5(a). Calibration curve for Sr using Rb m.a.c.s.

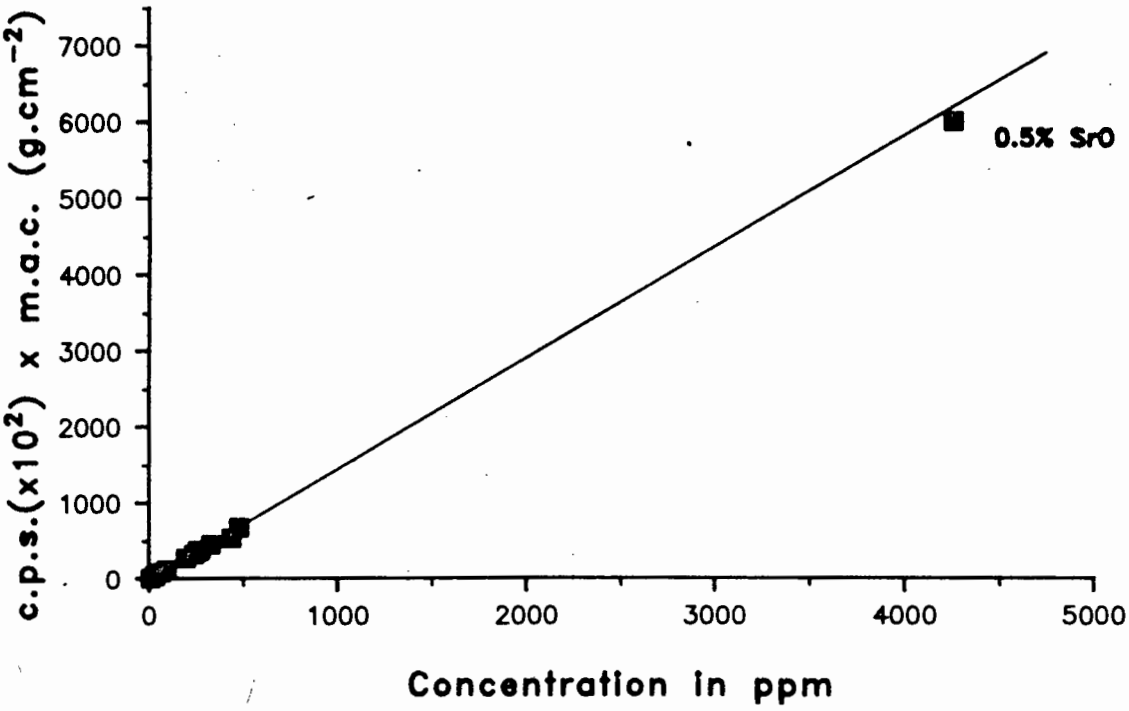

Figure 3:5(b). Calibration curve for Sr using Rb m.a.c.s.

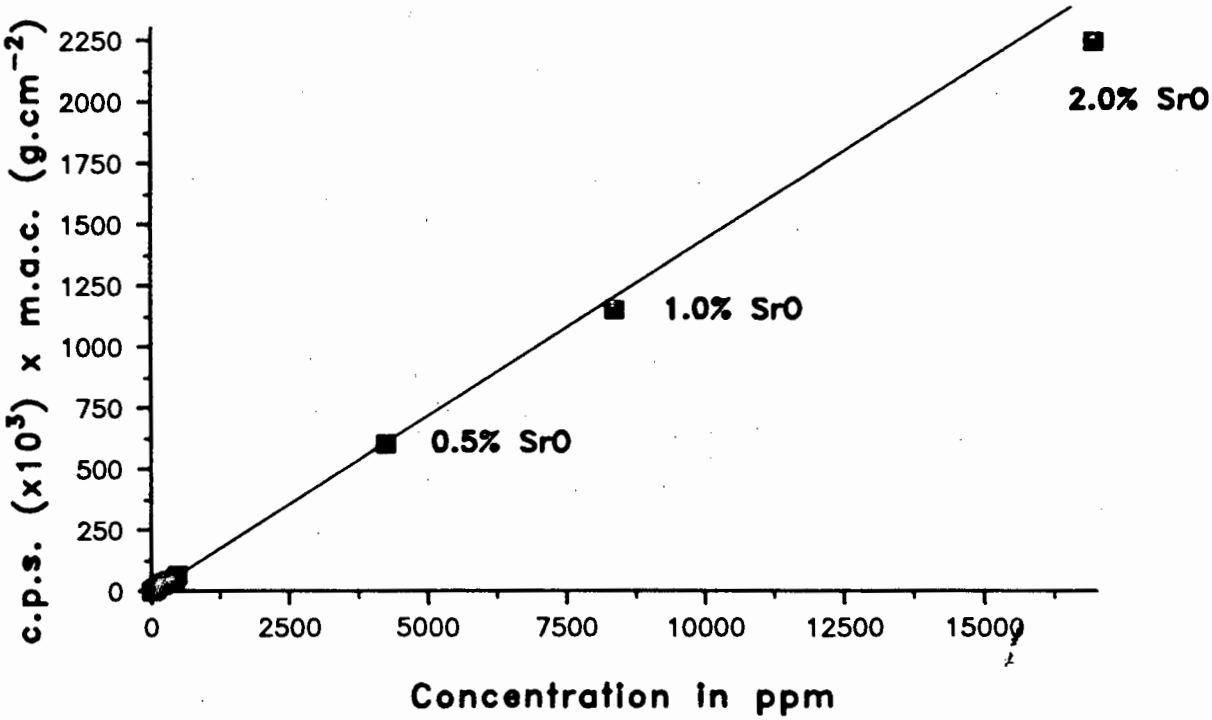

Figure 3:6(a). Calibration curve for Pb using W X–ray tube with no correction for lanthanum.

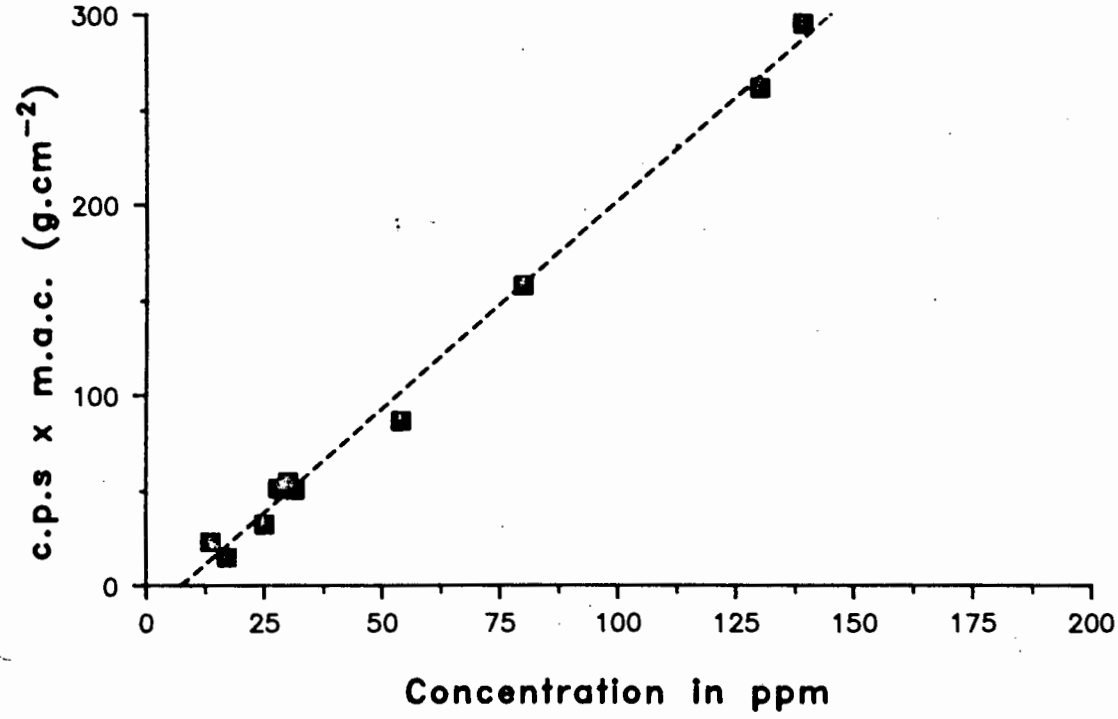

Figure 3:6(b). Calibration curve for Pb using W X–ray tube with correction for lanthanum interference.

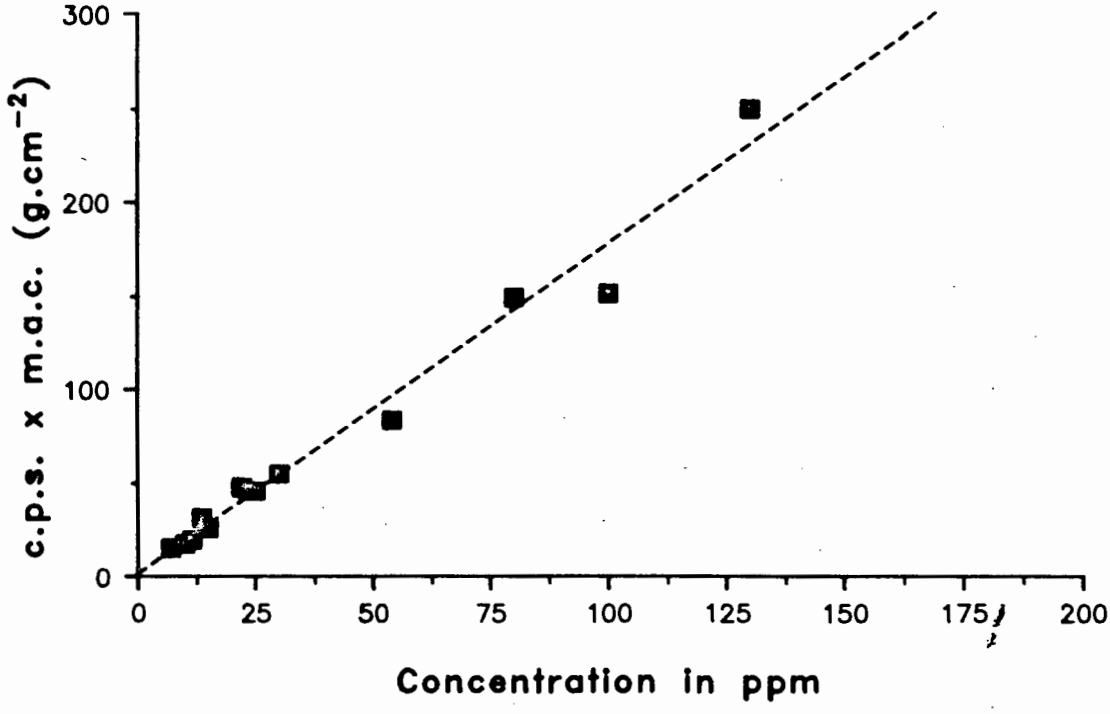

improvement as the present version of the calculation program, TRACE, corrects for the interference of La on all analyte elements, Figure 3:6(b). This is an error in the program, TRACE, which requires modification so that only corrections are made for the observed spectral line interferences. Further investigation revealed that third order LaK_b interferes on the PbL_b line, this is illustrated in Figure 3:1. The calibration curve in Figure 3:6(b) is still not satisfactory and the problems are thought to be associated with W X-ray tube as the W L_1 abs. edge is very close to the high angle Pb background at 29.29°2θ. The effect of this interference varies with the m.a.c. of the analytical specimens. Other elements U, Rb and Th that use this background position are affected to a lesser degree by this W interference. Bower and Valentine (1986) have also suggested that Pb could be lost during the fusion process. To test for W tube interference the discs were re-analyzed using the Mo tube which improves sensitivity for the L_a and L_b lines. This analytical run is discussed later.

For all the analyte elements except Nb the m.a.c.s calculated at the RbK_a wavelength have been used to correct matrix differences due to high concentrations of Sr in lamproites and kimberlites. The results of the determination of Nb-Pb in low dilution fusion discs are summarized in Table 3:5 and 3:6. Comparisons with international standards (Govindaraju 1984, Abbey 1986) are also presented. Available trace element data for lamproites and kimberlites obtained by INAA at the Open University (Fraser et al 1986) and at Mainz (Smith pers.comm) are compared with Low Dilution XRF data in the summary at the end of this chapter. Data for lamproite and kimberlite samples analyzed by this method are reported in Appendix G.

Table 3:5

Comparison of Nb-Pb data obtained by low dilution fusion method with international standards data. (in ppm).

sample		Nb	Zr	Y	Sr	Rb	U	Th	Pb
BCR-1	(a)	13.5	185	34.0	330.	47.0	-	6.0	13.6
	(b)	12.9	183	33.3	327.	48.3	-	6.6	21.8
BHVO-1	(a)	19.0	-	27.0	420+70	10.0	-	-	-
	(b)	16.2	-	27.2	387.	8.8	-	-	-
G-2	(a)	13.0	320.	11.0	480.	170.	-	25.0	30.0
	(b)	10.6	333.	7.8	484.	174.	-	28.5	29.5
GSP-1	(a)	26.0	-	29.0	240.	250.	-	105.	54.0
	(b)	28.3	-	25.0	235.	256.	-	101.	56.4
NIM-G	(a)	53.0	300.	143.	10.0	325.	15.0	51.0	40.0
	(b)	56.7	291.	143.	11.3	335.	19.8	45.2	36.9
NIM-N	(a)	-	-	-	260.	-	-	-	-
	(b)	-	-	-	261.	-	-	-	-
NIM-S	(a)	-	-	-	62.	530.	-	-	-
	(b)	-	-	-	64.9	538.	-	-	-
NIM-P	(a)	-	-	-	32.	-	-	-	-
	(b)	-	-	-	30.3	-	-	-	-
MRG-1	(a)	-	105.	13.0	270.	8.0	-	-	10.0
	(b)	-	99.8	8.9	269.	7.4	-	-	11.5
SY-2	(a)	-	290.	130.	275.	220.	290.	360.	85.0
	(b)	-	291.	130.	273.	223.	332.	362.	98.4
SY-3	(a)	-	320.	-	-	-	650.	-	135.
	(b)	-	311.	-	-	-	631.	-	123.
S-7	(a)	105.	250.	14.0	-	53.0	-	14.0	25.0
	(b)	109.	247.	13.7	-	53.0	-	15.5	32.3
S-13	(a)	27.0	320.	64.0	93.0	145.	-	21.0	17.0
	(b)	23.8	324.	64.9	91.8	141.	-	21.8	17.9
S-16	(a)	213.	300.	463.	31.0	290.	27.0	113.	-
	(b)	211.	306.	463.	31.1	285.	31.5	111.	-
S-18	(a)	7.0	85.0	24.0	198.	14.0	-	-	28.0
	(b)	6.2	84.6	24.1	196.	13.6	-	-	31.6

(a) International standard values (Govindaraju 1984, Abbey 1986)
(b) Low dilution fusion discs
\- not used as a standard

Table 3:6

Lower limits of detection and counting errors for low dilution fusion discs and powder pellets analyzed by XRFS using analytical conditions outlined in Table 3:4.

	Counting error (ppm) 1 S.D.	Lower limit of detection (ppm)
Nb	0.85-1.28 (0.76-0.88)	2.60-3.19 (1.90-2.18)
Zr	0.81-2.57 (1.69-2.24)	2.51-4.57 (2.67-3.61)
Y	0.94-1.55 (0.90-1.13)	2.81-4.62 (2.64-3.36)
Sr	0.87-3.11 (1.73-2.66)	2.58-3.75 (2.08-2.26)
U	2.53-3.73 (1.89-2.17)	7.57-11.2 (5.68-6.49)
Rb	0.88-1.81 (1.01-1.46)	2.64-3.86 (2.17-2.46)
Th	2.22-3.26 (1.87-2.09)	6.65-9.66 (5.48-6.18)
Pb	2.68-3.77 (2.11-2.33)	7.64-11.2 (6.07-6.77)

Figures in brackets refer to pressed powder pellets counting times are the same for pellets and discs.

Table 3:7(a)

Analytical conditions for the determination of Zn, Cu and Ni on low dilution fusion discs analyzed on a Philips PW1400 XRF spectrometer using a Au X-ray tube at 60kV, 45mA, and LiF(220) analyzing crystal.

Element, Line + order	Time (s)	Coll	Det	UPL	LWL	peak ($^{o}2\theta$)	background +off* ($^{o}2\theta$)	background -off* ($^{o}2\theta$)
Au L_a (1)	40	Fine	FS	80	20	53.285	-	-
Zn K_a (1)	80	Fine	FS	80	20	60.545	4.24	1.08
Cu K_a (1)	80	Fine	FS	80	20	65.545	4.44	-
Ni K_a (1)	80	Fine	FS	80	20	71.255	2.52	-

Note :

Secondary collimator associated with scintillation counter, but peak shape is determined by the flow counter.
2 counting cycles
Samples analyzed under vacuum
Background counting times was 40 seconds

The following backgrounds were used

Zn - Zn-, Zn+
Cu - Zn+, Cu+
Ni - Cu+, Ni+

* ± background angle offset relative to peak angle

Table 3:7(b)

Possible spectral line interferences on elements, Zn, Cu and Ni using analytical conditions outlined in Table 3:7(a).

Element		Possible Spectral line Interference (background positions)
Zn K_a	-	Cu K_a
Cu K_a	-	Ni K_a, (tube impurities)
Ni K_a	-	(tube impurities)

ANALYTICAL RUN - Zn, Cu, Ni.

The analytical conditions used to determine Zn, Cu and Ni on the low dilution fusion discs are detailed in Table 3:7(a). Possible interferences on background positions are detailed in Table 3:7(b). Wavelength scans, from 55 - 75 $^{o}2\theta$ were run for the special interference elements - La, Ce, Nd, and Ba. No new interferences were observed. Several lamproites were also scanned to check for any unusual problems in this range. Interference standards for zinc, copper and nickel were analyzed. Corrections for the concentrations of nickel and copper present as impurities in the gold X-ray tube were carried out using the method outlined earlier (page 41). International standards data are compared in Table 3:8 with data obtained from low dilution fusion discs. Lower limits of detection and errors are reported in Table 3:9.

Data for the lamproite and kimberlite samples analyzed by the low dilution method are reported in Appendix G.

Table 3:8

Comparison of Zn, Cu, Ni data determined on low dilution fusion disc and international standards data.(in ppm)

Sample		Zn	Cu	Ni
BCR-1	(a)	125.	16.0	10.0
	(b)	128.	12.7	7.0
BHVO-1	(a)	102.	130.	117.
	(b)	99.	127.	118.
G-2	(a)	84.	10.0	5.0
	(b)	83.	10.7	6.2
GSP-1	(a)	105.	33.0	9.0
	(b)	103.	33.2	8.1
NIM-G	(a)	50.0	12.0	-
	(b)	50.3	9.3	-
NIM-N	(a)	57.0	14.0	120.
	(b)	55.7	8.5	117.
NIM-P	(a)	100.	18.0	556.
	(b)	103.	19.8	557.
NIM-S	(a)	-	19.0	-
	(b)	-	18.1	-
MRG-1	(a)	208.	135.	210.
	(b)	207.	140.	207.
SY-2	(a)	250.	5.0	10.0
	(b)	252.	3.1	8.2
SY-3	(a)	240.	16.0	-
	(b)	238.	12.4	-

(a) International standard value (Govindaraju 1984, Abbey 1986)
(b) Low dilution Fusion Discs
\- not used as a standard

Table 3:9

Lower limits of detection and errors for Zn, Cu and Ni, analyzed by XRFS using Au tube and LiF (220) crystal.

	Counting error (ppm) 1 S.D.	Lower limit of detection (ppm)
Zn	0.40-1.08 (0.41-1.10)	1.19-2.25 (1.20-2.73)
Cu	0.61-1.15 (0.50-1.38)	1.82-3.06 (1.41-2.77)
Ni	0.52-2.77 (0.47-1.27)	1.56-3.09 (1.50-3.03)

Figures in brackets relate to pressed powder pellets analyzed at U.C.T.
Counting times were the same for pellets and discs.

ANALYTICAL RUN - Scandium

Scandium was determined on the low dilution fusion discs using the analytical conditions detailed in Table 3:10. No wavelength scans were run but wavelength tables were checked for any possible interferences. Calcium was the only interference standard analyzed.

International standards data are compared with data obtained by this method in Table 3:11. Lower limits of detection and counting errors are detailed in Table 3:12. Scandium data obtained by INAA by Fraser et al (1986) and Smith (in press) are compared with low dilution fusion disc data (XRFS) in the summary. Data for lamproite and kimberlite samples are reported in Appendix G.

Table 3:10

Analytical conditions for the determination of Sc in low dilution fusion discs analyzed on a SRS-1 XRF spectrometer using a Cr X-ray tube at 50kV, 60mA, and LiF(200) analyzing crystal.

Element, Line +order	Time (s)	Coll	Det	UPL	LWL	peak ($^{o}2\theta$)	background +off* ($^{o}2\theta$)	-off*
Sc K_a (1)	100	Fine	FS	250	750	97.710	-	2.71
Ca K_b (1)	20	Fine	FS	250	750	100.220	-	-

Note :

background counting time = 40 seconds, 2 counting cycles

samples analyzed under vacuum

Sc- used as background for Sc and Ca.

Ca - interference element

* $\pm$ background angle offset relative to peak angle

Table 3:11

Comparison of Scandium data from the low dilution fusion discs with international standards data. (data in ppm)

Standard		Sc
BCR-1	(a)	33.0
	(b)	33.1
GSP-1	(a)	6.6
	(b)	6.2
BHVO-1	(a)	31.0
	(b)	31.1
MRG-1	(a)	55.0
	(b)	55.3
NIM-N	(a)	39.0
	(b)	39.0
PCC-1	(a)	9.0
	(b)	7.9
G-2	(a)	3.5
	(b)	3.9

(a) International standards data (Govindaraju 1984, Abbey 1986)
(b) Low dilution Fusion discs

Table 3:12

Lower limits of detection and errors for Sc determined on Siemens SRS-1 spectrometer.

	Counting error (ppm) 1 S.D.	Lower limit of detection (ppm).
Sc	0.47-1.03 (0.37-0.89)	1.23-2.64 (0.93-1.83)

Figures in brackets relate to pressed powder pellets analyzed at U.C.T.
counting times were the same for pellets and discs

Table 3:13(a)

Analytical conditions for the determination of Co, Cr, V in low dilution fusion discs analyzed on a Philips PW1400 XRF spectrometer using W X-ray tube at 50kV, 55mA, and LiF(220) analyzing crystal.

Element, Line + order	Time (s)	Coll	Det	UPL	LWL	peak ($^{o}2\theta$)	background +off* ($^{o}2\theta$)	background -off* ($^{o}2\theta$)
Fe K_b (1)	40	Fine	FS	80	15	76.250	4.40	-
Co K_a (1)	80	Fine	FS	80	15	77.920	-	-
Ba L_γ (1)	80	Fine	FS	70	15	103.905	-	3.32
Cr K_a (1)	80	Fine	FS	70	15	107.185	2.90	4.10
V K_a (1)	80	Fine	FS	70	15	123.290	-	2.70
Ti K_b (1)	16	Fine	FS	70	15	124.145	2.20	-

Note :

background counting time = 40 seconds
2 counting cycles,
samples analyzed under vacuum

The following backgrounds were used -

Fe, Co - Fe+
Ba, Cr - Ba-, Cr+
V - V-
Ti - Ti+

* ± background angle offset relative to peak angle

Table 3:13(b)

Possible spectral line interferences on elements Co, Cr and V using analytical conditions outlined in Table 3:13(a).

Element		Possible Spectral Line Interference
Co K_a	-	Fe K_{b0} (satellite line)
Cr K_a	-	V K_b, (tube impurities)
V K_a	-	Ti K_b, Ba L_{b3}

ANALYTICAL RUN - Co, Cr, V.

Analytical conditions for this run are outlined in Table 3:13. Possible spectral line interferences are outlined in Table 3:13(b). Wavelength scans between 70° - 130° 2θ for the special interfering elements were run. Several lamproites were scanned and the peaks identified to check for any unusual interferences.

An important interference previously unrecognized is BaL_{b3} which interferes on TiK_b, which in turn interferes with VK_a, Figure 3:7. To correct for Ba interference on Ti, the intensity of BaL_γ was measured at 103.905° 2θ. Interference standards analyzed were V, Cr, Co, Ti, Ba, and Fe. The Co, Cr, and V interference standards contained 2000 ppm of the analyte in Specpure quartz. The TiO_2, BaO and Fe_2O_3 interference standards contained 5%, 2% and 20% of the analyte in Specpure quartz respectively.

Data obtained by the Low dilution fusion technique are summarized in Table 3:14 and 3:15. The data in Table 3:14 show that there is poor agreement of Cr at low concentration levels. This is most likely due to a combination of over correction of the tube interference and counting statistics, although the data for GSP-1, G-2 and NIM-S are within counting error (3 S.D.).

Data for lamproite and kimberlite samples are reported in Appendix G. Cobalt data from some lamproite and kimberlite samples are compared to data obtained from the low dilution fusion discs in the summary.

Figure 3:7. Barium and Titanium interference on Vanadium

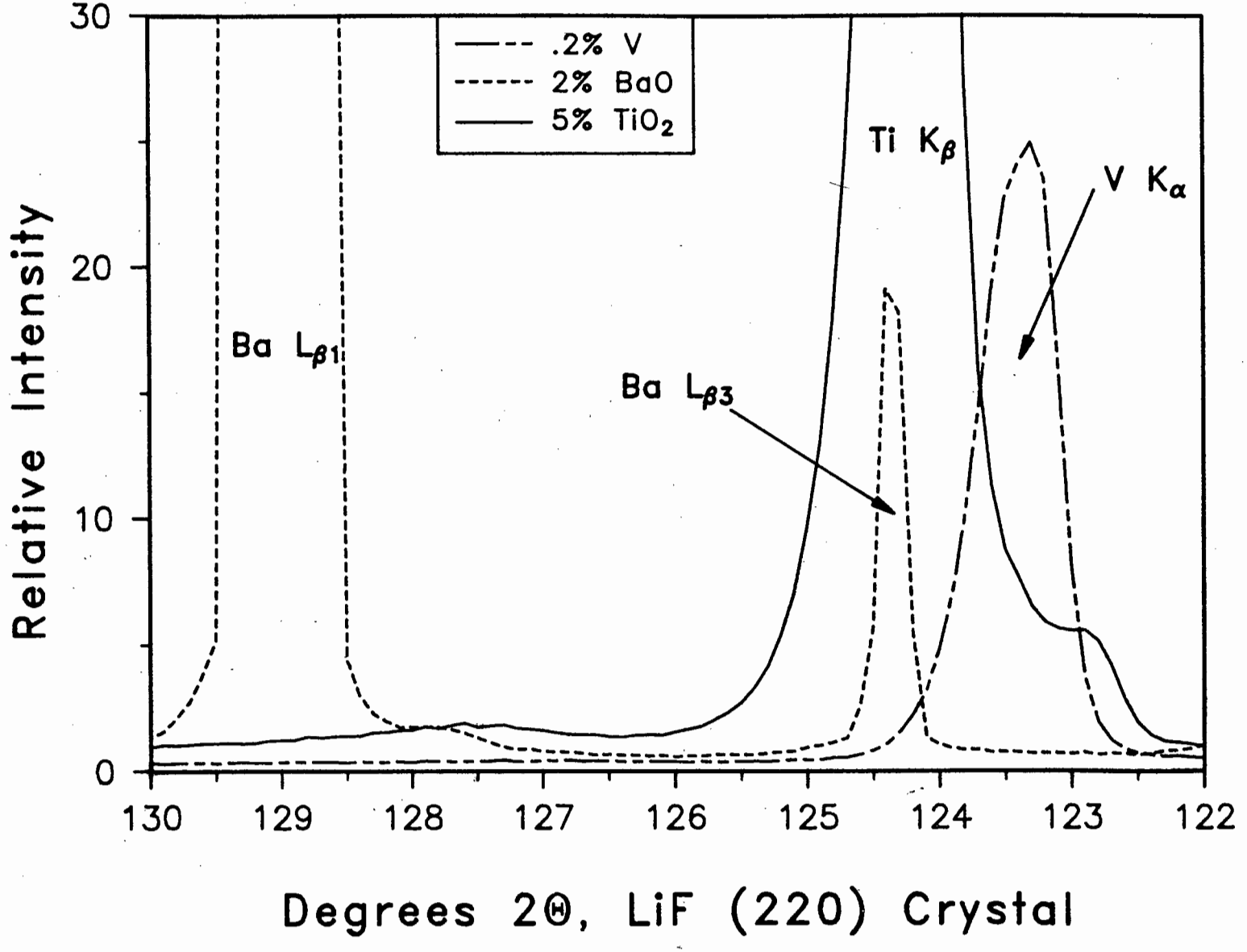

Table 3:14

Comparison of Co, Cr, V data obtained by the low dilution technique with international standard values. (in ppm)

Sample		Co	Cr	V
BCR-1	(a)	36.0	15.0	420.
	(b)	38.9	7.2	410.
BHVO-1	(a)	45.0	280.	314.
	(b)	44.8	273.	312.
G-2	(a)	5.0	8.0	36.0
	(b)	5.2	9.9	34.5
GSP-1	(a)	7.8	12.0	54.0
	(b)	6.8	8.9	46.9
NIM-D	(a)	210.	-	40.0
	(b)	207.	-	39.4
NIM-N	(a)	58.0	-	220.
	(b)	62.6	-	213.
NIM-S	(a)	-	12.0	10.0
	(b)	-	7.7	10.8
MRG-1	(a)	86.0	420.	520.
	(b)	89.7	431.	533.
SY-2	(a)	10.0	-	52.0
	(b)	9.1	-	48.6

(a) International standard value (Govindaraju 1984, Abbey 1986)
(b) Low Dilution Fusion Discs
\- not used as a standard

Table 3:15

Lower limits of detection and counting errors for Co-Cr-V. determined using conditions outlined in Table 3:13

	Counting error (ppm) 1 S.D.	Lower limit of detection (ppm)
Co	0.71-1.60 (0.82-1.65)	2.02-4.28 (2.29-4.53)
Cr	0.60-3.58 (0.78-2.40)	1.81-3.44 (2.35-3.57)
V	0.71-2.66 (1.25-2.55)	1.68-6.77 (3.61-6.01)

Figures in brackets refer to pressed powder pellets (U.C.T.) counting times were the same for pellets and discs.

Table 3:16(a)

Analytical conditions for the determination of La, Ce, and Nd in low dilution fusion discs analyzed on a Philips PW1400 XRF spectrometer using W X-ray tube at 50kV, 55mA, and LiF(220) analyzing crystal.

Element, Line + order	Time (s)	Coll	Det	UPL	LWL	peak ($^{o}2\theta$)	background +off* ($^{o}2\theta$)	background -off* ($^{o}2\theta$)
La L_a (1)	200	Fine	FS	70	30	138.955	4.22	2.78
Nd L_a (1)	200	Fine	FS	70	30	112.820	4.82	-
Ce L_b (1)	200	Fine	FS	70	30	111.790	-	1.64
Ba L_γ (1)	80	Fine	FS	70	30	103.905	-	3.32

Note :

La, Ce, Nd background counting times = 100 seconds
Ba background counting time = 40 seconds
2 counting cycles
samples analyzed under vacuum

The following backgrounds were used -

La	- La+, La-
Nd, Ce	- Nd+, Ce-
Ba	- Ba-, Ce-

* $\pm$ background angle offset relative to peak angle

Table 3:16(b)

Possible spectral line interferences on elements La, Ce, and Nd using analytical conditions outlined in Table 3:16(a).

Element		Possible Spectral Line Interference
La L_a	-	Cs L_{b4}, Nd L_L
Ce L_b	-	Nd L_{a1}, La L_{b6}, Ba L_{b7}, (Ba L_{III}abs. edge)
Nd L_a	-	Ce L_{b1}, La L_{b6}, Ba L_{b7} (Ba L_{III}abs. edge)

ANALYTICAL RUN - La, Ce, Nd

Analytical conditions for the determination of La, Ce and Nd on low dilution fusion discs are detailed in Table 3:16(a). Possible spectral line interferences are detailed in Table 3:16(b). Wavelengths scans were run to check for any interferences, these are illustrated in Figure 3:8 and they indicate that the 3 analyte elements require correction for the mutual interference of La, Ce and Nd. No additional interferences are shown by the scans.

The data obtained from TRACE indicated that Ba interferes on the La and Ce backgrounds and on the Nd peak. The calculated background factors for the Ba artificial standards showed the interference to be on the background positions. The calculated background factors for La and Ce were lower and for Nd higher than the background factors for Specpure SiO_2. This is illustrated in Table 3:17, the calculated background factors vary systematically with the concentration of BaO in the low dilution fusion discs.

Table 3:17

Comparison of calculated background factors for La, Ce, and Nd showing the interference of Barium.

sample	calculated background factors		
	La	Ce	Nd
2% BaO	.5305	.5078	.5570
4% BaO	.5030	.4920	.5939
8% BaO	.4576	.4802	.6550
Spec Pure SiO_2	.5532	.5271	.5120

Figure 3:8. Wavelength scan showing the La, Ce, Nd and Ba lines in the region 100–143 degrees 2Θ.

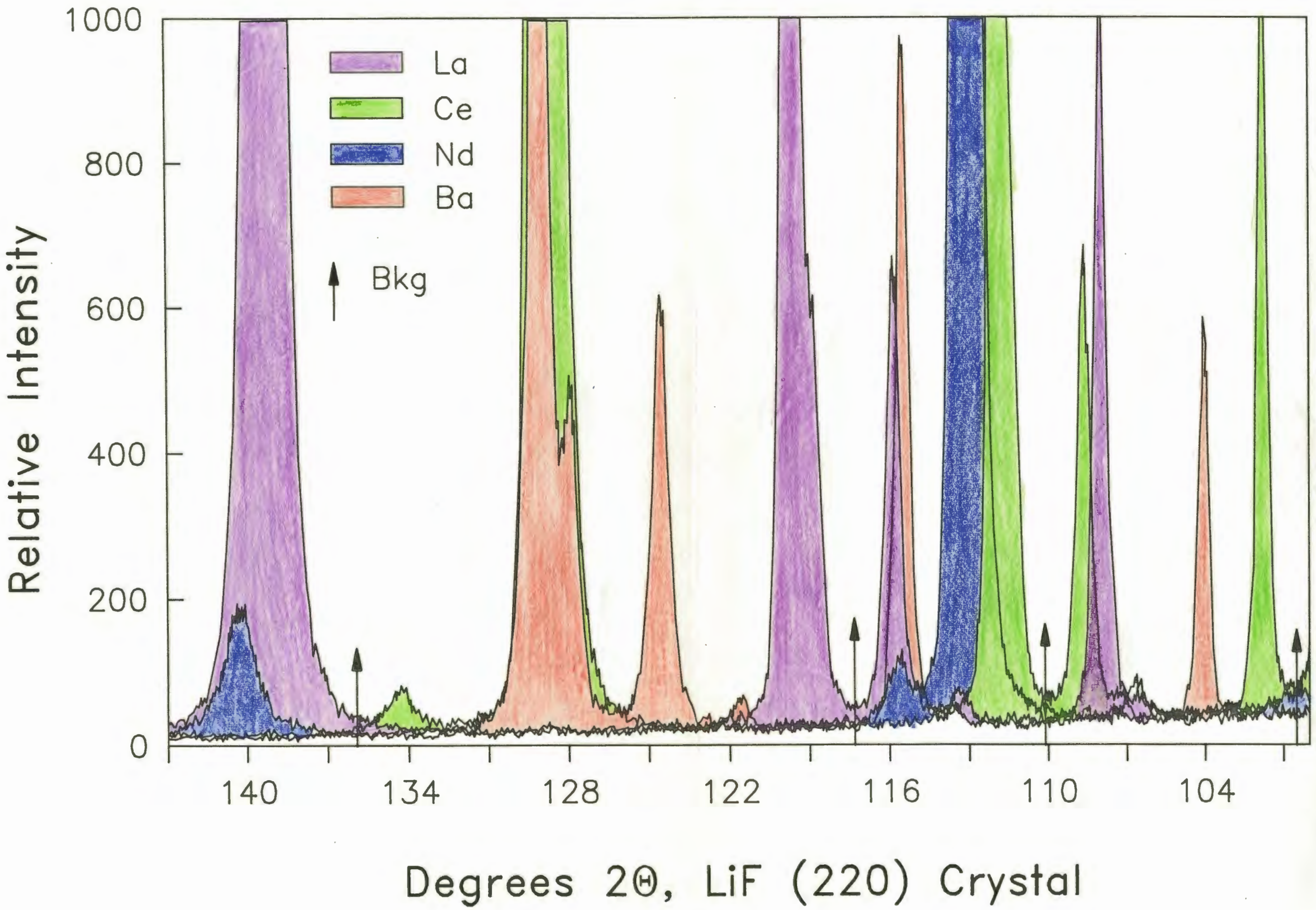

The LiF(220) wavelength tables indicated that sixth order BaK_b and seventh order BaK_a lines interfere on the Ce low angle background position and La high angle background position respectively. The wavelength scans, Figure 3:8, show that these Ba lines are not detected. On further investigation it was found that the BaL_{III} absorption edge lies between the CeL_b and NdL_a lines and thus between the two background positions used for these elements (Figure 3:9) therefore single backgrounds should be used for Ce and Nd, Ce- and Nd+ respectively. The presence of this absorption edge is responsible for the inverse relationship of the background factors for Ce and Nd as the concentration of BaO increases, as shown in Table 3:17. On the long wavelength side of the absorption edge the background intensity increases and the absorption decreases as the BaO concentration increases, resulting in the systematic variation in the Nd background factors.

This pseudo-interference due to the L-series absorption edges of Ba is very important when samples with high BaO concentrations are analyzed. Consequently La, Ce, Nd and Ba interference standards were analyzed, these standards contained .5% of the analyte in 99.5% Specpure SiO_2. To correct for the Ba interference the intensity of the Ba L line at 103.905 $^{o}20$ was measured.

The data for La, Ce and Nd are summarized in Table 3:18 and 3:19. Data for lamproite and kimberlite samples analyzed by this method are reported in Appendix G.

Figure 3:9. Position of the Ba L absorption edges in relation to the La, Ce and Nd analyte lines.

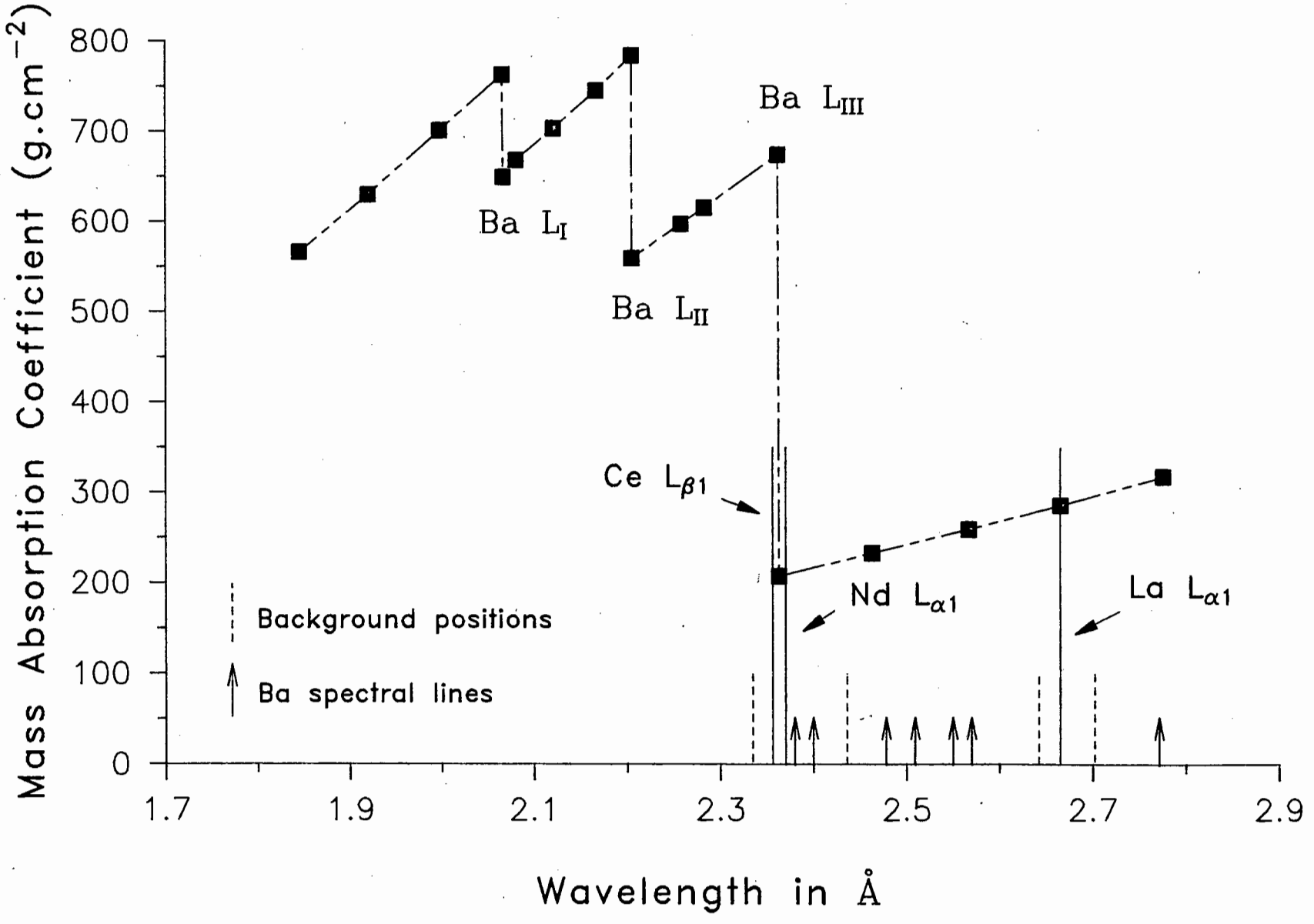

Table 3:18

Comparison of La, Ce, and Nd data obtained from the low dilution fusion discs with international standards. (in ppm)

standard		La	Ce	Nd
BCR-1	(a)	27.0	53.0	29.0
	(b)	29.4	52.9	23.6
BHVO-1	(a)	-	39.0	24.0
	(b)	-	41.5	20.3
G-2	(a)	92.0	160.	58.0
	(b)	90.7	156.	50.2
GSP-1	(a)	195.	-	190.
	(b)	191.	-	195.
NIM-G	(a)	109.	195.	72.0
	(b)	118.	201.	71.2
NIM-S	(a)	-	11.9	6.0
	(b)	-	9.3	3.8
SY-2	(a)	74.0	170.	74.0
	(b)	75.1	161.	72.1
SY-3	(a)	1350.	2200.	-
	(b)	1351.	2200.	-

(a) International standards data (Govindaraju 1984, Abbey 1986)
(b) low dilution fusion disc
\- not used as a standard

Table 3:19

Lower limits of detection and errors for La, Ce, Nd analyzed by XRFS conditions detailed in Table 3:16.

	Counting error (ppm) 1 S.D.	Lower limit of detection (ppm)
La	1.13-3.55 (0.87-1.06)	3.30-5.03 (2.26-2.81)
Ce	2.09-4.26 (1.68-2.06)	6.18-8.86 (4.37-5.83)
Nd	1.04-2.34 (1.06-1.34)	3.08-4.41 (2.83-3.82)

Figures in brackets refer to pressed powder pellets, U.C.T.

An interesting problem was brought to the investigator's attention at a conference on Kimberlites held at U.C.T. (February 1986). Smith (pers.comm) reported conflicting results for La, Ce, and Nd concentrations in kimberlites analyzed by XRFS (powder pellets) at U.C.T. and by INAA at the Max Planck Institute, Mainz. These results are summarized in Table 3:20. To investigate this problem low dilution fusion discs were made for the six kimberlites and the discs and powder pellets were re-analyzed on the same analytical run except that the fusion discs were corrected for the known Ba interference. The XRFS values for the low dilution fusion discs are comparable to the INAA values. The powder pellets gave the same results as Smith reported. The differences in the XRFS data are too large to be associated with the Ba interference, since in most cases the Ce concentration has increased between 15 and 75% in the low dilution fusion discs.

Further investigation revealed that the differences in the La, Ce, and Nd concentrations are due to mineralogical effects. In kimberlite samples, La, Ce and Nd reside in perovskite, but in the rock standards used at U.C.T (G-2, GSP-1) these elements reside chiefly in apatite and zircon. Perovskite is essentially a calcium titanate $(CaNaFe^{2+},Ce)(Ti,Nb)O_3)$ and apatite is a calcium phosphate $(Ca_5(PO_4)_3(OH,F,Cl))$ and zircon is a zirconium silicate $(Zr(SiO_4))$. Willis (pers comm) showed that the TiK absorption edge lies between the LaL_a and the NdL_a and CeL_b wavelengths. This is illustrated in Figure 3:10. The routine method of analyzing La, Ce, Nd at U.C.T. by XRFS involves the use of pressed powder pellets. The rocks are ground to approximately -300 mesh but this is not sufficient to remove the problem of La, Ce and Nd in kimberlites residing in a titanate

Figure 3:10. Position of La, Ce and Nd analyte lines in relation to the Titanium K absorption edge.

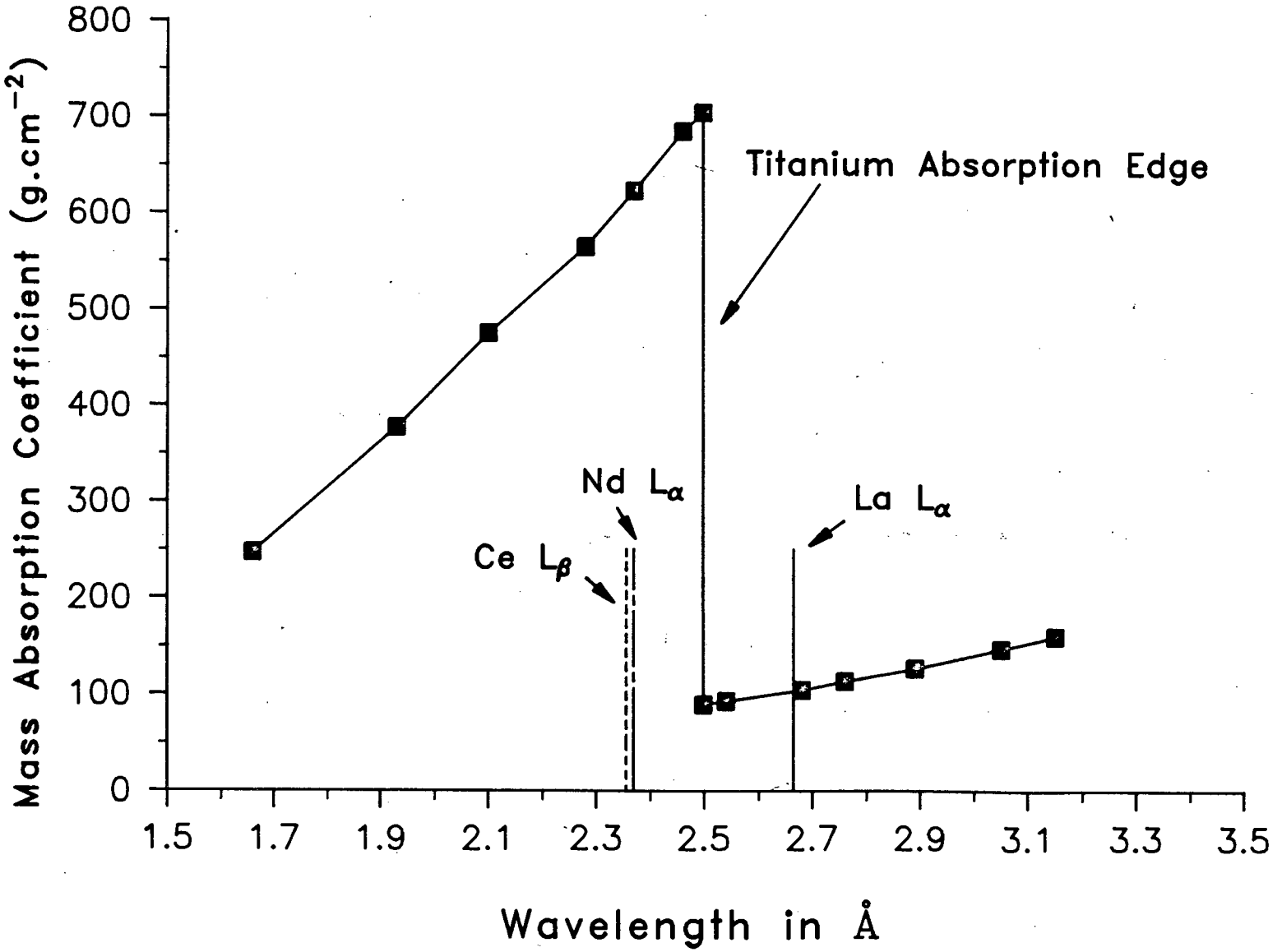

mineral. The titanium absorption edge will significantly affect the overall absorption coefficient of perovskite, but will have little effect on that of apatite and zircon, resulting in incorrect data for these elements in kimberlites. The net intensity in cps/ppm of especially Nd and Ce will be too low in perovskite relative to that from apatite and zircon due to the absorption by titanium. By grinding very fine this difference would be removed. This is a classic particle size - mineralogical effect as described in Chapter 1.

Comparison of the La, Ce and Nd data analyzed by INAA and by XRFS using low dilution fusion technique, Table 3:20, shows that the use of a homogeneous glass disc, in which the sample powders are completely dissolved and the elements homogenised, removes the effect of the titanium absorption edge on the La, Ce and Nd concentrations in different minerals.

La, Ce and Nd data obtained by INAA (Fraser et al 1986, Smith in press) is compared to low dilution fusion disc data in the summary.

Table 3:20

Comparison of La, Ce and Nd data analyzed by INAA (Max Planck), XRFS-powder pellets (UCT) and XRFS - low dilution fusion discs (UCT). (in ppm)

sample		La	Ce	Nd
CKP 9	(a)	310	580	224
	(b)	231	397	176
	(c)	231	392	190
	(d)	329	622	229
K64/55	(a)	240	461	130
	(b)	237	402	149
	(c)	231	399	159
	(d)	262	463	139
K61/35	(a)	356	740	290
	(b)	294	533	220
	(c)	285	507	233
	(d)	376	696	242
RJ53/54	(a)	103	204	77.1
	(b)	61	103	46.0
	(c)	61.5	107	48.7
	(d)	102	211	78.6
JAG K9	(a)	425	1090	470
	(b)	280	624	317
	(c)	263	599	322
	(d)	423	1056	440
VIN 1	(a)	246	539	207
	(b)	184	309	146
	(c)	171	296	146
	(d)	252	518	206

(a) INAA - Smith, Mainz
(b) XRFS - Smith 1984, powder pellets U.C.T.
(c) XRFS - 1986, powder pellets, U.C.T.
(d) XRFS - 1986, low dilution fusion discs.

Table 3:21(a)

Analytical conditions for the determination of Sr, U, Rb, Th, Pb, Br, Se, Bi, As, Ge, W, Ga in low dilution fusion discs analyzed on a Philips PW1400 XRF spectrometer using a Mo X-ray tube at 50 kV, 55 mA and LiF(200) analyzing crystal.

Element	Line	Time (s)	Coll	Det	UPL	LWL	peak (o2θ)	background +off* (°2θ)	background -off* (°2θ)
Sr	K_a	80	Fine	SC	68	35	25.175	0.62	-
U	L_a	80	Fine	SC	68	35	26.185	-	-
Rb	K_a	80	Fine	SC	68	35	26.640	-	-
Th	L_a	80	Fine	Sc	68	35	27.515	-	-
Pb	L_b	80	Fine	SC	68	35	28.290	1.00	-
Br	K_a	80	Fine	SC	68	35	29.985	1.32	-
Se	K_a	80	Fine	FS	75	25	31.895	-	0.60
Bi	L_a	80	Fine	FS	75	25	33.035	-	-
As	K_a	80	Fine	FS	75	25	34.010	1.32	0.60
Ge	K_a	80	Fine	FS	60	30	36.340	-	1.00
W	L_b	80	Fine	FS	60	30	37.155	-	-
Ga	K_a	80	Fine	FC	60	30	38.935	0.70	0.90

Note :

Background counting times = 40 seconds

2 counting cycles, samples analyzed under vacuum

Secondary collimator associated with the scintillation counter

The following background positions were used :

Sr	-	Sr+
Rb, U, Th, Pb	-	Sr+, Pb+
Br	-	Pb+, Br+
Se, Bi	-	Se-, As-
As	-	As-, As+
Ge, W	-	Ge-, Ga-
Ga	-	Ga-, Ga+

* $\pm$ background angle offset relative to peak angle

Table 3:21(b)

Possible spectral line interferences on elements Sr, U, Rb, Th Pb, Br, Se, Bi, AS, Ge, W, Ga using analytical conditions outlined in Table 3:21(a).

Element		Possible Spectral Line Interference
Sr K_a	-	Pb $L\gamma_5$
U L_a	-	Rb K_a
Rb K_a	-	U L_a, Br K_{b2}
Th L_a	-	Pb $L_{b3,5}$, Bi L_{b2}
Pb L_b	-	La $K_{b1,3}(3)$, Th L_{a2}, Bi L_{b4}, Se $K_{b1,2}$
Br K_a	-	As $K_{b1,2}$
Se K_a	-	Pb L_n, W $L\gamma_1$
Bi L_a	-	Hf $L\gamma_2$
As K_a	-	Pb $L_{a1,2}$
Ge K_a	-	Mo $K_{b1,2}(2)$, W L_{b2}
W L_b	-	Mo K_b, Mo K_b compton
Ga K_a	-	Pb L_L, Hf L_{b2}

Note: interference by adjacent elements on background positions is common.

ANALYTICAL RUN -Sr, U, Rb, Th, Pb, Br, Se, Bi, As, Ge, W, Ga

Analytical conditions for the determination of these elements are outlined in Table 3:21(a). Possible spectral line interferences are outlined in Table 3:21(b). Wavelength scans from 24 - 40°2θ indicated that La, Ce, Nd and Ba did not interfere with these elements. Interference standards for all the analyte elements were analyzed so that corrections for peak-on-peak and peak-on-background interferences could be made.

Strontium, rubidium, uranium, thorium and lead were re-analyzed using the Mo X-ray tube. These elements have absorption edges just longer than the wavelengths of the characteristic lines from the Mo X-ray tube leading to very efficient excitation of the analyte lines resulting in increased sensitivity for elements heavier than Ge (K series lines) and Os (L series lines). The Mo X-ray tube also gives the lowest background intensities as these originate from the continuum and are dependent on the atomic number of the target material. The effect of using the Mo X-ray tube is illustrated in Table 3:23, as the lower limits of detection and counting errors are considerably reduced compared to those reported in Table 3:6 for the W X-ray tube.

Mass absorption coefficients calculated at RbK_a were used to correct for matrix differences. Data obtained from this analytical run are summarized in Table 3:22-3:23. It should be noted that only Sr, Rb, U, Th, Pb and Ga could be standardized. As, Br, W, Se, Bi, and Ge were not detected in any of the fusion discs.

The use of a Mo X-ray tube improves the data for Pb in the low dilution fusion discs, this is illustrated by comparing the

calibration curve for Pb in Figure 3:11 to those in Figure 3:6 where Pb was determined using a W X-ray tube. The data in Table 3:22 indicates that agreement with international standards data is improved and lower limits of detection and counting errors (Table 3:23) are reduced using a Mo X-ray tube for Pb determination.

Data for lamproite and kimberlite samples analyzed using the Mo X-ray tube are reported in Appendix G.

Figure 3:11. Calibration curve for Pb using Mo X-ray tube with no correction for lanthanum interference.

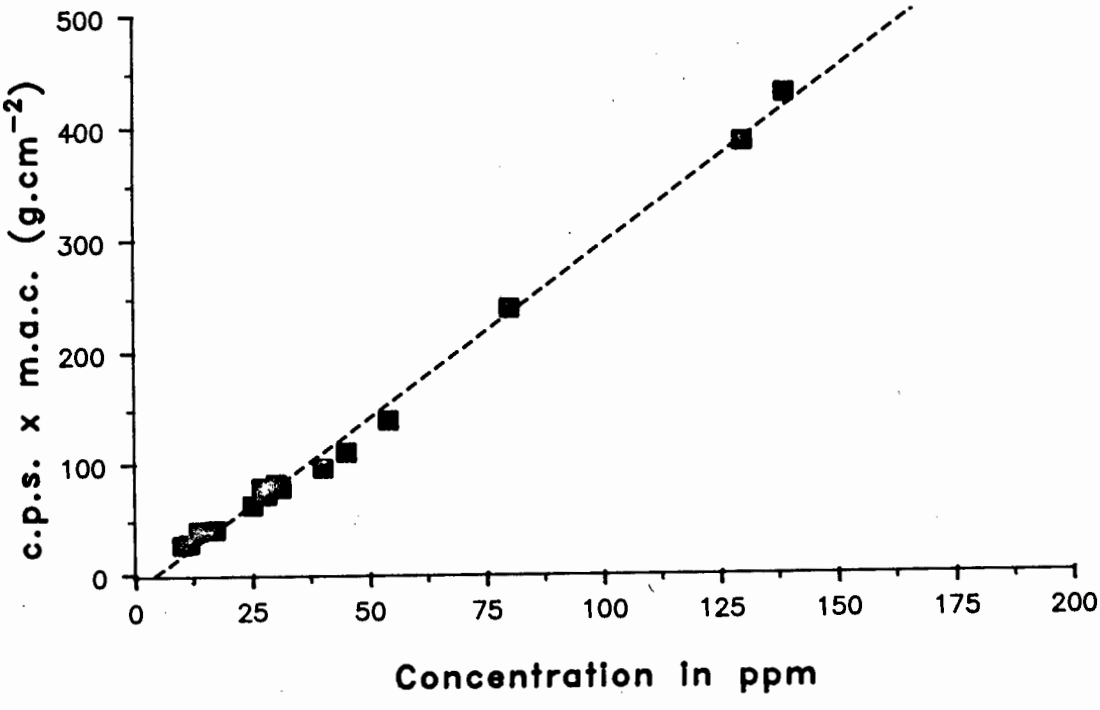

Table 3:22

Comparison of Sr, U, Rb, Th, Pb, Ga data obtained by low dilution fusion technique, using analytical conditions detailed in Table 3:21, with international standards data. (in ppm)

sample		Sr	Rb	U	Th	Pb	Ga
BCR-1	(a)	330.	47.0	-	6.00	13.6	22.0
	(b)	331.	47.1	-	6.17	14.6	22.5
BHVO-1	(a)	420+70	10.0	-	-	-	22+3
	(b)	390	9.3	-	-	-	20.3
G-2	(a)	480	170	-	25.0	30.0	23.0
	(b)	489	171	-	21.2	28.3	21.9
GSP-1	(a)	240.	250.	-	105.	54.0	23.0
	(b)	236.	254.	-	106.	51.2	21.8
NIM-G	(a)	10.0	325.	15.	51.0	40.0	27.0
	(b)	10.7	331	17.3	48.9	36.5	27.9
NIM-N	(a)	260.	-	-	-	-	16.0
	(b)	261.	-	-	-	-	17.5
NIM-S	(a)	62.0	530.	-	-	-	11.0
	(b)	65.1	534.	-	-	-	11.4
NIM-P	(a)	32.0	-	-	-	-	8.0
	(b)	30.0	-	-	-	-	7.9
MRG-1	(a)	270.	8.0	-	-	10.0	-
	(b)	269.	8.3	-	-	9.8	-
SY-2	(a)	275.	220.	290.	-	85.0	28.0
	(b)	275.	219.	282.	-	88.3	27.9
SY-3	(a)	306.	208.	650.	990.	135.	26.0
	(b)	296.	196.	653.	990.	136.	23.9
S-7	(a)	-	53.0	-	-	25.0	7.0
	(b)	-	50.3	-	-	22.1	6.9
S-13	(a)	93.0	145.	-	21.0	17.0	43.0
	(b)	90.7	139.	-	19.9	14.8	38.9
S-16	(a)	31.0	290.	27.0	113.	-	-
	(b)	30.5	281.	27.0	114.	-	-
S-18	(a)	198.	14.0	-	8.0	28.0	-
	(b)	195.	12.9	-	6.8	27.2	-

(a) International standard values (Govindaraju 1986, Abbey 1984)
(b) Low dilution fusion discs
\- not used as a standard

Table 3:23

Comparison of Lower limits of detection and counting errors for low dilution fusion discs analyzed by XRFS using a Mo and a W X-ray tube.

	Counting error (ppm) 1 S.D.		Lower limit of detection (ppm)	
	Mo Tube	W Tube	Mo Tube	W Tube
Sr	0.51-1.69	0.87-3.11	1.46-1.97	2.58-3.75
Rb	0.53-1.11	0.88-1.81	1.59-2.35	2.64-3.86
U	1.23-2.21	2.53-3.73	3.58-4.45	7.57-11.2
Th	1.46-3.02	2.22-3.26	4.16-5.54	6.65-9.66
Pb	1.49-2.11	2.68-3.77	4.25-5.79	7.64-11.2
Ga	0.73-1.07	-	2.11-3.27	-

- not analyzed using W X-ray tube

Barium

Barium net intensity data obtained from the major element analytical run described in the following chapter has been reduced using mass absorption coefficients, i.e. treated as a trace element. Two different sets of m.a.c.s have been used to correct Ba for matrix differences.

In the Geochemistry Department, U.C.T., primary and secondary m.a.c.s calculated at CrK_a and KK_a respectively are used to correct for matrix differences in samples analyzed for Ba on powder pellets. The calibration curves in Figure 3:12 show a linear relationship between concentration and corrected net intensity for the powder pellets but not for the low dilution fusion discs. The use of a m.a.c. calculated at K K_a results in the crossing of two major element absorption edges, namely Ca K and K K but this was necessary to achieve a linear calibration curve for Ba determined on powder pellets for a range of rock types. In basalts and granites, which are the normal rock standards used for calibration, Ba resides in different minerals, consequently mineralogical and particle size effects are important.

In the low dilution fusion discs the mineralogical and particle size effects are eliminated and the dilution of the rock by the flux results in less absorption by Ba. To correct the Ba net intensities for matrix effects the m.a.c. calculated at Sc K_a was correctly used as the secondary m.a.c. The position of the absorption edges in relation to the analyte lines are illustrated in Figure 3:13 and no major element absorption edges are crossed.

Figure 3:12(a). Calibration Curve for Ba using Cr and K m.a.c.s for Powder Pellets.

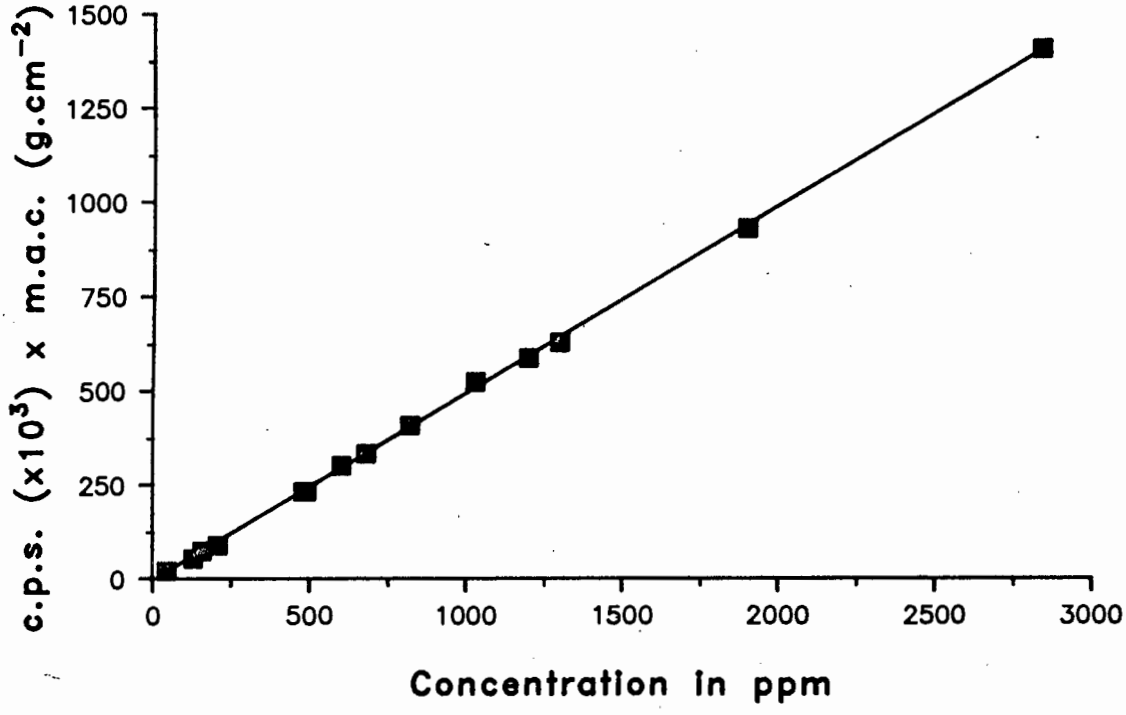

Figure 3:12(b). Calibration Curve for Ba using Cr and K m.a.c.s for Low Dilution Fusion Discs.

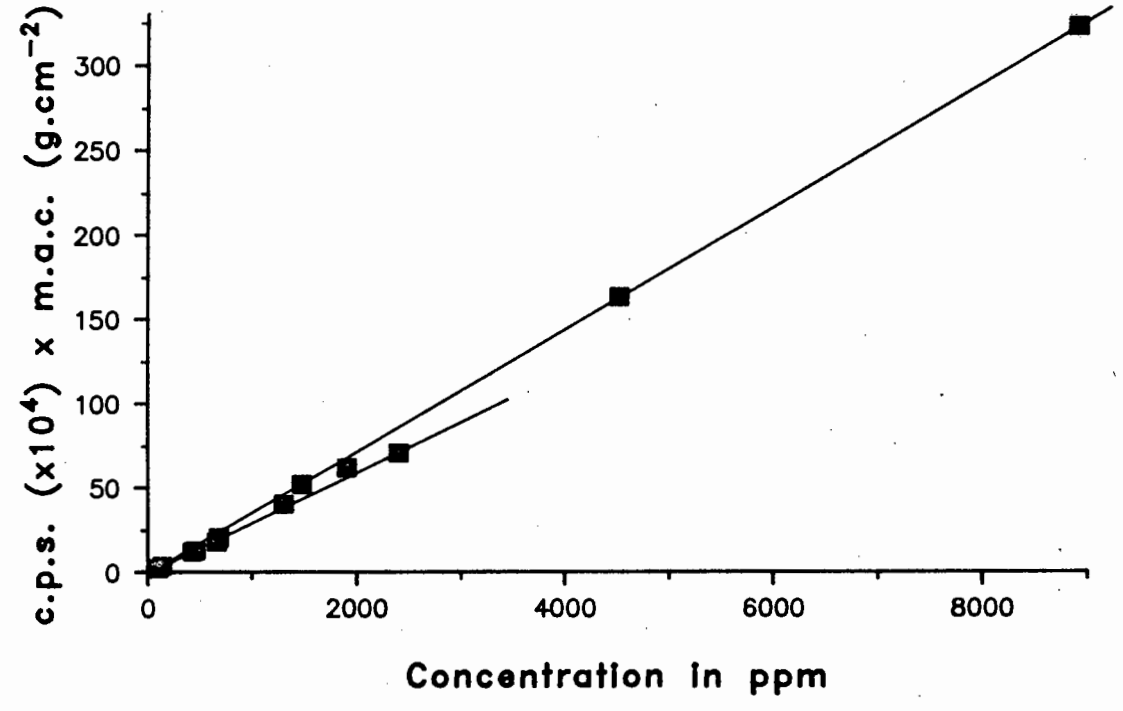

Figure 3:13. Position of the Absorption Edges in relation to Ba L_α Analyte Line.

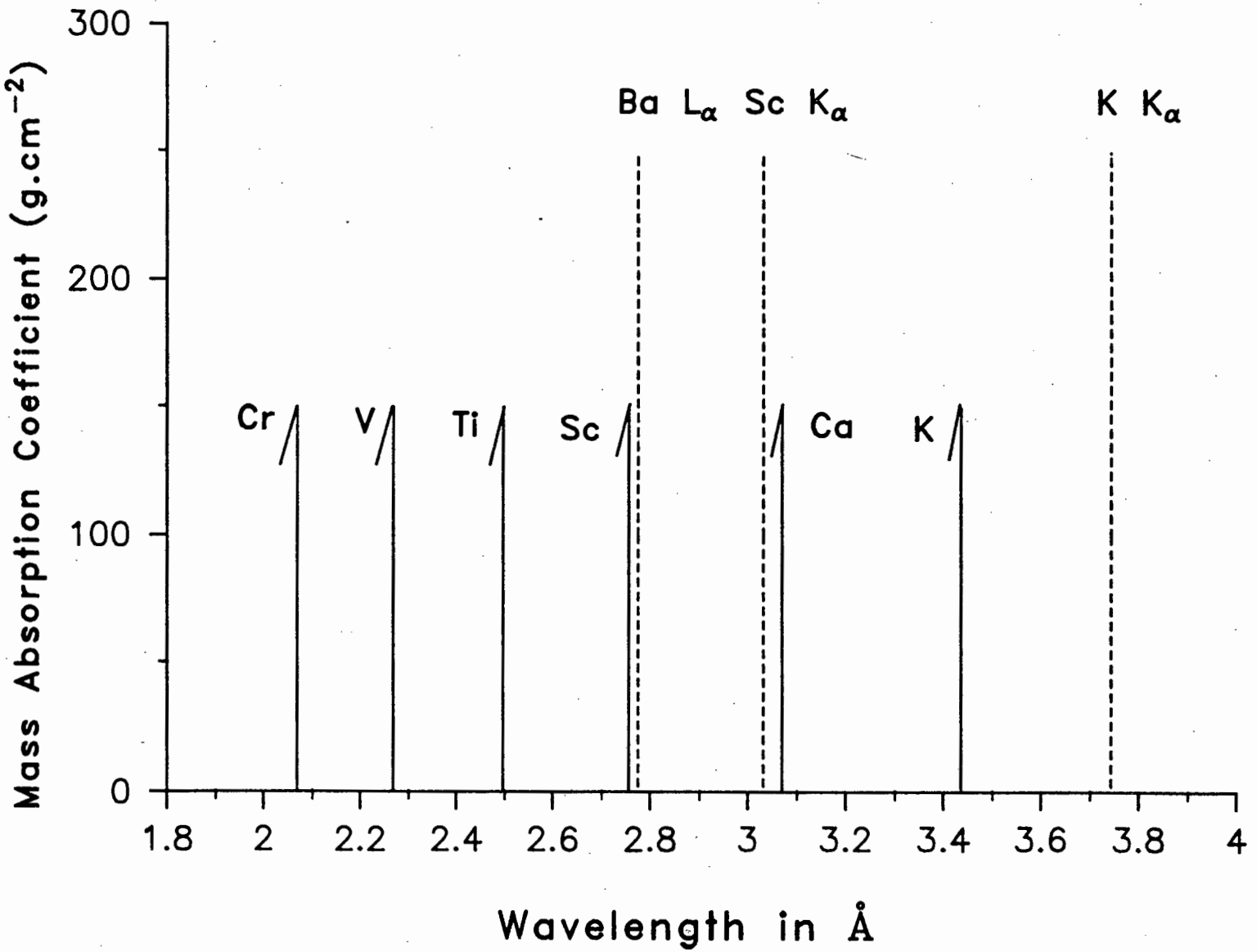

Figure 3:14(a). Calibration curve for Ba using Cr and Sc m.a.c.s for Powder Pellets.

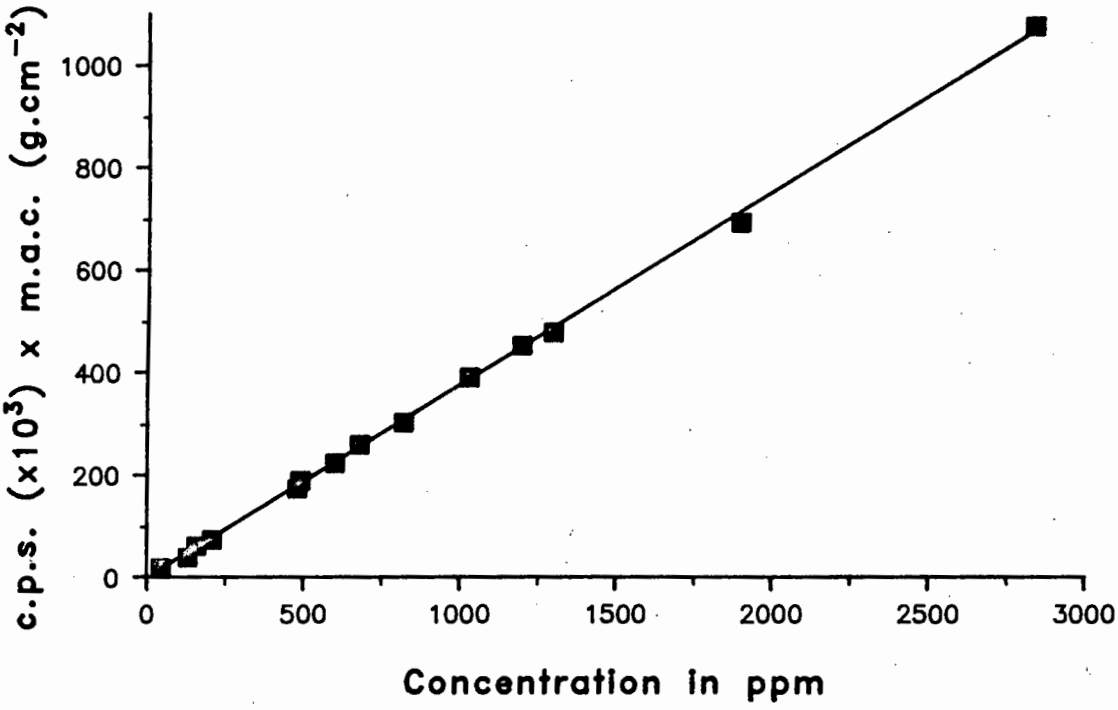

Figure 3:14(b). Calibration Curve for Ba using Cr and Sc m.a.c.s for Low Dilution Fusion Discs.

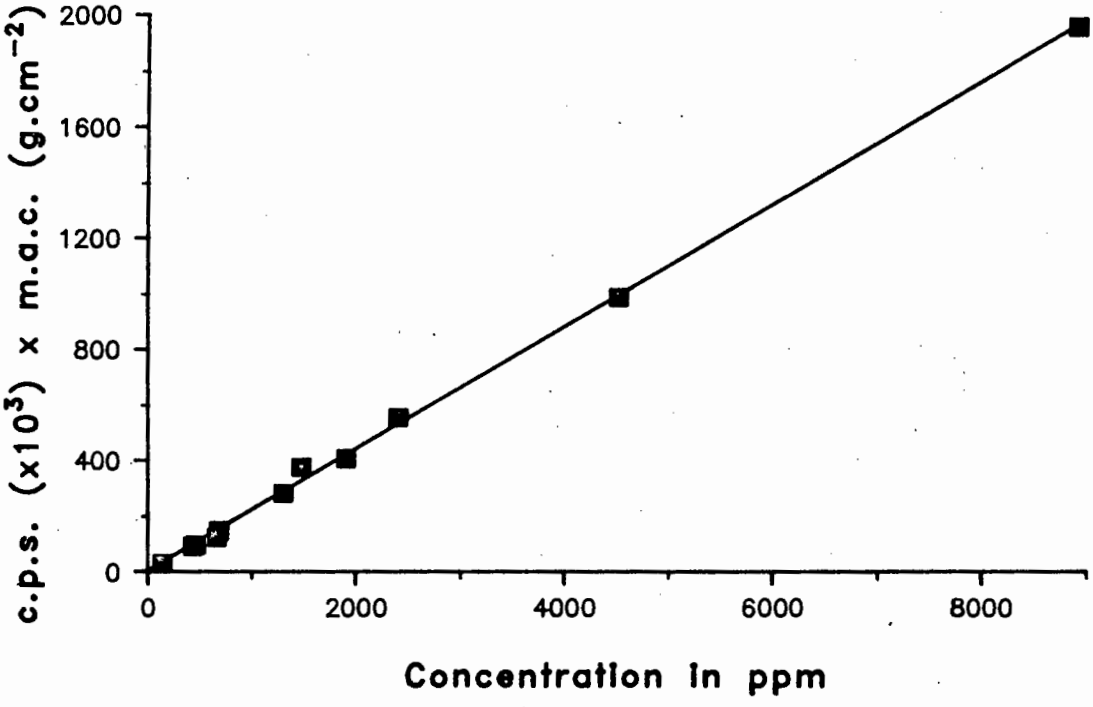

The calibration curves for Ba using Cr and Sc m.a.c.s for the powder pellets and low dilution fusion discs are presented in Figure 3:14. Examination of these curves illustrate that the m.a.c. calculated at Sc gives better results for the fusion discs but slightly worse results for the powder pellets.

Data obtained for the low dilution fusion disc are compared to international standards data in Table 3:24, and lower limits of detection and counting errors are presented in Table 3:26. The determination of barium is discussed further in Chapter 4 where it is treated as a major element and matrix corrections are performed using alpha coefficients.

Table 3:24

Comparison of Ba data obtained from low dilution fusion discs, international recommended values and artificial standards.
(in ppm except NIM-S and artificial standards)

		Barium	Artificial Standards in Wt. % Ba		
BCR-1	(a)	680.			
	(b)	700.	.5% BaO	(a)	0.453%
MRG-1	(a)	49.		(b)	0.455%
	(b)	58.	1% BaO	(a)	0.893%
BHVO-1	(a)	135.		(b)	0.895%
	(b)	134.	2% BaO	(a)	1.797%
G-2	(a)	1900.		(b)	1.792%
	(b)	1906.			
NIM-N	(a)	100.			
	(b)	89.			
NIM-S	(a)	0.27%			
	(b)	0.28%			

(a) international recommended value except for artificial standards.
(b) low dilution fusion discs

Table 3:25

Lower limits of detection and counting errors for Ba determined using conditions outlined in Table 4:1.

	Counting error (ppm) 1 S.D.	Lower limit of detection (ppm)
Ba	1.03-11.55 (0.00-0.00)	2.67-13.47 (0.00-0.00)

Errors and LLD taken from spiked samples (up to 5% BaO)

Figures in brackets refer to pressed powder pellets

Table 3:26

Average relative errors for trace elements determined on low dilution fusion discs for concentrations greater than 20ppm.

	Ave. Rel. Error %	X-ray Tube		Ave. Rel. Error %	X-ray Tube
Nb	4.91	W			
Zr	3.59	W			
Y	2.28	W			
Sr	2.14	W	Sr	2.05	Mo
Rb	2.08	W	Rb	2.01	Mo
U	8.06	W	U	1.07	Mo
Th	5.88	W	Th	1.48	Mo
Pb	11.20	W	Pb	4.42	Mo
			Ga	2.29	Mo
Zn	1.64	Au			
Cu	2.20	Au			
Ni	1.23	Au			
Sc	0.29	Cr			
Co	4.43	W			
Cr	2.56	W			
V	4.26	W			
La	3.87	W			
Ce	2.91	W			
Nd	5.18	W			

Summary

Previous workers have used low dilution fusion discs to determine a limited number of trace elements. Hutton and Elliot (1980) determined Cu, Zn, Rb, Sr, Ba and Pb on low dilution fusion discs containing a heavy absorber, using matrix correction coefficients based on Norrish and Hutton's (1969) work. They obtained relative errors between 4-10 %. Lee and McConchie (1982) determined V, Ni, Cu, Zn, Rb, Sr, Y, Zr, Ba and Pb on low dilution fusion discs using matrix correction factors and the Compton scatter method to correct for matrix differences and obtained errors of about 8%.

This work has shown that low dilution fusion discs can be used for the routine determination of most trace elements that exist in geological samples which are normally analyzed by XRF spectrometry.

The data presented here for the determination of trace elements on low dilution fusion discs generally agree very well with the literature data. Average relative errors for concentrations greater than 20 ppm for the trace elements analyzed are reported in Table 3:26, for most of the trace elements the relative errors are less than 5%.

In most cases, for the trace elements determined on low dilution fusion discs, only slight modifications have been made to the normal analytical procedures used in the Department of Geochemistry, U.C.T. These modifications were necessary due to the high concentration of Ba (up to 2.2% BaO) and higher concentrations of Sr, La, Ce, and Nd in the lamproite and kimberlite samples. The use of a Mo X-ray tube for the

determination of Pb in low dilution fusion discs is advised as the average relative error is approximately one third of the value for Pb analyzed using the W X-ray tube. Consequently the use of this low dilution fusion technique for samples that give preparation problems would be quite simple.

The good reproducibility of data is shown in Table 3:27, the (A) fusion discs of the samples were cast in January, 1985 and the (B) discs in April, 1986. The 1985 discs were analyzed for La, Ce and Nd in that year and the 1985 and 1986 discs were analyzed in April 1986. The data in Table 3:27 indicate that reproducible results can be obtained even after a long period of time.

Data for La, Ce, Nd, Sc, Co, Rb and Th obtained by INAA (Fraser et al 1986, Smith in press) are compared to data obtained using the low dilution fusion discs in Figures 3:15 to 3:21. International standards data from Govindaraju (1984) are also plotted for comparison. On the whole there is relatively good agreement between the different sets of data. Sc, Th and Rb show the most scatter even though there is agreement between the standards data and that obtained from the low dilution fusion discs analyzed by XRF spectrometry. The agreement of the La, Ce and Nd data from the low dilution fusion discs (XRFS) with the data obtained by INAA (Fraser et al 1986, Smith in press) is excellent as normally INAA is a superior method of analyzing these particular elements.

A disadvantage of analyzing trace elements on fusion discs is that the net peak intensity is lower and the background is higher compared to that from powder pellets. This is a direct result of the dilution of the samples by a factor of 3 in the

Figure 3:15. Comparison of INAA, International standards and low dilution fusion disc data for Lanthanum.

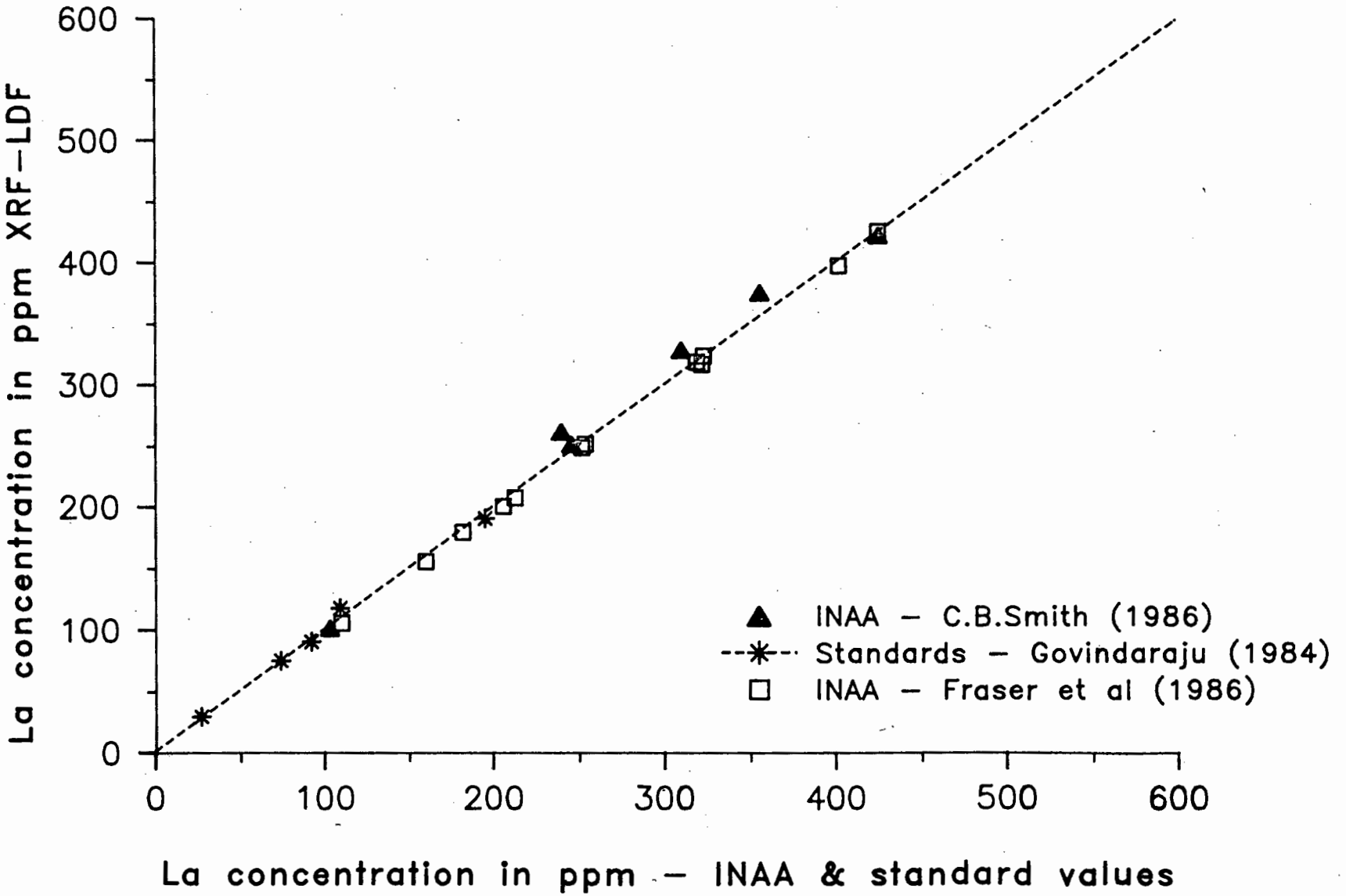

Figure 3:16. Comparison of INAA, International standards and low dilution fusion disc data for Cerium.

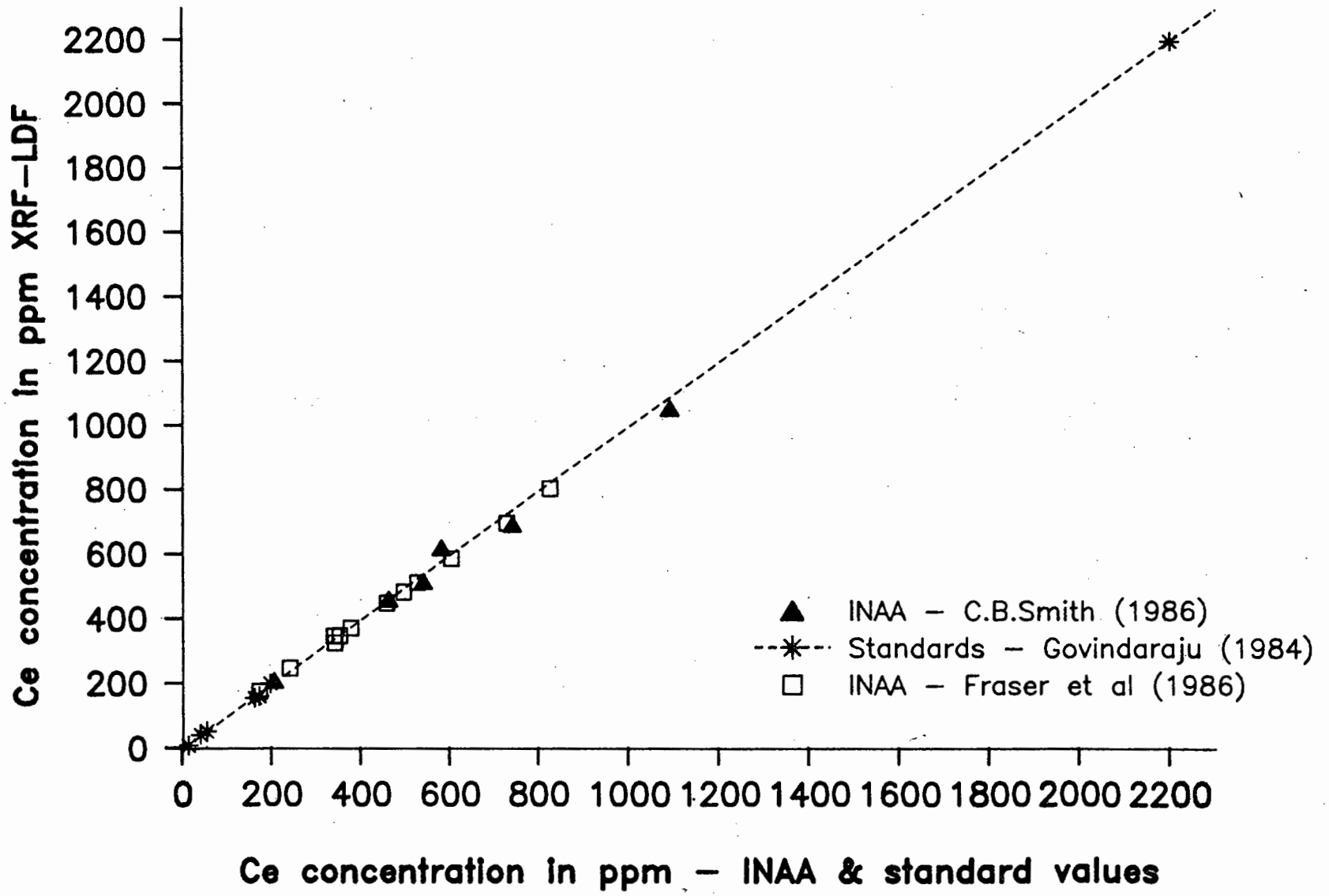

Figure 3:17. Comparison of INAA, International standards and low dilution fusion disc data for Neodymium.

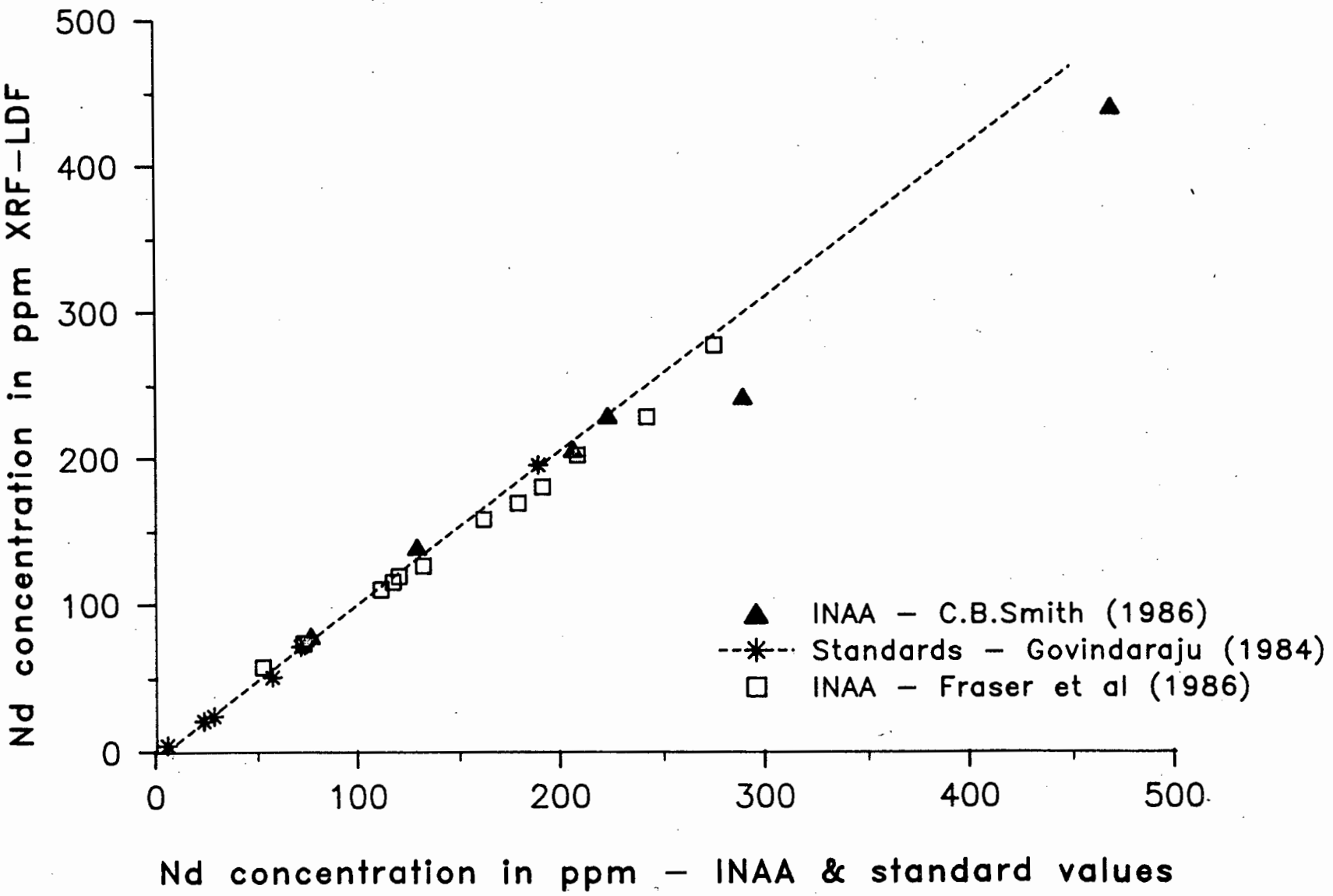

Figure 3:18. Comparison of INAA, International standards and low dilution fusion disc data for Scandium.

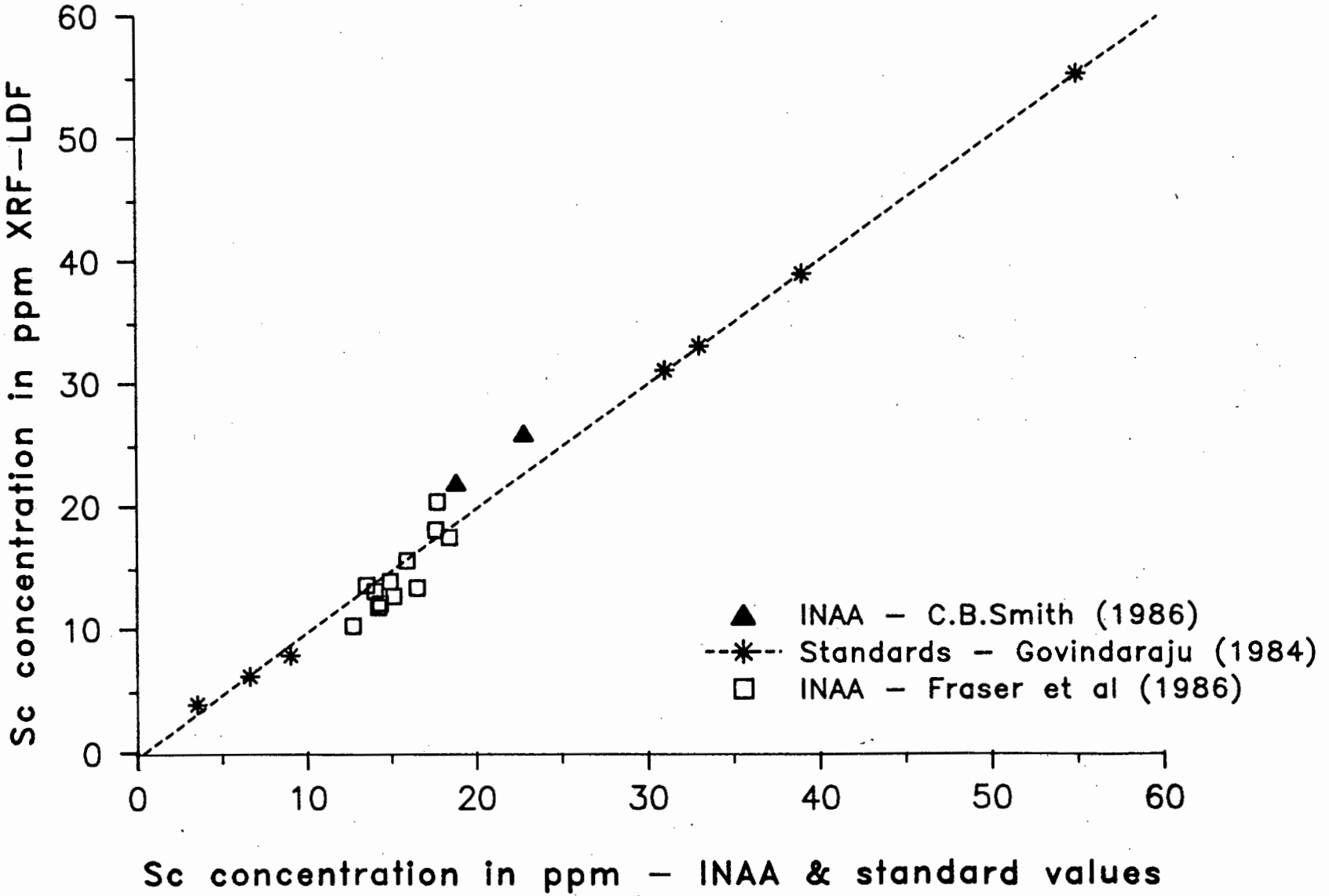

Figure 3:19. Comparison of INAA, International standard and low dilution fusion disc data for Cobalt.

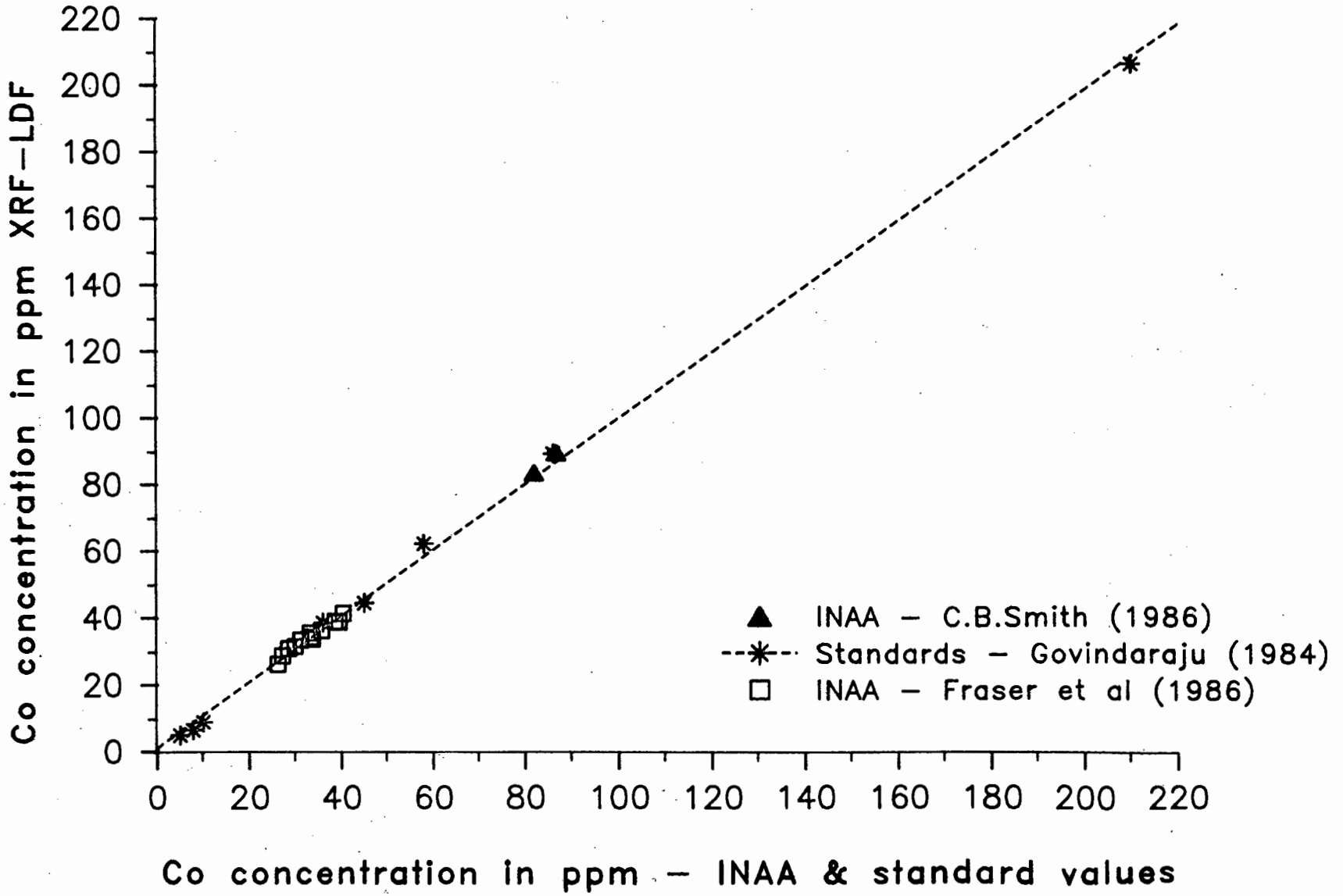

Figure 3:20. Comparison of INAA, International standard and low dilution fusion disc data for Rubidium.

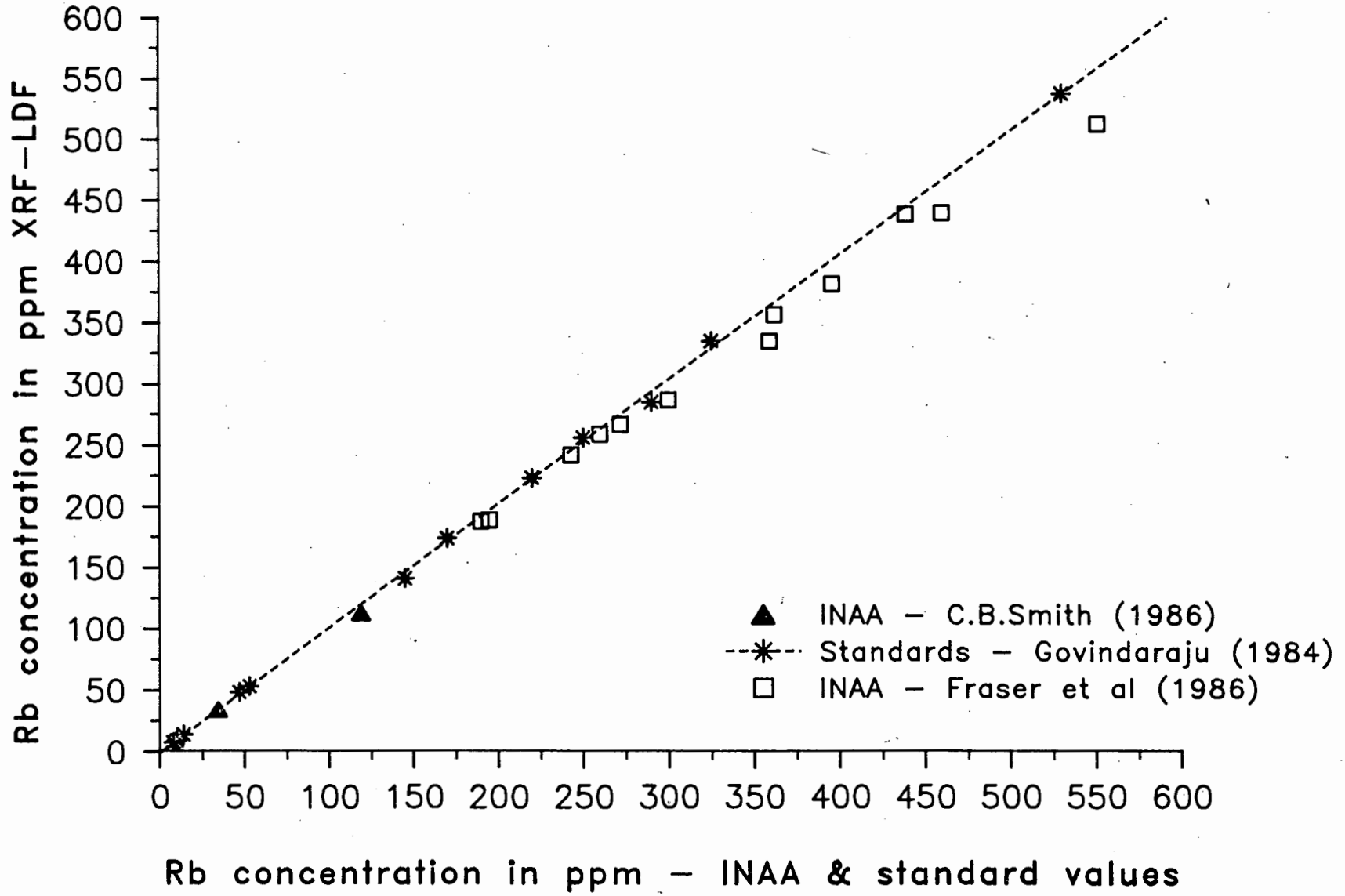

Figure 3:21. Comparison of INAA, International standard and low dilution fusion disc data for Thorium.

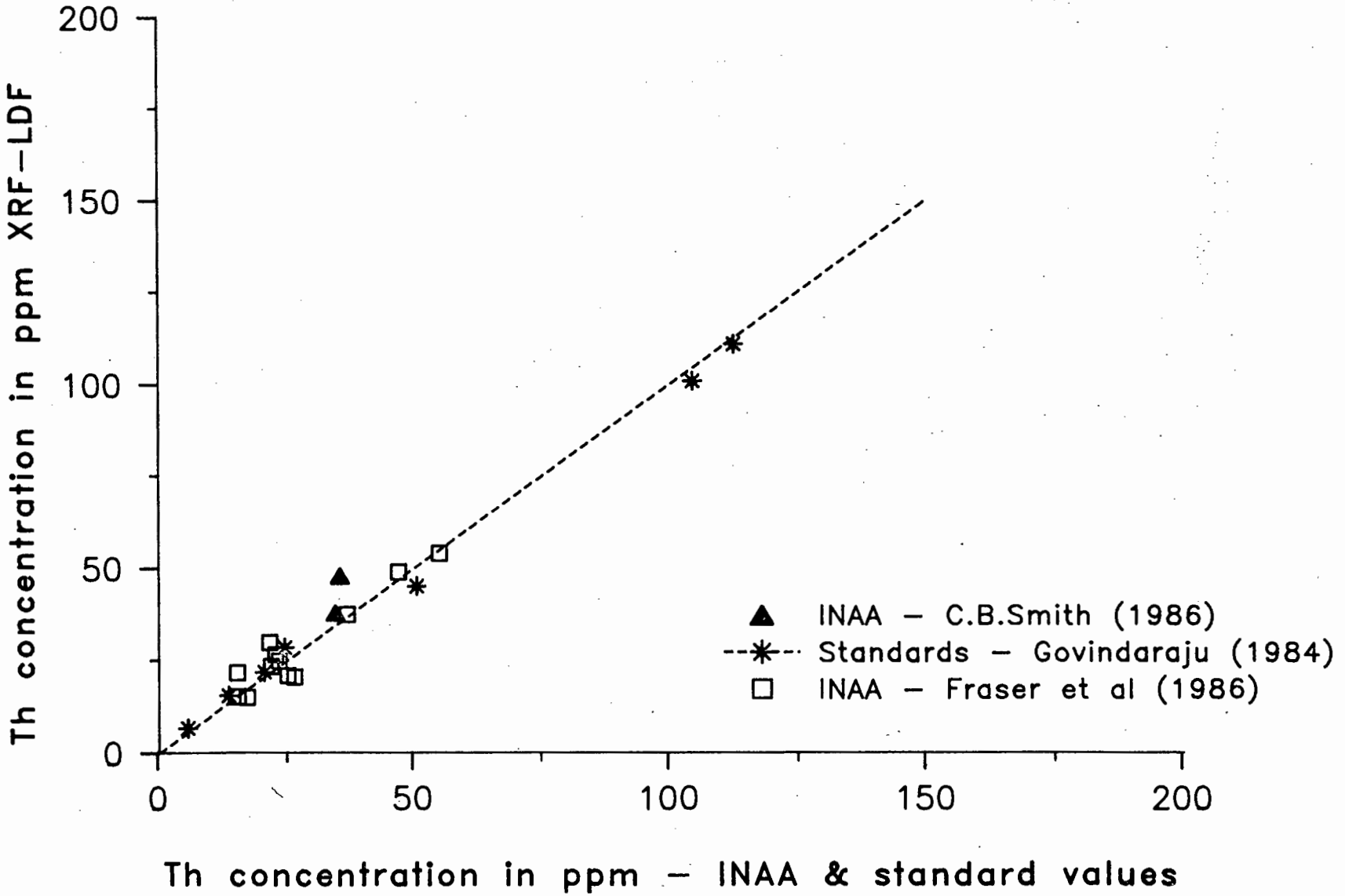

fused disc and the lower m.a.c. of the discs. This also leads to an increase in the lower limit of detection and counting error for all the trace elements as indicated in Tables in the relevant sections.

However, the advantages of using a fused glass disc to determine trace element concentrations in many cases outweigh the disadvantages. The use of a homogeneous glass disc, free from mineralogical and particle size effects is of vital importance for some of the trace elements. The determination of La, Ce and Nd in kimberlites described earlier is a good example of the deleterious effects the mineralogy of the samples can have on XRFS data. Geochemists and geologists are increasingly analyzing the more exotic rock types rather than common basalts and granites, and the use of a fusion technique to analyze for trace elements using international standards for calibration (normally basalts, granites, gabbros etc.) will be necessary to eliminate mineralogical and particle size effects. The use of a low dilution fusion technique also allows the determination of minor and major elements on the same glass disc as discussed in the Chapter 4.

Table 3:27

Reproducibility of La, Ce and Nd results analyzed on low dilution fusion discs.

		K64/55		CKP 9	
		(A)	(B)	(A)	(B)
La	(85)	264.		339.	
	(86)	262.	262.	328.	329.
Ce	(85)	460.		611.	
	(86)	463.	463.	618.	622.
Nd	(85)	139.		236.	
	(86)	138.	139.	229.	229.
Ave Rel Error %		0.71		2.45	

(85) fusion discs analyzed in 1985

(86) fusion discs analyzed in 1986

(A) discs cast in 1985 (January)

(B) discs cast in 1986 (April)

Further Research

The work reported here has suggested a number of problems that require further research :

1) To investigate infinite thickness for the short wavelength elements. Bower and Valentine (1986) have used 10g fusion discs in a 2:1 flux:sample ratio. This may also solve the loss on fusion problems that occur with rock samples with very low volatile content.

2) To investigate the background positions especially when dealing with elements in the range Mo-Pb where the background interferences are critical.

3) To investigate whether the interference standards containing 2000 ppm of the analyte are having the required effect on samples with concentrations of some of the analytes in excess of 5000 ppm.

CHAPTER 4

MAJOR ELEMENT ANALYSIS

MAJOR ELEMENT ANALYSIS

Introduction

Instrumental and analytical conditions for the determination of the twelve oxides - Fe_2O_3, MnO, TiO_2, BaO, CaO, K_2O, SO_3, P_2O_5, SiO_2, Al_2O_3, MgO and Na_2O are detailed in Table 4:1 approximate analysis time for a sample, with two counting cycles, is 1.25 hours for the twelve oxides.

The intensity of the analyte line is subject to influence by other matrix elements and by systematic and random errors. Random errors can be reduced to acceptable limits if counting times are sufficiently long and the spectrometer is well designed. Systematic errors resulting from detector dead time and spectral overlap may be significant. These errors are instrument dependent and need to be completely separated from the matrix dependent terms so that they are not associated with influence/matrix or alpha coefficients which are governed by different physical laws. The curves in Figure 4:1 (taken from Jenkins, 1980) show the different characteristics of matrix and instrumental effects on the relationship between concentration and intensity.

Various artificial and international rock standard low dilution fusion discs were scanned, using the appropriate analytical conditions for the various elements, to determine background angular positions and to search for any spectral interferences especially from Ba, La, Ce, and Nd. The background angular positions had to be checked carefully as the major element

Figure 4:1. Basic Shapes of Intensity/Concentration Curves. (after Jenkins 1980)

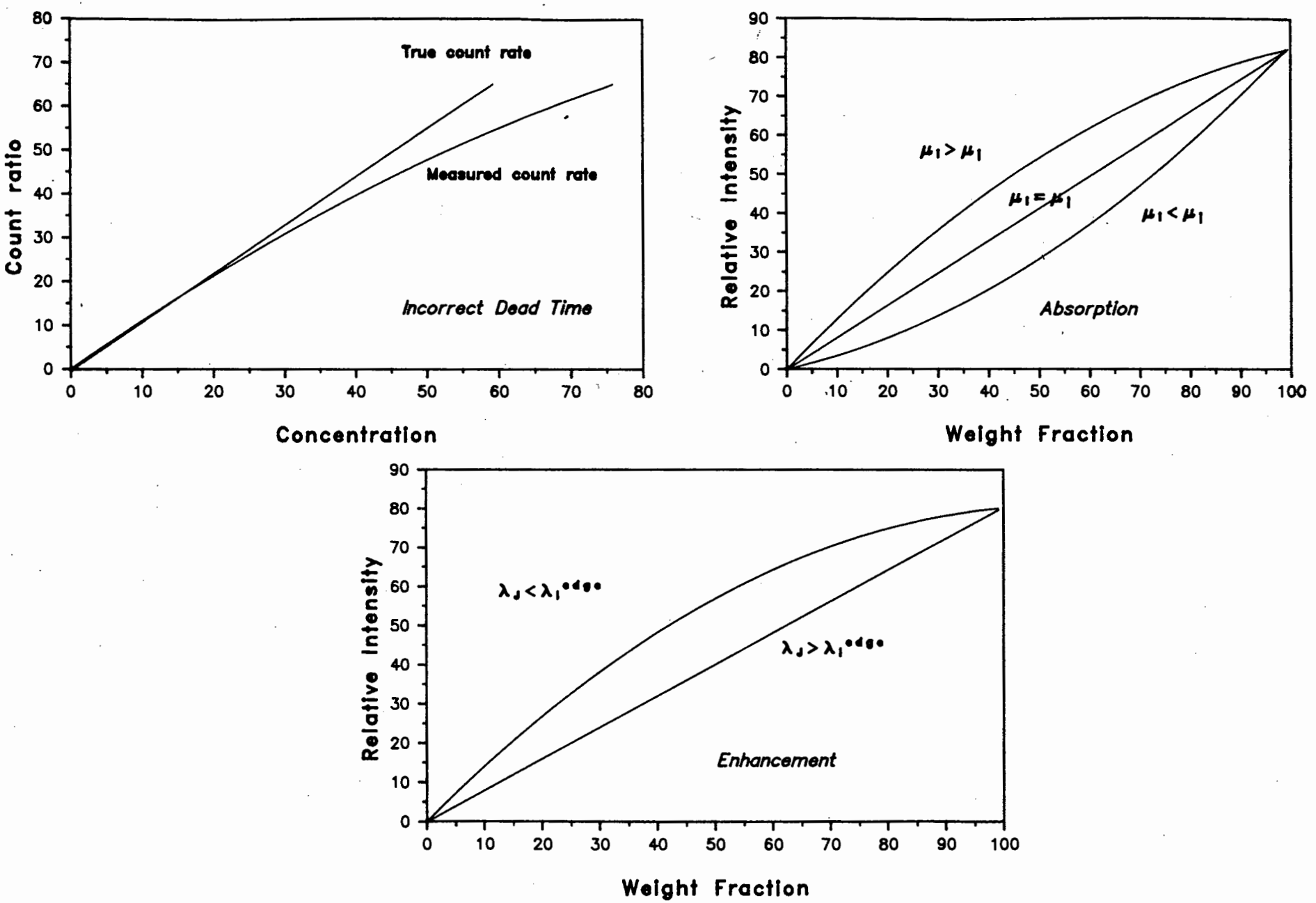

Table 4:1a

Analytical conditions for the determination of the 12 major element oxides using Philips PW 1400 XRF spectrometer with a Cr X-ray tube operating at 50 kV and 55 mA.

	Time (s)	Coll	Det	Xtal	UPL	LWL	Peak Angle (°2θ)	Background +off* (°2θ)	Background -off* (°2θ)
FeKa	16	Fine	FC	LiF220	75	15	85.785	4.540	-
MnKa	160	Fine	FC	LiF220	70	12	95.265	7.815	4.940
TiKa	16	Fine	FC	LiF200	75	25	86.195	-	5.195
BaLa	80	Fine	FC	LiF200	75	25	87.220	7.785	6.220
CaKa	16	Fine	FC	LiF200	75	25	113.180	3.500	5.100
K Ka	16	Fine	FC	LiF200	75	25	136.705	3.400	-
S Ka	80	Coarse	FC	Ge	72	30	110.825	5.000	5.000
P Ka	80	Coarse	FC	Ge	75	25	141.150	3.940	10.15
SiKa	16	Coarse	FC	InSb	75	25	144.610	-	8.110
AlKa	40	Coarse	FC	PET	75	25	145.110	-	7.110
MgKa	320	Fine	FC	TLAP	62	30	45.115	1.900	4.600
NaKa	160	Coarse	FC	TLAP	62	30	55.080	1.200	1.900

Note:

counting times on background positions were as follows :-

Fe, Ti, Ba, Ca, K and Si	16 seconds
S, P, Al	40 seconds
Mg	160 seconds
Mn, Na	80 seconds

Aluminium filter (0.5mm thick) used for Mn determinations

2 counting cycles

samples analyzed under vacuum

* ± Background angle offset relative to peak angle

Table 4:1b

Possible spectral line interferences on the major elements determined using the analytical conditions outlined in Table 4:1a.

element		Possible spectral line interferences
Ba L_a	-	Ti K_a
Ti K_a	-	Ba L_a
Al K_a	-	Ba L_a(3)
P K_a	-	Zr $L_{a1,2}$ (background positions)
Mn K_a	-	Cr X-ray tube lines (Al filter)

oxide run for the Norrish and Hutton (1969) type fusion discs used in the Geochemistry Department, U.C.T. does not count on background positions.

In the departmental run, using the Norrish and Hutton (1969) technique , backgrounds are calculated for all elements using the intensity from a blank at the peak positions.

Wavelength scans in Figures 4:2 - 4:4 show the various problems encountered. The careful choice of background positions is extremely important when dealing with rocks containing unusual concentrations of trace elements. This is illustrated in Figure 4:2 where $ZrL\alpha_{1,2}$ interferes on the originally chosen background position. The mutual interference of $BaL\alpha$ and $TiK\alpha$ is shown in Figure 4:3, and the interference of third order $BaL\alpha$ on $AlK\alpha$ in Figure 4:4. Joslin and Salt (1985) also report on the indirect interference of a barium escape peak on $AlK\alpha$ when using argon - methane gas in the flow counter. Barium is determined in the analytical run so corrections for these interferences can be made.

Several blank discs (100 % SiO_2 and 100 % Al_2O_3) and artificial standards (0.5 % BaO + 99.5 % SiO_2, 1 % BaO + 99 % SiO_2, 2 % BaO + 98 % SiO_2, 1 % P_2O_5 + 99 % SiO_2 5 % P_2O_5 + 95 % Si 5 % TiO_2 + 95 % SiO_2) were analyzed. Blanks used for the various elements are given in Table 4:2.

The elements - Fe, Ca, K, S, P, Si, Mg and Na are not affected by spectral interferences and the raw intensities were only corrected for instrumental drift, detector dead time and backgrounds. For Mn an aluminium filter was used to reduce the spectral interference from the Cr X-ray tube lines. The other elements - Ba, Al, and Ti have to be corrected for the line

Figure 4:2. Interference of Zr on P background positions.

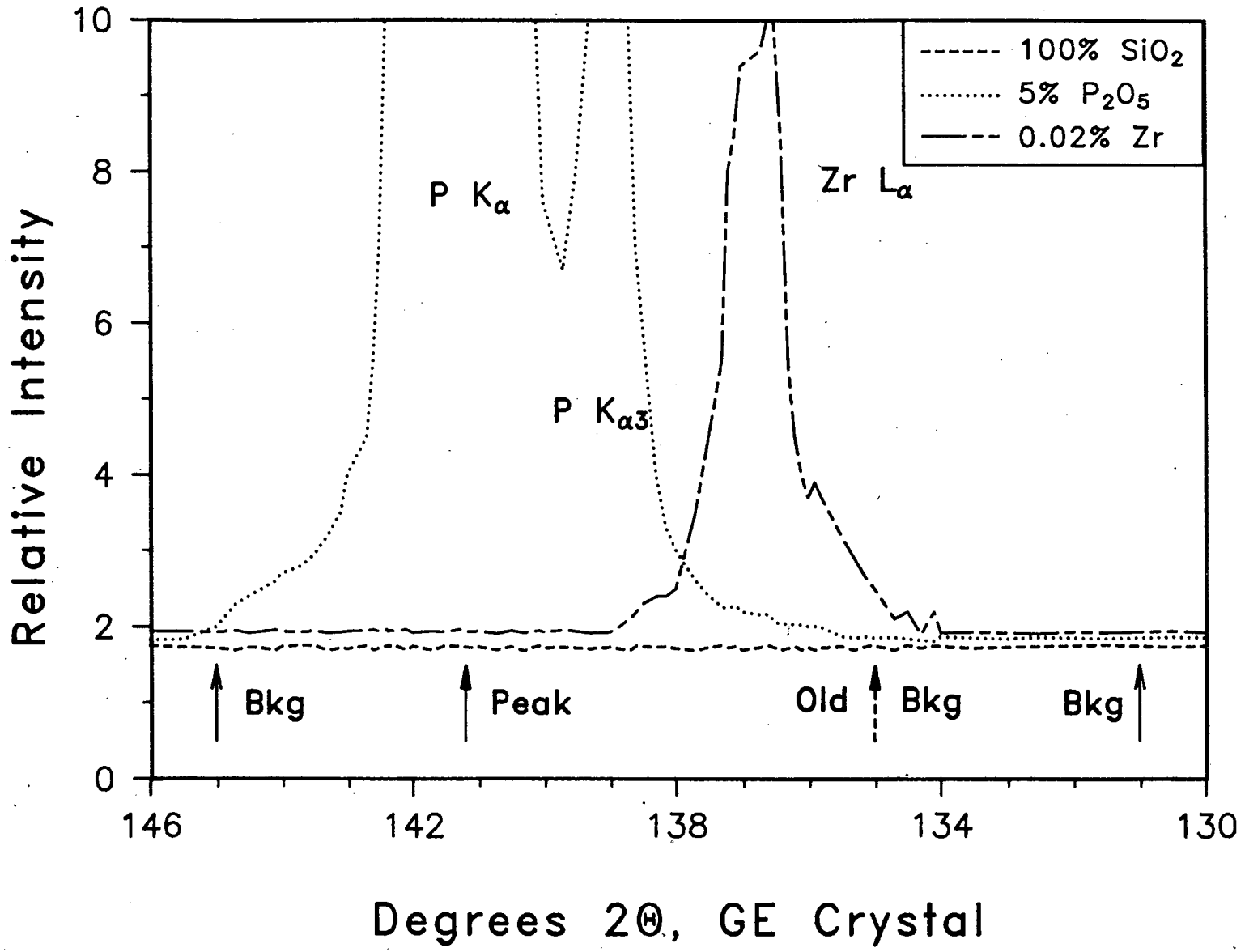

Figure 4:3. Wavelength scan showing mutual interference of Ba L_α and Ti K_α.

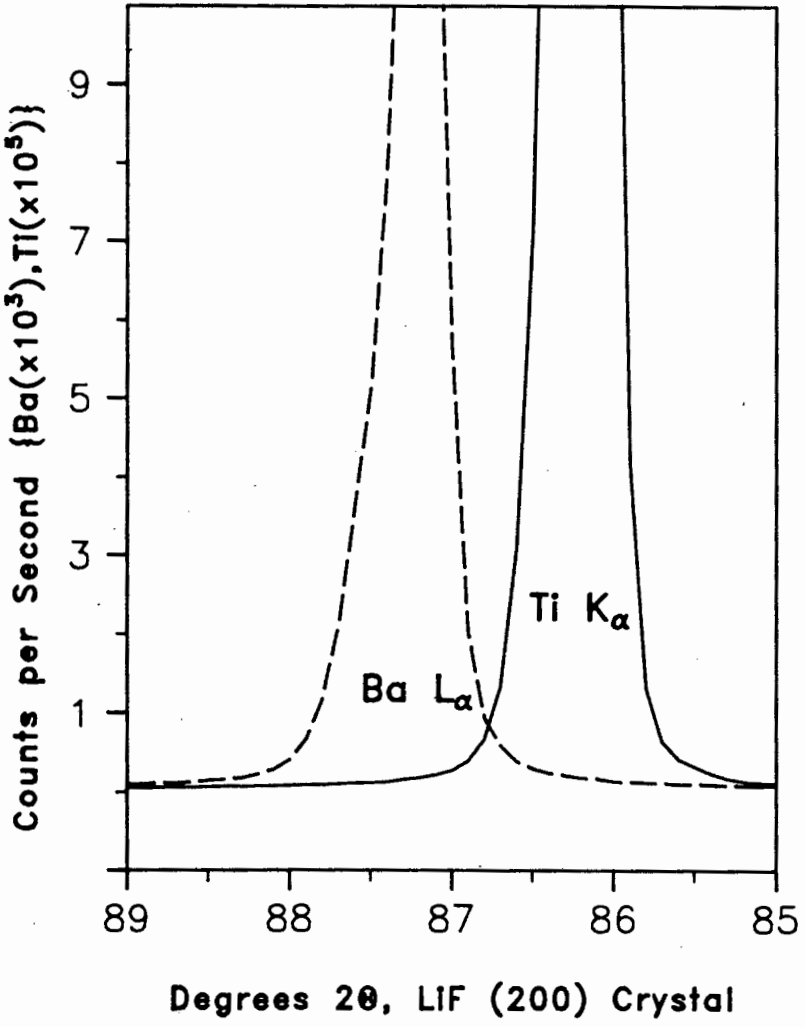

Figure 4:4. Wavelength scan showing interference of Ba $L_\alpha(3)$ on Al K_α

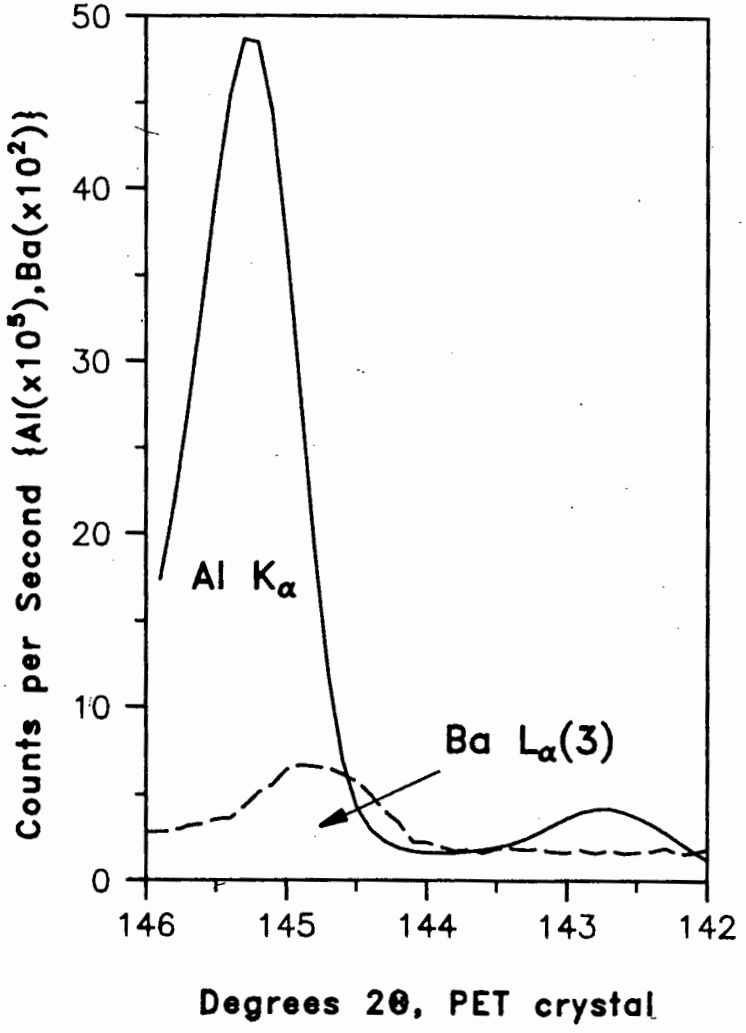

overlaps described previously. For these elements, Ba and Ti interference standards were analyzed so that the relevant interference factors could be calculated.

In the Norrish and Hutton (1969) major element oxide technique currently used in the Geochemistry Department, U.C.T., interference correction factors are used to correct for crystal fluorescence and/or spectral overlap. These factors are used to calculate interference in weight percent which is subtracted from the concentration of the oxide of interest after iteration using matrix correction factors. Crystal fluorescence is corrected for in the analysis of low dilution fusion discs by measuring analyte peak and background intensities, and then background correcting the peak, as the effect of crystal fluorescence is to increase the background.

Table 4:2

Summary of blank fusion discs used for the calculation of background factors.

Blank	Elements
100 % SiO_2	Fe, S, P, Na, Ti, Ba, Al
100 % Al_2O_3	Na, P, Si, Mg
5 % TiO_2	Fe, Mn, K, S, P, Na
1 % P_2O_5	Mn
5 % P_2O_5	Mn, Ca

Note: For some elements more than 1 blank was used to calculate the background factors. The 100 % SiO_2 blank was not used for the Ca and K background factors as this blank had exceptionally high factors indicating Ca and K impurities.

Relationship between Intensity and Concentration in major element oxide analysis.

In X-ray fluorescence spectrometry there are three basic types of mathematical correction models to correct for matrix effects and convert measured intensities to concentrations. These are (a) fundamental algorithm approach (Criss et al. 1978., Rousseau 1984a+b,), (b) concentration correction method (Lachance and Traill, 1966; Claisse and Quintin, 1967); and (c) intensity correction method (Lucas-Tooth and Pyne, 1963). For multi-element analysis the general forms of the equations for models (b) and (c) are given in Table 4:3. The Lucas-Tooth and Pyne (1963) method using intensities has severe drawbacks as it is spectrometer dependent and is only applicable over relatively limited concentration ranges. Consequently this method has limited use for the low dilution fusion discs in which the concentration ranges are relatively large.

The fundamental algorithm approach until recently required extensive computer facilities. The algorithms are derived directly from Sherman (1955) and Shiraiwa and Fujino (1968) basic equations relating X-ray fluorescence intensity from a sample to its composition. Criss et al. (1978) and more recently Rousseau (1984) fully explain the theory behind the fundamental algorithm approach. Rousseau (1984) established a fundamental algorithm relating concentration to intensity which corrects for all matrix effects.

Table 4:3

Mathematical correction models relating intensity to concentration.

Lachance-Traill (1966)

$$W_i = R_i' \left[k_i + \sum_j \alpha'_{ij} W_j \right] - B_i$$

where R_i' = intensity ratio relative to a reference standard.

B_i = background term in %

note α_{ij} term is used where concentration (W) of element j is used for correction (**alpha** coefficient).

Lucas-Tooth & Pyne (1963)

$$W_i = R_i' \left[k_i + \sum_j k_{ij} I_j \right] - B_i$$

note K_{ij} term is used where intensity (I) of element j is used for correction (**influence** coefficient)

Alpha Coefficients

For the accurate determination of major element oxides, the apparent concentrations are corrected for interelement effects using alpha coefficients. An alpha coefficient corrects for the absorption and enhancement effects of the matrix element on the analyte element. The term α_{ij}, referred to as the alpha coefficient, is a constant that expresses the direction and relative strength of the effect of element j on the concentration of element i, positive terms indicate absorption and negative terms enhancement. Enhancement tends to be less important than absorption in the analysis of geological materials and can be considered as negative absorption. The enhancement of analyte intensities is of greater importance in the analysis of alloys, a classic example being the enhancement of Cr by Fe.

Dilution of the sample by flux and the use of heavy absorbers, e.g. lanthanum oxide, partially suppress the interelement effects by strong absorption of the primary and secondary X-ray radiation. This partial suppression of the interelement effects leads to a linearisation of the calibration curve and permits a broad range of measurements independent of the matrix.

Lachance (1979) explains fully the family of alpha coefficients. A basic alpha coefficient is one that describes the relationship between the weight fraction of an element and the intensity relative to the pure element. A modified alpha coefficient is one in which the relative intensity is expressed in terms of a standard or standards rather than the pure element. In rock analysis, a variation of the modified alpha is used. Generally rock analysis involves the fusion of a powdered sample in a

fixed sample to flux ratio to produce an homogeneous glass disc. With geological materials, analysts usually prefer to work with oxides. 'Oxide alphas' are a hybrid member of the alpha family. Conversion from the basic alpha to oxide hybrid is seen as a two stage process. The basic alphas, including α_{ij} where **j** is equal to oxygen, are modified to compensate for the fact that intensities are relative to pure oxide and not pure element. Then the weighted contribution of both modified alphas is added to obtain the oxide alpha. The contribution for oxygen is the difference in oxygen concentration between oxide **j** and oxide **i**. Consequently for a fused rock sample doubly modified hybrid alpha coefficients are used. The use of a loss factor to account for LOI or LOF adds a further modification to the alpha coefficients.

Alpha coefficients can be determined by multiple regression analysis, graphically, experimentally from artificial standards, calculation from mass absorption coefficients, and from fundamental algorithms.

In multiple regression analysis and the graphical method, intensity measurements on a series of standards are required. These intensities are then used to give best fit of slope, background and the alpha coefficient constants. In multiple regression analysis the influence of all analyzed elements on the X-ray intensity from the analyte element are evaluated simultaneously.

Alpha coefficients are referred to as empirical constants, but they do have a theoretical basis and can be calculated using the following equation :-

$$\alpha_{ij} = \frac{\mu_j(\lambda_e) + A\mu_j(\lambda_i)}{\mu_i(\lambda_e) + A\mu_i(\lambda_i)}$$

where e = effective wavelength
μ_i = m.a.c. of analyte element
μ_j = m.a.c. of interfering element
A = geometric constant (spectrometer specific)

This equation illustrates the simple binary case, and the term involves primary and secondary absorption coefficients and a geometric constant, A, calculated from the geometry of the spectrometer. This α_{ij} term can be modified according to Lachance's (1979) alpha coefficient 'family' for dilution by flux and for elements determined as oxides.

The experimental determination of alpha coefficients is a long and tedious process, and can easily yield values that have no physical meaning (Rousseau 1984). Binary artificial standards at various concentrations are required from which the intensities are measured and related to intensities of pure elements. Norrish and Hutton (1969) reported experimental data for the departure of fluorescent intensity of Si K_a in different artificial standards from that in pure SiO_2 and compared calculated and experimentally determined alpha coefficients. In many cases these two sets of data were in disagreement as the authors did not consider absorption of the primary beam. The Norrish and Hutton (1969) method of calculation of alpha coefficients is discussed in detail later.

The determination of alpha coefficients from fundamental parameters (Criss et al., 1978; de Jongh,1973; Rousseau, 1984 and Tao, Pella and Rousseau, 1985) are generally based on Sherman (1955) and Shiraiwa and Fujino (1968) theoretical formalism which permits the calculation of X-ray intensity emitted by an element in a specimen of known concentration. The fundamental parameters required to calculate alpha coefficients are: (1) mass absorption coefficients; (2) fluorescent yields; (3) absorption edge jump ratios; (4) analyte wavelengths; (5) absorption edge wavelengths, and (6) the spectral distribution of primary radiation from the X-ray tube.

de Jongh (1973) calculated alpha coefficients from fundamental parameters. The α_{ij}'s are calculated using partial derivatives of the Sherman equation and the alpha coefficients are only valid over limited concentration ranges and for specific sample types.

Lachance (1981) showed how the parameters geometry, operating voltage, mass absorption coefficients and polychromaticity of primary radiation combine in the generation of alpha coefficients. He also introduced a new alpha coefficient algorithm that contained three different alpha coefficients. This is based on the fact that the alpha coefficients change with weight fraction of element i and that this change occurs at different rates. Lachance (1981) described the alpha coefficients as follows :-

α_1 - at the $W_i = 1.0$ limit

α_2 - at the $W_i = 0.0$ limit

α_3 - rate of decrease from $W_i = 1.0$ to $W_i = 0.0$

The three alpha coefficients are combined in the following equation :

$$\alpha'_{ik} = \alpha_1 + \frac{W_m \alpha_2}{1 + \alpha_3 - W_m \alpha_3}$$

where W = weight fraction
m = sum of all elements except i

This is referred to as the basic alpha algorithm. Modifications "family". The use of the three alpha coefficients means that this algorithm is valid over the complete concentration range.

It is important to remember that theoretically determined alpha coefficients by any of the above mentioned methods only provide the general relationship of matrix influences on the analyte. Consequently it is of vital importance to use well characterized standards to obtain good results.

Previous calculation procedures for low dilution fusions.

Low dilution fusion techniques for the determination of major element oxides in geological samples have been documented by Haukka and Thomas (1977), Hutton and Elliot (1980) and Lee and McConchie (1982).

Haukka and Thomas (1977) calculated theoretical matrix correction factors for their low dilution fusion disc system from tabulated m.a.c.s values of Heinrich (1966), normalized them to a reference standard and modified them according to certain predicted effects (enhancement and primary beam absorption).

factors reported were all positive and included a flux constant and factors for BaO and SO_3 effects on the major elements but not for the effects of the major elements on Ba and S. They then used a technique called computer-assisted-matrix-fitting (CAMF) which involved an iterative process of plotting differences, changing parameters and re-running original intensity data. The basic equation relating intensity to concentration used by Haukka and Thomas (1977) was:

$$C_i = R_i C_{i,ref} \left(K_{if} + \sum_{j=1} \alpha_{ij} W_j \right) - B_i$$

where K_{if} = mass absorption contributed by flux which is a constant

R_i = total (peak + background) intensity ratio of component i to Reference Standard

$C_{i,ref}$ = nominal percentage of i in reference

W_j = weight fraction of component j in specimen, unignited basis (successively estimated during iterative process)

B_i = background concentration which is constant for all samples

Hutton and Elliot (1980) calculated theoretical matrix correction factors for the low dilution fusion discs using the Norrish and Hutton (1969) method which is discussed in detail later.

Lee and McConchie (1982) used alpha coefficients that had been recalculated from 'delta' coefficients derived by de Jongh (1973) for 1:10 sample to lithium tetraborate fusions. The initial theoretical values calculated by Lee and McConchie (1982) were large, and the recalculated alpha factors slowly increased in magnitude to a dilution factor of 5, after which

the changes accelerated. Consequently Lee and McConchie (1982) used an empirical approach by theoretically calculating the alpha factors for a dilution factor of 5 using de Jongh's (1973) method and then obtained alpha factors for a dilution ratio of 3.02 using the following equation :-

$$\alpha_{ij}^{3.02} = \alpha_{ij}^{5.0} * \frac{5.0}{3.02}$$

The alpha coefficients reported were all positive and no barium or loss factors were given. Loss from a sample is eliminated in de Jongh's (1973) method of alpha coefficient calculation.

The incomplete, with regard to the proposed low dilution technique, sets of alpha coefficients produced by Haukka and Thomas (1977), and Lee and McConchie (1982) rendered these unusable in this work. De Jongh's (1973) coefficients are available only on a commercial basis in the form of a program called ALPHA.

Consequently three different methods of generating alpha coefficients were investigated and their results will be discussed and compared. It should be noted that the lack of heavy absorber and the low dilution ratio in this method has drastically increased the matrix effects and degree of correction required. These effects have been documented elsewhere by other workers (Bower and Valentine, 1986; Norrish, pers comm.)

The three methods investigated were :-

(1) A computer program called XRF4 which corrects for interelement effects using multiple regression analysis. (U.S.

Dept of Interior, Information Circular 8712).

(2) The Norrish and Hutton (1969) method, using programs XRF01 and MAJOR (Geochemistry Department, U.C.T.) with alpha coefficients theoretically calculated and the two programs modified to suit the composition of the low dilution fusion discs.

(3) A computer program called NBSGSC (Tao, Pella and Rousseau, 1985, NBS Technical Bulletin 1213) which calculates alpha coefficients from fundamental parameters and uses the Lachance and Claisse (1980) alpha coefficient algorithm (COLA) to convert intensities to concentrations.

The program NBSGSC and papers referred to by this program were only obtained by the investigator after methods 1 and 2 above had already been extensively evaluated.

Multiple Regression Analysis - Program XRF4

XRF4 is a computer program written in Basic by Marr (1976) and is available from the U.S. Department of Interior, Information Circular 8712. The original program was rewritten in Fortran and extensively modified by J.P. Willis in 1982 to suit the computer facility and the analytical requirements of the Geochemistry Department, U.C.T.

The program uses concentrations and net intensities of standards to calculate alpha factors through multiple regression analysis. Multiple regression analysis is a logical extension of simple regression analysis and the influences of all the analyzed elements on the X-ray intensity from the analyte element are calculated simultaneously. Various models relating concentration to intensity can be used from a simple linear regression model, to models such as Lucas-Tooth and Pyne (1963), Lachance-Traill (1966), Rasberry-Heinrich (1974) and Claisse-Quintin (1967). The program is designed to allow various options for the treatment of the X-ray data. For example the analyst can choose which standards and regression constraints to use, and whether to use gross or net peak intensities. Consequently for each element the regression constraints, standards and model can be changed. In some models, for example Lachance-Traill (1966), a loss correction can be made as the alpha coefficients are calculated using concentrations. The dilution ratio or composition of the flux are not taken into account.

Input to the program consists of concentration data for standards and corresponding net intensities after correction for systematic errors described previously. The program allows for a choice of suitable standards for each analyte element to generate a best fit calibration curve. The accuracy of both

concentration values and measured intensities are poor for very low concentrations and such values were therefore excluded from the calculations. Generally standards with less than 0.5% of the analyte element were omitted. For some elements it was necessary to obtain the initial slope of the calibration curve using the simple linear regression model (no interelement corrections). The coefficient generated by this model for the analyte is then stored and subsequently used in the Lucas-Tooth and Pyne (1963) or the Lachance-Traill (1966) models.

Concentrations for unknown samples were calculated using either Lucas-Tooth and Pyne (1963) or the no-correction model. These models give a reasonable estimate of the concentration which can be further refined by using one of the other more complex models.

The Lucas-Tooth and Pyne (1963) model described earlier, calculates the concentrations by using the intensities to correct for interelement effects and produce a linear calibration curve. The silica calibration curve, Figure 4:5, illustrates the limited concentration range between 50 - 75 % over which this model gives a linear calibration between concentration and intensity. The iron and calcium calibration curves in Figure 4:6 and 4:7 illustrate that the Lucas-Tooth and Pyne (1963) model is satisfactory over limited concentration ranges. The Lucas-Tooth and Pyne (1963) model gives good correction for absorption effects.

The concentration data for the unknowns from the Lucas-Tooth and Pyne (1963) model and the standards concentration and net intensity data for unknowns and standards was then re-entered to XRF4 and a model that uses concentration to correct for

Figure 4:5 Calibration Curve for SiO_2 using Lucas–Tooth & Pyne (1963) correction model

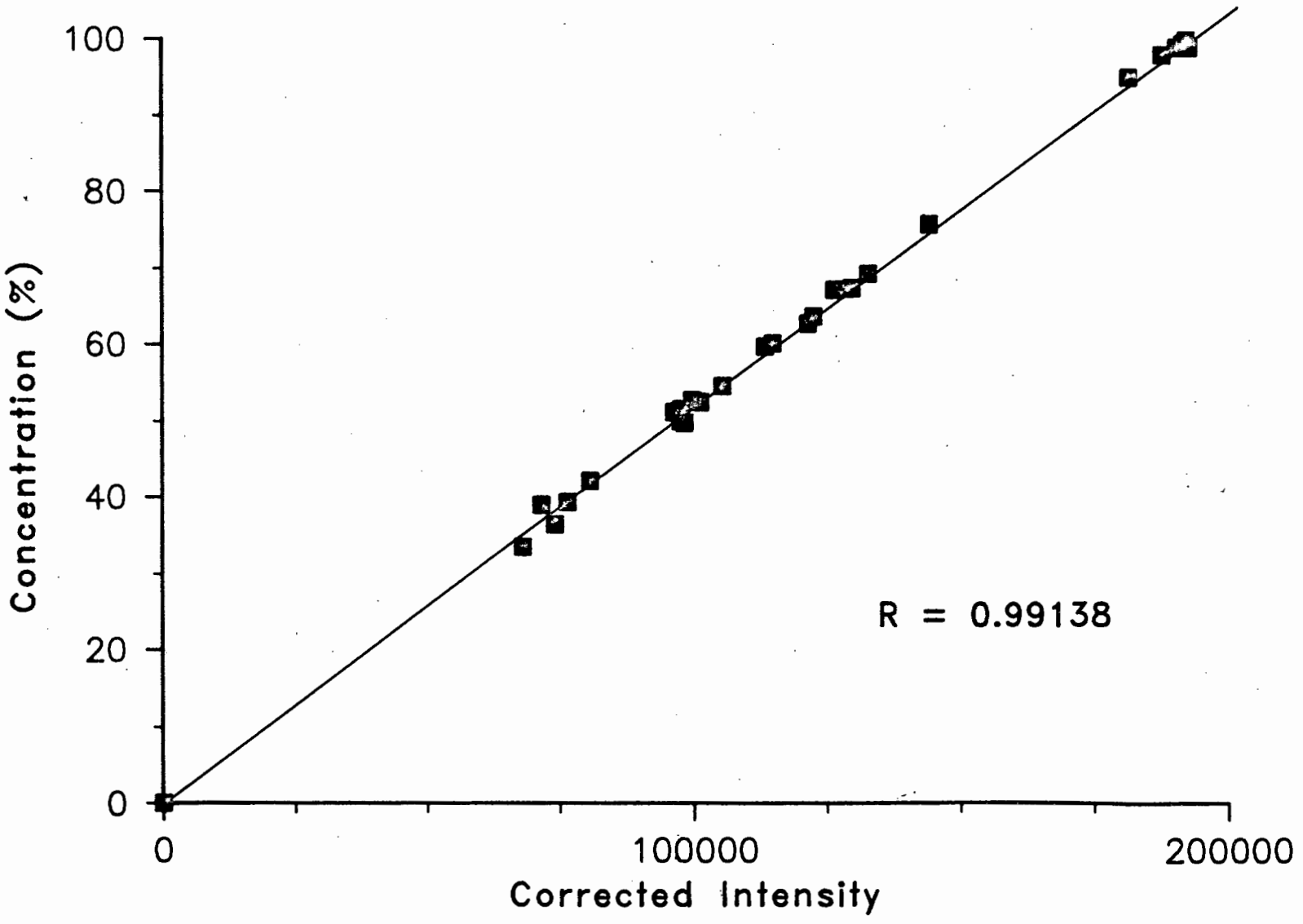

Figure 4:6. Calibration curve for CaO using Lucas Tooth–Pyne (1963) correction model.

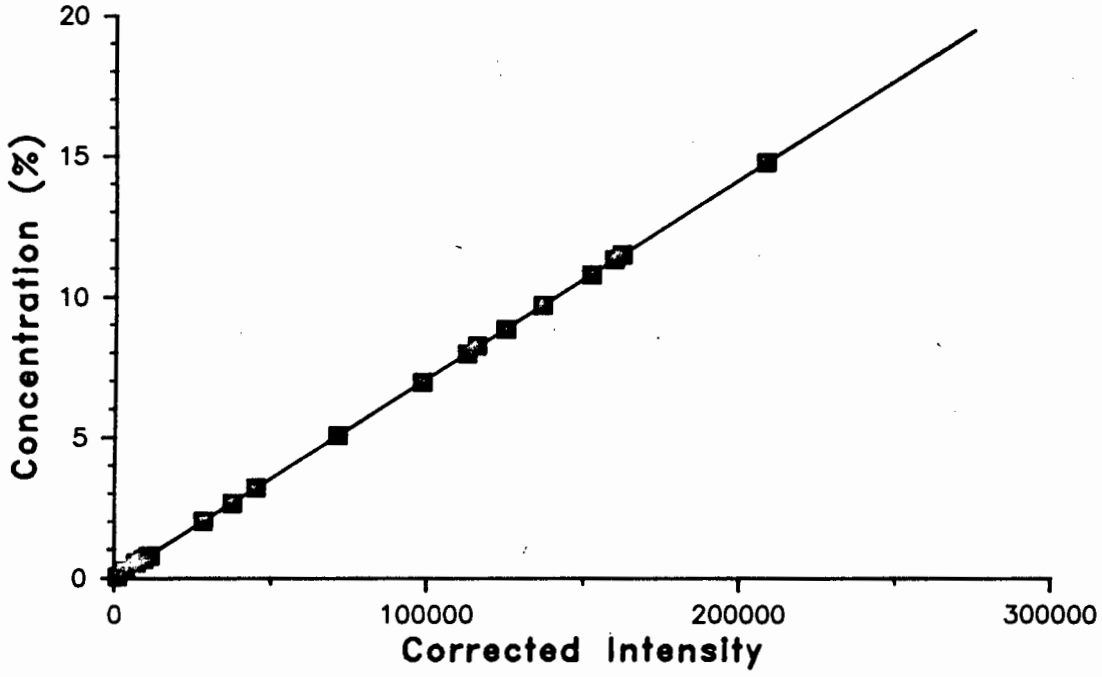

Figure 4:7. Calibration curve for Fe_2O_3 using Lucas Tooth–Pyne (1963) correction model.

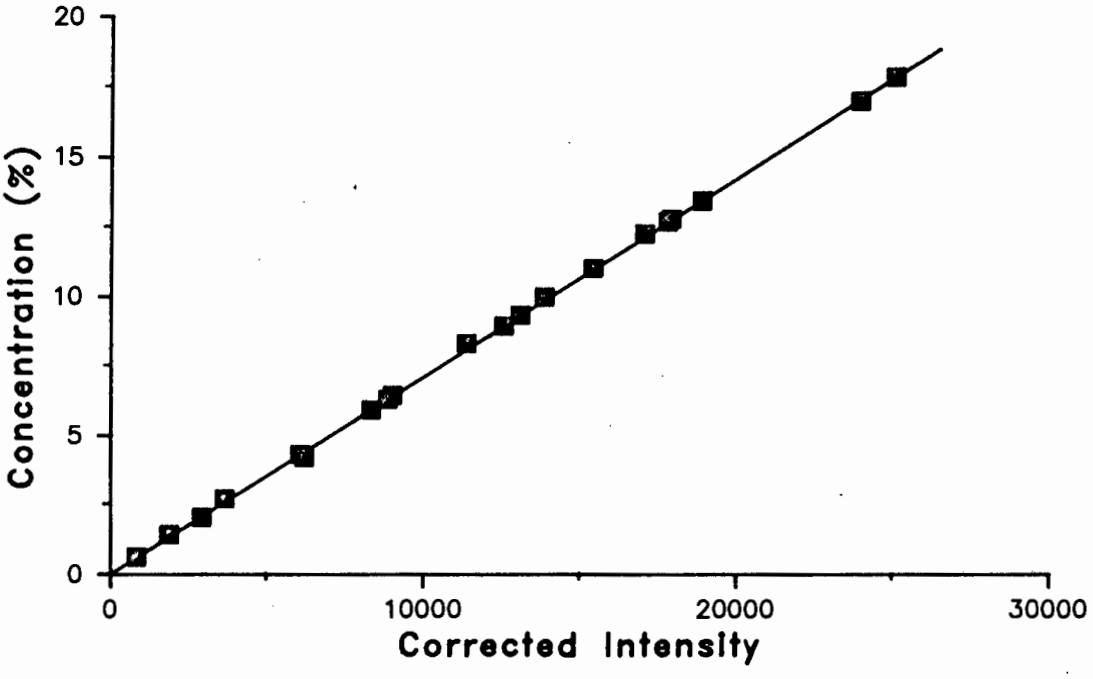

interelement effects, e.g. Lachance-Traill (1966), was used. The alpha coefficients generated are factors by which the observed intensities are multiplied.

To calculate coefficients for loss, the concentration data file must contain the LOF values for the standards and the unknowns. The data in Table 4:4 illustrates the effect of using LOF on the sign and magnitude of alpha coefficients for CaO and BaO calculated using the Lachance-Traill (1966) model. An examination of the data in Table 4:4 indicates that the use of loss can change both the magnitude and sign of the coefficient. For example, the alpha coefficient for the effect of Ti on BaO when including LOF is -.00315 but excluding LOF is .12872. The statistical data, least squares fit and average absolute and relative errors, given in Table 4:4 indicate that the inclusion of LOF does not really improve the "goodness of fit" of the calibration curve.

A calibration curve for SiO_2, derived using an iterative procedure for the Lachance-Traill (1966) correction model, is presented in Figure 4:8. Comparison of this curve with the Lucas-Tooth and Pyne (1963) model calibration curve in Figure 4:5 confirms the limitations of the latter correction model.

Problems were experienced with the calibration of barium and titanium and the matrix effects of these elements on other analyte elements as the international rock standards used did not contain Ba and Ti in concentrations similar to the lamproite and kimberlite samples. The international rock standards, on the whole, gave good results. The average absolute and relative errors, and composition ranges of the standards are presented in Table 4:5.

Figure 4:8. Calibration curve for SiO_2 using Lachance–Traill (1966) correction model.

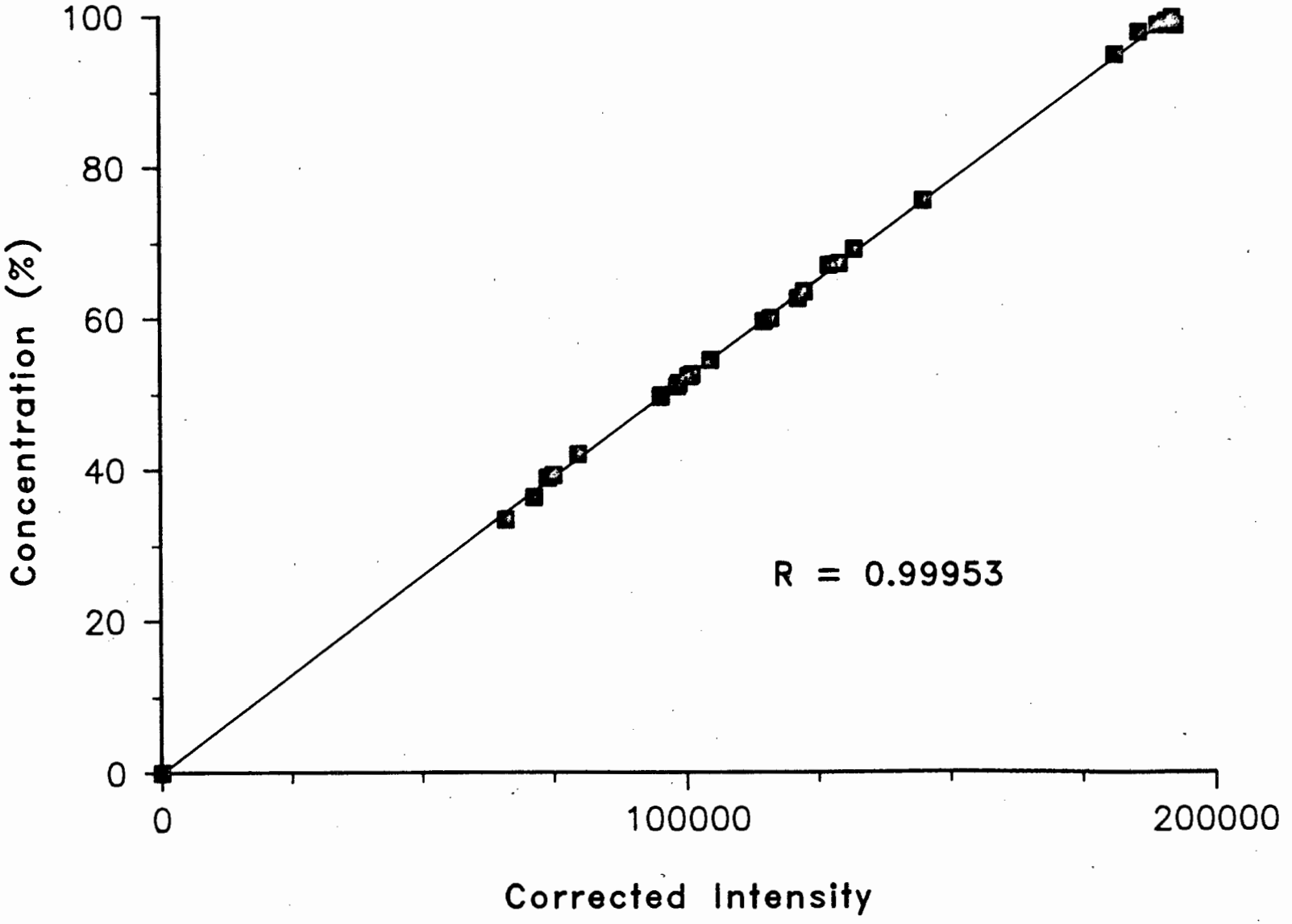

Table 4:4

Comparison of alpha coefficients for CaO and BaO calculated using XRF4 and the Lachance-Traill (1966) model using the same standards set.

	BaO		CaO	
	LOF as a Variable	LOF not a Variable	LOF as a Variable	LOF not a Variable
Fe	.03410	-.00250	-.00351	.00005
Mn	-.37095	.15943	.08574	.07743
Ca	-.03910	-.03261		
K	.01158	.00845	.00968	.01158
P			-.02515	-.02483
Si	.00006	.00001	-.00081	.00107
Mg	-.00115	-.00002	-.00268	-.00250
Na	.05328	.03724	-.00596	-.00319
Ti	-.00315	.12872	.00104	-.00094
Ba			.18566	.04822
Al	-.01388	-.00687	-.00235	-.00139
Lo	.03170		-.00610	
Lsq Fit	.99971	.99970	.99999	.99998
Av Abs Err	.005	.005	.014	.025
Max Abs Err	.013	-.015	.070	-.071
Av Rel Err	10.26	9.24	1.22	1.71
Max Rel Err	49.96	48.64	6.32	6.31

The data for the unknown samples produced using iterative cycles of the Lachance-Traill (1963) model resulted in high whole rock totals for some of the lamproites and low whole rock totals for kimberlites. One of the major differences between these two rock types are the BaO and TiO_2 concentrations. The data from XRF4 was, however, useful as it gave some indication of the approximate range in composition of these rock types. These are summarized in Table 4:6.

Consequently spiked standards were used to calculate alpha coefficients by multiple regression analysis using the program XRF4. Several of the secondary international standards were spiked with 2 and 5% barium oxide, and 5 and 10% titanium oxide.

The concentrations of the other elements in the spiked discs were corrected for the dilution by the spike. This spiking method gave ranges in concentrations detailed in Table 4:6.

Table 4:5

Absolute and relative errors for the international rock standards used for calibration of the major element oxides by multiple regression analysis. (16-20 standards, data in wt %)

	Range in Comp	Ave. Abs. Error %	Max. Abs. Error %	Ave. Rel. Error %	Max. Rel. Error %
SiO_2	33-99	.246	-.870	.46	1.37
TiO_2	.10-5.0	.005	-.019	2.00	13.03
Al_2O_3	1.0-88	.055	-.183	.50	2.26
Fe_2O_3	.59-18	.019	.051	.39	1.74
MnO	.03-.8	.002	-.004	1.60	6.83
MgO	.28-44	.016	-.059	.42	2.41
CaO	.28-15	.029	.074	1.43	4.21
Na_2O	.43-8.0	.023	.056	1.18	5.52
K_2O	.25-15	.007	-.024	.67	5.39
P_2O_5	.06-5.0	.005	.013	4.95	20.72
BaO	.05-2.0	.002	.007	.97	4.41

Table 4:6

Approximate composition range in the Lamproites and Kimberlites and the spiked standards. (data in percent, 20-30 standards)

	Lamproites + kimberlites	Spiked standards
SiO_2	19 - 63	28 - 100
TiO_2	.61 - 9	.4 - 11.5
Al_2O_3	1 - 11	3 - 88
Fe_2O_3	4 - 16	.5 - 17
MnO	.05 - .27	.01 - .25
MgO	2 - 36	.14 - 44
CaO	.1 - 16	.28 - 12
Na_2O	.06 - 3.5	.4 - 4
K_2O	.15 - 13	.22 - 16
P_2O_5	.4 - 3	.06 - 1.5
BaO	.1 - 2.2	.08 - 5.2
Loss	.4 - 16.5	.1 - 11

The average absolute and relative errors for the spiked standards are reported in Table 4:7. Comparison of this data with that in Table 4:5 indicates that "spiking" with barium and titanium has increased the average absolute and relative errors, for example the average absolute error for silica has doubled in magnitude.

Data from the Lachance-Traill (1966) model for the lamproites remained unsatisfactory after 3 iteration cycles as the analytical totals were low. Two examples are given in Table 4:8.

Table 4:7

Absolute and relative errors for the "spiked" rock standards used for calibration of the major element oxides by multiple regression analysis.

	Ave. Abs. Error %	Max. Abs. Error %	Ave. Rel. Error %	Max. Rel. Error %
SiO_2	.489	-1.409	.90	2.79
TiO_2	.096	-.331	2.08	6.99
Al_2O_3	.063	-.198	.51	1.92
Fe_2O_3	.077	.426	1.45	4.72
MnO	.002	-.005	1.35	3.05
MgO	.034	-.155	1.77	12.80
CaO	.052	.210	1.11	4.67
Na_2O	.038	-.121	2.63	10.22
K_2O	.021	.084	2.38	11.65
P_2O_5	.003	.009	2.11	6.75
BaO	.041	.132	4.92	24.88

Table 4:8

Data for two lamproite samples using multiple regression analysis and "spiked" standards to calculate alpha coefficients. (wt.%)

	PK 3/9 lamproite	PK 7/1 lamproite
SiO2	28.79	51.07
TiO2	5.44	4.99
Al2O3	3.27	8.63
Fe2O3	7.15	6.59
MnO	0.07	0.05
MgO	9.68	7.31
CaO	15.84	2.17
Na2O	0.47	0.69
K2O	6.56	10.08
P2O5	1.35	0.83
BaO	2.14	1.07
LOF	16.22	3.10
TOTAL	96.98	96.58

Discussion

The poor results obtained from XRF4 led to further research into alpha coefficients. Various workers have commented on the use of multiple regression analysis for the generation of alpha or influence coefficients. Norrish (pers comm) stated that he would avoid generating alpha coefficients by multiple regression analysis for the following reasons :

1) Most natural materials have cross correlations between elements which generally cause problems.

2) Natural variations in element concentrations are not sufficiently large to give good estimates of alpha coefficients.

3) It is necessary to make sure that any program used reports errors in the coefficients as well as in the concentrations. When the errors for the coefficients are given it is generally found

that the errors are greater than the coefficients.

Lachance (1981) stated that it is dangerous to read all available standards and proceed to obtain the whole set of alphas directly by multiple regression analysis. In theory this should not pose any problems, but Lachance and co-workers found that alphas determined theoretically and those computed by multiple regression analysis could not only differ by orders of magnitude but also in their algebraic sign, Table 4:9.

Table 4:9

Comparison of alpha coefficients determined by multiple regression analysis and theoretical alphas.
(after Lachance 1981)

	Theoretical	Experimental
Na_2O-P_2O_5	.07	-.38
MnO-Cr_2O_3	-.09	-1.56
Na_2O-K_2O	-.02	-.21
TiO_2-P_2O_5	-.06	.14
TiO_2-MnO	-.18	.04
SiO_2-Al_2O_3	.356	.356
SiO_2-Fe_2O_3	.289	.279

Theoretical calculation of alpha coefficients by the Norrish and Hutton (1969) method.

The low totals from the multiple regression analysis (XRF4) and the comments of various workers indicated that a better method of calculation of alpha coefficients was required.

Theoretical alpha coefficients have been calculated by numerous workers. The use of the Norrish and Hutton (1969) coefficients and their method of reduction of the major element data (modified in the Geochemistry Department, U.C.T.) influenced the choice of which method to use to calculate the theoretical alpha coefficients.

Various problems were encountered, as the method outlined in the original paper (Norrish and Hutton 1969) did not give the correct results, even with back calculation. After communicating with Dr Norrish these problems were rectified and the method of calculation is outlined in Table 4:10. The general relationship of intensity to concentration involving the Norrish and Hutton (1969) method of calculating correction factors is given in Table 4:11. Norrish (pers. comm.) pointed out that the mass absorption coefficients published by Heinrich (1966) for oxygen are incorrect. This matter was investigated and the graphs of atomic number versus mass absorption coefficients at the major element K_a wavelengths were generated. The resulting graphs are given in Figure 4:9. Determination of the modified oxygen values was performed by fitting second order polynomial regression lines to the data points (excluding oxygen) in the various graphs. The modified values are compared to the original reported values in Table 4.12.

Figure 4:9(a). M.A.C. for Na,Mg and Al K_α lines (Heinrich 1966)

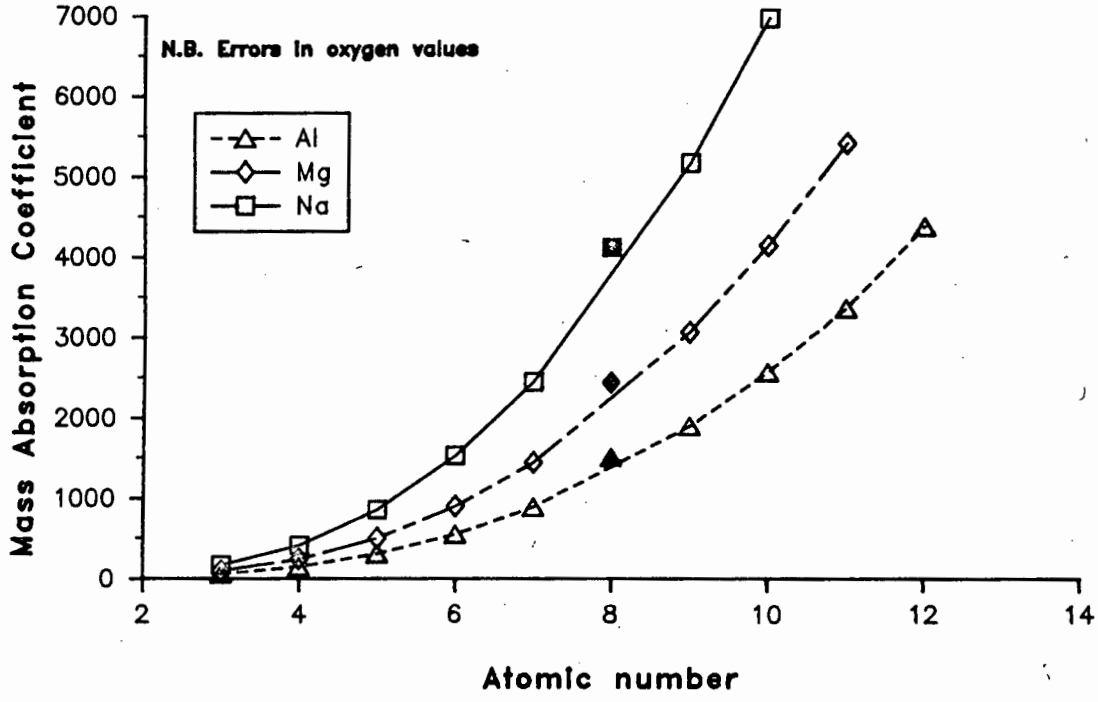

Figure 4:9(b) M.A.C. for Si, P and K K_α lines (Heinrich 1966)

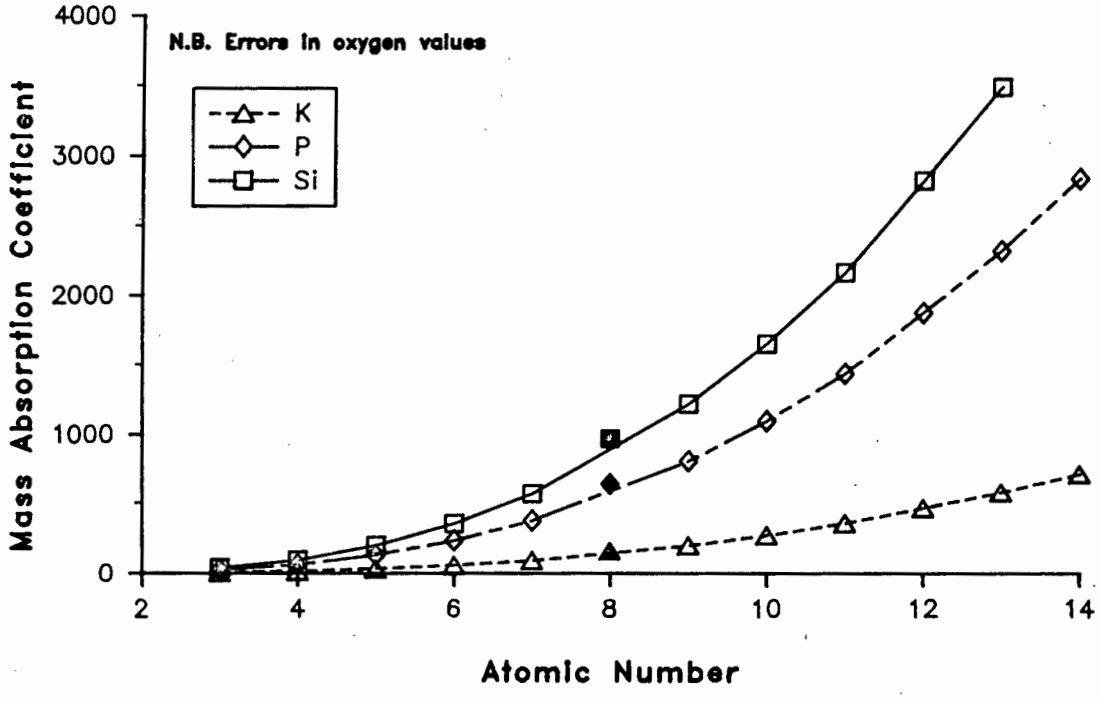

Table 4:10. Calculation of alpha coefficients by the Norrish and Hutton (1969) method for LDF discs using primary and secondary wavelengths.

α–coefficients for primary λ for Fe K_α and Mn K_α are calculated at .85 of respective absorption edges.

General equation (A = geometric factor)

$$\frac{\left\{\begin{matrix}\mu/\rho \text{ oxide} \\ \text{at primary } \lambda\end{matrix} + \left(A \times \begin{matrix}\mu/\rho \text{ oxide} \\ \lambda \text{ of interest}\end{matrix}\right) - \begin{matrix}\mu/\rho \text{ flux} \\ \text{at primary } \lambda\end{matrix} + \left(A \times \begin{matrix}\mu/\rho \text{ flux} \\ \lambda \text{ of interest}\end{matrix}\right)\right\} \times .303}{\begin{matrix}\mu/\rho \text{ flux} \\ \text{at primary } \lambda\end{matrix} + \left(A \times \begin{matrix}\mu/\rho \text{ flux} \\ \lambda \text{ of interest}\end{matrix}\right)}$$

Therefore the α–coefficient for SiO_2 at Na K_α using a PW 1400 is

$$\frac{\{106.90 + (1.347 \times 2599.50) - 27.49 + (1.347 \times 2619.39)\} \times .303}{27.49 + (1.347 \times 2619.39)}$$

$= .00448$ prior to normalisation *{B 113}*

General equation for flux coefficient : $M = \frac{Am}{Am} = 1$

$$Am = \begin{matrix}\mu/\rho \text{ flux} \\ \text{at primary } \lambda\end{matrix} + \left(1.347 \times \begin{matrix}\mu/\rho \text{ flux} \\ \text{at Na K}\alpha\end{matrix}\right)$$

Normalisation of Alpha factors and calculation of flux coefficient

$$= \sum \text{wt fraction of } \begin{matrix}\\ \text{of } SiO_2\end{matrix} \times \overset{\{B\ 113\}}{\alpha_{NaSi}} + \text{wt fraction of } \begin{matrix}\\ \text{of } TiO_2\end{matrix} \times \overset{\{B\ 114\}}{\alpha_{NaTi}} + \ldots\ldots$$

$$= (.626 \times .00448) + (.0066 \times .31627) + (.146 \times -.03212) + (.06530 \times .64906) + (.001 \times .60430) + (.035 \times -.07317) + (.062 \times .21010) + (.027 \times -.13189) + (.035 \times .15467) + (.00115 \times .03227)$$

$= 0.05555$ *{B 212}*

$\therefore$ M + TOTAL = 1.05555 *{B 215}*

$$\frac{1}{M + TOTAL} = 0.94738 \quad - \textit{ flux coefficient for Na } K_\alpha \quad \textit{\{B 218\}}$$

This value is also the normalisation value for α–coefficients

$\therefore$ normalized α–coefficient for SiO_2 at Na K_α = .00425 *{B 228}*

Loss factor for Na K_α :

μ/ρ loss = 0

$\therefore$ using the general equation

$$\text{Loss Factor (Na)} = \frac{(0 - 2619.39)}{2619.39} \times .30303 \qquad \textit{\{B 080\}}$$

$= -.30303$ *{B 125}*

This value is again normalised to the average of G–1 and W–1 (using *{B 218}*)

$\therefore$ Loss Factor (Na) = $-.30303 \times .94738 = -.28708$ *{B 240}*

{B 113} etc refer to locations on spreadsheet LDFMA2
ie. column B line 113

Table 4:11

General relationship between intensity and concentration using Norrish and Hutton (1969) method of calculating alpha coefficients.

$$\text{True wt. \% } C_i = (\text{apparent Wt. \% } \times A_i) - \text{Bkg}$$

Where

$$A_i = X_i + [\sum_j (\alpha_{ij} \times C_j)/100] + WC$$

i = analyte element

j = interfering element

A_i = alpha factor to correct apparent wt % of oxide i.

X_i = flux absorption factor for radiation of analyte element

C_i = wt % conc of analyte element i.

C_j = wt % conc of interfering element j

α_{ij} = matrix correction factor for effect of element j on analyte element i.

WCF = weight correction factor

$$= \frac{\text{sample wt - specified wt}}{\text{specified wt}} \times \alpha_{i,loss}$$

$\alpha_{i,loss}$ = loss factor

Table 4:12

Comparison of reported and calculated Heinrich Mass Absorption Coefficient values (Heinrich 1966) for oxygen at K_a wavelengths.

	Modified 'O' values	Reported 'O' values
Na	3711.7	4109.1
Mg	2200.3	2432.8
Al	1348.3	1503.3
Si	860.8	965.6
P	569.9	638.9
K	140.2	157.0
Ca	103.4	115.8
Ti	58.7	65.7
Mn	27.6	30.9
Fe	21.8	24.5

The lengthy repetitive calculations involved in generating alpha coefficients for all the major elements of interest resulted in the use of a computer program MATH/1000 (COMPROG 1981-1984) to set up a spreadsheet to calculate the alpha coefficients.

The calculation procedure was designed so that the flux composition and dilution factor could be altered in order that coefficients for any fusion method could be generated. The spreadsheets used to calculate the alpha coefficients are given in appendix D and these should be read in conjunction with Table 4:10. Part A of the spreadsheets contain the actual numbers used and Part B is a listing of the mathematical definitions (in reverse polish notation) used in the calculations.

The spreadsheet contains two types of data. The permanent data set consists of the mass absorption coefficients of the major

elements and flux constituents at the K_a wavelengths of the analyte elements, the oxide conversion factors and the average composition of G-1 and W-1 to normalise the calculated alpha coefficients. The mass absorption coefficients are taken from Heinrich (1966). The oxygen mass absorption coefficients have been modified according to the data in Figure 4:9 and Table 4:12. The m.a.c.s for Na at the Na K_a wavelength and Ba at the Mn K_a wavelength have also been estimated by the method used for oxygen. The temporary data set consists of the composition of the flux, expressed in weight fractions of Li_2O, B_2O_3 and La_2 and the sample, flux and nitrate weight (to calculate the dilution factor).

The rest of the data contained on the spreadsheet is calculated by the method outlined in Table 4:10 by relative addressing of the rows and columns of the matrix. A minor change in any of these values will result in the whole matrix being recalculated. Two sets of coefficients are generated, one using primary and secondary radiation, the other using secondary radiation only.

In the Norrish and Hutton (1969) fusion method, the relatively high dilution ratio and the use of the heavy absorber, lanthanum oxide, decreases the effect of primary beam absorption and only secondary absorption is considered in the calculation of the alpha coefficients. For the low dilution fusion discs, both primary and secondary absorption effects need to be taken into consideration for the calculation of alpha coefficients. Using the effective wavelength concept (Jenkins 1974) and a Cr X-ray tube, the primary absorption coefficient is calculated at 2.29 Å (CrK_a), where this is shorter than the absorption edge of the analyte of interest. This wavelength is used for Ti, Ba, Ca, K, P, Si, Al, Mg and Na. Where the excitation is by continuum

radiation only, the primary beam absorption coefficient is calculated at .85 (Norrish, pers. comm.) of the absorption edge of the excited element. This concept is used for Fe, Ni and Mn. In this work, the m.a.c.s of the oxides at Cu K_a (1.542 Å) and Ni K_a (1.659 Å) have been used to approximate the Fe K_{abs} x 0.85 wavelength (1.481 Å) and Mn K_{abs} x 0.85 wavelength (1.612 Å), respectively. The use of the m.a.c.s at these two wavelengths to approximate 0.85 of Fe K_{abs} and Mn K_{abs} is valid as no major element absorption edges occur in the region between 1.481 - 1.659 Å. The calculated coefficients are normalized to the average composition of G-1 and W-1 using the method outlined in Table 4:10. The normalized coefficients were used as input to programs XRFLD and MAJLD, modified versions of the Geochemistry Department, U.C.T. programs XRF01 and MAJOR.

XRF01 is a Fortran program that provides calibration curve data for silicate major element analysis using the Norrish and Hutton (1969) technique. A summary of the calibration data is stored in a file for input to MAJOR.

MAJOR is a Fortran program that reduces measured X-ray intensities from samples to concentrations. The working curve data and errors are read from the summary file created by XRF01.

For the low dilution fusion discs the two programs have been modified to correct for the use of 2g of sample instead of 0.28g as in the Norrish and Hutton (1969) technique. The LOF values are entered into the program as H_2O+ so no correction for loss is made to the concentration values. The intensity data for the standards and samples are entered as net intensities with a constant reference count since the intensities had previously been corrected in TRACE for instrumental drift. The dead time

correction factor was set to zero. These slight modifications to the input data avoided extensive alterations to the two programs.

Prior to processing of the low dilution fusion disc intensity data the method of theoretically calculating the alpha coefficients using MATH/1000 (COMPROG 1981-1984) was initially tested for the Norrish and Hutton (1969) flux containing lanthanum oxide. The resulting coefficients differed from those normally used for the Norrish and Hutton (1969) technique which are Norrish's "preferred" values from theoretical and experimental work. The two sets of alpha coefficients are presented in Table 4:13 and 4:14. The underlined values in the Tables indicate a change in sign. On examining the Tables, it is obvious that many of the theoretical coefficients are significantly larger than Norrish and Hutton's (1969) published coefficients. For example the Norrish and Hutton (1969) value for $\alpha_{FeKa-Fe2O3}$ is -0.027 yet the calculated value is -0.096. Average absolute and relative errors for the major elements using the Norrish and Hutton's (1969) published coefficients and the calculated coefficients using the same set of standards are presented in Table 4:15.

Table 4: 13

Norrish and Hutton (1969) published Matrix Correction factors for discs containing lanthanum oxide

ELEMENT BEING DETERMINED	INTERFERING ELEMENT EXPRESSED- AS OXIDE											
ELE-MENT	FE203	MNO	T102	CAO	K20	P205	S102	AL203	MGO	NA20	LOSS	FLUX
FE Ka	-.027	-.031	.146	.134	.126	-.060	-.065	-.074	-.090	-.110	-.163	1.046
MN Ka	-.044	-.044	.146	.135	.130	-.063	-.063	-.074	-.078	-.100	-.163	1.045
TI Ka	..081	.077	.179	.647	.644	.181	.110	.078	.069	.051	.132	.851
CA Ka	.090	.092	.065	.130	.723	.182	.128	.105	.068	.051	-.134	.865
K Ka	.098	.086	.017	.000	.069	.179	.119	.101	.080	.057	-.139	.897
P Ka	.108	.094	-.020	-.037	-.047	-.063	.127	.110	.094	.046	-.139	.896
SI Ka	.082	.086	-.034	-.042	-.055	-.061	-.061	.122	.093	.063	-.158	1.014
AL Ka	.112	.116	-.032	-.037	-.048	-.060	-.088	-.072	.116	.058	-.164	1.056
MG Ka	.136	.126	.010	-.021	-.043	-.016	-.070	-.078	-.084	.080	-.163	1.050
NA Ka	.000	.000	.000	.000	.000	.000	.000	.000	.000	.000	.000	.000

Table 4:14

Calculated Matrix Correction factors (this work) using Norrish and Hutton (1969) method [Table 4:10] for fusion discs containing lanthanum oxide

ELEMENT BEING DETERMINED	INTERFERING ELEMENT EXPRESSED AS OXIDE											
ELEMENT	Fe_2O_3	MnO	TiO_2	CaO	K_2O	P_2O_5	SiO_2	Al_2O_3	MgO	Na_2O	LOSS	FLUX
Feka	-.096	-.099	.130	.108	.112	-.074	-.085	-.092	-.100	-.107	-.168	1.068
Mnka	-.084	-.088	.172	.148	.153	-.059	-.071	-.079	-.088	-.096	-.165	1.051
Tika	.079	.070	-.003	.682	.696	.147	.117	.095	.072	.051	-.132	.837
Caka	.085	.075	-.001	-.025	.737	.158	.126	.104	.080	.058	-.137	.871
Kka	.089	.078	-.001	-.025	-.037	.165	.132	.109	.085	.061	-.141	.893
Pka	.094	.083	.004	-.021	-.034	-.062	.143	.121	.096	.072	-.139	.883
Sika	.110	.098	.006	-.023	-.038	-.070	-.078	.143	.115	.086	-.159	1.017
Alka	.115	.102	.008	-.022	-.038	-.071	-.079	-.089	.123	.093	-.165	1.051
Mgka	.141	.126	.025	-.009	-.023	-.061	-.069	-.081	-.093	.118	-.165	1.047
Naka	0	0	0	0	0	0	0	0	0	0	0	0

Table 4:15.

Comparison of average absolute and relative errors for major element concentrations using calculated (this work) and published coefficients from the Norrish and Hutton (1969) technique.(same set of standards and intensity data)

	Published Coefficients		Calculated Coefficients	
	Ave. Abs. Errors	Ave. Rel. Errors	Ave. Abs. Errors	Ave. Rel. Errors
SiO_2	.25	0.42	.418	0.70
TiO_2	.016	15.3	.020	6.68
Al_2O_3	.082	5.30	.137	2.10
Fe_2O_3	.069	1.66	.084	1.89
MnO	.008	13.3	.007	11.61
MgO	.117	13.3	.098	29.58
CaO	.035	2.21	.042	1.00
Na_2O**	.045	2.23	.045	2.23
K_2O	.024	7.38	.033	4.31
P_2O_5	.009	26.7	.015	16.49

** powder briquettes

Table 4:16.

Comparison of concentration data for basalts obtained using calculated coefficients (this work) and published coefficients. (Norrish and Hutton 1969) (data in wt. percent)

	10-3 A		10-5 A	
	Cal. Coeff.	Pub. Coeff.	Cal. Coeff.	Pub. Coeff.
SiO_2	50.84	50.17	51.03	50.67
TiO_2	1.60	1.60	1.61	1.61
Al_2O_3	14.94	14.84	15.01	15.13
Fe_2O_3	11.16	11.08	11.08	11.06
MnO	0.17	0.17	0.18	0.19
MgO	7.22	7.08	7.17	6.88
CaO	11.58	11.58	11.53	11.52
Na_2O*	2.83	2.83	2.89	2.89
K_2O	0.41	0.41	0.47	0.47
P_2O_5	0.20	0.20	0.19	0.19
Total	100.95	99.96	101.16	100.61

* determined on powder pellets

Table 4:17

Calculated Matrix Correction factors (this work) using Norrish and Hutton (1969) technique [Table 4:10] for Low Dilution Fusion Discs

ELEMENT BEING DETERMINED	INTERFERING ELEMENT EXPRESSED AS OXIDE													
ELEMENT	Fe_2O_3	MnO	TIO_2	CaO	K_2O	P_2O_5	SiO_2	AI_2O_3	MgO	Na_2O	CR_2O_3	BaO	LOSS	FLUX
Feka	1.160	1.144	1.791	1.650	1.673	.474	.408	.360	.310	.264	0	4.619	-.128	.424
Mnka	1.147	1.124	1.784	1.644	1.669	.473	.408	.359	.310	.264	0	4.096	-.129	.426
Tika	.345	.324	.689	1.723	1.754	.500	.431	.381	.329	.280	0	1.441	-.139	.459
Caka	.373	.350	.552	.476	1.904	.545	.469	.416	.360	.306	0	1.303	-.151	.499
Kka	.394	.369	.497	.421	.401	.579	.499	.442	.383	.326	0	1.259	-.161	.531
Pka	.389	.364	.268	.204	.175	.043	.506	.451	.393	.335	0	.911	-.166	.548
Sika	.556	.519	.341	.250	.208	.049	.024	.652	.569	.484	0	1.223	-.241	.795
Alka	.608	.568	.338	.239	.191	.043	.017	-.017	.630	.535	0	1.269	-.270	.891
Mgka	.612	.570	.315	.216	.165	.036	.009	-.025	-.063	.546	0	1.025	-.279	.923
Naka	.615	.572	.299	.199	.146	.031	.004	-.030	-.069	-.125	0	.777	-.287	.947
Crka	0	0	0	0	0	0	0	0	0	0	0	0	0	0
Baka	.346	.325	.680	1.726	1.757	.501	.432	.382	.329	.280	0	1.431	-.139	.458

Data for several basalts, Le Roex (pers comm) corrected for matrix effects using the calculated coefficients and Norrish and Hutton (1969) published coefficients are compared in Table 4:16. The same set of standards and initial intensity data were used. The data show that there is good agreement between all the elements except silica. The average absolute and relative errors for this element are higher for the calculated coefficients and this is mirrored in the concentration data.

The alpha coefficients calculated by this method for the low dilution fusion discs are presented in Table 4:17. Comparison of the alpha coefficients for the LDF in Table 4:17 with those for the Norrish and Hutton (1969) discs in Table 4:14 indicate that the lower dilution ratio and the lack of the heavy absorber in the LDF discs has greatly increased the magnitude of all the alpha coefficients and in many cases the sign of the coefficients had also changed. The flux factors for the LDF are smaller than those for the Norrish and Hutton (1969) discs. The magnitude of the flux factor is dependent on the magnitude of the individual α_{ij}, as the flux factor is the value required to normalise the total correction factor of a 1:1 mixture of G-1 and W-1 to 1. Consequently the larger size of the LDF α_{ij}'s leads to a smaller flux factor. For the LDF discs the alpha coefficients are generally positive indicating that absorption effects are predominant which is in agreement with the alpha coefficients calculated by Thomas and Haukka (1977).

The data for the international and "spiked" standards and unknown samples were entered into the two modified programs (XRFLD and MAJLD) in the form described earlier.

The absolute and relative errors for the standards are given in Table 4:18. The data indicate a serious problem with the calibration of silica, as the average absolute error for this oxide is 1.079% which is greater by a factor of four than that obtained for the Norrish and Hutton (1969) discs using the published It should, however, be noted that the average absolute errors on all the elements for the calculated Norrish and Hutton (1969) type coefficients (Table 4:15) are higher than those for the published coefficients (Norrish and Hutton 1969).

On examination of a plot of corrected concentration (using alpha coefficients) versus uncorrected concentration for silica (Figure 4:10), the calibration curve, with no matrix corrections, shows poor agreement and does not pass through the origin, but intercepts the concentration axis at approximately 6%. This is an interesting feature as Willis (pers. comm.) reports that the calibration curve for silica analyzed on powder pellets intercepts the concentration axis at approximately 17%. This indicates that the matrix effects have been decreased slightly by the dilution effect of the flux in the low dilution fusion discs but not completely eliminated. This large intercept is indicative of the severity of the matrix problems in the low dilution fusion discs due to the lack of a heavy absorber, the higher sample to flux ratio and the use of only one alpha coefficient that does not correct for variation of this coefficient with changing analyte concentration (Lachance et al. 1980).

The average absolute and relative errors for the remaining major elements analyzed in the low dilution fusion discs are also generally larger than those for the published Norrish alpha coefficients using discs containing lanthanum oxide. The use of

Figure 4:10. SiO_2 – standard concentrations vs uncorrected concentrations.

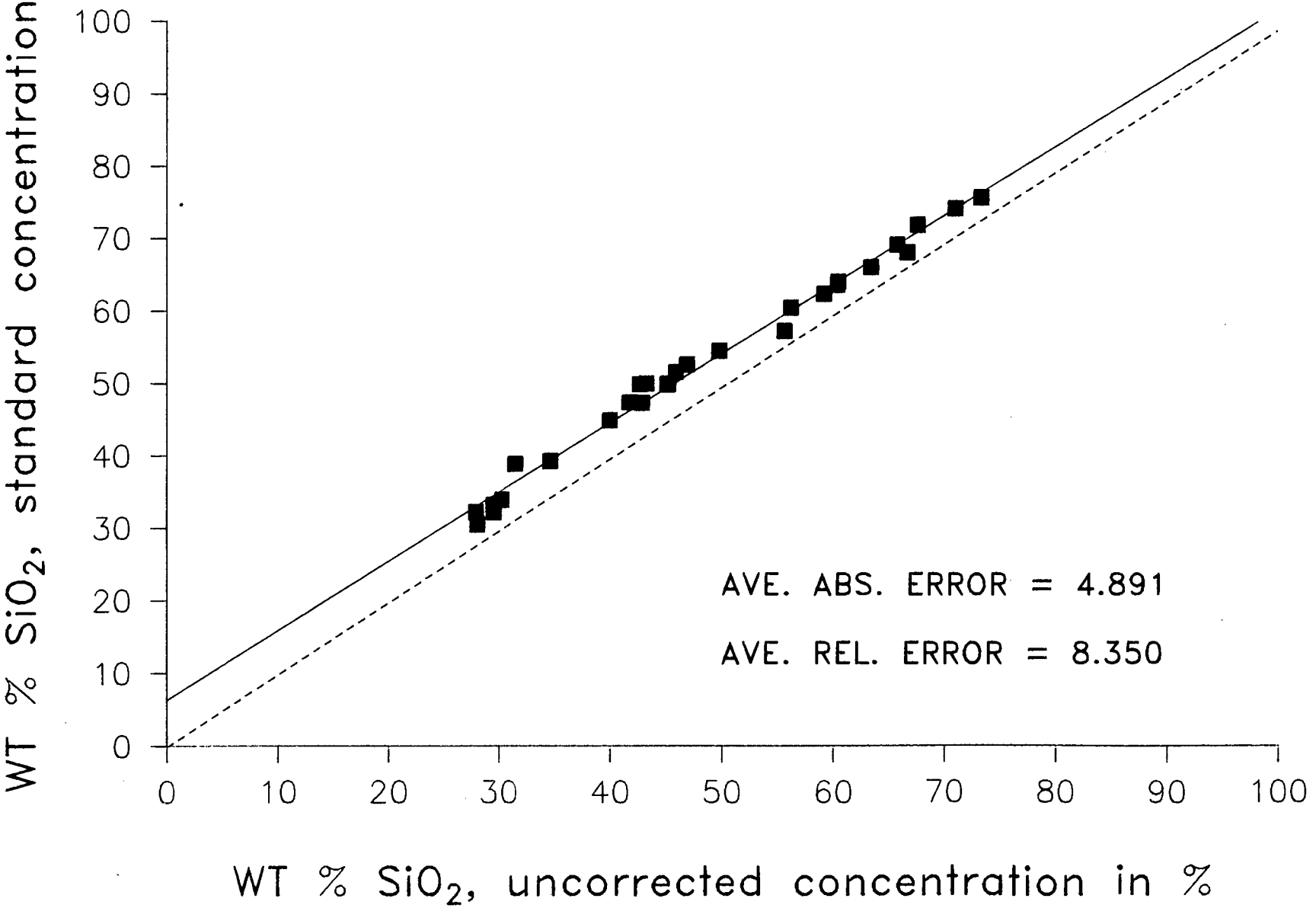

two different sets of standards for calibration accounts for part of the differences. The "spiked" NIM standards (BaO and TiO_2) were used to calibrate the low dilution fusion discs. The Norrish and Hutton (1969) discs were calibrated using normal international rock standards such as G-2, BCR-1, MRG-1, and BHVO-1.

Data for 2 kimberlites analyzed using the Norrish and Hutton (1969) technique with their published coefficients and the low dilution fusion method with the calculated coefficients are given in Table 4:19. The data indicate a calibration problem mainly with silica. This is serious since the silica concentrations are geochemically very important and are also used in calculating the correction factors for all the other elements.

Table 4:18

Average absolute and relative errors for the low dilution fusion discs using theoretical alphas from Table 4:17, Fused disc system.

	Ave. Abs. Error	Ave. Rel. Error
SiO_2	1.078	1.989
TiO_2	0.078	2.864
Al_2O_3	0.174	1.454
Fe_2O_3	0.144	3.736
MnO	0.009	19.947
MgO	0.162	1.016
CaO	0.102	2.736
Na_2O	0.071	7.651
K_2O	0.104	4.027
P_2O_5	0.008	4.086
BaO	0.062	3.063

Table 4:19

Comparison of kimberlite data obtained using the Norrish technique (published Norrish and Hutton alphas, 1969) and the low dilution technique (calculated Norrish and Hutton 1969 type alphas this work). (wt. %)

	K64/55		MAIN 15/1	
	Norrish	LDF	Norrish	LDF
SiO_2	33.59	32.54	30.54	31.20
TiO_2	0.62	0.63	1.66	1.67
Al_2O_3	1.29	1.23	5.75	5.74
Fe_2O_3	7.84	7.42	8.13	7.12
MnO	0.14	0.14	0.20	0.14
MgO	36.00	35.02	15.25	15.78
CaO	5.51	5.28	15.52	14.56
Na_2O***	0.06	<0.10	0.20	0.21
K_2O	1.43	1.81	6.29	5.77
P_2O_5	1.11	1.07	1.64	1.72
LOI	11.66		13.11	
LOF*		10.55		13.31
Total	99.25	95.79	98.29	97.22

* LOF values have been corrected for gain in weight by oxidation of S to SO_3
The difference in LOI and LOF values is most likely due to the loss of S in the LOI technique.

*** Na_2O was determined on powder pellets for the Norrish technique.

Using the low dilution fusion method and the calculated alpha coefficients, data for the lamproites either gave high or low analytical totals (between 97 - 102%). In Table 4:20 major element data for the low dilution fusion discs reduced using alpha coefficients calculated by XRF4 (multiple regression analysis) and the Norrish and Hutton (1969) method (Table 4:10) for two lamproite samples are compared. The disagreement of the results for PK3/3 and PK7/1 in Table 4:20 is so large that the data could represent four different rock samples instead of two. The main problem is the large difference in the silica concentrations. Many of the other elements show good agreement, e.g. P_2O_5, Na_2O, K_2O, TiO_2, BaO and MnO.

Table 4:20

Comparison of data obtained using Multiple regression analysis (XRF4) and the Norrish and Hutton (1969) method of calculating alpha coefficients for the low dilution fusion discs. (wt.%)

	PK3/3		PK7/1	
	LDF Norrish	LDF XRF4	LDF Norrish	LDF XRF4
SiO_2	50.36	48.84	51.71	51.07
TiO_2	6.34	6.37	4.84	4.99
Al_2O_3	6.95	6.73	8.71	8.62
Fe_2O_3	7.70	7.31	6.24	6.58
MnO	0.07	0.08	0.03	0.05
MgO	8.75	8.54	7.33	7.31
CaO	3.66	3.76	2.04	2.17
Na_2O	1.01	0.99	0.67	0.69
K_2O	9.53	9.47	9.66	10.07
P_2O_5	1.73	1.71	0.83	0.84
BaO	1.55	1.65	0.99	1.07
LOF	2.46	2.46	3.10	3.10
TOTAL	100.10	97.91	96.15	96.56

Discussion

These poor results led to further research into the theoretical calculation of alpha coefficients. The problems encountered with the calculation of alpha coefficients and calibration of the standards using the Norrish and Hutton (1969) method for the low dilution fusion disc seem to substantiate the findings of Lachance (1981). He reported that the value of the alpha coefficient is not constant but varies with weight fraction as described earlier.

Consequently the theoretical calculation of alpha coefficients using the Norrish and Hutton (1969) method presents a problem as the following are not taken into consideration: variation of alpha coefficient with weight fraction, X-ray tube operating voltage, geometry of the spectrometer (unless primary and secondary absorption are considered), which represents the fundamental parameters described earlier.

Lachance (1981) stated "Why is it that theoretical coefficients obtained by breaking the rules can prove beneficial in the correction of inter-element effects. One case that comes into mind is Norrish who obtains coefficients from calculations of mass absorption coefficients at characteristic emission lines only."

It was concluded from these two methods of calculating alpha coefficients, namely XRF4 and the Norrish and Hutton (1969) method, that for the low dilution fusion discs a program was required that calculated alpha factors from fundamental parameters and which took into consideration the variation of alpha coefficients with concentration which is documented by Lachance (1981).

Major element analysis using Fundamental Parameters.

NBSGSC, (Tao, Pella and Rousseau, 1985, NBS Technical Bull 1213), is a computer program written in Fortran IV for quantitative X-ray fluorescence analysis. The program is in two parts. The first part, CALCO, computes theoretical alpha coefficients, and part two, CALCOMP, calculates the composition of the analyte specimens. The program corrects for X-ray absorption/enhancement phenomena using the comprehensive alpha coefficient algorithm, known as COLA, proposed by Lachance et al. (1980). The COLA expression used in NBSGSC is outlined in Table 4:21. The COLA expression includes all three alpha coefficients described by Lachance et al. (1980) and there are various modifications to the expression if the elements are diluted either by oxides or a combination of oxides and flux. These modifications are explained in Table 4:21.

In NBSGSC there is a choice of three systems namely elemental, oxide and fused disc. Theoretical alpha coefficients are calculated for one of these three systems according to the COLA expression. In the fused disc system, various flux compositions can be selected.

The theoretical alpha coefficients are calculated in CALCO using fundamental parameters which include - mass absorption coefficients, fluorescent yields, jump ratios, analyte wavelengths, geometry of the spectrometer and absorption edge wavelengths. Many of these are either computed by or are stored in the program. The X-ray spectral distribution required in the fundamental parameter method, when the source of excitation of specimen is an X-ray tube, can either be calculated using an NBS algorithm (Pella et al. 1985) or can be entered as a measured

Table 4:21. The COLA expression as used in NBSGSC

$$C_1 \pm R_I \left(1 + \sum_j \alpha'_{ij} C_j + \sum_j \sum_k \alpha'_{ijk} C_j C_k \right) \quad 1$$

$$\alpha'_{ij} = \alpha_1 + \frac{\alpha_2 C_m}{1 + \alpha_3(1 - C_m)} \quad 2$$

α_1 = value of coefficient near $C_I = 1$ limit
α_2 = value within which α'_{ij} varies when analyte concentration decreases to the $C_I = 0.0$ limit
α_3 = rate at which α'_{ij} is made to vary hyperbolically between the two stated limits, .001 and .999

$C_m = C_I + C_k + \ldots$

$$\alpha'_{ijk} = \frac{1}{C_I C_k} \left\{ \frac{C_I}{R_I} (1 + \alpha'_{ij} C_I + \alpha'_{ik} C_k \right\} \quad 3$$

For multi-element analysis of alloys all coefficients in equation 1 are calculated.
For specimens such as cements α_3 is nearly equal to zero and equation 2 can be simplified to
$\alpha'_{ij} = \alpha_1 + \alpha_2 C_m$
For fusions α_2, α_3 and α'_{ij} are approximately zero and equation 1 can be simplified to
$C_I = R_I(1 + \Sigma \alpha_{ij} C_j)$ ← usual Lachance-Traill equation

spectrum. The calculated spectrum for a Cr X-ray tube operated at 50 kV and 55 mA is shown in Figure 4:11 and Table 4:22. The program allows for the use of either Sc, Cr, Mo, Rh, Ag, W or Au X-ray tubes and calculates the spectrum at the operating voltages specified. If a Cr tube is selected, the use of an aluminium filter for Mn and Cr determinations is assumed, and the primary spectrum is automatically corrected in the program for the absorption by the filter.

Mass absorption coefficients are either calculated by the program using Heinrich's (1966) algorithm using the general relationship :

$$\mu = C\lambda^{n}$$

where λ = wavelength

C = coefficient calculated by least squares fit.

n = constant for all absorbers

or from Thinh and Leroux's (1979) tabled values using the following equation :

$$\mu = C\ E_{ab}\lambda^{n}$$

where E_{ab} = the lower energy of the two edges enclosing energy E of the radiation

The values for Thinh and Leroux's (1979) data are not calculated in the program but are stored in a permanent data file. The m.a.c. values for oxygen in Heinrich (1966) as reported earlier are incorrect, but in NBSGSC the m.a.c.s are calculated directly from the equations listed above and are correct.

Figure 4.11 Cr X-ray tube spectrum at 50 kV calculated by NBSGSC (Pella et al 1985)

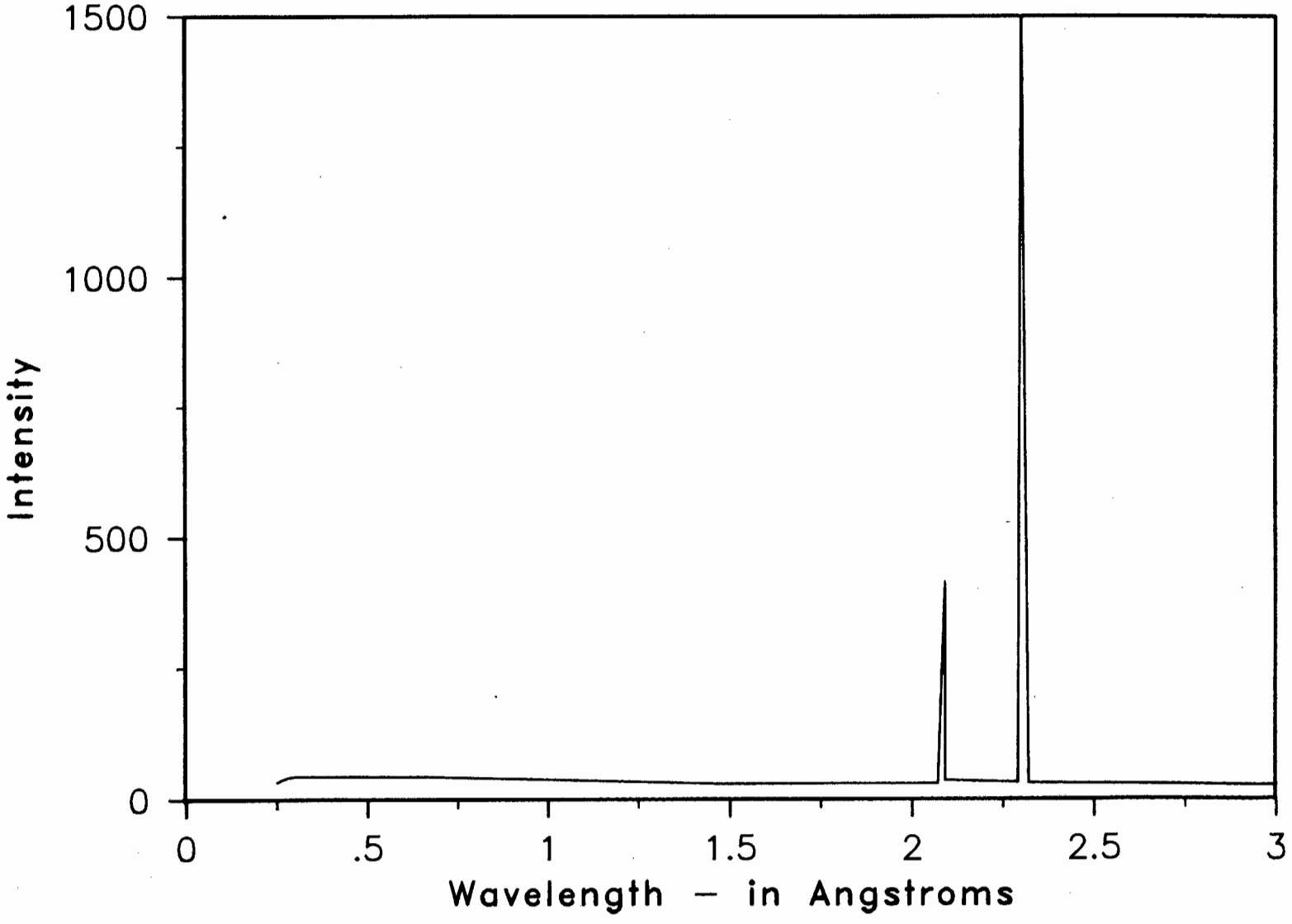

TABLE 4:22 CALCULATED X-RAY TUBE SPECTRAL DISTRIBUTION USING NBS ALGORITHM

X-RAY TUBE TARGET: CR KV: 50.0
TAKE OFF ANGLE(DEGREES): 26.0 BE WINDOW THICKNESS(MM): .500

LAMDA(A)	I	LAMDA(A)	I	LAMDA(A)	I	LAMDA(A)	I	LAMDA(A)	I
.2480	.0000E+00	.2680	.7323E-04	.2880	.1267E-03	.3080	.1660E-03	.3280	.1948E-03
.3480	.2160E-03	.3680	.2314E-03	.3880	.2423E-03	.4080	.2498E-03	.4280	.2548E-03
.4480	.2576E-03	.4680	.2589E-03	.4880	.2588E-03	.5080	.2578E-03	.5280	.2560E-03
.5480	.2535E-03	.5680	.2505E-03	.5880	.2471E-03	.6080	.2434E-03	.6280	.2395E-03
.6480	.2354E-03	.6680	.2311E-03	.6880	.2267E-03	.7080	.2222E-03	.7280	.2177E-03
.7480	.2131E-03	.7680	.2085E-03	.7880	.2039E-03	.8080	.1994E-03	.8280	.1948E-03
.8480	.1903E-03	.8680	.1858E-03	.8880	.1813E-03	.9080	.1769E-03	.9280	.1725E-03
.9480	.1682E-03	.9680	.1639E-03	.9880	.1598E-03	1.0080	.1558E-03	1.0280	.1518E-03
1.0480	.1478E-03	1.0680	.1440E-03	1.0880	.1402E-03	1.1080	.1364E-03	1.1280	.1328E-03
1.1480	.1292E-03	1.1680	.1257E-03	1.1880	.1222E-03	1.2080	.1189E-03	1.2280	.1156E-03
1.2480	.1123E-03	1.2680	.1092E-03	1.2880	.1061E-03	1.3080	.1031E-03	1.3280	.1001E-03
1.3480	.9725E-04	1.3680	.9444E-04	1.3880	.9170E-04	1.4080	.8902E-04	1.4280	.8641E-04
1.4480	.8387E-04	1.4680	.8139E-04	1.4880	.7898E-04	1.5080	.7663E-04	1.5280	.7434E-04
1.5480	.7211E-04	1.5680	.6995E-04	1.5880	.6784E-04	1.6080	.6579E-04	1.6280	.6379E-04
1.6480	.6185E-04	1.6680	.5997E-04	1.6880	.5814E-04	1.7080	.5636E-04	1.7280	.5463E-04
1.7480	.5296E-04	1.7680	.5133E-04	1.7880	.4975E-04	1.8080	.4822E-04	1.8280	.4673E-04
1.8480	.4529E-04	1.8680	.4389E-04	1.8880	.4253E-04	1.9080	.4121E-04	1.9280	.3993E-04
1.9480	.3870E-04	1.9680	.3750E-04	1.9880	.3633E-04	2.0080	.3521E-04	2.0280	.3411E-04
2.0480	.3305E-04	2.0680	.3203E-04	2.0880	.7074E-04	2.1080	.6933E-04	2.1280	.6793E-04
2.1480	.6656E-04	2.1680	.6520E-04	2.1880	.6387E-04	2.2080	.6255E-04	2.2280	.6126E-04
2.2480	.5998E-04	2.2680	.5872E-04	2.2880	.5748E-04	2.3080	.5626E-04	2.3280	.5505E-04
2.3480	.5387E-04	2.3680	.5270E-04	2.3880	.5155E-04	2.4080	.5042E-04	2.4280	.4931E-04
2.4480	.4821E-04	2.4680	.4713E-04	2.4880	.4607E-04	2.5080	.4503E-04	2.5280	.4400E-04
2.5480	.4299E-04	2.5680	.4200E-04	2.5880	.4102E-04	2.6080	.4006E-04	2.6280	.3911E-04
2.6480	.3819E-04	2.6680	.3727E-04	2.6880	.3638E-04	2.7080	.3550E-04	2.7280	.3463E-04
2.7480	.3378E-04	2.7680	.3295E-04	2.7880	.3213E-04	2.8080	.3133E-04	2.8280	.3054E-04
2.8480	.2977E-04	2.8680	.2901E-04	2.8880	.2827E-04	2.9080	.2754E-04	2.9280	.2682E-04
2.9480	.2612E-04	2.9680	.2544E-04	2.9880	.2476E-04				

I = Intensity

KA	KB	LA1	LB1	LB2	LB3	LB4	LG1	LG2	LG3	LL
2.2910	2.0850	0.0000	0.0000	0.0000	0.0000	0.0000	0.0000	0.0000	0.0000	0.0000
.2558E-01	.4027E-02	.0000E+00	.0000E+00	.0000E+00	.0000E+00	.0000E+00	.0000E+00	.0000E+00	.0000E+00	.0000E+00

Alpha coefficients are calculated for loss assuming the hypothetical compound CO_3 as an approximation to CO_2 and H_2O.

In CALCOMP, concentration data for unanalyzed elements, including loss (either as LOI or LOF) can be entered as given concentrations for each standard or specimen. There is also a choice of four calibration curves which are as follows :-

1	straight line	$Y = A0 + A1 \times X$
2	quadratic line	$Y = A0 + A1 \times X + A2 \times X^2$
3	straight line constrained to zero intercept	$Y = A1 \times X$
4	quadratic line constrained to zero intercept	$Y = A1 \times X + A2 \times X^2$

Tao, Pella and Rousseau (1985) recommended the use of curve 4 as they report that this curve partially compensates for inaccuracies in fundamental parameters used in the calculation of theoretical alpha coefficients especially over wide concentration ranges.

The second part of the program, CALCOMP, also allows the comparison of calculated data with previously known data and consequently average absolute and relative errors can be generated for the standards. This is invaluable for evaluating data reduction techniques.

Further information on the actual program structure can be obtained from the NBS Technical Bulletin 1213 (1985). Various system specific modifications had to be made to the program to enable it to run on the HP 1000 computer system

operating in the Geochemistry Department, U.C.T. The program was initially tested using the examples supplied in the NBS Technical Bulletin. The examples of the elemental, oxide and fused disc systems reproduced identical data with that listed in the Bulletin thus indicating that the program was working properly.

Various modifications have been made to the program to suit the analytical requirements of the Geochemistry Department and to make the program more "user friendly". The net intensity data for the specimens and standards and concentration data for the standards can now be entered via the terminal or be read from a file previously created. The concentration data can be entered as either weight fractions or as weight percentages. If entered as percentages the data is converted to weight fractions within the program. The program has been re-dimensioned to handle 20 elements (21 including loss) and 40 standards and unknown specimens. It was originally designed for 12 elements (13 including loss) and 20 standards and unknown specimens.

For the fused disc system the original program contained only three choices of flux composition. Two more compositions have been added: one for the Norrish and Hutton (1969) flux containing lanthanum oxide; and one to suit the flux composition and dilution ratio used in the low dilution fusion method.

In the original program for the fused disc systems, LOI was fixed at 25% and alpha coefficients calculated accordingly. The program has now been modified to calculate alpha coefficients for loss at any given value. This is generally the average loss value for the analytical specimens.

The program has been used to calculate alpha coefficients and

compute concentration data for low dilution fusion discs including international rock standards, lamproites and kimberlites, and Norrish and Hutton (1969) type fusion discs of international rock standards from the Geochemistry Department U.C.T., normal major element analytical run.

For the low dilution fusion technique, the spiked NIM and secondary standards have been used, as the composition of the standards needs to be similar to that of the analyte samples.

Fused disc system

Prior to reducing LDF data through NBSGSC the program was tested on Norrish and Hutton (1969) type fusion disc data taken from one of the normal departmental major element analytical runs.

Alpha coefficients for the fused disc system using the Norrish and Hutton (1969) flux containing lanthanum oxide are presented in Table 4:23. The results for the international rock standards derived using NBSGSC are in good agreement with those obtained using the Norrish and Hutton (1969) coefficients, and the average absolute and relative errors are comparable. The average absolute and relative errors using calibration curve 2, $Y = A0 + A1 \times X + A2 \times X^2$, are given in Table 4:24. This equation was used as the intensity data were not blank corrected and the calibration curve should not therefore be forced through the origin. In Table 4:25, recommended international standards data are compared to data obtained from NBSGSC. For all the standards the number of iteration cycles to reach the convergence criteria of 0.01% was less than or equal to 3. It should be noted that in the Norrish and Hutton (1969) method, proper blank corrections and crystal fluorescence corrections for Mg and P have been made. In NBSGSC, no blank, background or crystal fluorescence corrections have been made. A detailed look at the data indicates that corrections for crystal fluorescence is required for the NBSGSC data.

TABLE 4:23 MODIFIED ALPHA COEFFICIENTS FOR USE IN COLA EQUATION

(FUSED DISC SYSTEM)
NORRISH & HUTTON DISCS

TARGET : CR 50 0 KV
GEOMETRY : 60,40 DEGREES

MATRIX CONSTITUENTS

			11	12	13	14	15	19	20	22	25	26
		LOI	NA2O1	MG1O1	AL2O3	SI1O2	P 2O5	K 2O1	CA1O1	TI1O2	MN1O1	FE2O3
MEAN CONC		7.50	10.00	12 00	12.00	65.00	4.00	12.00	15 00	7.00	1.00	12.00
ANALYTE												
11	NA2O1	- 068	0.000	.021	037	.049	.058	.053	.070	099	.297	.318
12	MG1O1	-.080	.228	0.000	.007	.018	.024	.017	.031	.054	.227	.244
13	AL2O3	-.087	.191	.218	0 000	.002	.008	.002	.014	.034	.194	.209
14	SI1O2	-.099	.173	.199	.232	0.000	-.002	-.002	.009	.026	.178	.194
15	P 2O5	- 111	.157	.183	.215	.244	0.000	-.007	.004	.023	.164	.179
19	K 2O1	-.255	-.028	-.005	.023	.049	.083	0.000	-.074	-.061	-.013	-.001
20	CA1O1	-.294	-.075	-.053	-.026	-.001	.033	.686	0.000	-.076	-.059	-.047
22	TI1O2	-.384	-.184	-.164	- 139	-.115	-.084	.521	.517	0 000	-.165	-.155
25 F	MN1O1	-.124	-.049	-.042	-.032	-.023	-.011	.221	.220	.249	0.000	.004
26	FE2O3	-.178	-.112	-.104	-.095	-.087	-.076	.138	.137	164	-.003	0.000

+ FUSED DISC . 2800G SAMPLE + .8900G LI2B4O7 + .3000G LIO2 from LI2CO3 + .3000G LA2O3

F DENOTES THE USE OF FILTER

Table 4:24

Average absolute and relative errors for Norrish and Hutton (1969) fusion discs using alpha coefficients (Table 4:23) calculated using NBSGSC - $Y = A0 + A1 \times X + A2 \times X^2$ calibration curve.

	Ave. Abs. Error	Ave. Rel. Error	Concentration Range (%)
SiO_2	0.235	0.440	35 - 100
TiO_2	0.010	1.258	.01 - 2.7
Al_2O_3	0.069	1.299	.25 - 27
Fe_2O_3	0.051	0.919	.6 - 17
MnO	0.004	4.462	.02 - .25
MgO	0.141	7.681	.75 - 45
CaO	0.037	1.261	.14 - 12
Na_2O	0.029	2.998	.04 - 4.5
K_2O	0.019	12.42 *	.01 - 5.6
P_2O_5	0.005	13.62 *	.1 - 1.7

* These high average relative errors are due to large errors on rock standards that have <.5% of analyte element and in most cases no recommended standard value.

Table 4:25

Comparison of international standards data with data obtained from NBSGSC for Norrish and Hutton (1969) type fusion discs. Data for loss is not reported. (wt.%)

		GSP-1	BCR-1	DTS-1
SiO_2	(a)	67.76	54.53	40.54
	(b)	67.79	54.79	40.64
TiO_2	(a)	0.66	2.26	0.01
	(b)	0.67	2.22	0.06
Al_2O_3	(a)	15.38	13.72	0.25
	(b)	15.22	13.62	0.34
Fe_2O_3	(a)	4.33	13.41	8.69
	(b)	4.38	13.52	8.64
MnO	(a)	0.04	0.18	0.12
	(b)	0.04	0.18	0.12
MgO	(a)	0.98	3.48	49.72
	**(b)	1.41	3.88	50.14
CaO	(a)	2.04	6.97	0.14
	(b)	2.02	6.93	0.16
Na_2O	(a)	2.83	3.30	0.01
	(b)	2.82	3.34	0.01
K_2O	(a)	5.55	1.70	0.00
	(b)	5.58	1.73	0.02
P_2O_5	(a)	0.28	0.36	0.00
	(b)	0.24	0.31	0.07
Total	(a)	99.85	99.91	99.48
	(b)	100.17	100.52	100.20

(a) recommended International standards value

(b) calculated by NBSGSC using fused disc system alpha coefficients detailed in Table 4:23.

** no correction for crystal fluorescence, therefore values to high.

The international and "spiked" standards data for the low dilution fusion discs from NBSGSC using alpha coefficients calculated using both the Heinrich (1966), Table 4:26(a) and Thinh and Leroux (1979), Table 4:26(b) algorithms for the fused disc system and a $Y = A1 \times X + A2 \times X^2$ calibration curve gave acceptable values for average absolute and relative errors. These values are reported in Table 4:27. The intensities used for calibration had been background corrected, and therefore no correction for the effect of crystal fluorescence was necessary.

Table 4:27

Average absolute and relative errors for "spiked" and international LDF rock standards using $Y = A1 \times X + A2 \times X^2$ calibration curve and fusion disc system alphas calculated with Heinrich's (1966) and Thinh and Leroux's (1979) algorithm.

	Heinrich		Thinh and Leroux	
	Ave. Abs. Error	Ave. Rel. Error	Ave. Abs. Error	Ave. Rel. Error
SiO_2	0.561	1.162	0.509	1.040
TiO_2	0.044	4.713*	0.041	4.409*
Al_2O_3	0.206	1.917	0.145	1.454
Fe_2O_3	0.070	1.483	0.074	1.587
MnO	0.014	52.595*	0.015	56.167*
MgO	0.112	8.433*	0.114	8.461*
CaO	0.100	1.552	0.094	1.575
Na_2O	0.065	12.792*	0.071	12.916*
K_2O	0.035	5.216*	0.039	5.385*
P_2O_5	0.007	15.847*	0.007	15.774*
BaO	0.034	5.497*	0.035	5.526*

* these high average relative errors reported here are due to large errors on rock standards that generally contain <.5% of the analyte element and in most cases do not have a recommended international value.

TABLE 4:26a MODIFIED ALPHA COEFFICIENTS FOR USE IN COLA EQUATION

(FUSED DISC SYSTEM)
LOW DILUTION DISC

HEINRICH (1986) ALGORITHM

TARGET : CR 50.0 KV
GEOMETRY : 60,40 DEGREES

MATRIX CONSTITUENTS

			11	12	13	14	15	19	20	22	25	26	56
		LOI	NA2O1	MGIO1	AL2O3	SIIO2	P 2O5	K 2O1	CAIO1	TIIO2	MNIO1	FE2O3	BAIO1
MEAN CONC		10.00	1.00	15.00	7.00	55.00	2.00	6.00	8.00	3.00	.50	10.00	1.50
ANALYTE													
11	NA2O1	-.241	0.000	.073	.125	.168	.195	.200	268	.392	1.031	1.104	1.073
12	MGIO1	-.311	.880	0.000	.029	.069	.095	.112	.173	.285	.863	.930	1.418
13	AL2O3	- 352	.772	.879	0.000	.010	.034	.065	.122	.229	.766	.829	1.618
14	SIIO2	-.388	.677	.780	.907	0.000	-.000	061	.111	.204	.685	.745	1.592
15	P 2O5	-.420	594	.693	.815	.925	0.000	.017	.067	.164	.608	.665	1.566
19	K 2O1	-.661	- 067	-.007	.067	.134	.224	0.000	-.195	-.147	-.038	-.005	.897
20	CAIO1	- 699	-.173	- 120	- 054	.006	.087	1.657	0.000	-.184	- 143	-.114	.802
22	TIIO2	- 767	- 362	-.320	-.269	-.222	-.159	1.068	1.061	0.000	-.333	-.312	.761
25 F	MNIO1	-.731	-.266	-.217	-.157	-.102	-.028	1.411	1.404	1.583	0.000	.025	4.160
26	FE2O3	-.795	-.456	-.420	- 375	-.335	-.280	.784	.780	.913	-.019	0 000	3 398
56	BAIO1	-.869	- 637	-.613	-.584	-.557	-.521	.177	.173	-.446	-.621	-.611	0 000

+ FUSED DISC 2.0000G SAMPLE + .8000G LI2B4O7 +3.2000G LIBO2 + .6000G LI2O from LiNO3

F DENOTES THE USE OF FILTER

TABLE 4:26(b) MODIFIED ALPHA COEFFICIENTS FOR USE IN COLA EQUATION

(FUSED DISC SYSTEM)

LOW DILUTION DISCS

THINH & LEROUX (1979) ALGORITHM

TARGET : CR 50.0 KV

GEOMETRY : 60,40 DEGREES

MATRIX CONSTITUENTS

			11	12	13	14	15	19	20	22	25	26	56
		LOI	NA2O1	MG1O1	AL2O3	SI1O2	P 2O5	K 2O1	CA1O1	TI1O2	MN1O1	FE2O3	BA1O1
MEAN CONC.		10.00	1.00	15.00	7.00	55 00	2.00	6.00	8.00	3.00	.50	10.00	1.50
ANALYTE													
11	NA2O1	-.232	0.000	.081	.132	176	.206	.193	.269	.378	.957	1.018	- 147
12	MG1O1	-.306	.806	0.000	.030	.071	.099	.102	.172	.269	.774	830	.932
13	AL2O3	-.346	.706	.798	0.000	.013	.040	.052	.118	.211	676	.729	1.556
14	SI1O2	-.381	.618	.706	.814	0.000	.004	.042	.101	.181	.594	.643	1.516
15	P 2O5	-.411	.542	.626	.729	.823	0.000	-.002	.055	.139	.517	.563	1.480
19	K 2O1	-.648	-.037	.017	.082	.142	.225	0.000	-.181	-.138	-.045	-.018	.951
20	CA1O1	-.694	-.147	-.099	-.041	.012	.086	1.589	0.000	-.181	-.152	-.129	.858
22	TI1O2	-.767	-.339	-.299	-.254	-.212	-.153	1.050	1.042	0.000	-.339	-.322	.846
25 F	MN1O1	-.740	-.263	-.194	-.142	-.092	-.022	1.427	1.417	1.595	0.000	.020	4.375
26	FE2O3	-.804	-.460	-.416	-.379	-.335	-.276	807	.798	.930	-.015	0.000	3 357
56	BA1O1	-.874	-.640	-.619	-.594	-.572	-.540	.114	.109	-.469	-.641	-.633	0.000

* FUSED DISC .2.0000G SAMPLE + .8000G LI2B4O7 +3.2000G LIBO2 + .6000G LI2O from LiNO3

F DENOTES THE USE OF FILTER

Table 4:28

Comparison of international standards data with data obtained from NBSGSC for Low Dilution Fusion discs using Heinrich (1966) and Thinh and Leroux (1979) algorithms. (wt.%)

		G-2	MRG-1	S-7 5%BaO	BCR-1
SiO_2	(a)	69.22	39.32	32.26	54.53
	(b)	69.42	39.17	31.71	55.21
	(c)	69.37	39.12	31.79	55.02
TiO_2	(a)	0.48	3.75	1.53	2.26
	(b)	0.48	3.82	1.45	2.26
	(c)	0.48	3.81	1.46	2.26
Al_2O_3	(a)	15.40	8.50	4.14	13.72
	(b)	15.12	8.81	4.23	13.82
	(c)	15.20	8.67	4.14	13.73
Fe_2O_3	(a)	2.69	17.84	9.01	13.41
	(b)	2.64	17.88	8.88	13.42
	(c)	2.63	17.92	8.89	13.43
MnO	(a)	0.03	0.17	0.16	0.18
	(b)	0.03	0.15	0.15	0.17
	(c)	0.03	0.15	0.15	0.17
MgO	(a)	0.75	13.49	25.63	3.48
	(b)	0.76	13.92	25.69	3.53
	(c)	0.77	13.92	25.33	3.54
CaO	(a)	1.96	14.77	9.33	6.97
	(b)	1.96	14.86	9.12	7.17
	(c)	1.95	14.85	9.16	7.14
Na_2O	(a)	4.06	0.71	0.42	3.30
	(b)	4.10	0.70	0.56	3.36
	(c)	4.15	0.71	0.55	3.38
K_2O	(a)	4.46	0.18	0.99	1.70
	(b)	4.45	0.17	0.99	1.73
	(c)	4.44	0.17	1.00	1.73
P_2O_5	(a)	0.13	0.06	1.45	0.36
	(b)	0.14	0.06	1.45	0.38
	(c)	0.14	0.06	1.45	0.37
BaO	(a)	0.21	0.01	5.15	0.08
	(b)	0.21	0.01	5.13	0.08
	(c)	0.21	0.01	5.15	0.08
Total (no LOF)	(a)	99.39	98.72	90.07	99.99
	(b)	99.31	99.55	89.36	101.13
	(c)	99.37	99.39	89.07	100.85

(a) recommended International standards value
(b) calculated by NBSGSC using Heinrich (1966)
(c) calculated by NBSGSC using Thinh and Leroux (1979)

The average absolute errors using the Thinh and Leroux (1979) algorithm to calculate the alpha coefficients are similar to those for the Heinrich (1966) algorithm except for Al_2O_3, for which Thinh and Leroux (1979) errors are significantly smaller.

International standards data and "spiked" standards data are compared with data obtained by NBSGSC and the two mass absorption coefficient algorithms in Table 4:28. These results reflect the high average absolute errors for SiO_2. Data for BCR-1 (Table 4:25 and 4:28), using NBSGSC alpha coefficients, indicate that the low dilution fusion technique yields better results for TiO_2, Al_2O_3, Fe_2O_3 and MgO but worse for SiO_2 than the Norrish and Hutton (1969) type fusion discs. The improvement of the MgO concentrations is a result of the correction for crystal fluorescence in the analysis of the low dilution fusion discs.

Unfortunately the lamproite and kimberlite data once again produced low analytical totals, ranging from 95% to 100%, several examples of which are given in Table 4:29. Even samples with low concentrations of barium did not give acceptable analytical totals. However the data did indicate the high degree of variability in the composition of the samples.

Table 4:29

Major element data for lamproite samples obtained from NBSGSC using fused disc system, Heinrich's (1966) algorithm and $Y = Al + X + A2 \times X^2$ calibration curve.(wt.%)

	CKP 9	PK3/9	PK12/1	PK11/1
SiO_2	19.16	28.01	60.29	47.39
TiO_2	3.19	5.53	5.16	5.03
Al_2O_3	2.35	3.23	8.08	6.98
Fe_2O_3	14.79	6.75	6.82	6.57
MnO	0.14	0.05	0.04	0.05
MgO	25.01	10.04	2.33	10.89
CaO	15.31	17.16	1.32	3.25
Na_2O	0.14	0.47	0.14	0.25
K_2O	0.25	5.39	8.16	8.71
P_2O_5	2.81	1.45	1.12	1.94
BaO	0.22	2.23	0.45	0.82
LOF	12.94	16.22	2.19	3.20
TOTAL	96.31	96.53	96.10	95.08

Discussion

Due to the large concentration ranges and the low dilution ratio it was thought that the fused disc system in NBSGSC, with the omission of α_2, α_3 and α_{ijk} (Table 4:21), might not hol true for the low dilution fusion discs. The only example for the fused disc system given in the Tech. Bull. 1213 (Tao et al. 1985) is for a sample:flux ratio of 1:5.3, i.e. similar to the Norrish and Hutton (1969) type fusion disc but without the addition of a heavy absorber. The low dilution fusion discs have a sample to flux ratio of 1:2.13 or approximately 2.5 times more sample than the example given in the Tech. Bull. 1213 (Tao et al 1985).

In the COLA expression (Lachance et al., 1980), Table 4:21, the fused disc system is the simplest form and the authors of NBSGSC, Tao, Pella and Rousseau (1985) suggest that with the flux being the major constituent of the disc and relatively constant with respect to weight percent. The α_2, α_3 and α'_{ijk} terms are approximately zero, so the α'_{ij} equation (2) reduces to the conventional Lachance-Traill (1966) expression (Table 4:21). This disregards the dependence of the alpha coefficient on weight fraction of analyte as reported by Lachance (1981).

In correspondence with Pella, he suggested that as long as the calibrations were carried out using 'type' standards the single coefficient model of Lachance-Traill (1966) should suffice. However, he conceded that this analytical problem was an interesting one which should be explored further. Bearing in mind the wide range of sample concentrations reported in Table 4:6 and 4:29, it is obviously impossible to analyze all samples and use "type" standards in a single run.

Oxide System

In an attempt to resolve the problem of low totals for the lamproite and kimberlite samples, it was decided to use the oxide system of NBSGSC and to calculate oxide alpha coefficients for the low dilution fusion discs, including the oxides from the flux and nitrate that are present in the fused disc, namely Li_2O and B_2O_3. The weight percent of Li_2O and B_2O_3 in the flux a lithium nitrate were calculated as detailed in Appendix C and alpha coefficients for the oxides computed. The use of the oxide alpha coefficient system computes the following alpha coefficients :-

α_1 - at the $W_i = 1.0$ limit

α_2 - at the $W_i = 0.0$ limit

and α_{ijk} - coefficient to compensate for the fact that total interelement correction can not be strictly represented by the sum of binary matrix coefficients.

The oxide alpha coefficients using both Heinrich's (1966) and Thinh and Leroux's (1979) algorithms are presented in Appendix E. The alpha coefficients for loss in the oxide system are calculated using CO_3, which is assumed as an approximation to CO_2 and H_2O.

In CALCOMP, part two of the program, the Li_2O and B_2O_3 contents of the fused discs were entered as fixed concentrations and the international and "spiked" standards concentration data were reduced by a factor of 3.065 to account for dilution by the Li_2O and B_2O_3 present. This resulted in the input concentration data for the standards being identical to the composition of the

glass disc. Loss on fusion values were also entered as fixed concentrations.

The results from CALCOMP using oxide alpha coefficients were encouraging.

In Table 4:30 data for one international and two "spiked" standards obtained from the low dilution fusion discs reduced using oxide alpha coefficients are compared to calculated and recommended values. Data for lamproites and kimberlites are also reported in Appendix G. The data reported in Appendix G have been produced using Thinh and Leroux's (1979) m.a.c. algorithm, as the data for Al_2O_3 are in better agreement with the recommended values for the standards.

To recalculate the standards, lamproite and kimberlite data to the original sample, i.e. without the Li_2O and B_2O_3 from the flux, the data were recalculated to the analytical total given in the program CALCOMP. For example if the analytical total was 100.28 with 67.32 % of this being flux, then the rock totalled 32.96% of the disc. The sample data were recalculated to a total of 100.28, i.e. x 100.28/32.96.

Table 4:30

Comparison of data for the standards used to calibrate the low dilution fusion discs using the oxide alpha coefficients - Heinrich (1966), and Thinh and Leroux (1979) algorithms.(wt.%)

		S-7 5% BaO	NIM G	S-13 10% TiO_2
SiO_2	(a)	32.26	75.70	44.91
	(b)	32.15	75.76	45.23
	(c)	32.27	75.68	45.11
TiO_2	(a)	1.53	0.10	11.63
	(b)	1.46	0.09	11.58
	(c)	1.47	0.09	11.60
Al_2O_3	(a)	4.14	12.08	23.98
	(b)	4.22	11.98	24.16
	(c)	4.16	12.03	24.14
Fe_2O_3	(a)	9.01	2.02	11.37
	(b)	8.85	1.97	11.37
	(c)	8.86	1.98	11.38
MnO	(a)	0.16	0.02	0.09
	(b)	0.25	0.02	0.08
	(c)	0.26	0.02	0.08
MgO	(a)	25.63	0.06	3.09
	(b)	25.63	0.06	3.04
	(c)	25.33	0.06	3.05
CaO	(a)	9.33	0.78	0.70
	(b)	9.19	0.77	0.69
	(c)	9.23	0.77	0.69
Na_2O	(a)	0.42	3.36	0.75
	(b)	0.58	3.31	0.66
	(c)	0.61	3.35	0.68
K_2O	(a)	0.99	4.99	2.87
	(b)	1.01	4.94	2.85
	(c)	1.02	4.93	2.85
P_2O_5	(a)	1.45	0.10	0.08
	(b)	1.44	.003	0.07
	(c)	1.44	.003	0.08
BaO	(a)	5.15	0.01	0.09
	(b)	5.16	.012	0.09
	(c)	5.18	.012	0.09
Total (no LOF)	(a)	90.07	99.22	99.56
	(b)	89.94	98.91	99.82
	(c)	89.83	98.92	99.75

(a) Standard or recalculated value (spiked standards)
(b) Using Heinrich algorithm
(c) using Thinh and Leroux algorithm

Table 4:31

Average absolute and relative errors for international and "spiked" standards using oxide alpha coefficients.

	Heinrich's Algorithm		Thinh and Leroux	
	Ave Abs Error	Ave Rel Error	Ave Abs Error	Ave Rel Error
SiO_2	.398	.771	.407	.807
TiO_2	.042	1.570	.037	1.447
Al_2O_3	.141*	1.272	.095*	.758
Fe_2O_3	.055	1.382	.058	1.363
MnO	.021	30.000+	.021	30.741+
MgO	.052	14.237+	.043	14.003+
CaO	.077	1.466	.070	1.569
Na_2O	.067	10.283+	.070	10.719+
K_2O	.046	1.784	.046	1.833
P_2O_5	.006	7.252+	.006	6.017+
BaO	.052	6.409+	.052	6.459+

* large difference in average absolute error between two data sets.

\+ these high average relative errors reported here are due to large errors on rock standards that generally contain <.5% of the analyte element and in most cases do not have a recommended international value.

The good agreement of the standards data and the acceptable analytical totals for the lamproites and kimberlites using the oxide type calculation model indicates that the single coefficient model, the fused disc system of NBSGSC, does not hold true for the low dilution fusion discs even though the alpha coefficients are calculated from fundamental parameters. It appears that the variation of the alpha coefficient with concentration of the analyte element is an **essential** ingredient for the reduction of major element data when a low dilution fusion technique is employed. The use of a heavy absorber in a low dilution fusion technique would most likely result in the single coefficient model holding true as the heavy absorber would suppress the interelement effects.

Average absolute and relative errors for the international and "spiked" standards using Heinrich (1966) and Thinh and Leroux's (1979) algorithm to calculate the oxide alpha coefficients are reported in Table 4:31. The average absolute errors reported by CALCOMP were multiplied by 3.065 to correct for the initial reduction of the standards concentration data by the same factor. The average absolute and relative errors in Table 4:31 are significantly lower than those reported for the Norrish and Hutton (1969) derived alpha factors in Table 4:18. The average absolute error for SiO_2 for the Norrish and Hutton (1969) derived alpha factors was 1.079 % which has been reduced to 0.407 % using oxide system alpha coefficients in NBSGSC. The latter average absolute error for SiO_2 is still a factor of 1.6 larger than the average absolute error for normal Norrish and Hutton (1969) type fusion discs containing lanthanum oxide. This

large difference is most likely due to the use of both "spiked" standards and international standards for calibration of the low dilution fusion discs and only international standards for the Norrish and Hutton (1969) type fusion discs.
Using the oxide system of the NBSGSC program the average absolute errors for SiO_2, Al_2O_3, MgO, CaO and Fe_2O_3 are reduced compared to the errors for the fused disc system, Table 4:27. With reference to Table 4:6, these five oxides are the major constituents of the lamproites and kimberlites and generally have the largest concentration range and variability. The other oxides, BaO, MnO, K_2O, Na_2O, TiO_2 and P_2O_5 that a generally present in low concentrations have higher average absolute errors for the data reduced using the oxide alpha coefficients.

The SiO_2 and MgO calibration curves in Figure 4:10, 4:12 (a+b) and 4:13 (a-c) show the effect of using oxide system alpha coefficients to correct for interelement effects in low dilution fusion discs. The two sets of calibration curves show the change in the form of the curve from a no correction model to the fused disc system and finally to the oxide system of NBSGSC. On examination of the figures it is obvious that the agreement between the standard and calculated values using the oxide system alpha coefficients for SiO_2 and MgO are significantly improved compared to the fused disc system alpha coefficients.

In Figure 4:14 (a-c), the use of the two sets of oxide alpha coefficients, Heinrich (1966) and Thinh and Leroux (1979), are graphically illustrated to show their effects on the interelement correction of Al_2O_3. The use of Thinh and Leroux's (1979) algorithm to calculate oxide alpha coefficients significantly improves the linear relationship between the

Figure 4:12 (a) Silica – NBSGSC theoretical alpha coefficients for fused disc system.

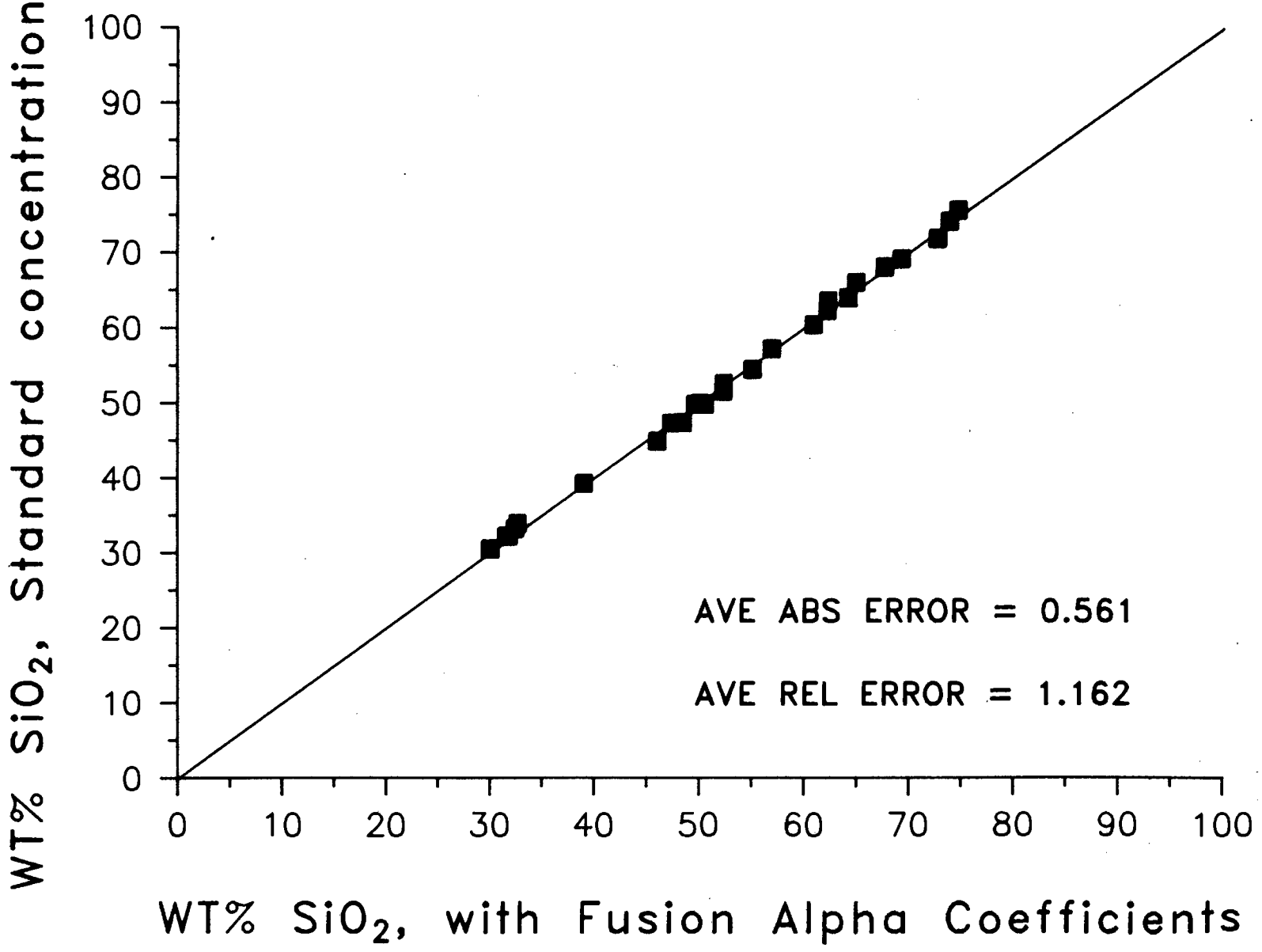

Figure 4:12(b) Silica – NBSGSC theoretical alpha coefficients for oxide system.

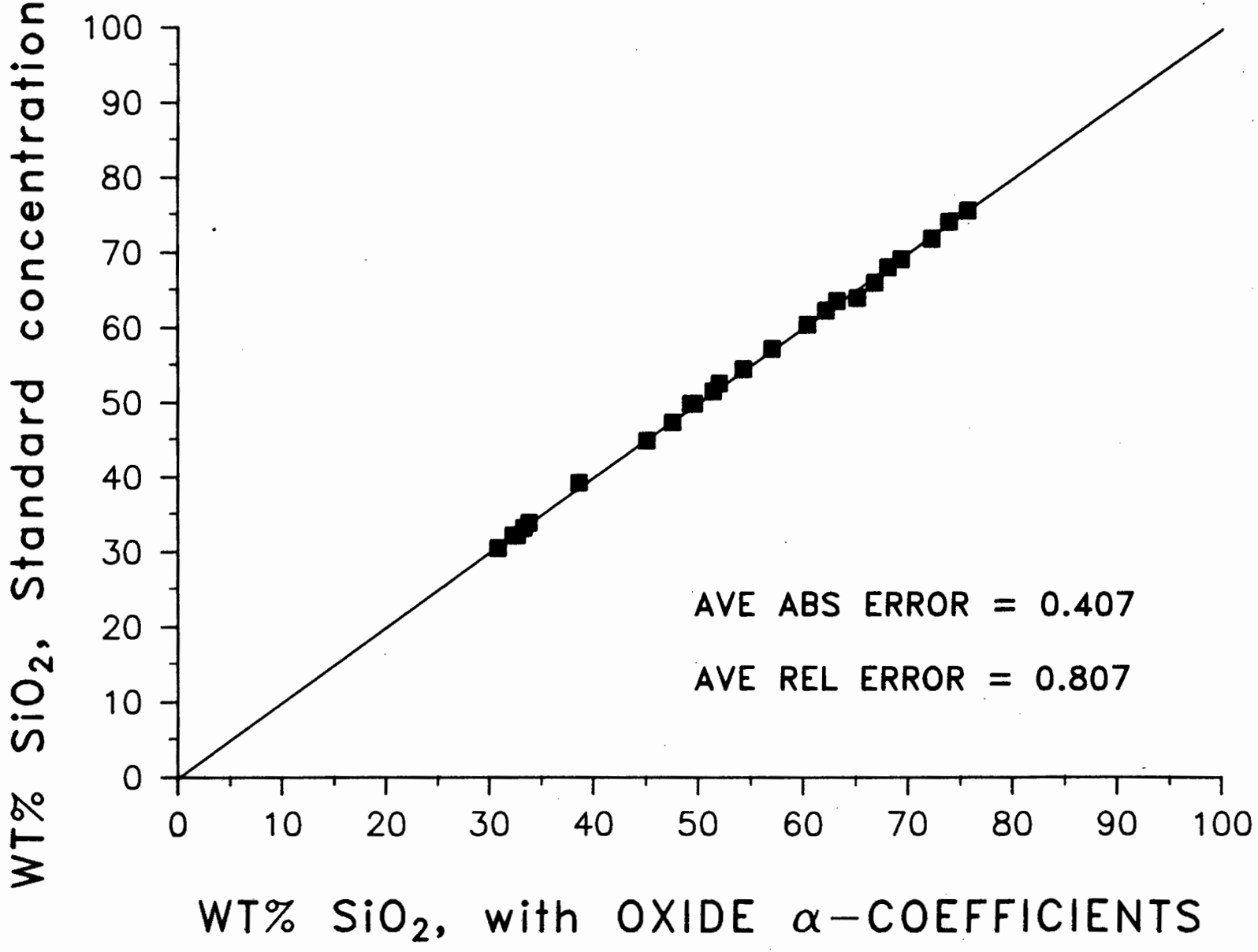

Figure 4:13(a) Magnesium – standard values vs uncorrected concentrations.

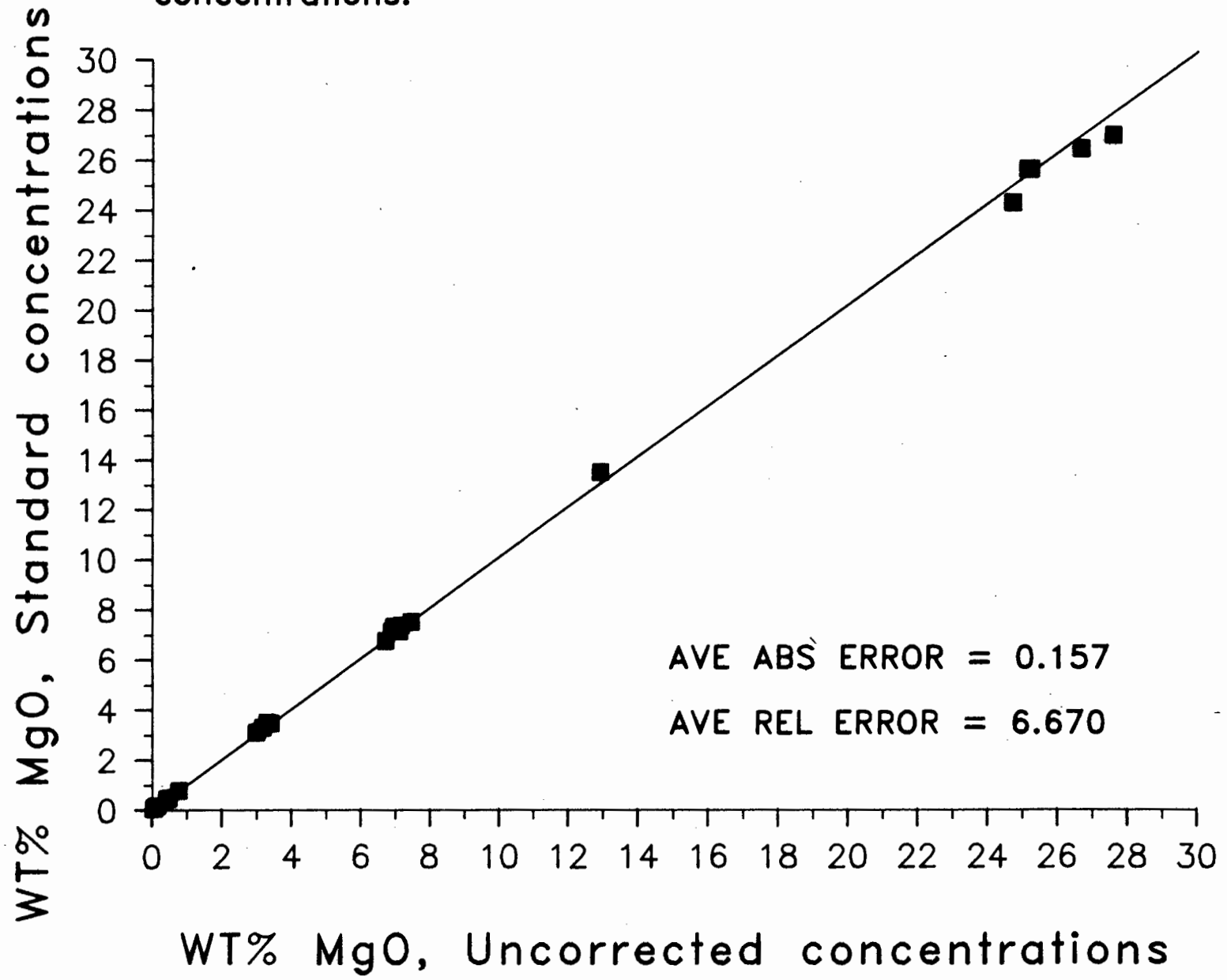

Figure 4:13(b) Magnesium – NBSGSC theoretical alpha coefficients for fused disc system.

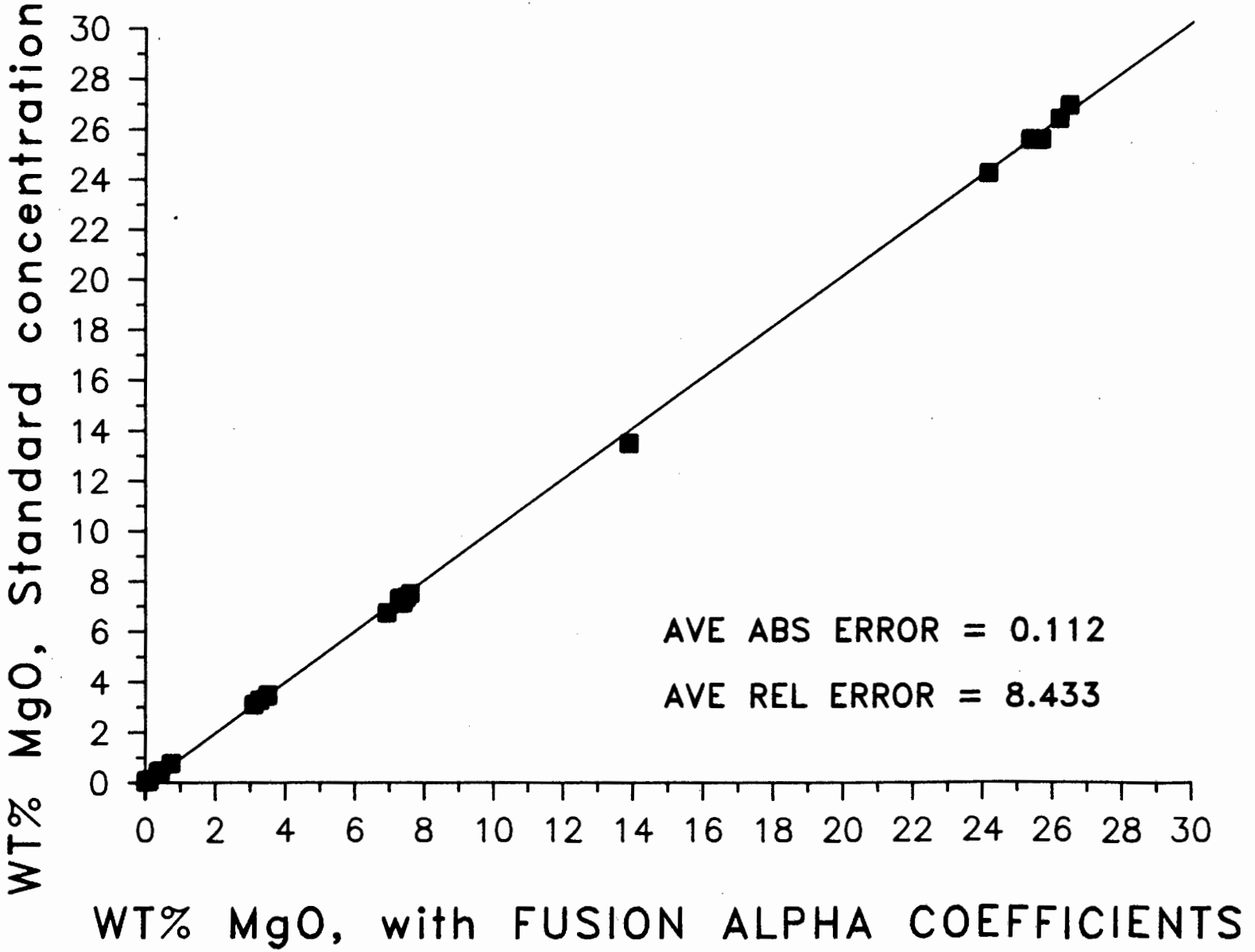

Figure 4:13(c) Magnesium – NBSGSC theoretical alpha coefficients for oxide system.

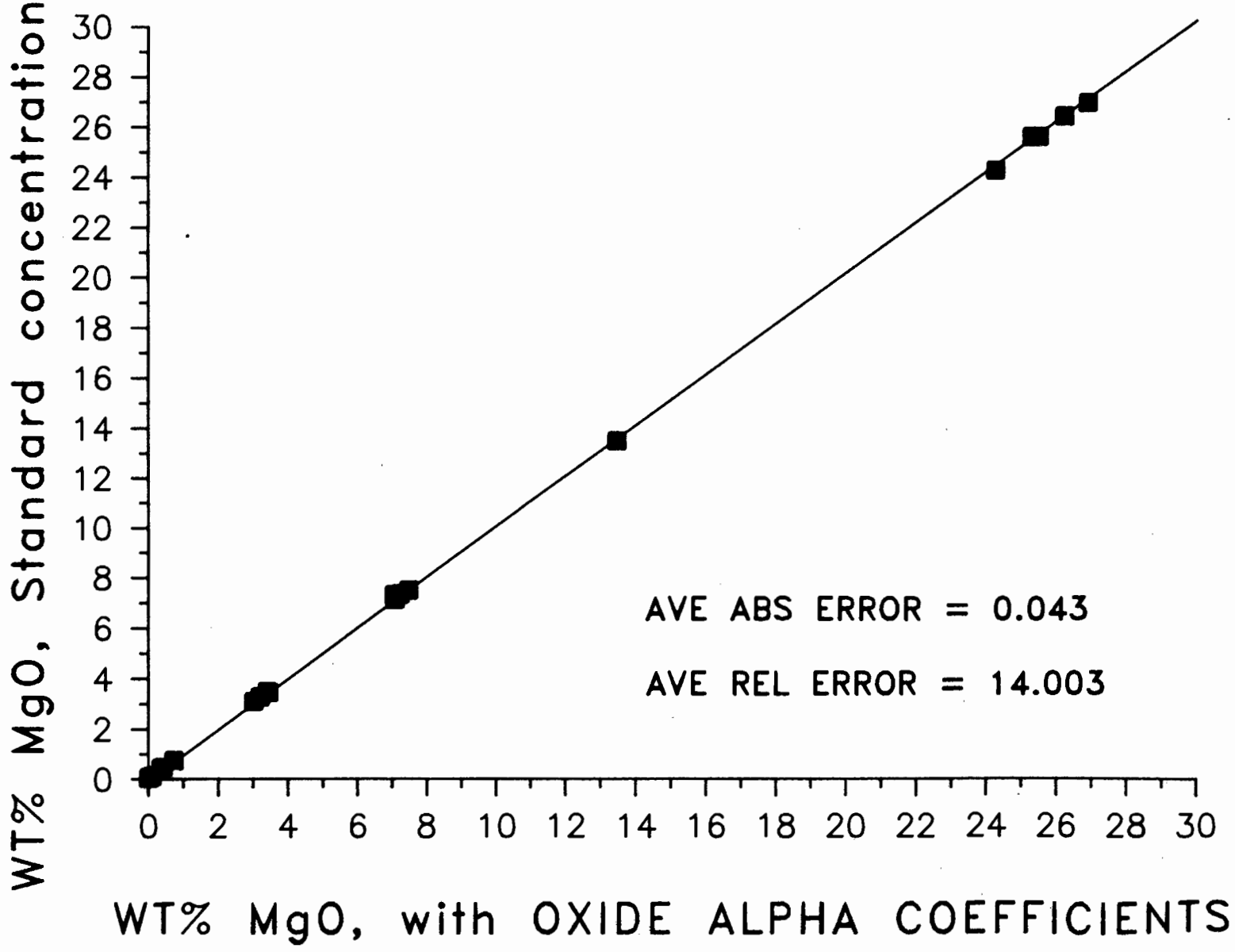

Figure 4:14(a). Aluminium – Standard values vs uncorrected concentrations.

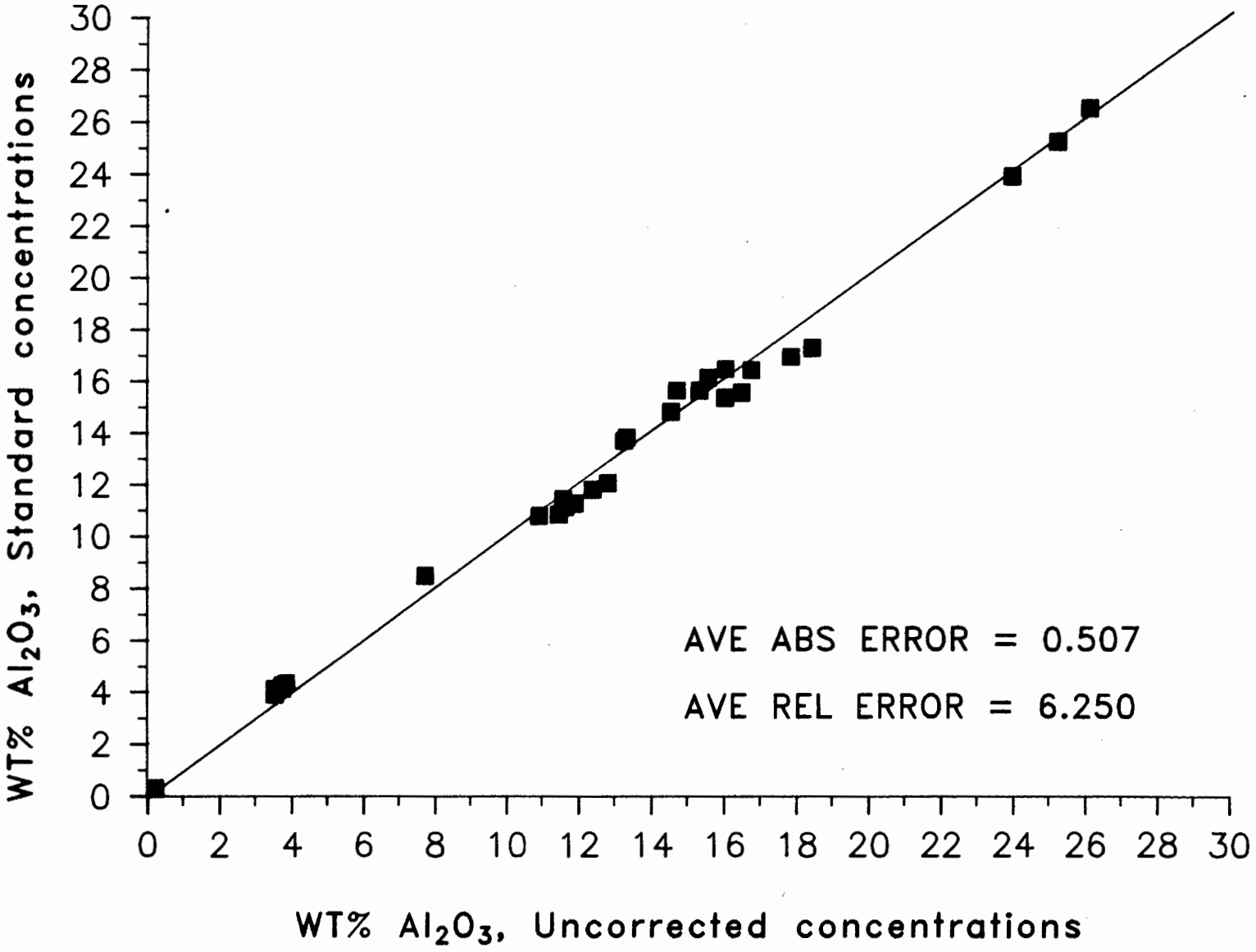

Figure 4:14(b). Aluminium – NBSGSC theoretical alpha coefficients for oxide system using Heinrichs (1966) m.a.c.

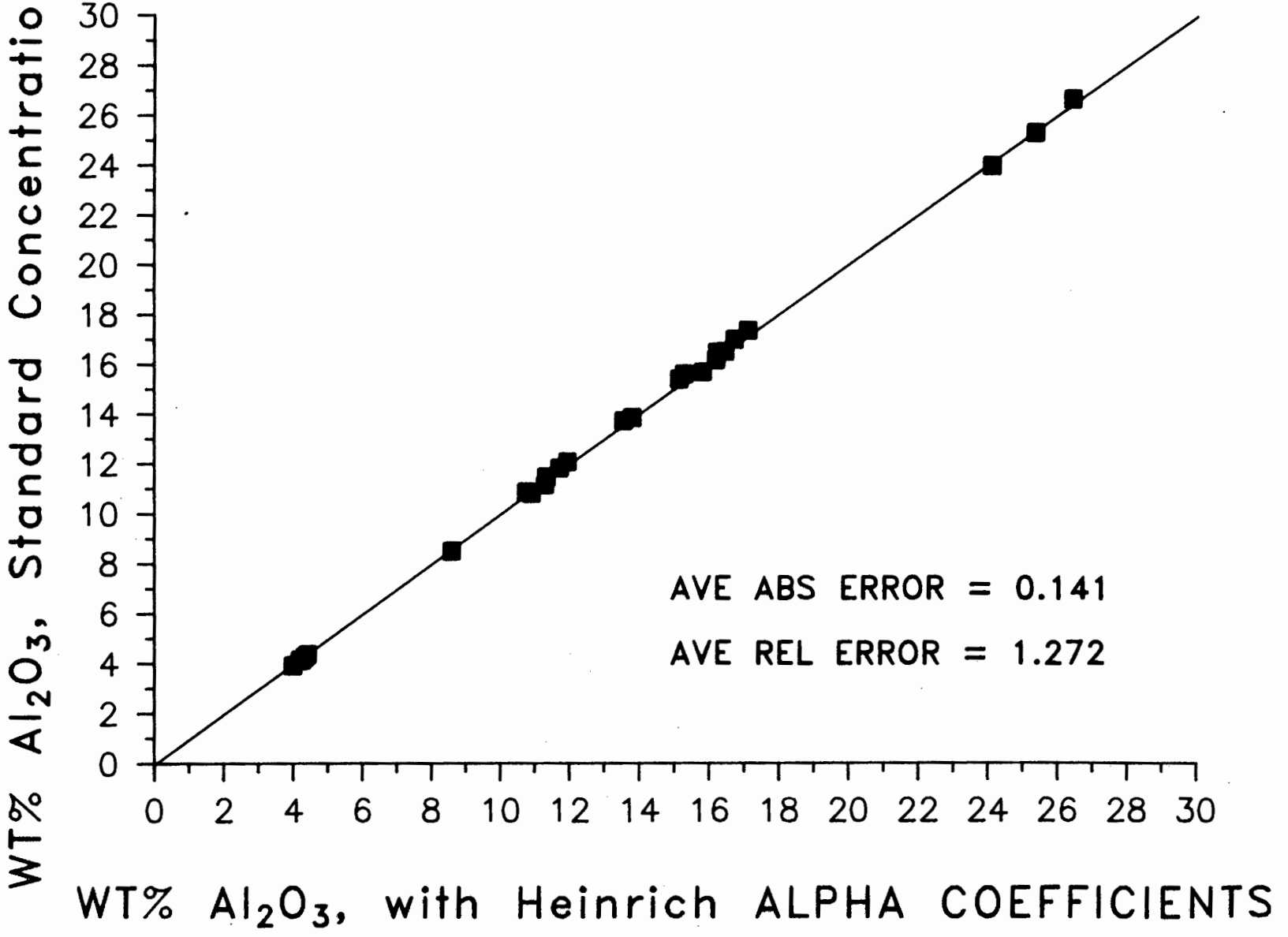

Figure 4:14(c). Aluminium – NBSGSC theoretical alpha coefficients for oxide system using Thinh and Leroux (1979) m.a.c.

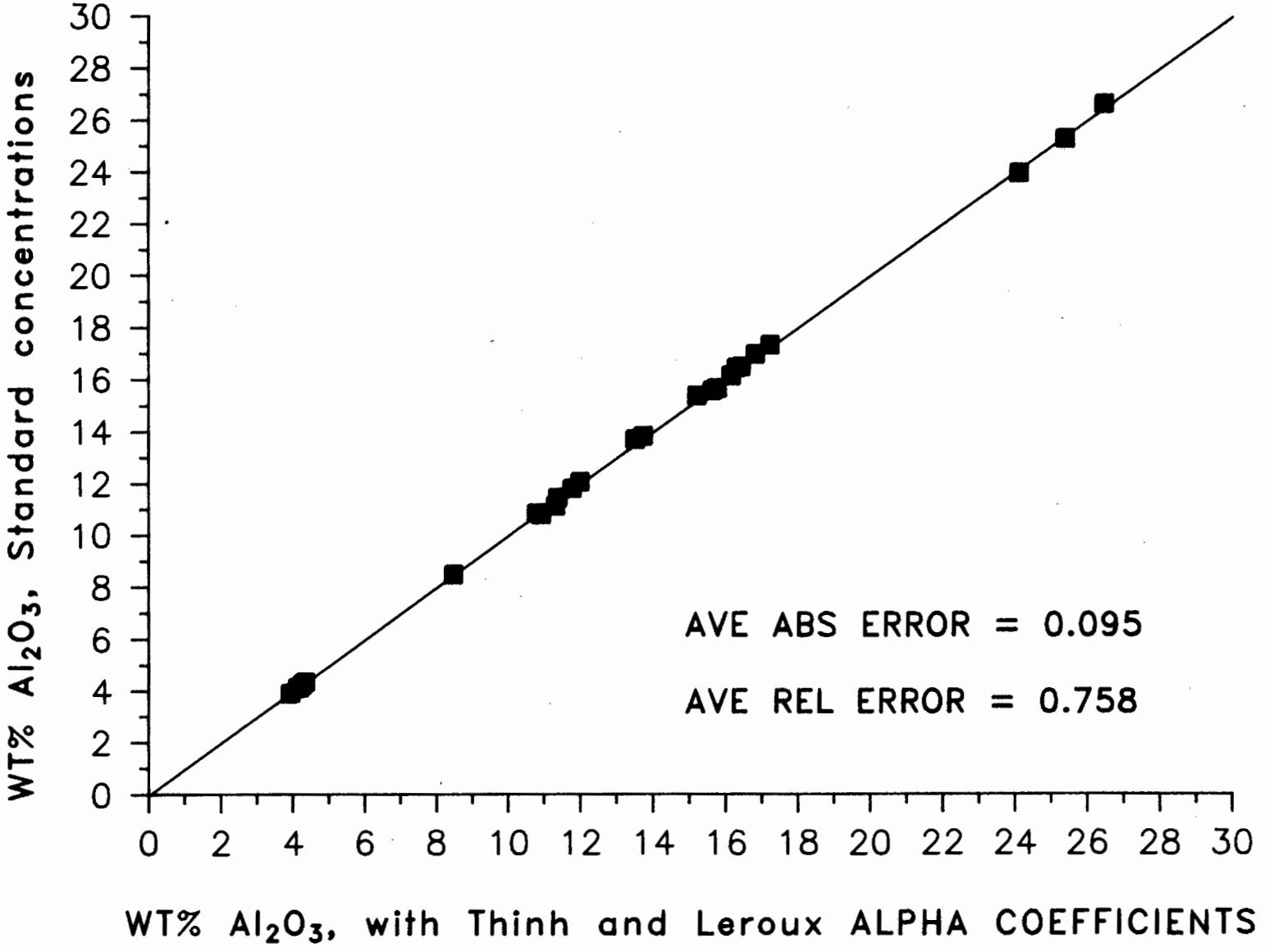

standard and calculated values. In Figure 4:14 (a) the standard values are plotted against the uncorrected concentrations to show the marked improvement the interelement correction models have on the calibration curves.

The authors of the NBSGSC program suggest that all the calibration curve equations be tested especially when the concentrations of the unknowns are out of range of the standards, as the extrapolation provided by the quadratic line can give large errors. Although the standards used in this technique matched to a certain extent the composition ranges of the unknowns due to the use of the "spiked" standards, all the calibration equations were used to check for consistency.

In Table 4:32, the average absolute and relative errors are reported for the four calibration curves available in NBSGSC, using Thinh and Leroux's (1979) algorithm to theoretically calculate the oxide alpha coefficients.

The data in Table 4:32 indicate that calibration equation 2, $Y = A0 + A1 \times X + A2 \times X^2$, generally has the lowest average absolute errors for the analyte elements except for TiO_2, MnO and K_2O. This calibration curve is not constrained to zero which limits its acceptability for quantitative analysis, as analysts generally prefer their calibration curves to pass as close to the origin as possible <u>provided</u> all necessary spectral interferences and backgrounds have been subtracted to give true net peak intensity to allow calibration from 0 to 100 weight percent. The use of equation 2, with a non-zero intercept, could introduce systematic bias for samples with low concentrations of elements such as TiO_2 and K_2O. Equation 4 is therefore the preferred option, in agreement with the recommendation by the

authors of NBSGSC.

For all 4 calibration curves 3 to 5 iteration cycles were required to reach the convergence criteria of 0.01% and only 4 cycles were needed for the unknown samples.

Table 4:32

Average absolute and relative errors for the oxide alpha coefficient system using Thinh and Leroux's (1979) algorithm for the four different calibration curves.

	Curve 1		Curve 2		Curve 3		Curve 4	
	Average Abs. Error	Rel.	Average Abs. Error	Rel.	Average Abs. Error	Rel.	Average Abs. Error	Rel.
SiO_2	.398	.755	.389	.747	.741	1.62	.407	.807
TiO_2	.077	23.65	.039	4.55	.073	1.90	.037	1.45
Al_2O_3	.086	.554	.083	.524	.107	0.967	.095	.758
Fe_2O_3	.049	.935	.049	1.59	.052	.906	.058	1.36
MnO	.018	23.95	.021	27.04	.018	33.09	.021	30.74
MgO	.086	47.09	.043	14.01	.089	15.07	.043	14.00
CaO	.077	1.78	.064	1.04	.077	1.37	.070	1.57
Na_2O	.073	10.68	.073	11.25	.073	10.47	.070	10.72
K_2O	.083	11.16	.049	3.27	.098	3.34	.046	1.83
P_2O_5	.006	5.78	.003	4.78	.003	4.79	.006	6.02
BaO	.052	6.82	.052	6.84	.055	6.48	.052	6.46

Curve 1 $Y = A0 + A1 \times X$

Curve 2 $Y = A0 + A1 \times X + A2 \times X^2$

Curve 3 $Y = A1 \times X$

Curve 4 $Y = A1 \times X + A2 \times X^2$

CHAPTER 5

SUMMARY AND CONCLUSION

SUMMARY and CONCLUSION

Summary

A low dilution fusion disc technique has been employed to prepare single glass fusion discs for the analysis of geological samples by XRF spectrometry. Successful determinations for eleven major and minor elements and nineteen trace elements have been achieved for international rock standards, lamproite and kimberlite samples using this method. A summary of the main points arising from this study is presented below.

1. The Low Dilution Fusion Technique.

(a). A low dilution ratio of flux:sample (2:1) has been used in this study and the flux composition and method of preparation of the discs is detailed in Table 2:1.

(b). Because of the low degree of dilution by the flux, sufficient count rates can be generated for trace element analysis.

(c). The fusion discs produced are generally infinitely thick for the measurement of wavelengths as short as 0.74 A, e.g. Nb K_a, although this is dependent on the overall mass absorption coefficient of the sample.

(d). The flux used in this technique did not contain a heavy absorber which is often used in fusion techniques to suppress matrix effects for major element analysis by XRF spectrometry. The absence of a heavy absorber has three main advantages :

i) Increased count rates and sensitivity for trace element

analysis.

ii) Elements often used as heavy absorbers such as La, Ce, Sr, and Ba can be determined.

iii) Increased homogeneity of the flux. Variations in the content of a heavy absorber in a particular flux batch greatly affects the measured intensities. Consequently standards have to be remade with each new flux batch, a problem which has been largely overcome in this study.

(e). The technique was used successfully to produce discs of blanks (pure SiO_2 and Al_2O_3) artificial standards (SiO_2 plus pure salts) and international rock standards.

(f) Precision is better than for the Norrish and Hutton (1969) technique.

(g) A single robust fusion disc is produced for the analysis of major, minor and trace elements.

(h). The fusion disc is a permanent and easily stored analytical sample available for later analysis. Results presented in Table 3:27 showed that reproducible data can be obtained after storage in a desiccator. Unlike powder pellets the sample powder is not recoverable from the fusion disc. The analytical surface of the discs may be easily cleaned (acetone wash) prior to analysis. This can not be done to a powder pellet.

2. Loss on Fusion

(a). The loss on fusion technique employed to determine the volatile content of the samples gave acceptable results, details of which are given in Tables 2:4-5.

(b). The use of lithium nitrate as an oxidant ensures complete oxidation of reduced species, for example Fe and S.

(c). The relative error of duplicate loss on fusion determinations was less than 12 % for values greater than 1%. The deliquescent nature of lithium nitrate can lead to the poor duplication of loss on fusion values unless care is exercised.

(d). The determination of the volatile content of the sample is complicated by the oxidation of S to SO_3 which results in the retention of sulphur. Although the data in Table 2:16 suggest that all the sulphur is retained as sulphate, further work is required to determine exactly the proportion of sulphur retained.

(e). Linear calibration curves obtained for volatile elements such as Rb indicate that these elements are not lost during the fusion process. However the complete retention of Pb may present a problem and requires further investigation.

3. Trace Element analysis.

(a). Data for trace elements analysed on low dilution fusion discs in this investigation are compared to those of other studies in Table 5:1. Data for Nd, Sc, Th and U analysed on low dilution fusion discs have not been previously reported.

(b). Average relative errors for most of the trace elements analysed in this investigation are less than 5% at concentration levels greater than 20 ppm.

Table 5:1

A comparison of the number and type of trace elements determined on low dilution fusion discs in this and other studies.

		Trace elements determined	total
This work		(Ba), Ce, Co, Cr, Cu, Ga, La, Nb, Nd, Ni, Pb, Rb, (S), Sc, Sr, Th, U, V, Y, Zn, Zr. () minor elements	21
Thomas & Haukka	1978	Ga, Mo, Nb, Ni, Pb, S, Sr, Zn	8
Hutton & Elliot	1980	Ba, Cu, Pb, Rb, Sr, Zn, Zr	7
Lee & McConchie	1982	Ba, Cu, Ni, Pb, Rb, Sr, V, Y, Zn, Zr	10
Bower & Valentine	1986	Ba, Ce, Co, Cr, La, Ni, Rb, Sr, V, Y, Zn, Zr	12

(c). Those trace elements analysed using less intense spectral lines generally reflect higher relative errors and an increase in the lower limit of detection. For example the average

relative error for Pb measured at its L_b wavelength is 11% and the lower limit of detection ranges between 7 - 11 ppm compared with 2% and 2-5 ppm respectively for Y, using the K_a line.

(d). The elimination of particle size effects including grain size, mineralogical and chemical effects in the homogeneous glass fusion discs is a major advantage over the use of powder pellets, especially for elements such as Ba, Cr and the REEs. A comparison of La, Ce and Nd data obtained for the same kimberlite samples by XRFS on powder pellets and by INAA showed significant differences in concentration, which have been attributed to mineralogical effects and are documented in Table 3:20 and discussed in Chapter 3. La, Ce and Nd determined on low dilution fusion discs by XRFS for these same kimberlite samples do not show the above mentioned concentration differences.

(e). Data for Sc, Th, Rb, La, Ce, Nd, and Co analysed by low dilution fusion XRF spectrometry and by INAA (Fraser et al.1986, Smith in press) are compared in Figures 3:15 - 21. A good agreement between recommended international standards and low dilution fusion XRFS data is indicated by linear calibration curves and the low dilution fusion XRFS data do not show any systematic bias. Data for Sc, Th and Rb determined by INAA show the most scatter but the overall good agreement of La, Ce and Nd data determined by low dilution fusion XRFS and by INAA (Fraser et al 1986 , Smith in press) is excellent. INAA is usually a superior technique for the determination of these elements.

(f). The data reported for the determination of trace elements on the low dilution fusion discs indicate that one of its main disadvantages is a decrease in the peak to background ratio which results in increased lower limits of detection compared

with those for powder pellets. However the lower limits of detection obtained by the low dilution fusion discs are only approximately 2 times greater than those of powder pellets and are still acceptable for the routine analysis of most rock types.

(g). Impurities in the flux may present a blank problem although this can be kept to a minimum if pure analytical reagents are used.

(h). Infinite thickness problems associated with the use of artificial standards, for example 1% SrO + 99% SiO_2, and rock types such as quartzites and sandstones requires further investigation as the low dilution fusion discs weighing approximately 6g may not have infinite thickness for the short wavelengths due to the low overall m.a.c. of the SiO_2.

4. Major element analysis.

(a). The calculation of concentrations from intensity data for the low dilution fusion discs was complicated by the following :

(i). The absence of a heavy absorber in the flux resulted in a large increase in the degree of matrix corrections required.

(ii). The chemistry of the lamproite and kimberlite samples, for which this fusion method was developed, is extremely variable and, in general, these rocks have larger concentration ranges than common rock types.

(iii). The presence of up to 2.5 % BaO in the lamproite samples required the calculation of alpha coefficients

to correct for inter-element effects of Ba on other elements and vice versa.

(b). The use of multiple regression analysis techniques and the Norrish and Hutton (1969) method of calculating alpha coefficients should be avoided when analyzing low dilution fusion discs for the following reasons :

(i). Data for standards, using multiple regression analysis to correct for interelement effects, produced low average absolute and relative errors but rather poor analytical totals for lamproite and kimberlite samples.

(ii). The theoretical calculation of alpha coefficients using the Norrish and Hutton (1969) method resulted in large relative errors on silica. It is worth noting that the published alpha coefficients for the Norrish and Hutton (1969) method, using lanthanum oxide, were calculated using the method outlined in Table 4:10 but were subsequently modified according to experimental work carried out by those workers.

(c). A Fortran program - NBSGSC - (Tao et al. 1985) designed to calculate alpha coefficients from fundamental parameters and the composition of the analyte specimens has been extensively used and evaluated.

(d). The data presented in Table 4:24 and 4:25 indicate that the single coefficient model, the fused disc system of NBSGSC (Tao et al. 1985), adequately corrects for the interelement effects for the Norrish and Hutton (1969) fusion method containing a heavy absorber.

(e). The NBSGSC (Tao et al. 1985) single coefficient fused disc model does not hold true for low dilution fusion discs as indicated in Tables 4:27-9. This is attributed to the use of a low dilution ratio, the high degree of variability in the chemistry of lamproite and kimberlite samples and the fact that in the single coefficient model the variation of alpha coefficients with weight fraction of the elements present is not taken into account.

(f). The oxide system of NBSGSC (Tao et al. 1985), which does take account of the variation of alpha coefficients with changing weight fraction, produced good analytical data for the low dilution fusion discs. Data presented in Tables 4:30-31 and Figures 4:12-14 indicate#ate that accounting for the variation of alpha coefficients with varying weight fraction is essential when using a low dilution fusion technique.

(g). The Thinh and Leroux (1979) m.a.c. algorithm produces significantly lower average absolute errors for Al_2O_3 than the Heinrich (1966) m.a.c. algorithm, Figure 4:14.

(h). Using the oxide system the average absolute errors for the five major oxides - SiO_2, Al_2O_3, MgO, CaO, and Fe_2O_3 are reduced compared to the fused disc system. However other oxides commonly analysed in geological samples (e.g. Na_2O, K_2O) have higher average absolute errors for the oxide system.

(i) The program NBSGSC, with the modifications made in this study, is extremely powerful as alpha coefficients can be calculated for element, oxide and fused disc systems for 20 (21 including LOI) elements at various operating conditions. The program also allows for the choice of different X-ray tubes, operating voltage and system geometries.

CONCLUSION

The low dilution fusion method described here is a viable analytical technique and gives good results for major, minor and trace elements in a variety of rock types. It is particularly good in eliminating particle size effects including mineralogical, inter-mineral and grain size effects, the major cause of systematic bias in X-ray fluorescence spectrometry.

A single, robust, homogeneous glass fusion disc is used for the determination of major, minor and trace elements, thus eliminating the preparation of powder pellets for trace element analysis. The fusion discs are easily cleaned using acetone, something that can not be done to powder pellets.

The loss on fusion technique employed ensures the complete loss of volatiles from the rock due to dissolution of minerals. Further work is required to quantify the losses (volatiles) and gains (oxidation of FeO and S) that occur during the sample preparation and fusion processes. The three methods (loss on ignition, loss on fusion, and determination of H_2O+ and CO_2) used in this study highlighted the problems encountered in the determination of volatile contents of geological samples.

The low dilution fusion method combined with the computer program NBSGSC (Tao et al.1985) for calculating alpha coefficients from fundamental parameters is an excellent and powerful technique for the analysis of rock types such as lamproites, kimberlites, syenites, carbonatites, lujavrites, and sulphide-rich rocks containing unusually high concentrations of elements such as Ba, Sr, Zr, Th, Pb, Ce.

ACKNOWLEDGEMENTS

I wish to express my sincerest gratitude to my supervisor, Prof. James Willis for his guidance, support and many hours of discussion during the last two and a half years. I am also grateful to Profs. A.J. Erlank, A.R. Duncan and J.J. Gurney and Drs. A.P. Leroex, H.S. Smith and D.L. Reid for their advice. Dave Hill is also thanked for the many hours he spent trying to make me more "computer literate".

De Beers Consolidated Mining Corporation are acknowledged for providing the lamproite samples and financial assistance towards the analytical costs involved in this thesis. The CSIR are thanked for their financial assistance, which was in the form of post-graduate research bursaries, for the period January 1984 to July 1986. The University of Cape Town are thanked for the Research Associateship that was awarded to me for the year 1986. The Geological Survey, Pretoria are thanked for analysing some of the lamproite samples for H_2O+, H_2O- and sulphur. Dr. C.B. Smith is thanked for supplying the kimberlite samples for La, Ce and Nd determinations.

Special thanks go to Simon Milner, who has spent many hours reading, correcting and criticising the thesis, and digitising some of the wavelength scans especially Figure 3:8.

Finally I wish to express my thanks to all the staff and post-graduate students in the Departments of Geochemistry and Geology

who have put up with me and supported me during the last 2 and half years, especially those that nick-named me "MOTHBALL".

And last but not least I wish to say thanks to my parents and brother for the encouragement and help that I have had from them especially when I had an extended stay in hospital.

In closing I must take my hat off to the computer program GRAFIT/1000 (GRAPHICUS) and the HP 7550 plotter, with this facility I could produce my diagrams with the minimum of heart ache and hair tearing. With out it well ....!

REFERENCES

Abbey, S., Gladney, E.S. (1986), A Re-evaluation of 3 Canadian Reference Rocks. Geostandards Newsletter X, 3-11.

Baker, J.W. (1982), Volatilization of Sulphur in Fusion Techniques for Preparation of Discs for X-ray Fluorescence Analysis. Adv. Xray Anal. 25, 91-94.

Bernstein, F. (1963), Particle Size and Mineralogical Effects in Mining Applications. Adv. X-ray Anal. 6, 436-445.

Bertin, E.P. (1978), Principles and Practice of X-ray Spectrometric Analysis. Plenum Press, New York, Second Edition. 1079p.

Bower, N.W., Valentine, G. (1986), Critical Comparison of Sample Preparation Methods for Major and Trace element Determinations using X-ray Fluorescence. X-ray Spec. 15, 73-78.

Claisse, F. (1956), Accurate X-ray fluorescence analysis without internal standard. Quebec Department Mines P.R. 327.

Claisse, F., Quintin, M. (1967), Generalisation of the Lachance-Traill Method for the Correction of Matrix Effects in X-ray Fluorescence Analysis. Can. Jour. Spec. 12, 129-133.

Claisse, F., Samson, C. (1962), Heterogeneity Effects in X-ray Analysis. Adv. X-ray Anal. 5, 335-354.

COMPROG Inc. (1982-1984), MATH/1000, version 5.1 computer program. Burbank CA 91507.

Criss, J.W., Birks, L.S., Gilfrich, J.V. (1978), Versatile X-ray Analysis Program combining Fundamental Parameters and Empirical Coefficients. Anal. Chem. 50(1), 33-37.

de Jongh, Willy.K. (1973), X-ray Fluorescence Analysis applying Theoretical Matrix Coefficients. Stainless Steel. X-ray Spec. 2, 151-158.

Fraser, K.J., Hawkesworth, C.J., Erlank, A.J., Mitchell, R.H.,

and Scott-Smith, B.H. (1986), Sr, Nd, and Pb Isotope and Minor Element Geochemistry of Lamproites and Kimberlites. E.P.S.L. 76, 57-70.

Govindaraju, K. (1984), 1984 Compilation of working values and sample description for 170 international reference samples of mainly silicate rocks and minerals. Geostandards Newsletter V111, Special Issue.

GRAPHICUS USER SYSTEMS, INC. (1983-1984), GRAFIT/1000 computer program, version 2.0. Santa Clara CA 95051.

Gurney, J.J. (1969), The Geochemical Distribution of some elements in ultrabasic rocks. Unpub. PhD thesis, Dept. Geochemistry, University of Cape Town.

Haukka, M.L., Thomas, I.L.(1977), Total X-ray Fluorescence Analysis of Geological Samples using a Low Dilution Lithium Metaborate Fusion Method. Matrix Corrections for Major Elements. X-ray Spec. 6, 204-211.

Heinrich, K.F.J. (1966), X-ray Absorption Uncertainty. In: The Electron Microprobe, T.D.Mckinley, K.F.J.Heinrich, D.B. Wittry, eds., pp.296-377, Wiley and Sons USA, 1966.

Hutton, J.T., Elliot, S.M. (1980), An Accurate XRF Method for the Analysis of Geochemical Exploration Samples for Major and Trace Elements using One Glass Disc. Chem. Geol. 29, 1-11.

Jenkins, R. (1974), An Introduction to X-ray Spectrometry. Heyden Press, New York, 1st edition, 163p

Jenkins, R. (1978), A Review of Empirical Influence Coefficient Methods in X-ray Spectrometry. Adv. X-ray Anal. 22, 281-292.

Jenkins, R., De Vries, J.L. (1970), Practical X-ray Spectrometry Philips Technical Library, London, Macmillan and Co Ltd. 2nd Edition.

Joslin, D., Salt, P.D. (1985), Analyses of Barytes by X-ray

Fluorescence Spectrometry using a Fusion Method for Sample Preparation. X-ray Spec. 14, 69-73.

Lachance, G.R. (1981), The Role of Alpha Coefficients in X-ray Spectrometry. In: Proceedings of XRF Program - International Conference on Industrial Inorganic Elemental Analysis, Metz, France, June 1981.

Lachance, G.R. (1979), The Family of Alpha Coefficients in X-ray Analysis. X-ray Spec. 8(4), 190-195.

Lachance, G.R., Claisse, F. (1980), A Comprehensive Alpha Coefficient Algorithm. Adv. X-ray Anal. 23, 87-92.

Lachance, G.R., Traill, G.R. (1966), A Practical Solution to the Matrix Problem in X-ray Analysis. Can. Spec. 11, 43-48.

Lee, R.F., McConchie, D.M. (1982), Comprehensive Major and Trace Element Analysis of Geological Materials by X-ray Fluorescence, using Low Dilution Fusions. X-ray Spec. 11(2), 55-63.

Lucas-Tooth, H.J., Pyne, C.C. (1963), The Accurate Determination of Major Constituents by X-ray Fluorescence Analysis in the presence of large interelement effects. Denver X-ray Conference.

Maessen, F.J.M.J., Boumanns, P.W.J.M. (1968), Critical Examination of the Borate Fusion Technique for Spectrochemical Trace analysis of Geological materials using D.C. Arc. Spectrochimica Acta 23B, 739 - 749.

Marr, III, H.E., (1976) XRF4 - Computer Programming for X-ray Analysis. U.S.Department of Interior Info. Circ. 8712.

Norrish, K., Chappell, B.W. (1967), X-ray Fluorescence Spectrometry. In: J. Zussman (editor) Physical methods in Determinative Mineralogy., Academic Press, London p 201-272.

Norrish, K.,Hutton, J.T. (1969), An Accurate X-ray Spectrographic Method for the Analysis of a wide range of Geological Samples. Geochim. Cosmochim. Acta 33, 431-453.

Pella, P.A., Feng, L.Y., Small, J.A. (1985), An Analytical Algorithm for Calculation of Spectral distributions for Quantitative X-ray Fluorescence Analysis. X-ray Spec. 14, 125-135.

Rasberry, S.D., Heinrich, K.F.J. (1974), Calibration for Interelement effects in X-ray fluorescence. Anal. Chem.46, 81-89.

Reynolds, R.C. (1963), Matrix Corrections in Trace Element Analysis by X-ray Fluorescence - Estimation of Mass Absorption Coefficient by Compton Scattering. Amer. Mineral. 48, 1133-1143.

Rose, H.J., Adler, I., Flanagan, F.J. (1962), Use of La2O3 as a Heavy Absorber in X-ray Fluorescence Analysis of Silicate Rocks. U.S.Geol Surv., Prof Papers 450B, 80-82.

Rousseau, R.M.(a) (1984), Fundamental Algorithm between Concentration and Intensity in XRF Analysis. 1 - Theory. X-ray Spec. 13, 115-120.

Rousseau,R.M.(b) (1984), Fundamental Algorithm between Concentration and Intensity in XRF Analysis. 2 - Practical Application. X-ray Spec. 13, 121-125.

Shapiro, L., Brannock, W.W. (1962), Rapid Analysis of silicate, carbonate and phosphate rocks. USGS Bulletin 1144-A.

Sherman. J. (1955), Theoretical Derivation of Fluorescent X-ray Intensities from Mixtures. Spectrochim. Acta 7, 283-306

Shiraiwa, T., Fujino, N. (1968), Micro Fluorescent X-ray Analyzer Adv. X-ray Anal. 11, 95-100.

Skinner, M. (1980), Brief Petrographic descriptions of Western Australian Lamproite specimens submitted for whole-rock geochemistry. Internal report, De Beers Consolidated Mines, Geology department.

Smith, C.B. (in press) , Kimberlite Geochemistry.

Tao, G.Y., Pella, P.A., Rousseau, R.M. (1985), NBSGSC - A FORTRAN Program for Quantitative X-ray Fluorescence Analysis. NBS Technical Bulletin 1213, National Bureau of Standards, Gaithersburg USA.

Thinh, T.P., Leroux, J. (1979), New Basic Empirical Expression for Computing Tables Of X-ray Mass Attenuation Coefficients. X-ray Spec. 8, 85-91.

Thomas, I.L., Haukka, M.T. (1978), XRF determination of trace and major elements using a single fused disc. Chem. Geol. 21 39-50.

Turekian, K.K., Wedepohl, K.H. (1961), Distribution of the elements in some major units of Earth's crust. Geol. Soc. Am. Bull 72, 175-192.

Van Der Heyde, H.A, (1986), A Geochemical study of some volcanic and related rocks from the Barberton Greenstone Belt. Unpub. M.Sc thesis, Dept. Geochemistry, University of Cape Town.

Zemany, P.D.(1960), Effects due to Chemical State of the Samples in X-ray Emission and Absorption. Anal. Chem. 32, 595-597.

APPENDIX A

Calculation of loss on fusion

Loss from lithium nitrate

$$2LiNO_3 \longrightarrow Li_2O + 2NO + 3/2\ O_2$$

137.8 29.8 60.0 48.0 molecular wts.

therefore loss $= \dfrac{2NO + 3/2O}{2LiNO_3}$

$$= \frac{60 + 48}{137.8} = 0.78374 \text{ lithium nitrate}$$

therefore

wt of NO and O_2 lost to atmosphere $=$ wt of $LiNO_3$ x 0.78374

loss from flux

determined by fusing accurately weighed portions of dried flux and lithium nitrate

loss from flux = total loss from flux + lithium nitrate − wt of NO and O_2

loss from sample

$$\frac{\text{total loss after fusing} - \text{wt of NO and } O_2 - \text{loss from flux}}{\text{weight of sample}}$$

CALCULATION OF LOSS ON FUSION AND DILUTION RATIO

Loss from flux and lithium nitrate

	FLUX 1	FLUX 2	FLUX 3	FLUX 4	
WT OF FLUX	4.00025	4.00063	3.99998	4.00034	
WT OF CRUCIBLE	23.73970	24.70525	23.73830	23.73622	
WT OF C+S+F	28.34038	29.31409	28.34103	28.34958	
WT AFTER 1000 C	27.85502	28.82120	27.85325	27.85388	
WT OF NITRATE	.60028	.61164	.60490	.61284	
NITRATE * .78374	.47046	.47937	.47408	.48031	.00000
TOTAL LOSS (F+N)	.01490	.01352	.01370	.01539	.00000
AVERAGE LOSS	.01438				

Loss from samples during fusion

Enter sample names in B24:P24

	CKP 9	K64/S5	MAIN 15/	33/K2/6F	24/K4/42	K1/402F	KDB 9	KBEL 2	KDT 24	KDT 28	126/PK3/3
WT OF SAMPLE	2.00069	2.00042	2.00051	2.00049	2.00089	2.00006	2.00061	2.00021	2.00074	2.00078	2.00077
WT OF FLUX	4.00013	4.00044	4.00003	4.00013	4.00060	4.00034	4.00022	4.00050	4.00031	4.00010	4.00007
WT OF CRUCIBLE	24.70771	23.74062	24.70724	23.74095	24.70796	23.74054	23.73236	24.70090	24.70795	23.73460	24.70763
WT OF C+S+F	31.31534	30.34480	31.30587	30.37638	31.31938	30.34790	30.33400	31.32093	31.30870	30.35475	31.31087
WT AFTER 1000 C	30.56551	29.64060	30.56231	29.61789	30.66299	29.69555	29.66973	30.57795	30.64287	29.67957	30.77305
WT OF NITRATE	.60804	.61076	.60261	.63599	.61066	.61210	.60043	.60555	.60336	.60862	.60503
NITRATE*.78374	.47655	.47868	.47229	.49845	.47860	.47973	.47058	.47459	.47288	.47700	.47419
TOTAL LOSS	.27328	.22552	.27127	.26004	.17779	.17262	.19369	.26839	.19295	.19818	.06364
LOSS ON FUSION	.25891	.21115	.25689	.24566	.16342	.15825	.17931	.25401	.17857	.18381	.04926
%LOSS	12.94	10.56	12.84	12.28	8.17	7.91	8.96	12.70	8.93	9.19	2.46
DILUTION RATIO	.32625	.32618	.32630	.32591	.32622	.32613	.32633	.32621	.32630	.32626	.32630

126/PK7/1	126/PK7/2	126/PK9/1	126/PK11/1	126/PK12/1	126/PK12/2	126/PK13/1	126/PK13/2	460/PK8/5	460/PK4/17	125/PK16/8
2.00041	2.00044	2.00086	2.00051	2.00039	2.00085	2.00056	2.00074	2.00034	2.00064	2.00042
3.99978	4.00017	4.00003	4.00062	4.00040	4.00096	3.99987	3.99976	4.00020	4.00047	4.00039
23.73929	24.70541	24.70281	23.73861	23.74100	23.74030	23.73644	24.70800	24.70492	23.73806	24.70545
30.34922	31.30660	31.31654	30.33661	30.35979	30.35450	30.35878	31.31086	31.36586	30.35746	31.30733
29.79907	30.77284	30.78437	29.78746	29.77508	29.77741	29.80045	30.76657	30.82556	29.77719	30.79433
.60441	.60110	.61212	.60055	.61769	.61303	.62730	.60850	.65964	.61999	.60157
.47370	.47111	.47974	.47068	.48411	.48046	.49164	.47691	.51699	.48591	.47147
.07645	.06265	.05243	.07847	.10060	.09664	.06669	.06738	.02331	.09436	.04153
.06207	.04828	.03805	.06410	.08622	.08226	.05231	.05301	.00893	.07998	.02715
3.10	2.41	1.90	3.20	4.31	4.11	2.61	2.65	.45	4.00	1.36
.32628	.32630	.32623	.32629	.32610	.32617	.32603	.32627	.32562	.32609	.32628

CALCULATION OF LOSS ON FUSION AND DILUTION RATIO

Loss from flux and lithium nitrate

	FLUX 1	FLUX 2	FLUX 3	FLUX 4	
WT OF FLUX	4.00025	4.00063	3.99998	4.00034	
WT OF CRUCIBLE	23.73970	24.70525	23.73830	23.73622	
WT OF C+S+F	28.34038	29.31409	28.34103	28.34958	
WT AFTER 1000 C	27.85502	28.82120	27.85325	27.85388	
WT OF NITRATE	.60028	.61164	.60490	.61284	
NITRATE * .78374	.47046	.47937	.47408	.48031	.00000
TOTAL LOSS (F+N)	.01490	.01352	.01370	.01539	.00000
AVERAGE LOSS	.01438				

Loss from samples during fusion

Enter sample names in B24:P24

	127/PK3/8	127/PK3/9	127/PK5/5	127/PK5/6	127/PK8/2	127/PK9/3	127/PK9/4	127/PK12/1	127/PK19/2	127/PK20/1	127/PK20/2
WT OF SAMPLE	2.00028	2.00055	2.00077	2.00076	2.00073	2.00074	2.00015	2.00081	2.00093	2.00044	2.00021
WT OF FLUX	4.00027	4.00056	4.00056	3.99993	4.00001	4.00011	4.00024	4.00056	4.00082	4.00032	4.00025
WT OF CRUCIBLE	24.70694	24.70627	23.73854	24.70521	23.73925	23.73720	23.73849	23.73575	24.70586	24.70596	24.70558
WT OF C+S+F	31.33442	31.30940	30.34517	31.30809	30.36908	30.34025	30.33543	30.33893	31.31294	31.30829	31.30310
WT AFTER 1000 C	30.55981	30.49846	29.79651	30.76826	29.82629	29.80344	29.79672	29.80884	30.76584	30.72176	30.78952
WT OF NITRATE	.62785	.60227	.60434	.60149	.62962	.61039	.60095	.60188	.60819	.60492	.59691
NITRATE*.78374	.49207	.47202	.47365	.47141	.49346	.47839	.47099	.47172	.47666	.47410	.46782
TOTAL LOSS	.28254	.33892	.07501	.06842	.04933	.05842	.06772	.05837	.07044	.11243	.04576
LOSS ON FUSION	.26816	.32454	.06064	.05404	.03495	.04404	.05335	.04399	.05606	.09805	.03138
%LOSS	13.41	16.22	3.03	2.70	1.75	2.20	2.67	2.20	2.80	4.90	1.57
DILUTION RATIO	.32597	.32628	.32628	.32635	.32602	.32623	.32627	.32631	.32624	.32625	.32632

APPENDIX B

FeO Determinations

The method used to determine FeO concentrations was titrimetric and followed the technique described by Shapiro and Brannock (1962). An in-house control standard was used (KL11a), previous workers (van Der Heyde 1986) reported values between 8.32-8.54% FeO for KL11a.

Values obtained in this work for KL11a are detailed in Table B:1.

Table B:1

FeO concentrations for KL11a (data reported in wt percent)

FeO	Date of titrations
8.32	
8.28	September 1984
8.32	
8.44	
8.28	October 1984
8.24	
8.32	
8.36	April 1986
8.36	

mean = 8.32%

1.92% spread in data

Gas Chromatograph - HP 185B

Carbon dioxide and chemically bound water (H_2O+) were determined in the rock samples using a Gas Chromatograph (HP185B CHN analyser) linked to a HP 3380A integrator which enables "desk

top" calculation of the final concentrations. For this technique 20-30 mg of sample powder, predried at 110°C and accurately weighed on a CAHN electrobalance, was combusted using conditions detailed in Table B:2.

An in-house standard (HSS 112) and two synthetic $CaCO_3$ - quartz mixtures were used to calibrate the data. These standards were run at regular intervals throughout the analytical period. The standards data is detailed in Table B:3.

Table B:2

Conditions for the determination of CO_2 and H_2O^+ using HP 185B Gas Chromatograph.

gas flow rate	120ml
oxidation furnace setting	4.7
oxidation furnace temperature	1050°C
reduction furance temperature	500°C
column oven temperature	100°C
oven shell temperature	90°C
Bridge current	150 mA
sensitivity selector	16

Table B:3

In-house standards data for CO_2 and H_2O+.

	CO_2	H_2O+	
HSS 112	2.87	9.54	recommended values
HSS 112	3.02	9.22	
	3.14	9.77	
	3.03	9.42	standardised by
	3.09	9.38	taking average of
	3.06	9.54	all readings
	3.16	9.84	
	3.10	9.95	
	3.14	9.79	
	3.10	9.34	
mean	3.09	9.58	
SD	0.05	0.26	
9.16% CO2 artificial standard	9.06		
	9.03		
	9.09		
	9.12		
mean	9.07		
SD	0.04		
18.32% CO2 artificial standard	18.52		
	18.45		
mean	18.48		
	0.05		

CO_2 standardised using the two artificial standards

% spread in calibration factor for H_2O+ = 4.47%

% spread in calibration factor for CO_2 = 2.74%

APPENDIX C

Calculation of oxide content and m.a.c.s. of Johnson-Mathey Spectroflux 100B

Spectroflux 100B contains 80 % $LiBO_2$ lithium metaborate

20 % $Li_2B_4O_7$ lithium tetraborate

LDF Discs contain 4g flux + 0.6g lithium nitrate

Therefore 80 % of 4g = 3.2g $LiBO_2$

20 % of 4g = 0.8g $Li_2B_4O_7$

0.6g $LiNO_3$

Atomic Weights

Li = 6.939
B = 10.811
O = 15.999

Lithium Metaborate - (3.2g)

$2\ LiBO_2$ ----------> Li_2O + B_2O_3

99.496 29.877 69.619 molecular wts

$\frac{29.877}{99.496}$ = 0.30028 of 3.2g = 0.96090g of Li_2O

$\frac{69.619}{99.496}$ = 0.69972 of 3.2g = 2.23910g of B_2O_3

Lithium Tetraborate - (0.8g)

$Li_2B_4O_7$ --------> Li_2O + B_4O_6

169.115 29.877 139.238 molecular wts

$$\frac{29.877}{169.115} = 0.17667 \text{ of } 0.8g = \underline{0.14134g} \text{ of } Li_2O$$

$$\frac{139.238}{169.115} = 0.82333 \text{ of } 0.8g = \underline{0.65866g} \text{ of } B_4O_6$$

Lithium Nitrate - (0.6g)

$$2\ LiNO_3 \xrightarrow{\qquad\qquad} Li_2O + 2NO + 3/2\ O_2$$
$$137.886 \qquad\qquad 29.877 \quad 60.012 \quad 47.997$$

$$\frac{29.877}{137.886} = 0.21668 \text{ of } 0.6g = \underline{0.13001g} \text{ of } Li_2O$$

THEREFORE

FLUX + NITRATE (4.6g) contains :

2.23910g	B_2O_3	) from $LiBO_2$
0.96190g	Li_2O	)
0.65866g	B_4O_6	) from $Li_2B_4O_7$
0.14134g	Li_2O	)
0.13001g	Li_2O	) from $LiNO_3$
0.46999g	NO + O_2 lost from $LiNO_3$ to atmosphere	
4.60000g		

Total oxide content =

1.23225g Li_2O

2.23910g B_2O_3

0.65866g B_4O_6

Therefore LDF fusion discs contain -

32.63 % sample

20.10 % Li_2O

36.52 % B_2O_3

10.74 % B_4O_6

Spectroflux 100B + lithium oxide from $LiNO_3$ contains

29.84 % Li_2O

54.22 % B_2O_4

15.94 % B_4O_6

Oxide content of Spectroflux 100B + Lithium oxide from $LiNO_3$ for NBSGSC major element reduction

32.63 % sample

20.10 % Li_2O

47.26 % B_2O_3 / B_4O_6

Content of Li, B and O for m.a.c. calculations

29.84 x .46450	=	13.86 %	Li	) from Li_2O
29.84 x .53550	=	15.98 %	O	)
54.22 x .31058	=	16.84 %	B	) from B_2O_3
54.22 x .65942	=	37.38 %	O	)
15.94 x .31058	=	4.95 %	B	) from B_4O_6
15.94 x .68942	=	10.99 %	O	)

Therefore Spectroflux 100B + lithium oxide from $LiNO_3$

contains 13.86 % Li
64.35 % O
21.79 % B

Figure C:1. Mass absorption coefficients for Flux components

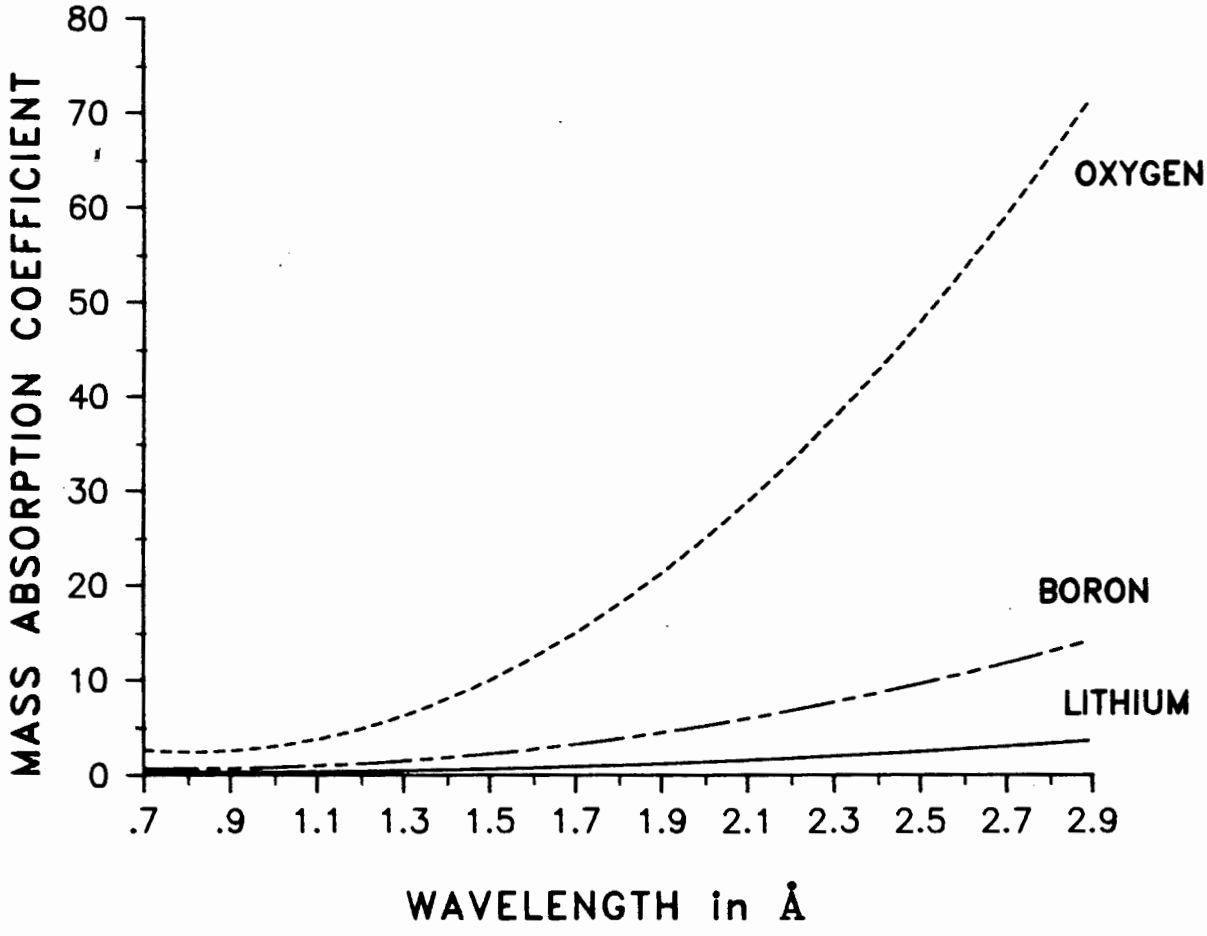

LITHIUM

$Y = 0.76728 \times X^2 - 1.2392 \times X + 0.77512$

BORON

$Y = 2.9728 \times X^2 - 4.5052 \times X + 2.2942$

OXYGEN

$Y = 15.784 \times X^2 - 25.402 \times X + 12.595$

Calculation of Mass Absorption Coefficient of the Flux.

From the m.a.c.s. tables of Jenkins and De Vries (1970) curves relating mass absorpton coefficients to wavelengths were generated as given in Figure C:1 and regression lines produced to enable calculation of m.a.c.s. of Li, B and O at the wavelengths of interest.

Therefore at Rb K_a (0.927 Å)

	m.a.c.
Li	0.297
B	0.667
O	2.640

m.a.c. of flux at Rb K_a = .1386 x .297 + .6435 x 2.64 + .2179 x .667

= 1.86 g/cm^2

m.a.c. of LDF disc at Rb K_a = m.a.c. of raw sample at Rb K_a x .32626 + m.a.c. of flux at Rb K_a x .67374

m.a.c. of raw sample at Rb K_a

oxide	A Composition of G-2	B m.a.c. of oxide	A x B
SiO_2	.6922	8.22	5.689
TiO_2	.0048	31.5	0.151
Al_2O_3	.1540	7.37	1.135
Fe_2O_3	.0269	57.0	1.533
MnO	.0003	52.0	0.016
MgO	.0075	6.57	0.049
CaO	.0196	30.8	0.604
Na_2O	.0406	5.66	0.229
K_2O	.0446	29.8	1.329
P_2O_5	.0013	8.84	0.011
H_2O^+	.0050	2.39	0.012
CO_2	.0080	2.25	0.018
Ba	.0019	97.5	0.185
Sr	.0005	28.9	0.014
		Total	10.975

Therefore m.a.c. of LDF disc at Rb K_a =

$$10.975 \times .32636 + 1.86 \times .67374 = 4.83 \text{ g/cm}^2$$

MATH/1000 (COMPROG 1982-1984) is a computer routine which enables the user to work with a matrix spreadsheet of up to 16384 elements in any combination of rows and columns dependent on the size of the memory partition the program is operating in. The MATH commands allow free movement around the spreadsheet. Normal arithmetic routines can be performed using either relative or specific addressing of the rows and columns in either reverse polish or algebraic notation. Areas of the matrix can be write protected and areas to be printed can be specified.

Further details on the operation of MATH 1000 can be obtained from COMPROG, INC P.O.Box 1459 BURBANK, CA 91507 U.S.A. or from a local Hewlett Packard dealer.

An example of a spreadsheet with definitions generated by MATH/1000 to calculate mass absorption coefficients from major and minor element compositions of rock samples is included here.

APPENDIX D

Spread sheets from MATH/1000 for calculation

of Norrish-type alpha coefficients

for Norrish-type discs and Low dilution fusion discs

HYBRID ALPHA COEFFICIENTS FOR USE IN COLA EQUATION

(OXIDE SYSTEM)

TARGET:CR 50.0 KV FILTER : NO

GEOMETRY : 60,40 DEGREES

ANALYTE : NA201 (11)

			3	5	6	11	12	13	14	15	19	20	22	25	26	56
			LI201	B 203	C 103	NA201	MG101	AL203	SI102	P 205	K 201	CA101	TI102	MN101	FE203	BA101
		A1	.508 4.463	1.086 -.585	1.422	0.000	.419	.664	.879	1.046	1.441	1.804	2.300	4.211		
		A2	-.000 -.062	-.000 .115	-.000	0.000	-.052	-.072	-.094	-.123	-.355	-.384	-.389	-.068		
AIJK	3	LI201	0.000													
	5	B 203	.000													
	6	C 103	.000	-.000												
	11	NA201	0.000	0.000	0.000											
	12	MG101	-.003	-.011	-.016	0.000										
	13	AL203	.000	-.011	-.016	0.000	.060									
	14	SI102	.003	-.011	-.017	0.000	.078	.079								
	15	P 205	.005	-.013	-.021	0.000	.104	.104	.106							
	19	K 201	-.157	-.263	-.317	0.000	.290	.281	.279	.302						
	20	CA101	-.160	-.272	-.329	0.000	.310	.300	.297	.320	.736					
	22	TI102	-.197	-.323	-.388	0.000	.300	.288	.281	.304	.747	.741				
	25	MN101	-.007	-.020	-.026	0.000	.023	.016	.007	-.004	-.459	-.481	-.565			
	26	FE203	-.007	-.018	-.024	0.000	.014	.006	-.002	-.014	-.501	-.525	-.616	-.009		
	56	BA101	-.205 -.324	-.263	-.296	0.000	-.068	-.040	-.018	.026	.710	.774	.714	-.289		

HYBRID ALPHA COEFFICIENTS FOR USE IN COLA EQUATION

(OXIDE SYSTEM)

TARGET:CR 50.0 KV FILTER : NO

GEOMETRY : 60,40 DEGREES

ANALYTE : MG101 (12)

		3	5	6	11	12	13	14	15	19	20	22	25	26	56
		LI201	B 203	C 103	NA201	MG101	AL203	SI102	P 205	K 201	CA101	TI102	MN101	FE203	BA101
	A1	.037 2.762	.428 3.170	.668	2.635	0.000	.154	.301	.415	.688	.934	1.268	2.588		
	A2	-.000 -.037	-.000 -.059	-.000	-.000	0.000	-.046	-.059	-.077	-.203	-.215	-.207	-.042		
AIJK	3 LI201	0.000													
	5 B 203	.000													
	6 C 103	.000	.000												
	11 NA201	.000	.000	-.000											
	12 MG101	0.000	0.000	0.000	0.000										
	13 AL203	.001	-.006	-.010	-.032	0.000									
	14 SI102	.003	-.006	-.010	-.037	0.000	.057								
	15 P 205	.004	-.007	-.013	-.048	0.000	.074	.076							
	19 K 201	-.103	-.169	-.204	-.404	0.000	.203	.203	.220						
	20 CA101	-.108	-.177	-.214	-.420	0.000	.212	.211	.228	.531					
	22 TI102	-.137	-.215	-.258	-.489	0.000	.197	.195	.212	.535	.529				
	25 MN101	-.006	-.014	-.019	-.042	0.000	.012	.007	-.000	-.282	-.298	-.357			
	26 FE203	-.005	-.013	-.017	-.037	0.000	.005	.000	-.007	-.310	-.328	-.392	-.006		
	56 BA101	-.057 -.078	-.085	-.101	-.195	0.000	.055	.060	.073	.217	.241	.056	-.061		

HYBRID ALPHA COEFFICIENTS FOR USE IN COLA EQUATION

(OXIDE SYSTEM)

TARGET:CR 50.0 KV FILTER : NO

GEOMETRY : 60,40 DEGREES

ANALYTE : AL203 (13)

			3	5	6	11	12	13	14	15	19	20	22	25	26	56
			LI201	B 203	C 103	NA201	MG101	AL203	SI102	P 205	K 201	CA101	TI102	MN101	FE203	BA101
		A1	-.135 2.149	.188 4.662	.394	2.041	2.308	0.000	.104	.201	.461	.662	.935	2.003		
		A2	-.000 -.028	-.000 -.139	-.000	-.000	-.000	0.000	-.051	-.067	-.178	-.184	-.171	-.033		
AIJK	3	LI201	0.000													
	5	B 203	.000													
	6	C 103	.000	-.000												
	11	NA201	.000	.000	.000											
	12	MG101	.000	.000	.000	.000										
	13	AL203	0.000	0.000	0.000	0.000	0.000									
	14	SI102	.003	-.004	-.008	-.031	-.034	0.000								
	15	P 205	.005	-.004	-.009	-.040	-.044	0.000	.067							
	19	K 201	-.075	-.127	-.158	-.322	-.346	0.000	.188	.203						
	20	CA101	-.081	-.135	-.168	-.336	-.362	0.000	.190	.206	.480					
	22	TI102	-.107	-.169	-.207	-.395	-.425	0.000	.173	.188	.478	.471				
	25	MN101	-.005	-.012	-.016	-.035	-.035	0.000	.004	-.001	-.221	-.235	-.286			
	26	FE203	-.005	-.011	-.014	-.031	-.032	0.000	-.001	-.007	-.245	-.261	-.315	-.005		
	56	BA101	-.001 .004	-.019	-.030	-.082	-.092	0.000	.088	.089	.045	.054	-.184	.014		

HYBRID ALPHA COEFFICIENTS FOR USE IN COLA EQUATION

(OXIDE SYSTEM)

TARGET:CR 50.0 KV FILTER : NO

GEOMETRY : 60,40 DEGREES

ANALYTE : SI102 (14)

		3	5	6	11	12	13	14	15	19	20	22	25	26	56
		LI201	B 203	C 103	NA201	MG101	AL203	SI102	P 205	K 201	CA101	TI102	MN101	FE203	BA101
	A1	-.256 1.719	.019 4.109	.202	1.625	1.857	2.140	0.000	.059	.332	.499	.729	1.593		
	A2	-.000 -.024	-.000 -.133	-.000	-.001	-.001	-.001	0.000	-.061	-.174	-.174	-.156	-.026		
AIJK	3 LI201	0.000													
	5 B 203	.000													
	6 C 103	.000	.000												
	11 NA201	.000	.000	.000											
	12 MG101	.000	.000	.000	.000										
	13 AL203	.000	.000	.000	.000	.000									
	14 SI102	0.000	0.000	0.000	0.000	0.000	0.000								
	15 P 205	.006	-.002	-.006	-.033	-.037	-.041	0.000							
	19 K 201	-.049	-.092	-.118	-.256	-.277	-.301	0.000	.200						
	20 CA101	-.056	-.101	-.129	-.271	-.293	-.319	0.000	.199	.457					
	22 TI102	-.082	-.133	-.166	-.323	-.349	-.379	0.000	.178	.452	.444				
	25 MN101	-.005	-.010	-.014	-.031	-.031	-.034	0.000	-.002	-.170	-.185	-.230			
	26 FE203	-.004	-.009	-.013	-.027	-.028	-.032	0.000	-.006	-.190	-.205	-.254	-.005		
	56 BA101	.006 .016	-.008	-.018	-.059	-.067	-.077	0.000	.083	.050	.056	-.170	.022		

HYBRID ALPHA COEFFICIENTS FOR USE IN COLA EQUATION

(OXIDE SYSTEM)

TARGET:CR 50.0 KV FILTER : NO

GEOMETRY : 60,40 DEGREES

ANALYTE : P 205 (15)

			3	5	6	11	12	13	14	15	19	20	22	25	26	56
			LI201	B 203	C 103	NA201	MG101	AL203	SI102	P 205	K 201	CA101	TI102	MN101	FE203	BA101
		A1	-.345 1.402	-.105 3.751	.054	1.318	1.524	1.774	2.001	0.000	.279	.420	.617	1.293		
		A2	-.000 -.022	-.001 -.139	-.001	-.001	-.001	-.001	-.001	0.000	-.191	-.187	-.166	-.023		
AIJK	3	LI201	0.000													
	5	B 203	.000													
	6	C 103	.000	.000												
	11	NA201	.000	.000	.000											
	12	MG101	.000	.000	.000	.000										
	13	AL203	.000	.000	.000	.000	.000									
	14	SI102	.000	.000	.000	.000	.000	-.000								
	15	P 205	0.000	0.000	0.000	0.000	0.000	0.000	0.000							
	19	K 201	-.018	-.054	-.076	-.196	-.214	-.234	-.252	0.000						
	20	CA101	-.027	-.064	-.088	-.210	-.230	-.252	-.271	0.000	.449					
	22	TI102	-.053	-.095	-.123	-.258	-.281	-.307	-.329	0.000	.443	.433				
	25	MN101	-.004	-.009	-.012	-.027	-.028	-.031	-.033	0.000	-.122	-.137	-.178			
	26	FE203	-.004	-.008	-.011	-.025	-.026	-.028	-.030	0.000	-.138	-.154	-.198	-.004		
	56	BA101	.016 .028	.005	-.003	-.037	-.044	-.052	-.059	0.000	.061	.064	-.161	.033		

HYBRID ALPHA COEFFICIENTS FOR USE IN COLA EQUATION

(OXIDE SYSTEM)

TARGET:CR 50.0 KV FILTER : NO

GEOMETRY : 60,40 DEGREES

ANALYTE : K 201 (19)

		3 LI201	5 B 203	6 C 103	11 NA201	12 MG101	13 AL203	14 SI102	15 P 205	19 K 201	20 CA101	22 TI102	25 MN101	26 FE203	56 BA101
	A1	-.746 .017	-.654 1.661	-.595	-.031	.054	.157	.250	.380	0.000	-.043	.038	-.022		
	A2	-.005 -.035	-.008 -.195	-.009	-.021	-.023	-.024	-.026	-.028	0.000	-.198	-.214	-.038		
AIJK	3 LI201	0.000													
	5 B 203	.000													
	6 C 103	.000	.000												
	11 NA201	.002	.001	.001											
	12 MG101	.002	.001	.001	.000										
	13 AL203	.003	.002	.001	.000	.000									
	14 SI102	.003	.002	.001	.000	.000	.000								
	15 P 205	.003	.002	.002	.000	.000	.000	.000							
	19 K 201	0.000	0.000	0.000	0.000	0.000	0.000	0.000	0.000						
	20 CA101	.080	.072	.066	.024	.018	.011	.005	-.003	0.000					
	22 TI102	.080	.070	.064	.018	.010	.002	-.005	-.014	0.000	.229				
	25 MN101	.005	.003	.001	-.007	-.008	-.009	-.010	-.011	0.000	.046	.041			
	26 FE203	.004	.002	.000	-.007	-.008	-.009	-.010	-.011	0.000	.039	.034	-.000		
	56 BA101	.072 .072	.069	.067	.054	.051	.049	.047	.045	0.000	.067	-.069	.073		

APPENDIX E

Oxide alpha coefficients calculated

by NBSGSC using

Thinh and Leroux algorithm

HYBRID ALPHA COEFFICIENTS FOR USE IN COLA EQUATION

(OXIDE SYSTEM)

TARGET:CR 50.0 KV FILTER : NO

GEOMETRY : 60,40 DEGREES

ANALYTE : LI201 (3)

			3	5	6	11	12	13	14	15	19	20	22	25	26	56
			LI201	B 203	C 103	NA201	MG101	AL203	SI102	P 205	K 201	CA101	TI102	MN101	FE203	BA101
		A1	0.000 -1.062	-1.002 -1.205	-1.004	1.609	-1.059	-1.078	-1.100	-1.131	-1.598	-1.611	-1.633	-1.070		
		A2	0.000 .073	.002 .241	.005	-.113	.059	.080	.105	.139	.680	.700	.732	.081		
AIJK	3	LI201	0.000													
	5	B 203	0.000													
	6	C 103	0.000	-.000												
	11	NA201	0.000	.181	.189											
	12	MG101	0.000	.006	.009	.103										
	13	AL203	0.000	.003	.007	.089	.029									
	14	SI102	0.000	-.001	.004	.070	.033	.033								
	15	P 205	0.000	-.006	.000	.036	.038	.039	.039							
	19	K 201	0.000	-.108	-.096	-.588	.020	.031	.041	.055						
	20	CA101	0.000	-.118	-.107	-.609	.006	.018	.028	.041	.128					
	22	TI102	0.000	-.132	-.123	-.647	-.015	-.004	.006	.020	.115	.107				
	25	MN101	0.000	-.015	-.015	.146	.019	.022	.024	.027	.006	-.008	-.029			
	26	FE203	0.000	-.014	-.014	.159	.020	.022	.025	.028	.009	-.006	-.028	-.001		
	56	BA101	0.000 -.013	-.047	-.046	-.191	-.001	.012	.019	.030	.110	.098	.054	-.012		

HYBRID ALPHA COEFFICIENTS FOR USE IN COLA EQUATION

(OXIDE SYSTEM)

TARGET:CR 50.0 KV FILTER : NO

GEOMETRY : 60,40 DEGREES

ANALYTE : B 203 (5)

		3	5	6	11	12	13	14	15	19	20	22	25	26	56
		LI201	B 203	C 103	NA201	MG101	AL203	SI102	P 205	K 201	CA101	TI102	MN101	FE203	BA101
	A1	-.737 -1.058	0.000 -1.187	-1.005	-.157	-.011	.101	.214	.419	-1.511	-1.529	-1.559	-1.065		
	A2	.005 .068	0.000 .226	.006	-.016	-.012	-.013	-.014	-.025	.573	.599	.642	.075		
AIJK	3 LI201	0.000													
	5 B 203	0.000													
	6 C 103	-.001	0.000												
	11 NA201	.039	0.000	.062											
	12 MG101	.040	0.000	.069	.079										
	13 AL203	.047	0.000	.085	.098	.092									
	14 SI102	.056	0.000	.104	.120	.114	.115								
	15 P 205	.077	0.000	.140	.159	.152	.153	.153							
	19 K 201	-.235	0.000	-.089	-.190	-.205	-.194	-.179	-.156						
	20 CA101	-.242	0.000	-.100	-.205	-.221	-.211	-.197	-.174	.124					
	22 TI102	-.252	0.000	-.116	-.232	-.250	-.241	-.228	-.206	.111	.104				
	25 MN101	-.028	0.000	-.014	.050	.062	.086	.114	.166	.006	-.008	-.028			
	26 FE203	-.025	0.000	-.013	.055	.067	.091	.121	.175	.008	-.006	-.027	-.001		
	56 BA101	-.081 -.013	0.000	-.044	-.087	-.026	.013	.046	.105	.104	.094	.051	-.012		

HYBRID ALPHA COEFFICIENTS FOR USE IN COLA EQUATION

(OXIDE SYSTEM)

TARGET:CR 50.0 KV FILTER : NO

GEOMETRY : 60,40 DEGREES

ANALYTE : C 103 (6)

			3	5	6	11	12	13	14	15	19	20	22	25	26	56
			LI201	B 203	C 103	NA201	MG101	AL203	SI102	P 205	K 201	CA101	TI102	MN101	FE203	BA101
		A1	-.673 -1.054	.244 -1.166	0.000	.154	.365	.531	.702	1.009	-1.483	-1.499	-1.525	-1.061		
		A2	.009 .068	.009 .224	0.000	-.030	-.035	-.047	-.062	-.094	.543	.567	.607	.075		
AIJK	3	LI201	0.000													
	5	B 203	0.000													
	6	C 103	0.000	0.000												
	11	NA201	.047	.025	0.000											
	12	MG101	.053	.024	0.000	.090										
	13	AL203	.068	.029	0.000	.118	.111									
	14	SI102	.086	.036	0.000	.151	.145	.146								
	15	P 205	.119	.057	0.000	.205	.197	.198	.197							
	19	K 201	-.264	-.610	0.000	-.277	-.300	-.287	-.267	-.242						
	20	CA101	-.270	-.618	0.000	-.291	-.315	-.303	-.283	-.257	.129					
	22	TI102	-.278	-.627	0.000	-.316	-.341	-.331	-.311	-.288	.114	.107				
	25	MN101	-.030	-.067	0.000	.053	.072	.108	.154	.226	.005	-.008	-.028			
	26	FE203	-.027	-.060	0.000	.059	.079	.115	.163	.237	.007	-.006	-.027	-.001		
	56	BA101	-.091 -.013	-.202	0.000	-.112	-.044	.009	.060	.140	.106	.095	.050	-.012		

MATH/1000 - CALCULATION OF NORRISH AND HUTTON TYPE ALPHA COEFFICIENTS FOR LOW DILUTION FUSION DISCS.

	A	B	C	D	E	F	G	H	I	J	K	L	M	N	O
000	ELEMENT MASS ABSORPTION COEFFICIENTS FROM HEINRICH (1966 ** locate to A25 for mass absorption coefficients for oxides **														
002		NaKa	MgKa	AlKa	SiKa	PKa	KKa	CaKa	TiKa	MnKa	FeKa	NiKa	CuKa	BaLa	CrKa
003	Li	169.40	99.20	60.70	38.60	25.30	6.00	4.40	2.50	1.10	.90	.60	.50	2.60	1.50
004	B	861.90	507.50	312.00	199.50	131.40	31.80	23.40	13.20	6.20	4.90	3.10	2.50	13.60	7.90
005	O	3,711.70	2,200.30	1,348.30	860.80	569.90	140.20	103.40	58.70	27.60	21.80	15.80	12.90	60.00	39.40
006	Na	640.02	5,409.10	3,359.40	2,168.10	1,440.80	359.40	265.90	151.90	72.00	57.20	37.20	30.30	156.10	91.40
007	Mg	770.10	463.60	4,376.50	2,824.60	1,877.00	468.20	346.40	197.90	93.80	74.60	48.40	39.50	203.30	119.10
008	Al	1,021.00	614.70	385.70	3,493.20	2,324.70	582.80	431.70	247.00	117.40	93.40	60.70	49.60	253.90	149.00
009	Si	1,332.50	802.20	503.40	327.90	2,840.10	715.60	530.60	304.30	145.00	115.50	75.20	61.40	312.60	183.80
010	P	1,695.90	1,021.00	640.60	417.90	279.80	870.30	645.30	370.00	176.40	140.50	91.40	74.70	380.20	223.60
011	K	3,729.20	2,245.10	1,408.80	917.80	615.30	158.10	1,189.80	685.00	328.20	261.80	171.00	139.80	703.70	415.40
012	Ca	4,412.80	2,656.70	1,667.00	1,086.00	728.10	187.10	139.40	772.20	371.00	296.20	193.70	158.60	793.20	469.20
013	Ti	6,056.70	3,646.40	2,288.00	1,490.60	999.30	256.80	191.30	110.60	472.50	377.50	247.30	202.60	113.60	597.00
014	Mn	9,041.80	5,443.60	3,415.60	2,225.30	1,491.80	383.40	285.50	165.10	79.50	63.50	343.60	281.60	169.50	100.50
015	Fe	10,166.60	6,120.70	3,840.60	2,502.10	1,677.40	431.10	321.10	185.60	89.40	71.40	379.60	311.10	190.60	113.00
016	Ni	12,805.60	7,709.50	4,837.50	3,151.60	2,112.80	543.00	404.40	233.80	112.60	90.00	58.90	48.30	240.10	142.30
017	Cu	12,165.00	8,569.00	5,376.80	3,503.00	2,348.30	603.60	449.50	259.80	125.20	100.00	65.50	53.70	266.90	158.10
018	Ba	10,032.20	7,463.70	5,559.60	3,696.90	2,526.00	692.60	523.10	310.40	688.10	645.40	425.40	349.40	318.40	622.10
019	La	10,596.50	7,889.10	5,880.00	3,909.70	2,671.40	732.50	553.20	328.20	720.00	672.90	444.20	365.20	336.70	647.40

MAC FOR OXIDES AT WAVELENGTHS OF INTEREST **locate to A 45 for oxide factors**

	NaKa	MgKa	AlKa	SiKa	PKa	KKa	CaKa	TiKa	MnKa	FeKa	NiKa	CuKa	BaLa	CrKa
SiO2	2,599.50	1,546.73	953.33	611.69	1,631.15	409.18	303.10	173.51	82.48	65.60	43.57	35.57	178.08	106.90
TiO2	5,117.53	3,067.24	1,911.65	1,238.36	827.33	210.10	156.10	89.81	294.32	235.04	154.58	126.63	92.13	373.68
Al2O3	2,287.70	1,361.15	838.86	2,253.95	1,498.59	374.44	277.15	158.35	75.12	59.69	39.56	32.32	162.62	97.40
Fe2O3	8,226.52	4,942.38	3,091.51	2,008.79	1,344.53	343.67	255.67	147.46	70.83	56.49	270.26	221.47	151.35	90.88
MnO	7,839.65	4,712.11	2,949.34	1,917.55	1,283.87	328.55	244.43	141.10	67.79	54.09	269.67	221.00	144.80	86.72
MgO	1,937.42	1,152.77	3,174.82	2,045.31	1,358.30	338.04	249.97	142.66	67.53	53.65	35.46	28.94	146.43	87.47
CaO	4,212.77	2,526.48	1,576.07	1,021.75	682.96	173.72	129.13	568.63	273.02	217.91	142.94	117.03	584.01	346.57
Na2O	1,432.94	4,580.78	2,840.25	1,830.63	1,215.99	302.82	223.95	127.84	60.54	48.06	31.68	25.81	131.29	77.98
K2O	3,726.23	2,237.49	1,398.52	900.12	607.59	155.06	1,005.28	578.62	277.14	221.04	144.64	118.25	594.37	351.54
P2O5	2,831.96	1,685.63	1,039.45	667.51	443.29	458.83	339.90	194.56	92.54	73.60	48.79	39.87	199.74	119.79
BaO	9,372.78	6,914.57	5,120.24	3,401.01	2,321.92	634.97	479.31	284.14	619.19	580.34	382.67	314.29	291.44	561.31

OXIDE FACTORS

	OXYGEN	ELEMENT
SiO2	.53253	.46747
TiO2	.40050	.59950
Al2O3	.47077	.52923
Fe2O3	.30056	.69944
MnO	.22554	.77446
MgO	.39683	.60317
CaO	.28531	.71469
Na2O	.25814	.74186
K2O	.16985	.83015
P2O5	.56358	.43642
BaO	.10433	.89567

LOCATE F45 FOR ****DILUTION**** FACTOR

DILUTION FACTOR (FLUX:SAMPLE RATIO)

	WEIGHT	F
sample	2.00	
flux	4.00	
nitrate	.60	
TOTAL	6.60	.30303

LOCATE TO A60 FOR FLUX COMPOSTION

FLUX COMPOSITION

			WT FRAC
Li2O	.53676	.46324	.27524
La2O3	.14732	.85268	.00000
B2O5	.68964	.31036	.72489

LOCATE TO A70 FOR FLUX MAC CALCULATION

CALCULATION OF FLUX MASS ABSORPTION COEFFICIENTS ***locate to A85 and A108 for unnormalised a-coefficients (X valu

	NaKa	MgKa	AlKa	SiKa	PKa	KKa	CaKa	TiKa	MnKa	FeKa	NiKa	CuKa	BaLa	CrKa
Li2O	2,070.77	1,226.99	751.83	479.92	317.62	78.03	57.54	32.67	15.32	12.12	8.76	7.16	33.41	21.84
La2O3	9,582.23	7,051.03	5,212.39	3,460.54	2,361.81	645.24	486.94	288.50	618.00	576.98	381.09	313.30	295.94	557.83
B2O5	2,827.24	1,674.92	1,026.67	655.56	433.81	106.56	78.57	44.58	20.96	16.55	11.86	9.67	45.60	29.62
TOTAL	2,619.39	1,551.85	951.16	607.30	401.88	98.78	72.79	41.31	19.41	15.34	11.01	8.98	42.25	27.49

CALCULATION OF a-COEFFICIENTS (X-values) USING SECONDARY WAVELENGTHS

	NaKa	MgKa	AlKa	SiKa	PKa	KKa	CaKa	TiKa	MnKa	FeKa	BaLa	CrKa
SiO2	-.00230	-.00100	.00069	.00219	.92690	.95299	.95877	.96990	.98465	.99323	.97423	.87556
TiO2	.28900	.29591	.30600	.31489	.32079	.34190	.34679	.35587	4.29181	4.34128	.35777	3.81676
Al2O3	-.03837	-.03724	-.03578	.82164	.82695	.84634	.85071	.85870	.86981	.87647	.86331	.77083
Fe2O3	.64867	.66207	.68190	.69931	.71078	.75189	.76130	.77877	.80269	.81323	.78247	.69890
MnO	.60392	.61710	.63660	.65378	.66504	.70548	.71451	.73214	.75537	.76586	.73554	.65304
MgO	-.07890	-.07793	.70844	.71753	.72116	.73462	.73758	.74358	.75124	.75702	.74724	.66135
CaO	.18433	.19032	.19909	.20680	.21194	.23022	.23452	3.86862	3.95939	4.00278	3.88565	3.51791
Na2O	-.13726	.59146	.60185	.61041	.61385	.62649	.62927	.63485	.64209	.64665	.63864	.55665
K2O	.12805	.13389	-.14253	.15010	.15511	.17294	3.88186	3.94193	4.02369	4.06453	3.95994	3.57862
P2O5	.02459	.02612	.02813	.03004	.03122	1.10539	1.11193	1.12430	1.14168	1.15133	1.12957	1.01763
BaO	.78128	1.04718	1.32823	1.39400	1.44775	1.64606	1.69231	1.78151	9.36367	11.16419	1.78727	5.88532
LOSS	-.30303	-.30303	-.30303	-.30303	-.30303	-.30303	-.30303	-.30303	-.30303	-.30303	-.30303	-.30303

***locate to A130 for mac of average of C-1 and W-1 and A152 for calculation of flux coefficient

CALCULATION OF a-COEFFICIENTS (X-values) USING PRIMARY AND SECONDARY WAVELENGTHS

	NaKa	MgKa	AlKa	SiKa	PKa	KKa	CaKa	TiKa	MnKa	FeKa	BaLa	CrKa
SiO2	.00448	.01038	.01907	.03058	.92448	.93973	.94055	.93870	.95852	.96414	.94209	.87556
TiO2	.31627	.34161	.37774	.42872	.48972	.93712	1.10653	1.50025	4.19139	4.22663	1.48420	3.81676
Al2O3	-.03212	-.02675	-.01884	.81999	.82423	.83341	.83322	.82965	.84503	.84954	.83319	.77083
Fe2O3	.64906	.66255	.68225	.69930	.71020	.74201	.74764	.75236	2.67942	2.73938	.75525	.69890
MnO	.60430	.61757	.63695	.65376	.66446	.69650	.70105	.70599	2.64133	2.70150	.70867	.65304
MgO	-.07317	-.06833	.70745	.71570	.71827	.72206	.72089	.71639	.72815	.73174	.71926	.66135
CaO	.21010	.23350	.26879	.31444	.37169	.79338	.95341	3.75266	3.86250	3.89460	3.76589	3.51791
Na2O	-.13189	.59101	.60090	.60867	.61109	.61453	.61337	.60900	.62045	.62275	.61194	.55665
K2O	.15467	.17851	.21457	.26136	.32024	.75528	3.81415	3.81981	3.92159	3.95007	3.83380	3.57862
P2O5	.03227	.03899	.04891	.06215	.07889	1.09036	1.09128	1.08903	1.11165	1.11828	1.09311	1.01763
BaO	.82073	1.10997	1.42394	1.54000	1.66218	2.37222	2.61036	3.13848	9.62099	10.90286	3.12190	5.88532
LOSS	-.30303	-.30303	-.30303	-.30303	-.30303	-.30303	-.30303	-.30303	-.30303	-.30303	-.30303	-.30303

AVERAGE COMPOSITION OF C-1 AND W-1 (CW-1)

SiO2	.62600
TiO2	.00660
Al2O3	.14600
Fe2O3	.06530
MnO	.00100
MgO	.03500
CaO	.06200
Na2O	.02700
K2O	.03500
P2O5	.00115

	NaKa	MgKa	AlKa	SiKa	PKa	KKa	CaKa	TiKa	MnKa	FeKa	BaLa	CrKa
MAC OF CW-1	2,944.95	1,987.92	1,233.04	1,044.57	1,461.77	379.10	304.89	191.95	93.07	74.07	197.05	120.01

CALCULATION OF M VALUES USING M=Am/Am

	NaKa	MgKa	AlKa	SiKa	PKa	KKa	CaKa	TiKa	MnKa	FeKa	BaLa	CrKa
M	1.00000	1.00000	1.00000	1.00000	1.00000	1.00000	1.00000	1.00000	1.00000	1.00000	1.00000	1.00000

Calculation of normalisation value using average of C-1 and W-1 (CW-1) using secondary wavelengths only

	NaKa	MgKa	AlKa	SiKa	PKa	KKa	CaKa	TiKa	MnKa	FeKa	BaLa	CrKa
SUM-P2O5	.04727	.06947	.10077	.22940	.81055	.83515	.97032	1.20745	1.25488	1.26664	1.21301	1.11345
P2O5	.00003	.00003	.00003	.00003	.00004	.00127	.00128	.00129	.00131	.00132	.00130	.00117
TOTAL	.04730	.06950	.10080	.22943	.81059	.83642	.97160	1.20874	1.25613	1.26796	1.21431	1.11462
M+TOTAL	1.04730	1.06950	1.10080	1.22943	1.81059	1.83642	1.97160	2.20874	2.25613	2.26796	2.21431	2.11462
1/M+TOTAL	.95484	.93502	.90843	.81339	.55231	.54454	.50720	.45275	.44324	.44092	.45161	.47290

Normalisation of a-coefficients (X-values) using secondary wavelengths

	NaKa	MgKa	AlKa	SiKa	PKa	KKa	CaKa	TiKa	MnKa	FeKa	BaLa	CrKa
SiO2	-.00220	-.00093	.00063	.00178	.51193	.51894	.48629	.43918	.43643	.43794	.43997	.41405
TiO2	.27595	.27668	.27798	.25612	.17718	.18618	.17589	.16112	1.90229	1.91418	.16157	1.80494
Al2O3	-.03664	-.03482	-.03250	.66831	.45673	.46086	.43148	.38877	.38553	.38646	.38988	.36453
Fe2O3	.61938	.61905	.61945	.56881	.39257	.40943	.38613	.35259	.35578	.35857	.35337	.33051
MnO	.57664	.57700	.57831	.53178	.36731	.38416	.36240	.33147	.33481	.33769	.33218	.30882
MgO	-.07533	-.07286	.64356	.58363	.39830	.40002	.37410	.33665	.33297	.33379	.33746	.31275
CaO	.17601	.17795	.18086	.16821	.11706	.12536	.11895	1.75151	1.75494	1.76493	1.75480	1.66361
Na2O	-.13106	.55303	.54673	.49650	.33904	.34115	.31917	.28743	.28460	.28512	.28841	.26324
K2O	.12226	.12519	.12947	.12209	.08567	.09417	1.96889	1.78469	1.78344	1.79215	1.78834	1.68948
P2O5	.02348	.02443	.02555	.02444	.01725	.60193	.56398	.50902	.50603	.50765	.51012	.48123
BaO	.74600	.97913	1.20660	1.13386	.79960	.89634	.85835	.80657	4.15032	4.92257	.80714	2.78315
LOSS	-.28935	-.28334	-.27528	-.24648	-.16737	-.16501	-.15370	-.13720	-.13431	-.13361	-.13685	-.14330

Calculation of normalisation value using average of C-1 and W-1 (primary and secondary wavelengths)

	NaKa	MgKa	AlKa	SiKa	PKa	KKa	CaKa	TiKa	MnKa	FeKa	BaLa	CrKa
SUM-K2O+P2O5	.05010	.07677	.11453	.24899	.81398	.85639	.86816	1.04267	1.21039	1.22097	1.04640	.98841
K2O+P2O5	.00545	.00629	.00757	.00922	.01130	.02769	.13475	.13495	.13853	.13954	.13544	.12621
TOTAL	.05555	.08306	.12210	.25821	.82528	.88408	1.00291	1.17762	1.34892	1.36051	1.18184	1.11462
M+TOTAL	1.05555	1.08306	1.12210	1.25821	1.82528	1.88408	2.00291	2.17762	2.34892	2.36051	2.18184	2.11462
1/M+TOTAL	.94738	.92331	.89119	.79478	.54786	.53076	.49927	.45922	.42573	.42364	.45833	.47290

Normalisation of a-coefficients (X-values) using primary and secondary wavelengths

	NaKa	MgKa	AlKa	SiKa	PKa	KKa	CaKa	TiKa	MnKa	FeKa	BaLa	CrKa
SiO2	.00425	.00958	.01699	.02430	.50645	.49877	.46959	.43107	.40807	.40845	.43179	.41405
TiO2	.29963	.31541	.33842	.34074	.26830	.49739	.55246	.68894	1.78439	1.79141	.68029	1.80494
Al2O3	-.03043	-.02470	-.01679	.65171	.45157	.44234	.41600	.38099	.35975	.35990	.38188	.36453
Fe2O3	.61490	.61174	.60802	.55579	.38909	.39426	.37327	.34550	1.14070	1.16050	.34615	.33051
MnO	.57250	.57021	.56764	.51960	.36403	.36968	.35002	.32420	1.12448	1.14446	.32480	.30882
MgO	-.06932	-.06309	.63047	.56883	.39351	.38325	.35992	.32898	.30999	.30999	.32966	.31275
CaO	.19904	.21560	.23955	.24991	.20363	.42109	.47601	1.72328	1.64437	1.64990	1.72601	1.66361
Na2O	-.12495	.54568	.53551	.48376	.33479	.32617	.30624	.27966	.26414	.26382	.28047	.26324
K2O	.14653	.16482	.19122	.20778	.17545	.40088	1.90430	1.75412	1.66953	1.67340	1.75714	1.68948
P2O5	.03057	.03600	.04359	.04939	.04322	.57872	.54485	.50010	.47326	.47375	.50101	.48123
BaO	.77754	1.02485	1.26900	1.22397	.91064	1.25909	1.30328	1.44124	4.09591	4.61886	1.43085	2.78315
LOSS	-.28708	-.27979	-.27006	-.24084	-.16602	-.16084	-.15129	-.13916	-.12901	-.12838	-.13089	-.14330

MATH/1000 - DEFINITIONS FOR NORRISH-TYPE ALPHA COEFFICIENTS FOR LOW DILUTION FUSION DISCS.

A	B	C	D	E	F	G	H	I	J	K	L	M	N	O
H					H									
	H	H	H	H	H	H	H	H	H	H	H	H	H	H
H	.1694E+03	.9920E+02	.6070E+02	.3860E+02	.2530E+02	.6000E+01	.4400E+01	.2500E+01	.1100E+01	.9000E+00	.6000E+00	.5000E+00	.2600E+01	.1500E+01
H	.8619E+03	.5075E+03	.3120E+03	.1995E+03	.1314E+03	.3180E+02	.2340E+02	.1320E+02	.6200E+01	.4900E+01	.3100E+01	.2500E+01	.1360E+02	.7900E+01
H	.3712E+04	.2200E+04	.1348E+04	.8608E+03	.5699E+03	.1402E+03	.1034E+03	.5870E+02	.2760E+02	.2180E+02	.1580E+02	.1290E+02	.6000E+02	.3940E+02
H	.6400E+03	.5409E+04	.3359E+04	.2168E+04	.1441E+04	.3594E+03	.2659E+03	.1519E+03	.7200E+02	.5720E+02	.3720E+02	.3030E+02	.1561E+03	.9140E+02
H	.7701E+03	.4636E+03	.4377E+04	.2825E+04	.1877E+04	.4682E+03	.3464E+03	.1979E+03	.9380E+02	.7460E+02	.4840E+02	.3950E+02	.2033E+03	.1191E+03
H	.1021E+04	.6147E+03	.3857E+03	.3493E+04	.2325E+04	.5828E+03	.4317E+03	.2470E+03	.1174E+03	.9340E+02	.6070E+02	.4960E+02	.2539E+03	.1490E+03
H	.1333E+04	.8022E+03	.5034E+03	.3279E+03	.2840E+04	.7156E+03	.5306E+03	.3043E+03	.1450E+03	.1155E+03	.7520E+02	.6140E+02	.3126E+03	.1838E+03
H	.1696E+04	.1021E+04	.6406E+03	.4179E+03	.2798E+03	.8703E+03	.6453E+03	.3700E+03	.1764E+03	.1405E+03	.9140E+02	.7470E+02	.3802E+03	.2236E+03
H	.3729E+04	.2245E+04	.1409E+04	.9178E+03	.6153E+03	.1581E+03	.1190E+04	.6850E+03	.3282E+03	.2618E+03	.1710E+03	.1398E+03	.7037E+03	.4154E+03
H	.4413E+04	.2657E+04	.1667E+04	.1086E+04	.7281E+03	.1871E+03	.1394E+03	.7722E+03	.3710E+03	.2962E+03	.1937E+03	.1586E+03	.7932E+03	.4692E+03
H	.6057E+04	.3646E+04	.2288E+04	.1491E+04	.9993E+03	.2568E+03	.1913E+03	.1106E+03	.4725E+03	.3775E+03	.2473E+03	.2026E+03	.1136E+03	.5970E+03
H	.9042E+04	.5444E+04	.3416E+04	.2225E+04	.1492E+04	.3834E+03	.2855E+03	.1651E+03	.7950E+02	.6350E+02	.3436E+03	.2816E+03	.1695E+03	.1005E+03
H	.1017E+05	.6121E+04	.3841E+04	.2502E+04	.1677E+04	.4311E+03	.3211E+03	.1856E+03	.8940E+02	.7140E+02	.3796E+03	.3111E+03	.1906E+03	.1130E+03
H	.1281E+05	7710E+04	.4838E+04	.3152E+04	.2113E+04	.5430E+03	.4044E+03	.2338E+03	.1126E+03	.9000E+02	.5890E+02	.4830E+02	.2401E+03	.1423E+03
H	.1217E+05	.8569E+04	.5377E+04	.3503E+04	.2348E+04	.6036E+03	.4495E+03	.2598E+03	.1252E+03	.1000E+03	.6550E+02	.5370E+02	.2669E+03	.1581E+03
H	.1003E+05	.7464E+04	.5560E+04	.3697E+04	.2526E+04	.6926E+03	.5231E+03	.3104E+03	.6881E+03	.6454E+03	.4254E+03	.3494E+03	.3184E+03	.6221E+03
H	.1060E+05	.7889E+04	.5880E+04	(198)	.2671E+04	.7325E+03	.5532E+03	.3282E+03	.7200E+03	.6729E+03	.4442E+03	.3652E+03	.3367E+03	.6474E+03
H				H										
	H	H	H	H	H	H	H	H	H	H	H	H	H	H
H	(4)	(4)	(4)	(4)	(4)	(4)	(4)	(4)	(4)	(4)	(4)	(4)	(4)	(4)
H	(5)	(5)	(5)	(5)	(5)	(5)	(5)	(5)	(5)	(5)	(5)	(5)	(5)	(5)
H	(7)	(7)	(7)	(7)	(7)	(7)	(7)	(7)	(7)	(7)	(7)	(7)	(7)	(7)
H	(9)	(9)	(9)	(9)	(9)	(9)	(9)	(9)	(9)	(9)	(9)	(9)	(9)	(9)
H	(10)	(10)	(10)	(10)	(10)	(10)	(10)	(10)	(10)	(10)	(10)	(10)	(10)	(10)
H	(11)	(11)	(11)	(11)	(11)	(11)	(11)	(11)	(11)	(11)	(11)	(11)	(11)	(11)
H	(1)	(1)	(1)	(1)	(1)	(1)	(1)	(1)	(1)	(1)	(1)	(1)	(1)	(1)
H	(14)	(14)	(14)	(14)	(14)	(14)	(14)	(14)	(14)	(14)	(14)	(14)	(14)	(14)
H	(15)	(15)	(15)	(15)	(15)	(15)	(15)	(15)	(15)	(15)	(15)	(15)	(15)	(15)
H	(16)	(16)	(16)	(16)	(16)	(16)	(16)	(16)	(16)	(16)	(16)	(16)	(16)	(16)
H	(2)	(2)	(2)	(2)	(2)	(2)	(2)	(2)	(2)	(2)	(2)	(2)	(2)	(2)
H					H									
H														
H	H	H												
H	.5325E+00	.4675E+00				H	H							
H	.4005E+00	.5995E+00												
H	.4708E+00	.5292E+00	H		H	.2000E+01								
H	.3006E+00	.6994E+00	H		H	.4000E+01								
H	.2255E+00	.7745E+00	H		H	.6000E+00								
H	.3968E+00	.6032E+00	H											
H	.2853E+00	.7147E+00			H	(156)	(157)							
H	.2581E+00	.7419E+00												
H	.1698E+00	.8302E+00												
H	.5636E+00	.4364E+00												
H	.1043E+00	.8957E+00			H									
H														
H			H		H									
H														
H	.5368E+00	.4632E+00	.2752E+00											
H	.1473E+00	.8527E+00	.0000E+00											
H	.6896E+00	.3104E+00	.7249E+00											
H														
H					H									
	H	H	H	H	H	H	H	H	H	H	H	H	H	H
H	(3)	(3)	(3)	(3)	(3)	(3)	(3)	(3)	(3)	(3)	(3)	(3)	(3)	(3)
H	(6)	(6)	(6)	(6)	(6)	(6)	(6)	(6)	(6)	(6)	(6)	(6)	(6)	(6)
H	(8)	(8)	(8)	(8)	(8)	(8)	(8)	(8)	(8)	(8)	(8)	(8)	(8)	(8)
H	(18)	(18)	(18)	(18)	(18)	(18)	(18)	(18)	(18)	(18)	(18)	(18)	(18)	(18)
H														
	H	H	H	H	H	H	H	H	H	H			H	H
H	(13)	(13)	(13)	(13)	(13)	(13)	(13)	(13)	(13)	(13)			(13)	(13)
H	(17)	(17)	(17)	(17)	(17)	(17)	(17)	(17)	(17)	(17)			(17)	(17)
H	(19)	(19)	(19)	(19)	(19)	(19)	(19)	(19)	(19)	(19)			(19)	(19)
H	(20)	(20)	(20)	(20)	(20)	(20)	(20)	(20)	(20)	(20)			(20)	(20)
H	(21)	(21)	(21)	(21)	(21)	(21)	(21)	(21)	(21)	(21)			(21)	(21)
H	(22)	(22)	(22)	(22)	(22)	(22)	(22)	(22)	(22)	(22)			(22)	(22)
H	(23)	(23)	(23)	(23)	(23)	(23)	(23)	(23)	(23)	(23)			(23)	(23)
H	(25)	(25)	(25)	(25)	(25)	(25)	(25)	(25)	(25)	(25)			(25)	(25)
H	(26)	(26)	(26)	(26)	(26)	(26)	(26)	(26)	(26)	(26)			(26)	(26)
H	(27)	(27)	(27)	(27)	(27)	(27)	(27)	(27)	(27)	(27)			(27)	(27)
H	(28)	(28)	(28)	(28)	(28)	(28)	(28)	(28)	(28)	(28)			(28)	(28)
H	(29)	(29)	(29)	(29)	(29)	(29)	(29)	(29)	(29)	(29)			(29)	(29)
H														
H														
H						H								
	H	H	H	H	H	H	H	H	H	H			H	H
H	(95)	(95)	(95)	(95)	(95)	(95)	(95)	(95)	(39)	(60)			(95)	(95)
H	(96)	(96)	(96)	(96)	(96)	(96)	(96)	(96)	(40)	(61)			(96)	(96)
H	(97)	(97)	(97)	(97)	(97)	(97)	(97)	(97)	(41)	(72)			(97)	(97)
H	(98)	(98)	(98)	(98)	(98)	(98)	(98)	(98)	(42)	(73)			(98)	(98)
H	(99)	(99)	(99)	(99)	(99)	(99)	(99)	(99)	(44)	(74)			(99)	(99)
H	(71)	(71)	(71)	(71)	(71)	(71)	(71)	(71)	(53)	(76)			(71)	(71)
H	(148)	(149)	(150)	(151)	(152)	(153)	(154)	(31)	(54)	(77)			(33)	(33)
H	(34)	(34)	(34)	(34)	(34)	(34)	(34)	(34)	(55)	(78)			(34)	(34)
H	(37)	(37)	(37)	(37)	(37)	(37)	(37)	(37)	(56)	(79)			(37)	(37)
H	(35)	(35)	(35)	(35)	(35)	(35)	(35)	(35)	(57)	(80)			(35)	(35)
H	(36)	(36)	(36)	(36)	(36)	(36)	(36)	(36)	(58)	(81)			(36)	(36)
H	(38)	(38)	(38)	(38)	(38)	(38)	(38)	(38)	(59)	(82)			(38)	(38)
H														
H	.6260E+00													
H	.6600E-02													
H	.1460E+00													
H	.6530E-01													
H	.1000E-02													
H	.3500E-01													
H	.6200E-01													
H	.2700E-01													
H	.3500E-01													
H	.1150E-02													
	H	H	H	H	H	H	H	H	H	H			H	H
H	(12)	(12)	(12)	(12)	(12)	(12)	(12)	(12)	(12)	(12)			(12)	(12)
H			H											
	H	H	H	H	H	H	H	H	H	H			H	H
H	(30)	(30)	(30)	(30)	(30)	(30)	(30)	(30)	(30)	(30)			(30)	(30)
H														
H														
	H	H	H	H	H	H	H	H	H	H			H	H
H	(45)	(45)	(45)	(45)	(45)	(45)	(45)	(45)	(45)	(45)			(45)	(45)
H	(48)	(48)	(48)	(48)	(48)	(48)	(48)	(48)	(48)	(48)			(48)	(48)
H	(62)	(62)	(62)	(62)	(62)	(62)	(62)	(62)	(62)	(62)			(62)	(62)
H	(32)	(32)	(32)	(32)	(32)	(32)	(32)	(32)	(32)	(32)			(32)	(32)
H	(49)	(49)	(49)	(49)	(49)	(49)	(49)	(49)	(49)	(49)			(49)	(49)
H														
	H	H	H	H	H	H	H	H	H	H			H	H
H	(43)	(43)	(43)	(43)	(43)	(43)	(43)	(43)	(43)	(43)			(43)	(43)
H	(43)	(43)	(43)	(43)	(43)	(43)	(43)	(43)	(43)	(43)			(43)	(43)
H	(43)	(43)	(43)	(43)	(43)	(43)	(43)	(43)	(43)	(43)			(43)	(43)
H	(43)	(43)	(43)	(43)	(43)	(43)	(43)	(43)	(43)	(43)			(43)	(43)
H	(43)	(43)	(43)	(43)	(43)	(43)	(43)	(43)	(43)	(43)			(43)	(43)
H	(43)	(43)	(43)	(43)	(43)	(43)	(43)	(43)	(43)	(43)			(43)	(43)
H	(43)	(43)	(43)	(43)	(43)	(43)	(43)	(43)	(43)	(43)			(43)	(43)
H	(43)	(43)	(43)	(43)	(43)	(43)	(43)	(43)	(43)	(43)			(43)	(43)
H	(43)	(43)	(43)	(43)	(43)	(43)	(43)	(43)	(43)	(43)			(43)	(43)
H	(43)	(43)	(43)	(43)	(43)	(43)	(43)	(43)	(43)	(43)			(43)	(43)
H	(43)	(43)	(43)	(43)	(43)	(43)	(43)	(43)	(43)	(43)			(43)	(43)
H	(43)	(43)	(43)	(43)	(43)	(43)	(43)	(43)	(43)	(43)			(43)	(43)
H														
H														
	H	H	H	H	H	H	H	H	H	H			H	H
H	(24)	(24)	(24)	(24)	(24)	(24)	(24)	(24)	(24)	(24)			(24)	(24)
H	(63)	(63)	(63)	(63)	(63)	(63)	(63)	(63)	(63)	(63)			(63)	(63)
H	(64)	(64)	(64)	(64)	(64)	(64)	(64)	(64)	(64)	(64)			(64)	(64)
H	(50)	(50)	(50)	(50)	(50)	(50)	(50)	(50)	(50)	(50)			(50)	(50)
H	(51)	(51)	(51)	(51)	(51)	(51)	(51)	(51)	(51)	(51)			(51)	(51)
H														
H														
	H	H	H	H	H	H	H	H	H	H			H	H
H	(52)	(52)	(52)	(52)	(52)	(52)	(52)	(52)	(52)	(52)			(52)	(52)
H	(52)	(52)	(52)	(52)	(52)	(52)	(52)	(52)	(52)	(52)			(52)	(52)
H	(52)	(52)	(52)	(52)	(52)	(52)	(52)	(52)	(52)	(52)			(52)	(52)
H	(52)	(52)	(52)	(52)	(52)	(52)	(52)	(52)	(52)	(52)			(52)	(52)
H	(52)	(52)	(52)	(52)	(52)	(52)	(52)	(52)	(52)	(52)			(52)	(52)
H	(52)	(52)	(52)	(52)	(52)	(52)	(52)	(52)	(52)	(52)			(52)	(52)
H	(52)	(52)	(52)	(52)	(52)	(52)	(52)	(52)	(52)	(52)			(52)	(52)
H	(52)	(52)	(52)	(52)	(52)	(52)	(52)	(52)	(52)	(52)			(52)	(52)
H	(52)	(52)	(52)	(52)	(52)	(52)	(52)	(52)	(52)	(52)			(52)	(52)
H	(52)	(52)	(52)	(52)	(52)	(52)	(52)	(52)	(52)	(52)			(52)	(52)
H	(52)	(52)	(52)	(52)	(52)	(52)	(52)	(52)	(52)	(52)			(52)	(52)
H	(52)	(52)	(52)	(52)	(52)	(52)	(52)	(52)	(52)	(52)			(52)	(52)
H	(52)	(52)	(52)	(52)	(52)	(52)	(52)	(52)	(52)	(52)			(52)	(52)

```
1:[,12]*C54+[,5]*B54
2:[,18]*C58+[,5]*B58
3:[,3]*C62+[,5]*B62
4:[,9]*C48+[,5]*B48
5:[,13]*C49+[,5]*B49
6:[,19]*C63+[,5]*B63
7:[,8]*C50+[,5]*B50
8:[,4]*C64+[,5]*B64
9:[,15]*C51+[,5]*B51
10:[,14]*C52+[,5]*B52
11:[,7]*C53+[,5]*B53
12:[,30]*B133+[,31]*B134+[,32]*B135+[,34]*B136+[,35]*B137+[,36]*B138+[,37]*B139+[,38]*B140+[,39]*B141
13:([,30]-[,80])*H54/[,80]
14:[,6]*C55+[,5]*B55
15:[,11]*C56+[,5]*B56
16:[,10]*C57+[,5]*B57
17:([,31]-[,80])*H54/[,80]
18:[,75]*D62+[,76]*D63+[,77]*D64
19:([,32]-[,80])*H54/[,80]
20:([,33]-[,80])*H54/[,80]
21:([,34]-[,80])*H54/[,80]
22:([,35]-[,80])*H54/[,80]
23:([,36]-[,80])*H54/[,80]
24:[,113]*B133+[,114]*B134+[,115]*B135+[,116]*B136+[,117]*B137+[,118]*B138+[,119]*B139+[,120]*B140
25:([,37]-[,80])*H54/[,80]
26:([,38]-[,80])*H54/[,80]
27:([,39]-[,80])*H54/[,80]
28:([,40]-[,80])*H54/[,80]
29:-[,80]*H54/[,80]
30:[,80]/[,80]
31:(((O36+(1.347*[,36]))-(O80+(1.347*[,80])))*H54)/(O80+(1.347*[,80]))
32:[,158]+[,172]
33:(((O36+(1.347*[,36]))-(O80+(1.347*[,80])))*H54)/(O80+(1.347*[,80]))
34:(((O37+(1.347*[,37]))-(O80+(1.347*[,80])))*H54)/(O80+(1.347*[,80]))
35:(((O39+(1.347*[,39]))-(O80+(1.347*[,80])))*H54)/(O80+(1.347*[,80]))
36:(((O40+(1.347*[,40]))-(O80+(1.347*[,80])))*H54)/(O80+(1.347*[,80]))
37:(((O38+(1.347*[,38]))-(O80+(1.347*[,80])))*H54)/(O80+(1.347*[,80]))
38:(O80+(1.347*[,80]))*-H54/(O80+(1.347*[,80]))
39:(((L30+(1.347*[,30]))-(L80+(1.347*[,80])))*H54)/(L80+(1.347*[,80]))
40:(((L31+(1.347*[,31]))-(L80+(1.347*[,80])))*H54)/(L80+(1.347*[,80]))
41:(((L32+(1.347*[,32]))-(L80+(1.347*[,80])))*H54)/(L80+(1.347*[,80]))
42:(((L33+(1.347*[,33]))-(L80+(1.347*[,80])))*H54)/(L80+(1.347*[,80]))
43:[,178]*[,-98]
44:(((L34+(1.347*[,34]))-(L80+(1.347*[,80])))*H54)/(L80+(1.347*[,80]))
45:[,90]*B133+[,91]*B134+[,92]*B135+[,93]*B136+[,94]*B137+[,95]*B138+[,96]*B139+[,97]*B140+[,98]*B141
48:[,99]*B142
49:1/[,175]
50:[,158]+[,212]
51:1/[,215]
52:[,218]*[,-115]
53:(((L35+(1.347*[,35]))-(L80+(1.347*[,80])))*H54)/(L80+(1.347*[,80]))
54:(((L36+(1.347*[,36]))-(L80+(1.347*[,80])))*H54)/(L80+(1.347*[,80]))
55:(((L37+(1.347*[,37]))-(L80+(1.347*[,80])))*H54)/(L80+(1.347*[,80]))
56:(((L38+(1.347*[,38]))-(L80+(1.347*[,80])))*H54)/(L80+(1.347*[,80]))
57:(((L39+(1.347*[,39]))-(L80+(1.347*[,80])))*H54)/(L80+(1.347*[,80]))
58:(((L40+(1.347*[,40]))-(L80+(1.347*[,80])))*H54)/(L80+(1.347*[,80]))
59:(L80+(1.347*[,80]))*-H54/(L80+(1.347*[,80]))
60:(((M30+(1.347*[,30]))-(M80+(1.347*[,80])))*H54)/(M80+(1.347*[,80]))
61:(((M31+(1.347*[,31]))-(M80+(1.347*[,80])))*H54)/(M80+(1.347*[,80]))
62:[,170]+[,171]
63:[,121]*B141+[,122]*B142
64:[,210]+[,211]
71:(((O35+(1.347*[,35]))-(O80+(1.347*[,80])))*H54)/(O80+(1.347*[,80]
72:(((M32+(1.347*[,32]))-(M80+(1.347*[,80])))*H54)/(M80+(1.347*[,80]
73:(((M33+(1.347*[,33]))-(M80+(1.347*[,80])))*H54)/(M80+(1.347*[,80]
74:(((M34+(1.347*[,34]))-(M80+(1.347*[,80])))*H54)/(M80+(1.347*[,80]
76:(((M35+(1.347*[,35]))-(M80+(1.347*[,80])))*H54)/(M80+(1.347*[,80]
77:(((M36+(1.347*[,36]))-(M80+(1.347*[,80])))*H54)/(M80+(1.347*[,80]
78:(((M37+(1.347*[,37]))-(M80+(1.347*[,80])))*H54)/(M80+(1.347*[,80]
79:(((M38+(1.347*[,38]))-(M80+(1.347*[,80])))*H54)/(M80+(1.347*[,80]
80:(((M39+(1.347*[,39]))-(M80+(1.347*[,80])))*H54)/(M80+(1.347*[,80]
81:(((M40+(1.347*[,40]))-(M80+(1.347*[,80])))*H54)/(M80+(1.347*[,80]
82:(M80+(1.347*[,80]))*-H54/(M80+(1.347*[,80]))
95:(((O30+(1.347*[,30]))-(O80+(1.347*[,80])))*H54)/(O80+(1.347*[,80]
96:(((O31+(1.347*[,31]))-(O80+(1.347*[,80])))*H54)/(O80+(1.347*[,80]
97:(((O32+(1.347*[,32]))-(O80+(1.347*[,80])))*H54)/(O80+(1.347*[,80]
98:(((O33+(1.347*[,33]))-(O80+(1.347*[,80])))*H54)/(O80+(1.347*[,80]
99:(((O34+(1.347*[,34]))-(O80+(1.347*[,80])))*H54)/(O80+(1.347*[,80]
148:(((O36+(1.347*[,36]))-(O80+(1.347*[,80])))*H54)/(O80+(1.347*[,80]
149:(((O36+(1.347*[,36]))-(O80+(1.347*[,80])))*H54)/(O80+(1.347*[,80]
150:(((O36+(1.347*[,36]))-(O80+(1.347*[,80])))*H54)/(O80+(1.347*[,80]
151:(((O36+(1.347*[,36]))-(O80+(1.347*[,80])))*H54)/(O80+(1.347*[,80]
152:(((O36+(1.347*[,36]))-(O80+(1.347*[,80])))*H54)/(O80+(1.347*[,80]
153:(((O36+(1.347*[,36]))-(O80+(1.347*[,80])))*H54)/(O80+(1.347*[,80]
154:(((O36+(1.347*[,36]))-(O80+(1.347*[,80])))*H54)/(O80+(1.347*[,80]
156:G50+G51+G52
157:G50/G54
198: 3909.7
```

MATH/1000 - CALCULATION OF NORRISH AND HUTTON TYPE ALPHA COEFFICIENTS FOR NORRISH AND HUTTON (1969) type
FUSION DISCS.

ELEMENT MASS ABSORPTION COEFFICIENTS FROM HEINRICH (1966) **locate to A25 for mass absorption coefficients for oxides**

	NaKa	MgKa	AlKa	SiKa	PKa	KKa	CaKa	TiKa	MnKa	FeKa	NiKa	CuKa	BaLa	CrKa
Li	169.40	99.20	60.70	38.60	25.30	6.00	4.40	2.50	1.10	.90	.60	.50	2.60	1.50
B	861.90	507.50	312.00	199.50	131.40	31.80	23.40	13.20	6.20	4.90	3.10	2.50	13.60	7.90
O	3,711.70	2,200.30	1,348.30	860.80	569.90	140.20	103.40	58.70	27.60	21.80	15.80	12.90	60.00	39.40
Na	640.02	5,409.10	3,359.40	2,168.10	1,440.80	359.40	265.90	151.90	72.00	57.20	37.20	30.30	156.10	91.40
Mg	770.10	463.60	4,376.50	2,824.60	1,877.00	468.20	346.40	197.90	93.80	74.60	48.40	39.50	203.30	119.10
Al	1,021.00	614.70	385.70	3,493.20	2,324.70	582.80	431.70	247.00	117.40	93.40	60.70	49.60	253.90	149.00
Si	1,332.50	802.20	503.40	327.90	2,840.10	715.60	530.60	304.30	145.00	115.50	75.20	61.40	312.60	183.80
P	1,695.90	1,021.00	640.60	417.90	279.80	870.30	645.30	370.00	176.40	140.50	91.40	74.70	380.20	223.60
K	3,729.20	2,245.10	1,408.80	917.80	615.30	158.10	1,189.80	685.00	328.20	261.80	171.00	139.80	703.70	415.40
Ca	4,412.80	2,656.70	1,667.00	1,086.00	728.10	187.10	139.40	772.20	371.00	296.20	193.70	158.60	793.20	469.20
Ti	6,056.70	3,646.40	2,288.00	1,490.60	999.30	256.80	191.30	110.60	472.50	377.50	247.30	202.60	113.60	597.00
Mn	9,041.80	5,443.60	3,415.60	2,225.30	1,491.80	383.40	285.50	165.10	79.50	63.50	343.60	281.60	169.50	100.50
Fe	10,166.60	6,120.70	3,840.60	2,502.10	1,677.40	431.10	321.10	185.60	89.40	71.40	379.60	311.10	190.60	113.00
Ni	12,805.60	7,709.50	4,837.50	3,159.60	2,112.80	543.00	404.40	233.80	112.60	90.00	58.90	48.30	240.10	142.30
Cu	12,165.00	8,569.00	5,376.80	3,503.00	2,348.30	603.60	449.50	259.80	125.20	100.00	65.50	53.70	266.90	158.10
Ba	10,032.20	7,463.70	5,559.60	3,696.90	2,526.00	692.60	523.10	310.40	688.10	645.40	425.40	349.40	318.40	622.10
La	10,596.50	7,889.10	5,880.00	3,909.70	2,671.40	732.50	553.20	328.20	720.00	672.90	444.20	365.20	336.70	647.40

MAC FOR OXIDES AT WAVELENGTHS OF INTEREST **locate to A45 for oxide factors**

	NaKa	MgKa	AlKa	SiKa	PKa	KKa	CaKa	TiKa	MnKa	FeKa	NiKa	CuKa	BaLa	CrKa
SiO2	2,599.50	1,546.73	953.33	611.69	1,631.15	409.18	303.10	173.51	82.48	65.60	43.57	35.57	178.08	106.90
TiO2	5,117.53	3,067.24	1,911.65	1,238.36	827.33	210.10	156.10	89.81	294.32	235.04	154.58	126.63	92.13	373.68
Al2O3	2,287.70	1,361.15	838.86	2,253.95	1,498.59	374.44	277.15	158.35	75.12	59.69	39.56	32.32	162.62	97.40
Fe2O3	8,226.52	4,942.38	3,091.51	2,008.79	1,344.53	343.67	255.67	147.46	70.83	56.49	270.26	221.47	151.35	90.88
MnO	7,839.65	4,712.11	2,949.34	1,917.55	1,283.87	328.55	244.43	141.10	67.79	54.09	269.67	221.00	144.80	86.72
MgO	1,937.42	1,152.77	3,174.82	2,045.31	1,358.30	338.04	249.97	142.66	67.53	53.65	35.46	28.94	146.43	87.47
CaO	4,212.77	2,526.48	1,576.07	1,021.75	682.96	173.72	129.13	568.63	273.02	217.91	142.94	117.03	584.01	346.57
Na2O	1,432.94	4,580.78	2,840.25	1,830.63	1,215.99	302.82	223.95	127.84	60.54	48.06	31.68	25.81	131.29	77.98
K2O	3,726.23	2,237.49	1,398.52	908.12	607.59	155.06	1,005.28	578.62	277.14	221.04	144.64	118.25	594.37	351.54
P2O5	2,831.96	1,685.63	1,039.45	667.51	443.29	458.83	339.90	194.56	92.54	73.60	48.79	39.87	199.74	119.79
BaO	9,372.78	6,914.57	5,120.24	3,401.01	2,321.92	634.97	479.31	284.14	619.19	580.34	382.67	314.29	291.44	561.31

OXIDE COEFFICIENTS

	OXYGEN	ELEMENT
SiO2	.53253	.46747
TiO2	.40050	.59950
Al2O3	.47077	.52923
Fe2O3	.30056	.69944
MnO	.22554	.77446
MgO	.39683	.60317
CaO	.28531	.71469
Na2O	.25814	.74186
K2O	.16985	.83015
P2O5	.56358	.43642
BaO	.10433	.89567

LOCATE F45 FOR ****DILUTION**** FACTOR

DILUTION FACTOR (FLUX:SAMPLE RATIO)

	WEIGHT	F
sample	.28	
flux	1.50	
nitrate	.00	
TOTAL	1.78	.15730

LOCATE TO A60 FOR FLUX COMPOSTION

FLUX COMPOSITION

			WT FRAC
Li2O	.53676	.46324	.29535
La2O3	.14732	.85268	.20900
B2O5	.68964	.31036	.49562

LOCATE TO A70 FOR FLUX MAC CALCULATION

CALCULATION OF FLUX MASS ABSORPTION COEFFICIENTS **locate to A85 and A108 for unnormalised a-coefficients (X-value

	NaKa	MgKa	AlKa	SiKa	PKa	KKa	CaKa	TiKa	MnKa	FeKa	NiKa	CuKa	BaLa	CrKa
Li2O	2,070.77	1,226.99	751.83	479.92	317.62	78.03	57.54	32.67	15.32	12.12	8.76	7.16	33.41	21.84
La2O3	9,582.23	7,051.03	5,212.39	3,460.54	2,361.81	645.24	486.94	288.50	618.00	576.98	381.09	313.30	295.94	557.83
B2O5	2,827.24	1,674.92	1,026.67	655.56	433.81	106.56	78.57	44.58	20.96	16.55	11.86	9.67	45.60	29.62
TOTAL	4,015.52	2,666.18	1,820.28	1,189.91	802.43	210.71	157.71	92.04	144.07	132.37	88.11	72.39	94.32	137.72

CALCULATION OF a-COEFFICIENTS (X-VALUES) USING SECONDARY WAVELENGTHS

	NaKa	MgKa	AlKa	SiKa	PKa	KKa	CaKa	TiKa	MnKa	FeKa	BaLa	CrKa
SiO2	-.05547	-.06605	-.07492	-.07644	.16246	.14816	.14503	.13925	-.06725	-.07935	.13970	-.03520
TiO2	.04317	.02366	.00790	.00641	.00488	-.00046	-.00161	-.00380	.16404	.12201	-.00364	.26951
Al2O3	-.06769	-.07700	-.08481	.14066	.13647	.12222	.11914	.11334	-.07528	-.08637	.11391	-.04605
Fe2O3	.16496	.13430	.10986	.10826	.10627	.09925	.09771	.09472	-.07997	-.09017	.09511	-.05350
MnO	.14981	.12071	.09757	.09619	.09438	.08797	.08650	.08386	-.08328	-.09302	.08420	-.05825
MgO	-.08141	-.08929	.11705	.11308	.10897	.09505	.09203	.08652	-.08357	-.09355	.08692	-.05739
CaO	.00773	-.00824	-.02110	-.02223	-.02342	-.02762	-.02850	.81455	.14079	.10165	.81671	.23855
Na2O	-.10117	.11296	.08814	.08470	.08107	.06876	.06608	.06119	-.09121	-.10019	.06167	-.06824
K2O	-.01133	-.02529	-.03645	-.03725	-.03820	-.04155	.84541	.83163	.14529	.10536	.83398	.24422
P2O5	-.04636	-.05785	-.06748	-.06906	-.07040	.18522	.18173	.17522	-.05627	-.06984	.17582	-.02048
BaO	.20986	.25065	.28517	.29230	.29787	.31672	.32079	.32833	.51874	.53233	.32876	.48382
LOSS	-.15730	-.15730	-.15730	-.15730	-.15730	-.15730	-.15730	-.15730	-.15730	-.15730	-.15730	-.15730

***locate to A130 for mac of average of G-1 and W-1 and to A152 for calculation of flux coefficient

AVERAGE COMPOSITION OF G-1 AND W-1 (GW-1)

SiO2	.68600
TiO2	.00660
Al2O3	.14600
Fe2O3	.06530
MnO	.00100
MgO	.03500
CaO	.06200
Na2O	.02700
K2O	.03500
P2O5	.00115

	NaKa	MgKa	AlKa	SiKa	PKa	KKa	CaKa	TiKa	MnKa	FeKa	BaLa	CrKa
MAC OF GW-1	2,944.95	1,987.92	1,233.04	1,044.57	1,461.77	379.10	304.89	191.95	93.07	74.07	197.05	120.01

CALCULATION OF M VALUES USING M=Am/Am

	NaKa	MgKa	AlKa	SiKa	PKa	KKa	CaKa	TiKa	MnKa	FeKa	BaLa	CrKa
M	1.00000	1.00000	1.00000	1.00000	1.00000	1.00000	1.00000	1.00000	1.00000	1.00000	1.00000	1.00000

Calculation of normalisation value using average of G-1 and W-1
using secondary wavelengths only

	NaKa	MgKa	AlKa	SiKa	PKa	KKa	CaKa	TiKa	MnKa	FeKa	BaLa	CrKa
SUM-P2O5	-.03890	-.04501	-.04807	-.01654	.13190	.11918	.14747	.19425	-.04889	-.06345	.19489	-.01104
P2O5	-.00005	-.00007	-.00008	-.00008	-.00008	.00021	.00021	.00020	-.00006	-.00008	.00020	-.00002
TOTAL	-.03895	-.04508	-.04814	-.01662	.13182	.11939	.14767	.19445	-.04895	-.06353	.19509	-.01107
M+TOTAL	.96105	.95492	.95186	.98338	1.13182	1.11939	1.14767	1.19445	.95105	.93647	1.19509	.98893
1/M+TOTAL	1.04053	1.04721	1.05058	1.01690	.88353	.89334	.87133	.83720	1.05147	1.06784	.83676	1.01119

Normalisation of a-coefficients (X-values) using secondary wavelengths

	NaKa	MgKa	AlKa	SiKa	PKa	KKa	CaKa	TiKa	MnKa	FeKa	BaLa	CrKa
SiO2	-.05778	-.06916	-.07871	-.07773	.14354	.13236	.12637	.11658	-.07071	-.08473	.11690	-.03559
TiO2	.04492	.02478	.00830	.00651	.00431	-.00041	-.00140	-.00318	.17248	.13028	-.00305	.27253
Al2O3	-.07043	-.08063	-.08910	.14304	.12058	.10919	.10381	.09489	-.07916	-.09223	.09531	-.04656
Fe2O3	.17165	.14063	.11541	.11009	.09389	.08867	.08514	.07930	-.08409	-.09629	.07959	-.05410
MnO	.15588	.12641	.10250	.09782	.08339	.07858	.07537	.07021	-.08757	-.09933	.07045	-.05890
MgO	-.08471	-.09351	.12298	.11499	.09628	.08491	.08019	.07244	-.08787	-.09990	.07273	-.05803
CaO	.00804	-.00863	-.02217	-.02261	-.02069	-.02467	-.02484	.68195	.14804	.10854	.68338	.24122
Na2O	-.10527	.11829	.09260	.08613	.07163	.06142	.05758	.05123	-.09590	-.10699	.05160	-.06900
K2O	-.01179	-.02649	-.03829	-.03788	-.03375	-.03712	.73663	.69624	.15277	.11251	.69784	.24695
P2O5	-.04824	-.06058	-.07089	-.07023	-.06220	.16547	.15834	.14669	-.05916	-.07458	.14712	-.02071
BaO	.21837	.26249	.29960	.29725	.26318	.28294	.27951	.27488	.54544	.56845	.27509	.48924
LOSS	-.16368	-.16473	-.16526	-.15996	-.13898	-.14053	-.13706	-.13170	-.16540	-.16797	-.13162	-.15906

HYBRID ALPHA COEFFICIENTS FOR USE IN COLA EQUATION

(OXIDE SYSTEM)

TARGET:CR 50.0 KV FILTER : NO

GEOMETRY : 60,40 DEGREES

ANALYTE : CA101 (20)

		3	5	6	11	12	13	14	15	19	20	22	25	26	56
		LI201	B 203	C 103	NA201	MG101	AL203	SI102	P 205	K 201	CA101	TI102	MN101	FE203	BA101
	A1	-.793 -.145	-.718 1.417	-.669	-.187	-.116	-.031	.047	.157	2.353	0.000	-.039	-.175		
	A2	-.004 -.033	-.007 -.189	-.008	-.021	-.022	-.024	-.025	-.028	-.055	0.000	-.208	-.036		
AIJK	3 LI201	0.000													
	5 B 203	.000													
	6 C 103	.000	.000												
	11 NA201	.002	.001	.001											
	12 MG101	.003	.002	.001	.000										
	13 AL203	.003	.002	.001	.000	.000									
	14 SI102	.003	.002	.002	.000	.000	.000								
	15 P 205	.004	.003	.002	.000	.000	.000	.000							
	19 K 201	.008	.006	.005	.002	.002	.002	.001	.001						
	20 CA101	0.000	0.000	0.000	0.000	0.000	0.000	0.000	0.000	0.000					
	22 TI102	.088	.081	.077	.044	.039	.033	.029	.022	-.072	0.000				
	25 MN101	.005	.003	.002	-.006	-.006	-.007	-.008	-.009	-.023	0.000	.068			
	26 FE203	.004	.002	.001	-.007	-.007	-.008	-.009	-.009	-.021	0.000	.061	-.000		
	56 BA101	.074 .080	.071	.070	.063	.061	.059	.058	.057	.036	0.000	-.055	.081		

HYBRID ALPHA COEFFICIENTS FOR USE IN COLA EQUATION

(OXIDE SYSTEM)

TARGET: CR 50.0 KV FILTER : NO

GEOMETRY : 60,40 DEGREES

ANALYTE : TI102 (22)

		3	5	6	11	12	13	14	15	19	20	22	25	26	56
		LI201	B 203	C 103	NA201	MG101	AL203	SI102	P 205	K 201	CA101	TI102	MN101	FE203	BA101
	A1	-.857 -.374	-.805 1.146	-.772	-.414	-.360	-.299	-.243	-.163	1.438	1.427	0.000	-.391		
	A2	-.004 -.038	-.006 -.039	-.008	-.023	-.024	-.027	-.029	-.031	-.067	-.067	0.000	-.043		
AIJK	3 LI201	0.000													
	5 B 203	.000													
	6 C 103	.000	.000												
	11 NA201	.003	.002	.002											
	12 MG101	.003	.002	.002	.000										
	13 AL203	.004	.003	.002	.000	.000									
	14 SI102	.004	.003	.002	.000	.000	.000								
	15 P 205	.005	.004	.003	.000	.000	.000	.000							
	19 K 201	.011	.009	.008	.003	.003	.002	.002	.002						
	20 CA101	.011	.009	.008	.003	.003	.002	.002	.002	.000					
	22 TI102	0.000	0.000	0.000	0.000	0.000	0.000	0.000	0.000	0.000	0.000				
	25 MN101	.008	.006	.005	-.003	-.003	-.004	-.005	-.006	-.016	-.016	0.000			
	26 FE203	.006	.004	.003	-.005	-.005	-.006	-.006	-.007	-.016	-.016	0.000	.001		
	56 BA101	.009 .026	.009	.009	.012	.012	.013	.013	.014	.029	.029	0.000	.026		

HYBRID ALPHA COEFFICIENTS FOR USE IN COLA EQUATION

(OXIDE SYSTEM)

TARGET:CR 50.0 KV FILTER : YE

GEOMETRY : 60,40 DEGREES

ANALYTE : MN101 (25)

		3 LI201	5 B 203	6 C 103	11 NA201	12 MG101	13 AL203	14 SI102	15 P 205	19 K 201	20 CA101	22 TI102	25 MN101	26 FE203	56 BA101
	A1	-.835 .028	-.775 6.098	-.736	-.312	-.214	-.140	-.070	.029	2.050	2.036	2.282	0.000		
	A2	-.004 -.001	-.007 -.175	-.008	-.029	-.034	-.038	-.041	-.045	-.113	-.113	-.119	0.000		
AIJK	3 LI201	0.000													
	5 B 203	.000													
	6 C 103	.000	.000												
	11 NA201	.006	.004	.003											
	12 MG101	.007	.005	.004	.000										
	13 AL203	.008	.006	.005	.000	.000									
	14 SI102	.009	.007	.006	.000	.000	.000								
	15 P 205	.010	.008	.007	.001	.000	.000	.000							
	19 K 201	.026	.022	.020	.008	.007	.006	.005	.004						
	20 CA101	.026	.022	.020	.008	.007	.006	.005	.004	.000					
	22 TI102	.027	.023	.021	.009	.007	.006	.006	.005	.000	.000				
	25 MN101	0.000	0.000	0.000	0.000	0.000	0.000	0.000	0.000	0.000	0.000	0.000			
	26 FE203	.003	.006	.007	.028	.032	.036	.039	.043	.099	.099	.103	0.000		
	56 BA101	.034 .137	.030	.028	.014	.012	.011	.010	.009	.001	.001	.001	0.000		

HYBRID ALPHA COEFFICIENTS FOR USE IN COLA EQUATION

(OXIDE SYSTEM)

TARGET:CR 50.0 KV FILTER : NO

GEOMETRY : 60,40 DEGREES

ANALYTE : FE203 (26)

		3	5	6	11	12	13	14	15	19	20	22	25	26	56
		LI201	B 203	C 103	NA201	MG101	AL203	SI102	P 205	K 201	CA101	TI102	MN101	FE203	BA101
	A1	-.883	-.840	-.813	-.509	-.448	-.398	-.336	-.255	1.199	1.189	1.363	-.020		
		0.000	4.509												
	A2	-.006	-.009	-.012	-.045	-.052	-.057	-.064	-.073	-.197	-.197	-.208	-.000		
		0.000	-.350												
AIJK	3 LI201	0.000													
	5 B 203	.000													
	6 C 103	.001	.000												
	11 NA201	.010	.007	.005											
	12 MG101	.012	.009	.007	.000										
	13 AL203	.014	.010	.008	.000	.000									
	14 SI102	.016	.012	.010	.001	.000	.000								
	15 P 205	.018	.014	.012	.001	.001	.000	.000							
	19 K 201	.050	.044	.040	.018	.015	.014	.012	.010						
	20 CA101	.050	.044	.040	.018	.016	.014	.012	.010	.000					
	22 TI102	.052	.046	.043	.020	.017	.015	.013	.011	.000	.000				
	25 MN101	.006	.010	.013	.047	.055	.060	.067	.076	.188	.188	.197			
	26 FE203	0.000	0.000	0.000	0.000	0.000	0.000	0.000	0.000	0.000	0.000	0.000	0.000		
	56 BA101	.074	.068	.064	.037	.034	.032	.029	.026	.005	.005	.004	.293		
		0.000													

HYBRID ALPHA COEFFICIENTS FOR USE IN COLA EQUATION

(OXIDE SYSTEM)

TARGET:CR 50.0 KV FILTER : NO

GEOMETRY : 60,40 DEGREES

ANALYTE : BA101 (56)

		3	5	6	11	12	13	14	15	19	20	22	25	26	56
		LI201	B 203	C 103	NA201	MG101	AL203	SI102	P 205	K 201	CA101	TI102	MN101	FE203	BA101
	A1	-.934 -.711	-.910 0.000	-.895	-.728	-.704	-.675	-.649	-.612	.142	.137	-.532	-.719		
	A2	-.000 -.008	-.000 0.000	-.001	-.003	-.003	-.003	-.003	-.004	-.012	-.012	-.007	-.009		
AIJK	3 LI201	0.000													
	5 B 203	.000													
	6 C 103	.000	.000												
	11 NA201	.001	.000	.000											
	12 MG101	.001	.000	.000	-.000										
	13 AL203	.001	.001	.000	.000	.000									
	14 SI102	.001	.001	.001	.000	.000	.000								
	15 P 205	.001	.001	.001	.000	.000	.000	.000							
	19 K 201	.003	.003	.003	.001	.001	.001	.001	.001						
	20 CA101	.003	.003	.003	.001	.001	.001	.001	.001	-.000					
	22 TI102	.005	.006	.006	.010	.010	.011	.011	.012	.021	.021				
	25 MN101	.003	.002	.002	-.000	-.000	-.001	-.001	-.001	-.006	-.006	.018			
	26 FE203	.002	.002	.001	-.001	-.001	-.002	-.002	-.002	-.008	-.008	.015	.001		
	56 BA101	0.000 0.000	0.000	0.000	0.000	0.000	0.000	0.000	0.000	0.000	0.000	0.000	0.000		

.PHAS STORED IN FILE :/XRF/ALPHASLDF_LEROEX.DAT

APPENDIX G

Analytical totals reported do not include SO_4^{2-} and CO_2, and H_2O+ data. Blanks indicate that the samples were not analysed for those elements.

Whole rock geochemical analysis of the following lamproite and kimberlite samples :-

Lamproites --- Western Australia

number		location	description (Fraser et al 1986)
601/126/PK3/3	-	Mt Percy	olivine leucite lamproite
601/126/PK7/1	-	Mt Rose	leucite lamproite
601/126/PK7/2	-	Mt Rose	
601/126/PK9/1	-	Old Leopold Downs	
601/126/PK11/1	-	Seltrust Pipe 1	olivine leucite lamproite
601/126/PK12/1	-	Seltrust Pipe 2	
601/126/PK12/2	-	Seltrust Pipe 2	leucite lamproite
601/126/PK13/1	-	Seltrust Pipe 3	
601/126/PK13/2	-	Seltrust Pipe 3	olivine leucite lamproite
601/127/PK3/8	-	Wolgidee Hills	altered
601/127/PK3/9	-	Wolgidee Hills	altered
601/127/PK5/5	-	Noonkanbah Hills	
601/127/PK5/6	-	Noonkanbah Hills	leucite lamproite
601/126/PK8/2	-	Machell's Pyramid	leucite lamproite
601/126/PK9/3	-	Mt Cedric	leucite lamproite
601/126/PK9/4	-	Mt Cedric	olivine leucite lamproite
601/126/PK12/1	-	Mt Gytha	
601/126/PK19/2	-	Oscar Plug	leucite lamproite
601/126/PK20/1	-	The Sisters West	olivine leucite lamproite
601/126/PK20/2	-	The Sisters West	leucite lamproite

Other lamproite samples

315/125/PK2/19	-	Leucite Hills, Wyoming
315/125/PK16/8	-	Leucite Hills, Wyoming
601/460/PK4/17	-	New South Wales, Australia
601/460/PK8/5	-	New South Wales, Australia

Kimberlites

CKP 9	-	South West Botswana Sill -Type I (C.B.Smith)
MAIN 15/1	-	Swartruggens - Type II (C.B.Smith)
K64/55	-	Bellsbank - Type II (C.B.Smith)
173/24/K1/402F	-	Finsch - Type II
173/33/K2/6F	-	St Augustina
173/33/K4/423F	-	Wesselton

MAJOR AND TRACE ELEMENT DATA FOR LAMPROITE AND KIMBERLITES LDF - XRFS

	PK3/3	PK7/1	PK7/2	PK9/1	PK11/1	PK12/1
SIO2	49.40	52.49	48.54	56.89	49.32	48.67
TIO2	6.34	5.02	6.21	5.43	5.20	6.68
AL2O3	6.91	8.92	8.02	7.13	7.21	9.23
FE2O3	8.01	6.82	8.92	6.51	6.75	8.88
MNO	.08	.05	.08	.07	.06	.09
MGO	8.79	7.57	8.59	6.05	11.15	6.20
CAO	3.83	2.24	3.74	3.44	3.30	2.28
NA2O	.99	.69	.52	.76	.27	.01
K2O	9.37	9.94	9.14	8.90	9.08	10.00
P2O5	1.70	.84	.99	.67	1.95	1.72
BAO	1.58	1.07	1.60	.93	.86	.65
SO4	.16	.41	.57	.04	.04	.01
H2O+	2.39	2.96	2.37	1.43	3.67	4.66
CO2	.24	0.32	.32	.18	.53	.97
LOF	2.48	3.18	2.47	2.65	3.30	4.41
TOTAL	99.49	98.77	98.22	99.46	98.41	98.85
NB	255	106	212	136	174	286
ZR	1745	1130	1320	1205	1340	1685
Y	24	13	16	11	14	29
SR	1990	1070	1005	1110	1495	1275
SR(MO)	2005	1060		1105	1495	1270
U	<11	<11		<11	<11	<11
U(MO)	<3	<3		<3	<3	5.5
RB	440	260	367	269	513	507
RB(MO)	430	254		261	505	498
TH	54	15	27	22	38	57
TH(MO)	47	11		13	30	55
PB	67	39	35	32	67	95
PB(MO)	65	36		29	59	98
ZN	79	82	86	69	82	101
CU	61	78	88	83	61	81
NI	448	916	260	99	418	576
SC	18	12	19	13	12	16
CO	39	32	40	28	34	42
CR	447	445	452	219	447	402
V	152	173	178	137	255	169
LA	426	209	215	186	325	527
CE	806	327	381	332	589	869
ND	278	119	126	109	203	306
GA	17	21		15	19	22

MAJOR AND TRACE ELEMENT DATA FOR LAMPROITE AND KIMBERLITES LDF - XRFS.

	PK12/2	PK13/1	PK13/2	PK3/8	PK3/9	PK5/5
SIO2	47.05	53.65	53.87	37.88	29.75	52.17
TIO2	5.41	5.54	5.69	4.69	5.63	5.98
AL2O3	8.04	8.45	8.60	4.76	3.40	9.36
FE2O3	7.31	7.18	7.07	7.10	9.78	6.75
MNO	.72	.06	.05	.10	.08	.05
MGO	6.95	7.26	7.41	8.74	10.50	6.20
CAO	5.59	3.03	2.95	15.39	17.76	1.99
NA2O	.12	.92	.69	.44	.50	.01
K2O	9.20	9.97	9.72	6.73	5.73	11.52
P2O5	4.33	.68	.54	.48	1.51	1.54
BAO	.55	.59	.79	1.37	2.24	.66
SO4	.03	.03	.03	.26	.49	.05
H2O+	4.48	2.79	3.44	3.68	2.16	2.44
CO2	1.02	.32	1.05	11.55	14.16	.48
LOF	4.21	2.61	2.64	13.17	16.18	3.07
TOTAL	98.82	99.92	100.00	100.80	100.03	99.27
NB	222	118	118	158	171	147
ZR	1375	1250	1280	1995	1615	1290
Y	23	12	11	14	13	17
SR	1825	1065	1015	1725	2395	1450
SR(MO)	1835	1070	1030	1730	2420	1440
U	11	<11	<11	<11	<11	<11
U(MO)	11	<3	<3	<3	<3	<3
RB	358	404	267	439	382	243
RB(MO)	349	400	264	435	374	236
TH	49	18	15	27	22	27
TH(MO)	40	12	16	16	16	21
PB	92	33	37	<12	21	61
PB(MO)	77	34	38	17	25	51
ZN	88	76	74	72	65	103
CU	62	66	70	80	99	57
NI	512	397	458	235	167	292
SC	14	12	13	18	20	11
CO	37	35	39	34	27	29
CR	447	529	524	289	226	256
V	277	194	175	57	60	561
LA	398	179	180	156	106	291
CE	699	338	348	249	177	491
ND	229	117	115	73	57	167
GA	18	20	20	11	8.7	26

MAJOR AND TRACE ELEMENT DATA FOR LAMPROITE AND KIMBERLITES LDF - XRF

	PK5/6	PK8/2	PK9/3	PK9/4	PK12/1	PK19/2
SIO2	51.57	50.35	52.07	51.74	62.24	52.25
TIO2	6.14	5.00	5.51	5.48	5.28	6.42
AL2O3	9.51	7.87	8.73	7.43	8.31	10.07
FE2O3	6.92	7.67	7.30	6.72	6.95	8.54
MNO	.06	.11	.05	.07	.04	.05
MGO	6.72	6.95	7.58	11.08	2.36	5.13
CAO	1.76	7.16	2.46	3.61	1.33	.41
NA2O	.06	.47	.68	.65	.15	.01
K2O	11.94	9.01	10.52	8.50	8.39	11.36
P2O5	1.38	1.68	.95	.76	1.13	.72
BAO	.64	.82	.97	.45	.47	1.33
SO4	.26	.21	.06	.03	.05	.07
H2O+	2.16	1.59	2.53	3.13	2.35	2.14
CO2	.65	.56	.23	.42	.13	.42
LOF	2.73	1.79	2.24	2.71	2.24	2.85
TOTAL	99.42	98.93	99.10	99.20	98.86	99.11
NB	154	167	146	130	174	168
ZR	1270	1155	1240	1130	1165	1485
Y	27	23	28	16	18	26
SR	828	1025	1385	1155	794	565
SR(MO)				1150	1270	
U	<11	<11	<11	<11	<11	<11
U(MO)				<3	5.5	
RB	287	190	242	187	239	335
RB(MO)				183	498	
TH	25	23	21	30	26	21
TH(MO)				20	55	
PB	70	28	61	51	32	45
PB(MO)				43	98	
ZN	94	77	81	71	56	154
CU	47	62	65	70	59	73
NI	299	188	429	383	91	521
SC	10	16	13	14	16	13
CO	31	36	29	35	22	42
CR	270	301	377	384	293	471
V	326	104	183	168	171	203
LA	318	253	319	201	223	250
CE	515	373	489	349	380	451
ND	180	126	169	110	121	158
GA				17	22	

MAJOR AND TRACE ELEMENT DATA FOR LAMPROITE AND KIMBERLITES LDF - XRFS

	PK20/1	PK20/2	PK8/5	PK2/19	PK4/17	PK16/8
SIO2	47.40	54.16	42.83	51.80	47.36	52.67
TIO2	5.05	4.48	4.14	2.36	4.57	2.57
AL2O3	6.82	8.88	8.65	10.27	9.56	9.88
FE2O3	7.68	6.97	12.39	5.16	11.86	4.77
MNO	.08	.06	.15	.08	.13	.06
MGO	15.50	6.36	12.37	7.30	6.65	7.75
CAO	3.51	1.98	9.71	5.96	9.11	4.63
NA2O	.55	.74	2.35	1.97	3.66	1.39
K2O	6.04	11.26	4.79	9.75	1.67	11.77
P2O5	.89	.79	1.37	1.92	1.33	1.71
BAO	.76	1.62	.15	.89	.21	.70
SO4	.05	.30	.03	.30	.03	.15
H2O+	6.91	1.75	.63	.93	4.46	.96
CO2	.20	.28	.37	.22	.26	.20
LOF	4.97	1.60	.45	1.71	3.91	1.38
TOTAL	99.22	98.90	99.42	99.15	100.10	99.25
NB	144	147	105	75	113	61
ZR	1050	1105	540	1390	671	1525
Y	16	25	26	12	32	10
SR	1365	1450	1455	2220	1495	2250
SR(MO)			1460	2245	1490	2275
U	<10	<11	<11	<10	<11	16
U(MO)			<3	7.9	4.9	6.9
RB	228	269	166	128	56	291
RB(MO)			162	125	53	283
TH	25	26	19	23	17	33
TH(MO)				21	9.1	14
PB	46	60	18	23	18	36
PB(MO)			.0	24	6.7	24
ZN	77		119	84	125	85
CU	71		107	38	71	83
NI	1075		393	185	339	258
SC	13		23	13	22	13
CO	49		60	24	58	26
CR	660		499	363	427	378
V	118		223	117	209	94
LA	236	269	100	178	108	153
CE	399	475	206	341	230	311
ND	127	160	92	126	104	126
GA				18	19	19

MAJOR AND TRACE ELEMENT DATA FOR LAMPROITE AND KIMBERLITES LDF - X RF

	PK16/8 B	KBEL 2	KDB 9	KDT 24	KDT 28	K4/423F
SIO2	52.73	32.71	35.29	31.79	31.71	34.28
TIO2	2.56	.84	.97	1.67	2.05	2.28
AL2O3	9.82	2.01	3.45	1.81	2.16	3.66
FE2O3	4.71	7.89	8.35	9.06	8.94	9.36
MNO	.06	.15	.14	.14	.14	.14
MGO	7.66	31.04	31.84	35.86	35.38	29.54
CAO	4.61	7.55	6.97	7.64	7.55	8.52
NA2O	1.39	.01	.60	.23	.13	.40
K2O	11.88	2.06	1.53	1.18	1.55	2.03
P2O5	1.71	2.05	1.11	.85	.81	1.00
BAO	.69	.62	.11	.11	.09	.15
SO4	.15	.46	.05	.09	.09	.08
H2O+	.96	7.59	6.21	6.25	5.83	4.84
CO2	.20	4.66	3.13	3.46	3.29	4.50
LOF	1.79	12.75	9.07	9.03	9.22	8.22
TOTAL	99.59	99.67	99.34	99.35	99.75	99.62
NB		217	135	122	163	137
ZR		387	284	211	215	244
Y		17	19	11	9.3	15
SR		1930	1040	782	783	1265
SR(MO)						
U		<10	10	<10	<10	<10
U(MO)						
RB		133	76	76	102	129
RB(MO)						
TH		55	19	12	17	12
TH(MO)						
PB		36	13	14	14	22
PB(MO)						
ZN	84	55	62	56	60	64
CU	52	26	38	52	47	55
NI	258	1410	1390	1470	1545	1180
SC	13	30	14	13	12	13
CO	25	81	84	96	96	81
CR	373	1765	1380	1655	1825	1395
V	93	84	65	78	87	148
LA	151	411	137	96	94	94
CE	311	706	260	174	173	176
ND	123	221	106	72	68	69
GA						

MAJOR AND TRACE ELEMENT DATA FOR LAMPROITE AND KIMBERLITES LDF - XRFS

	K4/423F	K1/402F	K2/6F	CKP 9	MAIN 15/1	K64/55
SIO2	33.74	38.90	31.96	20.07	30.86	33.12
TIO2	2.23	.87	1.73	3.30	1.69	.63
AL2O3	3.65	3.67	2.15	2.42	5.93	1.32
FE2O3	9.32	8.72	9.53	15.13	7.66	8.07
MNO	.14	.14	.15	.22	.14	.14
MGO	29.38	28.77	32.19	25.73	16.29	36.06
CAO	8.61	5.73	8.77	16.00	15.90	5.55
NA2O	.39	.09	.01	.15	.21	.01
K2O	2.03	4.17	.16	.26	5.70	1.81
P2O5	1.01	.66	.92	2.82	1.74	1.11
BAO	.14	.23	.20	.23	.85	.59
SO4	.08	.08	.15	1.79	.71	.35
H2O+	4.84	6.15	8.00	5.54	2.43	
CO2	4.50	1.91	5.53	9.13	10.55	
LOF	9.35	7.92	12.25	13.09	12.85	10.73
TOTAL	100.00	99.89	100.00	99.37	99.87	99.13
NB		53	130	311	156	159
ZR		173	240	550	472	265
Y		6.7	14	39	29	8.4
SR		793	851	1915	838	1440
SR(MO)						
U		<10	<10	<11	<11	<10
U(MO)						
RB		162	17	34	251	113
RB(MO)						
TH		11	13	48	34	38
TH(MO)						
PB		19		29	40	35
PB(MO)						
ZN	64	58	66	123	85	56
CU	61	49	61	85	41	24
NI	1180	1335	1440	557	730	1780
SC	14	19	14	26	28	22
CO	83	85	92	84	66	90
CR	1400	1855	1500	529	1250	1480
V	149	141	65	138	150	45
LA	93	66	110	329	291	262
CE	177	123	204	622	506	463
ND	68	51	82	229	186	139
GA						